International Conference

Advanced Laser Technologies

ALT'13

The 21th annual International Conference on Advanced Laser Technologies ALT'13

Budva, Montenegro
September 16–20, 2013

BOOK OF ABSTRACTS

Contents

Organizers

General Physics Institute
of Russian Academy of Sciences,
Russia

University of Montenegro

Center of Laser Technology
and Material Science, Russia

International Laser Center,
Lomonosov Moscow State University,
Russia

Sponsors

Municipality of Budva,
Montenegro

Russian Foundation for Basic Research,
Russia

Keldysh Institute
of Applied Mathematics,
Russia

Forum of University Professors
and Researchers of Montenegro

The Optical Society of America

Conference Chairman

Ivan SHCHERBAKOV, Russia

Program Committee Chair

Vitaly KONOV, Russia

International Program Committee

Kerim ALLAKHVERDIEV (Turkey)
Ekaterina BORISOVA (Bulgaria)
Jean-Louis COUTAZ (France)
Aladar CZITROVSKY (Hungary)
Boris DENKER (Russia)
Dan DUMITRAS (Romania)
Costas FOTAKIS (Greece)
Thomas GRAF (Germany)
Sergey GARNOV (Russia)
Frans HARREN (Netherlands)
Lan JIANG (China)
Pavel KASHKAROV (Russia)
Armando LUCHES (Italy)
Yong Feng LU (USA)
Vladimir MAKAROV (Russia)
Andreas MANDELIS (USA)
Vladimir MAZHUKIN (Russia)
Ion MIHAILESCU (Romania)
Vladislav PANCHENKO (Russia)
Zarko PAVICEVIC (Montenegro)
Ivan PELIVANOV (Russia)
Alexander PRIEZZHEV (Russia)
Bojan RADAK (Serbia)
Valerio ROMANO (Switzerland)
Marc SENTIS (France)
Alexander SHKURINOV (Russia)
Valery TUCHIN (Russia)
Sergey VARTAPETOV (Russia)
Vadim VEIKO (Russia)
Alexey ZHELTIKOV (Russia)

Organizing Committee

Co-chairs Vladimir PUSTOVOY (Russia)
Lazar RADENOVIC (Montenegro)

Natalia KHAKAMOVA (Russia)
Valery KHAVAEV (Russia)
Andrey NIKOLAYCHIK (Russia)
Tatiana VOLYAK (Russia)

PLENARY TALKS

Plenary Talk 1

ADVANCES IN MULTI-SPECTRAL OPTOACOUSTIC TOMOGRAPHY

Vasilis Ntziachristos

Institute for Biological and Medical Imaging,
Helmholtz Zentrum München & Technische Universität München, Germany

Optical imaging is unequivocally the most versatile and widely used visualization modality in the life sciences. Yet it is significantly limited by photon scattering, which complicates imaging beyond a few hundred microns. For the past few years however there has been an emergence of powerful new optical imaging methods that can offer high resolution imaging beyond the penetration limits of microscopic methods. These methods can prove essential in cancer research. Of particular importance is the development of multi-spectral opto-acoustic tomography (MSOT) that brings unprecedented optical imaging performance in visualizing anatomical, physiological and molecular imaging biomarkers. Some of the attractive features of the method are the ability to offer 10–100 microns resolution through several millimetres to centimetres of tissue and real-time imaging. In parallel we have now achieved the clinical translation of targeted fluorescent probes, which opens new ways in the interventional detection of cancer in surgical and endoscopic optical molecular imaging. This talk describes current progress with methods and applications for in-vivo optical and opto-acoustic imaging in cancer and outlines how new opto-acoustic and fluorescence imaging concepts are necessary for accurate and quantitative molecular investigations in tissues.

Plenary Talk 2

RECENT ADVANCES IN SEMICONDUCTOR DISK LASERS

Oleg G. Okhotnikov

Optoelectronics Research Centre, Tampere University of Technology,
Korkeakoulunkatu 3, 33720 Tampere, Finland

oleg.okhotnikov@tut.fi; phone +358 40 849 0010; fax +358 3115 3400

Optically-pumped semiconductor disk lasers (SDLs) represent a proven approach for generation of multi-watt output powers with excellent beam quality. They combine many advantages of solid-state lasers with the added benefit of wavelength tailoring provided by the semiconductor gain material. During the past few years a wafer fusion technique has been used extensively in the producing of vertical-cavity surface-emitting lasers operating at the telecom wavelengths of 1.3–1.55 μm. This technique allows the integration of non-lattice-matched semiconductor materials, e.g. GaAs and InP, which cannot be grown monolithically. The quantum dot semiconductors provide an interesting alternative to quantum-well (QW) structures since these materials alleviate the requirement for lattice matching. Recently, we have demonstrated first quantum dot based gain medium in SDL architecture. Since then, different wavelengths have been demonstrated both in continuous-wave and mode-locked regimes with a performance comparable to quantum-well-based lasers. The (AlGaIn)(AsSb) material system establishes a steady platform for optoelectronic devices operating in the mid-infrared spectral range. Lattice-matched or strain-compensated structures employing InGaAsSb as an active material and AlGaAsSb for barrier and cladding layers grown on GaSb substrates are demonstrated to be compounds of choice for long-wavelength lasers and photodetectors. An optically-pumped semiconductor disk laser emitting radiation around 2.5 μm tunable over 130 nm will be presented. SDLs with intracavity frequency conversion and pumping of solid-state gain media will also be considered.

Plenary Talk 3

INTERACTION OF LASER RADIATION WITH NANOPARTICLES FOR PRECISION PHOTOSURGERY

V.B. Loschenov

A.M. Prokhorov General Physics Institute RAS, Vavilova str. 38-5, Moscow 119991, Russia

loschenov@mail.ru

This report summarizes the results on the interaction between laser radiation and nanoparticles (NPs) in the living objects in order to improve performance of photodynamic therapy and laser hyperthermia for further using in precision photosurgery. Three types of NPs were investigated: metalic and dielectric particles conjugated with molecules of photosensitizers and crystalline NPs from organic dyes.

The NPs from organic dyes – photosensitizers. Possibility of high accumulation of such particles in tumor cells has been demonstrated. For these types of NPs the biotransformation from solid to liquid phase on the border of intercellular medium/cell and inside of the lysosomes was investigated using luminescence spectra changes record. Also the photodynamic effect was evaluated upon excitation in the absorption band for the NPs and dissolved in various cellular structures photodynamic active molecules. Possibility to control for NPs phototoxicity when they dissolved offers additional advantages in selectivity for the using these type of NPs.

The plasmonic NPs conjugated with metal phthalocyanines onto their surface. Metal particles by the plasmon resonance can significantly increase the intensity of electromagnetic field near their surface and serve as an antenna, which can be used to more efficiently excite the conjugated molecule of photosensitizers. The effect of the singlet oxygen generation substantial strengthening by aluminum- and zinc-phthalocyanines in the presence of silver NPs was demonstrated in different water media. Furthermore, their ability to penetrate through cell membrane, and the phototoxicity mechanisms were investigated.

The upconversion dielectric NPs. These NPs can fluoresce not only in the VIS region, but also in the IR, that extends their range of application. We investigated the upconversion properties of inorganic NPs containing trivalent rare earth ions of ytterbium, erbium, thulium, holmium in biological environments upon excitation at the absorption band of ytterbium. A method for the up-conversion NPs kinetic characteristics study in the intercellular space is described. The upconversion NPs long luminescence lifetime is another advantageous property; it can be useful for the time-resolved bioimaging. The dependencies of the upconversion luminescence intensity on the pump power were obtained and analyzed.

These three classes of NPs seem promising for the visualization of biological tissues by the methods of video fluorescence deep tissue imaging, light scattering, NMR tomography as well as for precision photodynamic therapy and laser hyperthermia. The presented results are based on joint activities of the large group of scientists: laser biospectroscopy lab of GPI RAS and leading scientists-chemists from Moscow (Luk'yanets E.A., Kaliya O.L. SSC NIOPIK; Klimov A.I., Krutyakov Yu.A., Lisichkin G.V. Department of Chemistry, Moscow State University; Ponomarev G.V. Orekhovich Institute of Biomedical Chemistry RAMS; Krut'ko V.A. Kurnakov Institute of General and Inorganic Chemistry RAS; Kuznetsov S.V., Federov P.P. GPI RAS).

Acknowledgements: This work was partially supported by the RFBR grant № 12-02-12080-ofi-m.

Plenary Talk 4

SELECTIVE ABLATION OF TRANSPARENT THIN-FILMS BY ULTRASHORT LASER PULSES

Andreas Ostendorf, Shizhou Xiao, Evgeny L. Gurevich

Ruhr-University Bochum, Applied Laser Technology, 44780 Bochum, Germany

andreas.ostendorf@ruhr-uni-bochum.de

Selective laser ablation of thin layers by short and ultrashort is one of the key topics of modern surface engineering and many industrial products like solar cells and flat panel displays rely on this technology. Depending on the laser and material properties thin film laser ablation can result in two very different process regimes: 1) pure thermal regime with evaporation of the film from the substrate and 2) thermomechanical spallation due to shockwaves and material mismatch between thin film and underlying substrate. Besides these two types of interaction it is important to distinguish between opaque, e.g. metal films and transparent, e.g. TCO layers because of largely different optical absorption lengths. Finally, also the influence of film thickness as well as incubation can play important roles in thin film laser ablation.

It will be shown that there are strong effects of the film thicknesses on the ablation threshold. However, they scale inversely when changing from metal to transparent films. From these investigations bulk and film ablation and be distinguished. Also simulation and experimental results have revealed the clear transition from long pulse to ultrashort pulse regime.

References:

1. S. Xiao, E.L. Gurevich, A. Ostendorf, “Incubation effect and its influence on laser patterning of ITO thin film” Appl. Phys. A, Vol. 107, pp. 333–338 (2012).
2. S. Xiao, B. Gröger, S. Abreu Fernandes, A. Ostendorf, “Laser selective patterning of ITO on flexible PET for organic photovoltaics”, Proc. SPIE, Vol. 7921, DOI:10.1117/12.873289 (2011).
3. S. Xiao, S. Abreu Fernandes, C. Esen, A. Ostendorf, “Picosecond Laser Direct Patterning of Poly(3,4-ethylene dioxythiophene)-Poly(styrene sulfonate) (PEDOT:PSS) Thin Films” J. of Laser Micro/Nanoengineering, Vol. 6, No. 2, pp. 249–254 (2011).

Plenary Talk 5

MILLIMETER WAVE AND TERAHERTZ TOMOGRAPHY: A SURVEY

J.P. Guillet[1], B. Recur[1], L. Frederique[2], B. Bousquet[1], L. Canioni[1], I. Manek-Hönninger[1], P. Desbarats[2], P. Mounaix[1]

[1]*Université de Bordeaux, LOMA, UMR CNRS 5798, 351 Cours de la Libération, 33405 Talence Cedex, France*
[2]*Université de Bordeaux, LaBRI, UMR CNRS 5800, 351 Cours de la Libération, 33405 Talence Cedex, France*

p.mounaix@loma.u-bordeaux1.fr

Terahertz and millimeter waves penetrate various dielectric materials, including plastics, ceramics, crystals, and concrete, allowing terahertz transmission and reflexion images to be considered. Terahertz imaging is a well established technique in various laboratory and industrial applications. However, these images are almost totally two-dimensional, and transmission-mode measurement of such images is limited to thin samples, due to the absorption of the sample accumulated in the propagation direction. Tomographic imaging procedure can be used to acquire and to render three-dimensional images in the terahertz frequency range, as in the optical, infrared or X-ray regions of the electromagnetic spectrum.

In this presentation, after a brief introduction to two dimensional millimeter wave and terahertz imaging we will establish principles of tomography such as: Terahertz Computed tomography (CT), tomosynthesis (TS), synthetic aperture radar (SAR), time-of-flight (TOF) terahertz tomography. For each technique, we will present advantages, drawbacks and limitations for imaging the internal structure of an object. We will describe usual reconstruction methods (and their major optimizations) to obtain a 3D image of observed objects. First, the direct methods are developed. Then, we will define the acquisition and reconstruction models, in the spatial domain with the Radon transform and in the frequency domain with the Fourier Slice Theorem. Second, we will detail another kind of reconstructions: the iterative methods. Especially, we will explain the Karcmarz method giving well-known algebraic reconstructions such as the Simultaneous Algebraic Reconstruction Technique SART and we will develop methods based on stochastic process such as the Expectation Maximization (EM). Several potential applications will be presented.

Acknowledgements: We would like to express sincere thankfulness to each of the persons who have permitted us to display some results of their work for the review paper. We would also acknowledge financial support from the European community thanks to the contract DOTNAC (Development and Optimization of THz NDT of Aeronautics Composite multilayered structures) – Contract N 266320/FP7-AAT-2010-RTD-1 – http://www.dotnac-project.eu/ and the Agence Nationale de la Recherche (ANR) for their support in the InPoSec project (www.inposec.org).

SECTION B

Biophotonics

Paper B-I-1

OCT FOR DYNAMIC MOUSE EMBRYONIC ANALYSIS

Irina V. Larina

Molecular Physiology and Biophysics, Baylor College of Medicine, Houston, TX, USA, 77030

larina@bcm.edu

Congenital heart defects are among the most common birth defects and the leading cause of death in children born with congenital defects. Understanding how the early embryonic heart functions and what regulatory mechanisms are involved in early cardiogenesis is highly important for advancement of heart defects research. Biomechanical stimuli, including blood flow and heart contraction, are important regulators of cardiovascular development. Thus, defining how these mechanisms coordinate mammalian heart tube function and morphogenesis is critically important for the diagnosis of congenital heart defects and for the development of new therapeutic interventions to treat/prevent them. Such analysis can only be performed through live high-resolution embryonic imaging.

Toward this goal, we are working on development and application of innovative methods for live dynamic imaging and analysis of mammalian embryos. Our approach combines live embryo manipulation protocols, state-of-the-art optical coherence tomography technology (OCT), confocal microscopy of vital fluorescent reporters, advanced computational analysis, and utilizes mouse models of human congenital heart diseases. We are now using these methods to address different aspects of normal and abnormal embryonic cardiovascular development.

Paper B-I-2

LASER-BASED TECHNOLOGIES IN REPRODUCTIVE MEDICINE

N. Shakhova[1,2], S. Gamayunov[3], E. Grebenkina[3], O. Kachalina[2], I. Kuznetsova[4], O. Onoprienko[3], O. Panteleeva[5], M. Kirillin[1]

[1]*Institute of Applied Physics RAS, Uljanov St. 46, Nizhny Novgorod, 603950 Russia*
[2]*State Medical Academy, Minin Sq. 10/1, Nizhny Novgorod, 603000 Russia*
[3]*Oncologic Clinic, Rodionov St. 190, Nizhny Novgorod, 603126 Russia*
[4]*Regional Clinic, Rodionov St. 190, Nizhny Novgorod, 603126 Russia*
[5]*Nizhny Novgorod Clinical Hospital of Russian Railways, Lenin Av. 18, Nizhny Novgorod, 603011 Russia*

shakh@ufp.appl.sci-nnov.ru

An increase of "indeterminate" infertility rate, a growing level of "silent" pelvic inflammatory diseases (PID) and endometriosis raise the requirement for novel diagnostical techniques [1]. One more modern hazard for reproductive potential is "rejuvenation" of cervical cancer (CC) [2]. All these situations demand accurate timely diagnostics and organ-preserving methods of treatment. In our study we demonstrate application of laser-based technologies, including optical coherence tomography (OCT) and photodynamic therapy (PDT).

OCT has been used as a new method of introscopy in combination with standard endoscopic procedures: in colposcopy for CC and in laparoscopy for PID and endometriosis. Based on comparative analysis of the OCT data and the results of histological studies OCT criteria of the considered diseases have been developed.

In PID OCT demonstrates high (85–91%) diagnostic accuracy optimizing diagnosis of latent forms of PID. Basing of the subjective criteria an attempt to develop independent criteria aimed for automated recognition of pathological states in fallopian tubes was made. Diagnostic accuracy 90–97% of the developed independent criteria was demonstrated. In endometriosis OCT may be employed as an alternative to conventional biopsy.

In CC OCT makes it possible to avoid random biopsies, to validate the choice of treatment method and in particular cases to substitute broad excisions with PDT. At the stage of follow-up OCT allows for noninvasive evaluation of healing process and for early recurrence diagnostics.

In our opinion, the developed diagnostic and treatment algorithm employing OCT and PDT will allow to apply individual tactics in female patients which finally will promote efficient preserving and reconstruction of reproductive function.

Acknowledgements: The authors are grateful to the staff and management of the Nizhny Novgorod Oncologic Clinic, Regional Clinic and Hospital of the Russian Railways for the possibility to conduct this study. The authors thank the Russian Basic Research Foundation (project 11-02-00916), Presidium of Russian Academy of Sciences (Fundamental Sciences for Medicine) and the Ministry of Education and Science of Russian Federation (project 8147) for the financial support of this work.

References:

1. R.L. Sweet, R.S. Gibbs, Infectious Diseases of the Female Genital Tract. Philadelphia: Wolters Kluwer / Lippincott Williams & Wilkins, 2009.
2. Ramez N. Eskander et al., "Fertility preserving options in patients with gynecologic malignancies" Amer. J. Obstet. Gynecol., Vol. 205, Iss. 2, pp. 103–110 (2011).

Paper B-I-3

LIGHT SHEET BASED FLUORESCENCE MICROSCOPY OF 3-DIMENSIONAL CELL CULTURES

Herbert Schneckenburger, Sarah Schickinger, Petra Weber, Michael Wagner, and Thomas Bruns

Hochschule Aalen, Institut für Angewandte Forschung, Beethovenstr. 1, 73430 Aalen, Germany

herbert.schneckenburger@htw-aalen.de

Abstract: A module for light sheet based fluorescence microscopy is described permitting high resolution imaging of 3-dimensional cell cultures at low light exposure. Applications include fluorescence lifetime imaging (FLIM), nanosecond ratio imaging as well as measurements of the uptake and interaction of fluorescent dyes and chemotherapeutic agents applied via an innovative microfluidic system.

Introduction: 3-dimensional cell cultures are used increasingly as test models for diagnosis of diseases or interaction of pharmaceutical agents. Often these 3D systems require microscopic methods of high lateral and axial resolution. Laser scanning microscopy (LSM) or structured illumination microscopy are well described methods for 3D imaging. However, for recording each layer the whole sample is illuminated, and light dose sums up when various layers are recorded or when measurements are repeated during a larger time interval. Thus, living cells are easily damaged. To overcome this problem, light sheet based or selective plane illumination microscopy (SPIM), where only selected parts of a 3D sample are illuminated, has recently been introduced [1]. However, present light sheet microscopes are rather complex instruments of limited flexibility requiring special sample preparation and comparably large sample chambers. In the present paper some of these disadvantages are overcome, and new applications are becoming possible.

Materials and Methods: A light sheet module [2] is described which is easily adapted to a conventional fluorescence microscope. The light sheet (created by a focused laser beam) and an objective lens for image detection are shifted simultaneously in axial direction. The sample (3D cell spheroid with genetically encoded fluorescence proteins) is located in rectangular micro-capillaries of 600–900 µm diameter and surrounded by stationary or flowing liquid media. By coupling to a microfluidic system small quantities of agents (fluorescent dyes, pharmaceutical agents) are easily applied. Samples can be rotated using an innovative technique and observed from various sides. Thus, the loss of information due to long path ways of penetrating light resulting in pronounced scattering is kept low.

Applications: Present applications include:

- 3D representation of cell architecture;
- measurement of the uptake of specific fluorescent dyes;
- ratio imaging of an intrinsic redox sensor for detection of oxidative stress;
- measurement of the uptake and cellular interaction of a chemotherapeutic drug dependent on various metabolites (e.g. cholesterol).

At least two different laser sources can be used simultaneously, e.g. for fluorescence lifetime imaging (FLIM) or ratio microscopy. Pulsed laser diodes with a nanosecond time delay between one another are used to create a prompt and a delayed fluorescence image on two parts of a time-gated camera. This permits quasi continuous registration of two fluorescence images in a “shake hand” mode and online measurement of fluorescence ratios.

Acknowledgment: This project is funded by the Land Baden-Württemberg and the European Union, Europäischer Fonds für die regionale Entwicklung.

References:

1. J. Huisken, J. Swoger, F. del Bene, J. Wittbrodt, E.H.K. Stelzer, “Optical sectioning deep inside live embryos by SPIM” Science, Vol. 305, pp. 1007–1009 (2004).
2. T. Bruns, S. Schickinger, R. Wittig, H. Schneckenburger, “Preparation strategy and illumination of 3D cell cultures in light-sheet based fluorescence microscopy” J. Biomed. Opt., Vol. 17, 101518 (2012).

Paper B-I-5

LASER-ASSISTED STUDY OF THE INTERACTION OF DIAMOND NANOPARTICLES WITH BLOOD COMPONENTS

A.V. Priezzhev[1], A.E. Lugovtsov[1], V.B. Koshelev[2], O.E. Fadyukova[2], G.M. Naumova[2], Chia-Liang Cheng[3], Yu-Chung Lin[3], E.V. Perevedentseva[3]

[1]Physics Department and International Laser Center of M.V. Lomonosov Moscow State University,
[2]Faculty of Medicine of M.V. Lomonosov Moscow State University,
Russia, 119991, Moscow, Leninskye Gory
[3]Physics Department of National Dong Hwa University, Hualien, Taiwan

avpriezz@gmail.com

In this work, we studied the interaction of nanoparticles of diamond (ND) with blood components and their effect on hemoglobin oxygenation and red blood cell (RBC) microrheology. In particular, we wondered whether the incubation of ND with whole blood sample leads to a distortion of the oxygenation/deoxygenation (O/D) cycle and of the ability of RBCs to deform in shear flow and to spontaneously aggregate. The research was motivated by the fact that the administration of NDs and other nanoparticles into a live organism for diagnostic and therapeutic reasons is usually supposed to be performed intravenously, i.e. via blood vessels. However the possible effects of nanoparticles on blood and on its ability to normally flow though the vessels of different radii are usually not accounted for.

In order to assess the effect of NDs on the O/D cycle, we used single cell Raman microspectroscopy and laser tweezers to trap single RBC. To assess the effect of NDs on RBC microrheology, we used laser technologies based on dynamic light scattering, FTIR, diffractometry of dilute suspensions of RBCs, diffuse light reflectometry of whole blood samples. We have conducted a series of *in vitro* measurements of the deformability index and several parameters of aggregation kinetics, as well as of the adsorption of protein molecules on ND surfaces. In our experiments, we used suspensions of NDs with the sizes of 5 and 100 nm of different concentrations in bidistilled water, added to samples of freshly drawn human and rat blood or protein solutions. The surface of ND particles was either raw or carboxylated (cND) to improve their biocompatibility.

We have found that depending on the size, concentration, surface properties of the particles and, also, on the properties of blood samples of human individuals (healthy donors or patients with various diseases) and rats, the ND and cND show different effects on the microrheologic properties of blood. In particular, blood plasma proteins albumin and globulins are adsorbed on the particle surface. Both ND and cND interact with RBC membrane, which leads to reduction of RBC deformability at higher concentrations of the incubated particles. 5 nm ND can penetrate inside the RBC through the membrane and interact with the hemoglobin molecules. However this interaction does not lead to the impairment of the O/D cycle. The RBC aggregation parameters may be shifted as a result of RBC/ND interaction at higher concentrations of the latter.

The obtained results substantiate our conclusion on the importance of thorough studies of the interaction of nanoparticles with blood components.

Acknowledgements: This work was supported by the RFBR grant 12-02-92008-HHC_a and the NSC grant 97-2923-M-259-001-MY3.

Paper B-I-6

NEW LASER ADAPTIVE TECHNOLOGIES FOR MEDICAL APPLICATION

Andrey V. Belikov

National Research University of Information Technologies, Mechanics & Optics,
49 Kronverksky, Saint-Petersburg, Russia, 197101

meddv@grv.ifmo.ru

Modern laser technologies are widely represented in medicine. Lasers are used successfully for the treatment of soft and hard tissues. Laser influence on tissue is accompanied by different optical, acoustic and thermal effects. These effects are interrelated and depend on the laser radiation parameters and the tissues properties. In the tissues destruction process by laser radiation accompanying effects parameters can be changed following the change in the tissue. In adaptive laser systems analysis of these changes and effective feedback allow to adjust opportunely the laser parameters and to optimize the course of treatment.

In present work we will discuss adaptive laser systems with feedback. We discuss features of registration of thermal signal during laser treatment of soft tissues. Represent results of investigation of laser-tissue interaction with high time resolving. Introduce modern laser technologies with feedback, such as TOP dental surgery [1, 2].

TOP dental surgery – a new method of contact surgery (thermo-optical surgery) based on automatic control of diode laser energy conversion by opto–thermal fiber (OTF) converter into heat energy and polychromatic optical radiation with wavelengths in the range of 1400–11000 nm (thermo-optical feedback). The absorption coefficient of the radiation in the soft tissue is 700–850 cm^{-1}.

In the paper features of the growing and properties of the opto-thermal fiber converters for TOP surgery are discussed. The results of time-resolving video of the growing stages and operating of one variation of the opto–thermal fiber converter are presented. The dynamics of the optical transmittance of laser radiation at wavelength of 970 nm was investigated. The surface temperature dynamics of the converter during its operation at various laser powers was investigated.

The mechanism of work the adaptive diode laser system for top surgery including computer control and maintain the desired temperature of OTF converter in condition of changes in cutting speed and tissues properties was described. The results of time-resolving video of dynamics of soft tissue destruction by laser radiation with and without thermo–optical feedback are presented. It was shown that the depth of the cut and coagulation weakly depended on the speed of soft tissue cutting during using a powerful adaptive diode laser with thermo-optical feedback.

References:

1. K.S. Magid, A.V. Belikov, A.E. Pushkareva, A.V. Skrypnik, F.I. Feldchtein, T.V. Strunina, et al. “Soft tissue surgery with thermo-optical tips with a real-time temperature control” ALD 2010 Annual Meeting. Miami FL: Academy of Laser Dentistry (2010).
2. G.B. Altschuler, “Thermo-Optically Powered (TOP) Surgery: A New Opportunity for the Dental Practice”, ALD 2012 Annual Meeting. Scottsdale, AZ: Academy of Laser Dentistry (2012).

Paper B-I-7

FEMTONEWTON MAGNETIC INTERACTION BETWEEN BROWNIAN PARTICLES PROBED BY ACTIVE MICROREOLOGY IN OPTICAL TWEEZERS

M.N. Skryabina, M.D. Khokhlova, E.V. Lyubin, A.A. Fedyanin

Faculty of Physics, Lomonosov Moscow State University, Moscow 119991, Russia

fedyanin@nanolab.phys.msu.ru

Brownian motion is the driving force in the wide class of biological, chemical and physical processes, such as organelles diffusion in living cells, dynamics of DNA supercoils and colloidal crystallization. Interaction between Brownian microparticles plays a key role in the collective dynamics and can be the reason of the disorder-to-order transition of the soft matter system. It governs such amazing processes as synchronizations of Brownian particles motion, self-organizations to the complex structures of particles and even macromolecules. Furthermore the interaction between Brownian particles define many common colloidal phenomena, such as rheological properties of suspensions, the kinetics of aggregation and phase separation. Recently a new method to study viscoelastisity of the red blood cell (RBC) membrane was proposed by attaching a functionalized ferrimagnetic microbead to the RBC membrane and exposing the system in the ac-magnetic field. The magnetic bead's motion caused the deformation of the membrane and elastic and frictional moduli were extracted from optically tracked bead motion. However the only method having the ability for ultrafine positioning, control and noninvasive probing of local object properties in aqueous solution having no impact from the bulk substrate is the optical tweezers technique which is a unique tool for exploring problems related to quantitative characterization of single objects at the microscale. This method is widely used to determine the elastic properties of cell membranes, in particular the RBC membranes.

Two main sets of experiments will be discussed [1, 2]. The first one is use of optical tweezers for studying the magnetic interaction force between two individual superparamagnetic microparticles which is directly measured as functions of particles separations and external magnetic field value. The influence of these forces on the particles Brownian motion is experimentally found and theoretically analyzed. It is shown that the gradient of the interaction forces affects on the particles coupling and defines the crosscorrelations in the particles positions fluctuations. Another problem discussed is active rheology combined with an analysis of forced RBC vibration when the cell is optically trapped in double optical tweezers. This approach allows marking out correlated displacements of trapped erythrocyte edges. The displacements determined using forced vibrations analysis in the frequency range up to 1 kHz quantitatively characterizes the viscoelastic properties of individual RBC. A new dynamic parameter, namely, the tangent of phase difference in the movement of the erythrocyte edges, is introduced as an effective finger-print characterizing the state of the cell.

References:

1. M.N. Skryabina, E.V. Lyubin, M.D. Khokhlova, A.A. Fedyanin, "Probing of pair interaction of magnetic microparticles with optical tweezers", JETP Lett., Vol. 95, p. 560 (2012).
2. E.V. Lyubin, M.D. Khokhlova, M.N. Skryabina, A.A. Fedyanin, "Cellular viscoelasticity probed by active rheology in optical tweezers" J. Biomed. Opt., Vol. 17, 101510 (2012).

Paper B-I-8

OPTICAL COHERENCE ELASTOGRAPHY OF SOFT TISSUES

Kirill V. Larin

Department of Biomedical Engineering, University of Houston, 4800 Calhoun Rd, Houston, Texas, USA

klarin@uh.edu

Mechanical forces play an important role in the behavior and development at all spatial scales, from cells and their constituents, to tissues and organs. Such forces have a profound influence on the health, structural integrity, and normal function of cells and organs. Accurate determination of tissue biomechanical properties (e.g., Young's or shear modulus) could help with clinical diagnosis and interpretation of various diseases.

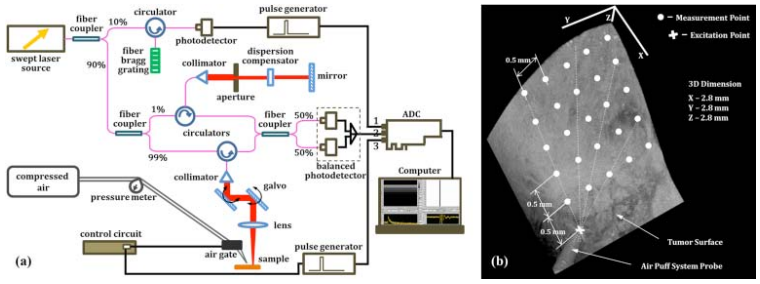

Fig. 1. (a) Schematic of AP-OCT system; (b) OCT 3-D image indicating the distribution of excitation and measurement positions across tissue surface.

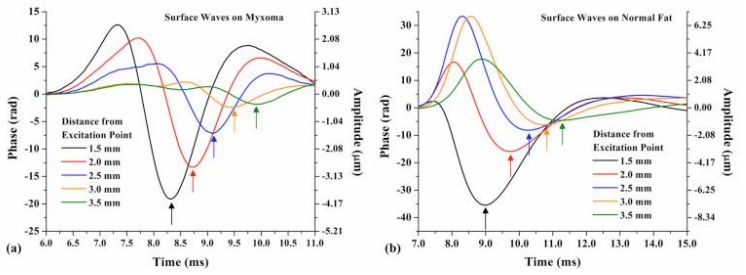

Fig. 2. (a) Surface waves recorded at different spatial locations showing time delays detected on (a) myxoma and (b) normal fat.

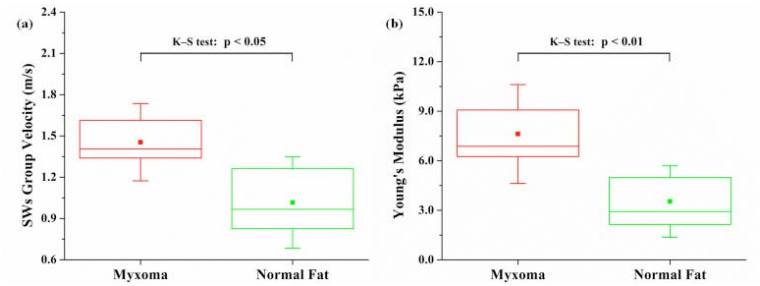

Fig. 3. Box plots of (a) the calculated group velocity of SWs and (b) the quantified Young's moduli for myxoma and normal fat. The solid dots and whiskers represent the mean values and standard deviations of data, respectively.

Optical Coherence Elastography (OCE) is an emerging tool that allows noninvasive assessment of tissue biomechanical properties with high lateral and axial resolution. In this talk I'll overview recent advances on developments and application of optical methods to assess mechanical properties of different tissues and show examples of the current state-ofthe-art optical elastography imaging of tissues, including tumors and ocular tissues. Particularly, I'll demonstrate the capability of OCE to assess surface mechanical wave propagation in phantoms and soft tissues both *ex vivo* and *in vivo* using a Phase Stabilized Swept Source Optical Coherence Elastography (PhS-SSOCE) system (Fig. 1). Low-amplitude (<10 μm) mechanical waves were introduced by focused air puff excitation on tissue surface. The tissue of myxoma, a type of soft-tissue tumor, turns out to have higher velocity of SWs propagation than the normal fat, which can be seen from Fig. 2. The SWs group velocity is calculated to be 1.45±0.28 m/s and 1.02±0.33 m/s for myxoma and normal fat, respectively. Also, we quantified a higher Young's modulus of 7.6±3.0 kPa for myxoma compared with 3.5±2.2 kPa for normal fat (see Fig. 3). These results demonstrate the OCE system can be useful for the intra-operative detection of soft tissue tumors based on the measurement of their elastic properties.

Acknowledgements: We acknowledge the funding from NIH grant 1R01EY022362 and Federal Target Program "Scientific and Scientific-Pedagogical Personnel of Innovative Russia" for 2009–2013 Grant 14.B37.21.1238.

Paper B-I-9

COHERENT ANTI-STOKES RAMAN SPECTROSCOPY AND 3D IMAGING FOR BIOLOGICAL AND MEDICAL RESEARCH

Y.F. Lu[1], X.N. He[1], P.N. Black[2], T. Baldacchini[1,3], X. Huang[1], L. Jiang[4]

[1]*Department of Electrical Engineering, University of Nebraska-Lincoln, Lincoln, NE 68588-0511*
[2]*Department of Biochemistry, University of Nebraska-Lincoln, Lincoln, NE 68588-0664*
[3]*Technology and Applications Center, Newport Corporation, Irvine, CA 92606*
[4]*Department of Mechanical and Automation Engineering, Beijing Institute of Technology, Beijing, 100081, P. R. China*

ylu2@unl.edu

Broadband coherent anti-Stokes Raman spectroscopy (CARS) and microscopy system based on a photonic crystal fiber light source has been used to study biological and medical samples. The pump pulses have a narrow bandwidth and define the spectral resolution. The Stokes pulses are spectrally broad in 700–1100 nm. The pump and Stokes pulses excite multiple Raman transitions within the bandwidth of the Stokes pulses. Vibrationally excited states are probed with a third spectrally narrow probe pulse, usually the same as the pump pulse. In a single shot, the entire CARS spectrum of the excited states is generated. Both the pump and Stokes beams are provided by a single fs laser in conjunction with a supercontinuum generator, which is optimized for performing broadband CARS microscopy. The supercontinuum ensures that broadband anti-Stokes spectra can be obtained without tuning the laser wavelength. The structure of the CARS system is shown in Fig. 1. The CARS system has been used to obtain CARS spectra and chemically specific images of biological (such as algal cells) and medical (such as neuro, artery, and liver cells) samples.

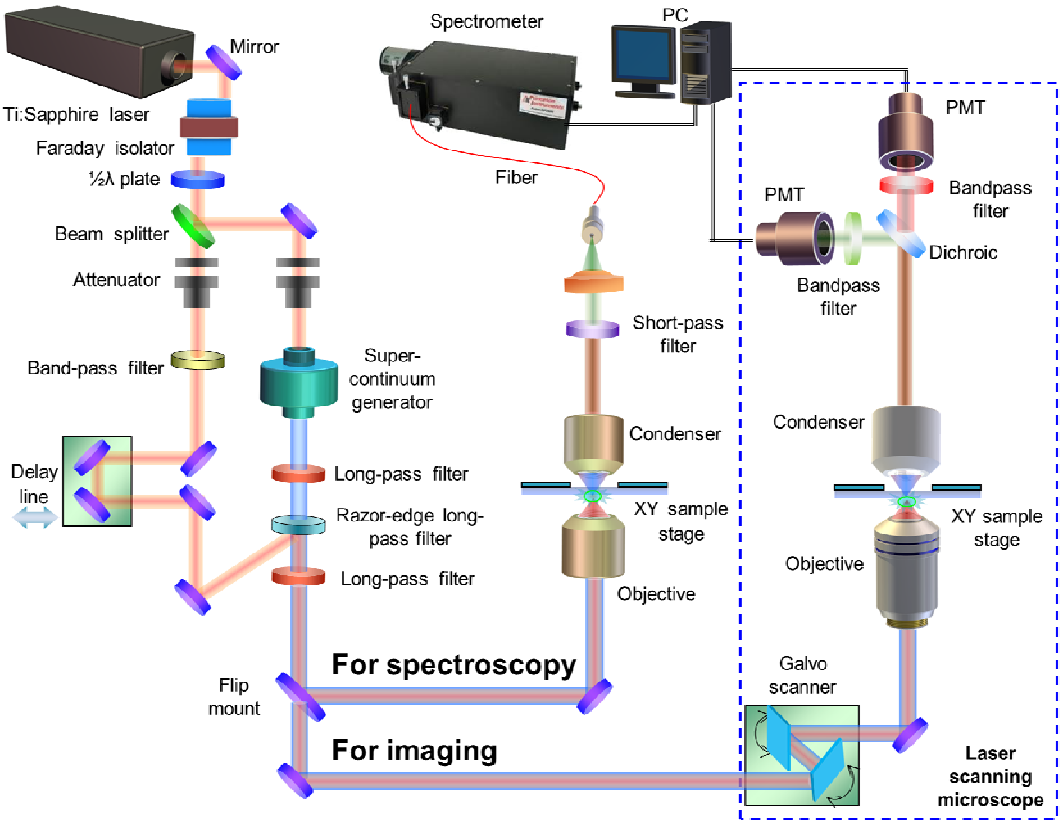

Figure 1. Schematic setup of the broadband forward CARS spectroscopy and microscopy system.

Paper B-I-10

LASER-INDUCED FLUORESCENCE SPECTROSCOPY FOR CLINICAL APPLICATION

Natalia Bulgakova

A.M. Prokhorov General Physics Institute of the R A S, Moscow, Russia

nnbulgakova@gmail.com

Laser-induced fluorescence spectroscopy (LIFS) is a sensitive technique that allows to measure tissue fluorescence emission spectra using a fiber-optic probe scanning in contact with the tissue surface. The main advantage of LIFS is noninvasive real-time collecting of quantitative information on the intensity and spectral features of the endogenous or exogenous tissue fluorescence emission which could be used for diagnostical or therapeutical purposes.

Our long term cooperation with the leading medical institutes shown that the most promising direction of LIFS application is the autofluorescence detection of cancer. We performed a comparative study of basic characteristics of autofluorescence emission spectra recorded from normal and pathological tissues in vivo. The statistical analysis and probabilistic estimations of nine basic quantitative characteristics were performed to reveal the spectral characteristics which may have potential to improve the detection accuracy of autofluorsecence diagnosis of early stage cancer. The different approaches for in vivo attributing the tested tissue to one of the histological status on the base of estimated spectral characteristics have been tested [1, 2]. As a result the complex of diagnostically informative spectral characteristics have been proposed which may maximize the autofluorescence contrast between normal mucosa and malignancy. Real time measurements and estimation of the important spectral information on the base of the probabilistic approach is assumed to be useful for real-time recommendation about biopsies and for minimizing a number of false-positive results of auto fluorescence detection of cancer.

The report presents the main results of in vivo LIFS clinical application obtained during last years in this field.

Acknowledgements: The work was supported partly by RFBR Grant No. 09-02-01204.

References:

1. N. Bulgakova, R. Ulijanov, K. Vereschagina, et al. “In vivo local fluorescence spectroscopy in PDD of superficial bladder cancer” Medical Laser Application, Vol. 24, pp.247–255 (2009).
2. N. Bulgakova, V. Sokolov, L. Telegina, et al. “Study of laser-induced autofluorescence emission spectra from normal and malignant bronchial epithelium” Photon Lasers Med., Vol. 2(2), pp. 93–99 (2013).

Paper B-I-11

ADVANCES IN TISSUE AND BLOOD OPTICAL CLEARING FOR LASER DIAGNOSTICS AND TREATMENT

Valery V. Tuchin

Research-Educational Institute of Optics and Biophotonics, Saratov State University, Saratov, 410012, Russia
Institute of Precise Mechanics and Control RAS, Saratov, 410028, Russia
Optoelectronics and Measurement Techniques Laboratory, P.O. Box 4500, Department of Electrical Engineering, University of Oulu, FIN-90014, Oulu, Finland

tuchinvv@mail.ru

The main limitations for laser-tissue interaction at application to laser diagnostics or treatment are the low penetration depth of laser beam, its random divergence, and low image contrast caused by high light scattering by tissues and blood. Doppler and speckle blood flow measuring techniques, optical coherence tomography (OCT), confocal microscopy, SHG imaging, multi-photon spectroscopy, polarization imaging, and Raman spectroscopy are strongly suffering from light scattering. Optical clearing due to reduction of tissue scattering ability is an attractive method for controlling of optical properties of a variety of tissues and blood. It provides many benefits for successful application of laser methods in biomedicine [1–4]. One of the optical clearing approaches is based on impregnation of tissue by an immersion liquid which refractive index is higher than refractive index of interstitial fluid (ISF) and/or tissue dehydration (losing water) another one is based on tissue compression or stretching.

In this paper optical clearing of different tissues will be analyzed in the framework of receiving of more precise and valuable information from reflectance spectroscopy, polarization measurements, optical coherence tomography (OCT), and full-field speckle imaging of blood microcirculation. *In vitro*, *ex vivo*, and *in vivo* spectroscopic, polarization, and OCT studies of human tissues and blood will be presented. Optical clearing agents and delivery techniques, as well as tissue enhanced permeation due to tissue compression, will be discussed. Some important applications of optical immersion and compression techniques in dermatology, ophthalmology, gastroenterology, and some other medical fields will be demonstrated. Optical clearing induced by metabolic processes and photothermal and photodynamic action on tissues will be discussed.

References:

1. V.V. Tuchin, Optical Clearing of Tissues and Blood, PM 154, SPIE Press, Bellingham, WA, 2006.
2. V.V. Tuchin, “A clear vision for laser diagnostics” IEEE J. Select. Topics on Quantum Electron., Vol. 13(6), pp. 1621–1628 (2007).
3. E.A. Genina, A.N. Bashkatov, V.V. Tuchin, “Tissue optical immersion clearing” Expert Rev. Med. Devices, Vol. 7(6), pp. 825–842 (2010).
4. K.V. Larin, M.G. Ghosn, A.N. Bashkatov, E.A. Genina, N.A. Trunina, V.V. Tuchin, “Optical clearing for OCT image enhancement and in-depth monitoring of molecular diffusion” IEEE J. Select. Topics on Quantum Electron., Vol. 18(3), pp. 1244–1259 (2012).
5. D. Zhu, K.V. Larin, Q. Luo, V.V. Tuchin, “Recent progress in tissue optical clearing” Laser Photon. Rev., 1–26 (2013) / DOI 10.1002/lpor.201200056.
6. O. Zhernovaya, V.V. Tuchin, M.J. Leahy, “Blood optical clearing study by optical coherence tomography” J. Biomed. Opt., Vol. 18(2), 026014-1–8 (2013).

Paper B-I-12

FLUORESCENT AND PHOTOACOUSTIC SMALL-ANIMAL IMAGING

Ilya Turchin[1,2], Pavel Subochev[1], Ilya Fiks[1], Mikhail Kleshnin[1],
Marina Shirmanova[2], Irina Balalaeva[3], Anna Orlova[1], Vladislav Kamensky[1,2]

[1]*Institute of Applied Physics of the Russian Academy of Sciences, 46 Ulyanov St., Nizhny Novgorod 603950, Russia*
[2]*Nizhny Novgorod State Medical Academy, Minin sq., 10/1, Nizhny Novgorod 603005, Russia*
[3]*University of Nizhny Novgorod, Prospekt Gagarina, 23, Nizhny Novgorod 603950, Russia*

ilya@ufp.appl.sci-nnov.ru

We present the results of fluorescent and photoacoustic imaging of small-animals with experimental tumors. For fluorescence small-animal imaging we created a multifunctional system which combines planar epi-illumination and trans-illumination geometries. We have demonstrated that the created system allows obtaining 2D fluorescent images for estimating the cross-sectional size of the superficial fluorescent objects and deep seated fluorescing inclusion by using trans-illumination imaging even in the case of low fluorescent intensity.

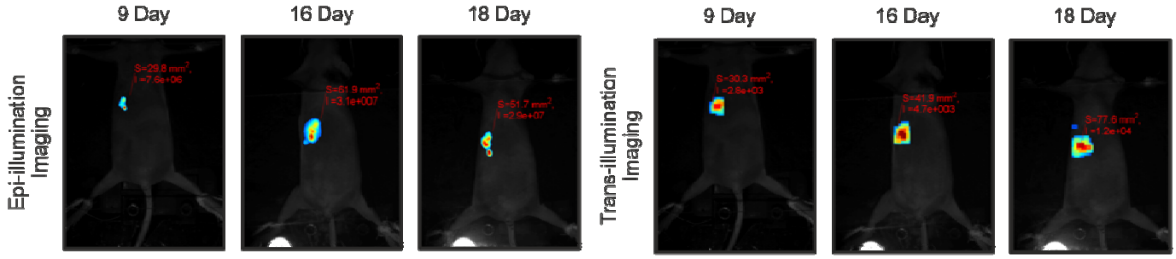

We also have shown that for high fluorescence signal the developed system provides 3D reconstruction of the fluorophore spatial distribution [1]. For the photoacoustic measurements we created an experimental setup which combines photoacoustic (PA) and optically mediated ultrasound (US) microscopy [2]. The probing US pulses were generated thermoelastically due to absorption of backscattered laser radiation by the metalized surface of a PVDF film. We achieved 70/45 μm transverse/longitudal resolution in US mode and 70/45 μm transverse/longitudal resolution in PA mode.

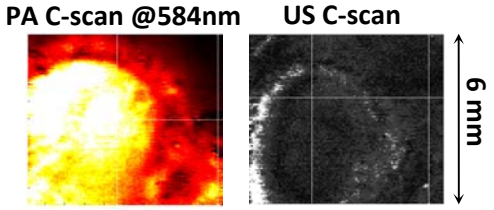

In this presentation we will demonstrate our first results validating simultaneous PA/US microscopy technique for in vivo imaging of experimental tumors in small-animals.

Acknowledgements: The work was supported by the by the Ministry of Education and Science of the Russian Federation (project # 14.512.11.0053), the Russian Foundation for Basic Research (projects #12-02-31361, 13-02-01289) and the Measures to Attract Leading Scientists to Russian Educational Institutions program (project no 11.G34.31.0017).

References:

1. M.S. Kleshnin, I.V. Turchin, “Fluorescence diffuse tomography technique with autofluorescence removal based on dispersion of biotissue optical properties” Laser Phys. Lett., Vol. 10, 075601 (2013).
2. P. Subochev, A. Katichev, A. Morozov, A. Orlova, V. Kamensky, I. Turchin, “Simultaneous photoacoustic and optically mediated ultrasound microscopy: Phantom study“ Opt. Lett., Vol. 37(22), pp. 4606–4608 (2012).

Paper B-I-13

NEW APPROACH FOR PHOTODYNAMIC THERAPY BASED ON THE GENETICALLY ENCODED PHOTOSENSITIZERS

E.V. Zagaynova[1], M V. Shirmanova[1], E O. Serebrovskaya[2], K A. Lukyanov[2], A. P. Ryumina[2], L. B. Snopova[1], I. V. Turchin[4,1], S. A. Lukyanov[1,2]

[1]Nizhny Novgorod State Medical Academy, Minin Sq, 10/1, Nizhny Novgorod 603005, Russia
[2]Shemyakin-Ovchinnikov Institute of Bioorganic Chemistry RAS, Miklukho-Maklaya St., 16/10, Moscow 117997, Russia
[3]Lobachevsky State University of Nizhny Novgorod, Gagarin Ave. 23, Nizhny Novgorod 603950, Russia
[4]Institute of Applied Physics RAS, Ulyanov St. 46, Nizhny Novgorod 603950, Russia

ezagaynova@gmail.com

Genetically encoded photosensitizers are a recently introduced optogenetic tool enabling local ROS production mediated by a fluorescent protein [1]. The first such protein was red fluorescent protein KillerRed capable of ROS production under exposure to green-orange (~520–590 nm) light [2].Recent studies showed that KillerRed is type I photosensitizer, which produces radicals and hydrogen peroxide but not singlet oxygen [3].

Then, it was demonstrated that light-oxygen-voltage–sensing (LOV) domains from bacterial and plant species can be mutated to generate flavin mononucleotide (FMN)–based fluorescent proteins [3]. Using this strategy, a protein that efficiently generates ROS on exposure to blue light was developed [3]. This protein called miniSOG (mini Singlet Oxygen Generator) was engineered from *Arabidopsis* phototropin 2.

The goal of this work is to evaluate the applicability of the phototoxic proteins KillerRed and miniSOG for PDT of tumors *in vivo*. The study was performed on subcutaneous HeLa tumor xenografts in nude mice using the cell lines stably expressing KillerRed and miniSOG in different cell compartments. *In vivo* fluorescence imaging was used throughout the selection of the treatment mode to assess photobleaching of the proteins. The tumors were exposed to laser irradiation at two regimens and examined pathomorphologically.

The results of the fluorescence imaging of the HeLa tumors producing KillerRed demonstrate 30% decrease of the intensity for 30 min at a power density 150 mW/cm^2 without heating. Irradiation with higher powers (225 and 300 mW/cm^2) resulted in more effective photobleaching but caused temperature growth (up to 37 and 41°C degrees respectively). Histological analysis of the treated tumors with KillerRed in mitochondria and nuclei and nuclei alone showed significant dystrophic changes in the tissue structure, such as nucleus swelling, cytoplasm vacuolization, cellular and nuclear membrane destruction, and activation of apoptosis.

Tumors expressing miniSOG were hardly distinguished from surrounding tissues on the fluorescence images *in vivo* due to strong skin autofluorescence in blue-and-green spectrum range. Nevertheless, considerable drop of fluorescence was revealed in the extracted specimens of the irradiated tumors. However, no difference between treated and untreated tumors was found either in pathomorphology or growth, which most likely related to the lack of FMN in poorly vascularized HeLa tumors.

Genetic encoding of the photosensitizer in a cancer cell seems very attractive for the promise of highly selective cellular photodamage. The first results in animals show the possibility to induce irreversible cell abnormalities using PDT with phototoxic proteins.

Acknowledgements: This work was supported by the Ministry of Education and Science of the Russian Federation (project 11.G34.31.0017, contracts # 8303, 8269).

References:

1. K.A. Lukyanov, E.O. Serebrovskaya, S. Lukyanov, D.M. Chudakov, “Fluorescent proteins as light-inducible photochemical partners” Photochem. Photobiol. Sci., Vol. 9, pp. 1301–1306 (2010).
2. M.E. Bulina, D.M. Chudakov, O.V. Britanova, et al. “A genetically encoded photosensitizer” Nat. Biotechnol., Vol. 24, pp. 95–99 (2006).
3. X. Shu, V. Lev-Ram, T.J. Deerinck, et al. “A genetically encoded tag for correlated light and electron microscopy of intact cells, tissues, and organisms” PLoS Biol., Vol. 9, e1001041 (2011).

Paper B-O-1

OPTIMIZING THE PHOTO-INDUCED MECHANISMS OF LIGHT INTERACTION WITH SOFT BIOTISSUES FOR LIGHT-THERAPY PURPOSES

Vladimir V. Barun[1,2], Arkady P. Ivanov[1]

[1]*B. I. Stepanov Institute of Physics, Belarus National Academy of Sciences, 68 Skaryna Pr., 220072 Minsk, Belarus*

[2]*Belarus State University of Informatics and Radioelectronics, 6 Brovka str., 220013 Minsk, Belarus*

barun@dragon.bas-net.by

This paper considers three mechanisms of light interaction with tissues, namely the photodynamic (PDE) and light-oxygen effects (LOE) as well as the photodissociation of blood oxyhemoglobin (PBO). All these mechanisms are or can be used in different kinds of light therapy treatments of a human organism. Their efficiencies are proportional to the light power absorbed by a target chromophore in tissue. These targets are, respectively, dissolved molecular oxygen for the light-oxygen mechanism, a photosensitizer for the photodynamic action, and oxyhemoglobin for the photodissociation. The goal of this paper is to maximize the absorbed light power by a suitable choice of a wavelength irradiating the skin surface. In succeeding so, one can optimize the non-invasive light therapy procedures. In other words, the desired maximization will enable one to utilize less irradiation power for achieving the same therapeutic effect or to achieve more positive effect for the same irradiation power. The idea of the optimization is rather simple. Really, optical properties of soft biotissues, especially their absorption coefficients, are spectrally selective, so that the tissue acts as a spectral filter with complex transmittance. The light power absorbed by a target chromophore at specific depth is proportional to the product of the fluence rate at this depth by the absorption coefficient of the chromophore. By varying the irradiation wavelength, one can change the filter transmittance and, hence, the fluence rate to maximize the said product. It is obvious that the optimal wavelength does not necessarily coincide with the maximum of the absorption coefficient.

A review of the author-designed methods for enhancing the absorbed light power is given in the presentation. For the PDE with using photosensitizer (PS) “Fotolon”, the optimal irradiation wavelength is shown [1] should be shifted to the red by 5 to 30 nm with respect the maximal PS absorption at 665 nm. The gain in the absorbed power can be up to 2 and more times. For the LOE near 586 nm [2], the irradiation at a wavelength shifted to the red by 5 to 8 nm provides the 3- of 4-fold increased singlet oxygen concentration generated in deep dermis layers. For the PBO, two cases are considered. The first one is the local O_2 formation at a specific depth. The more the depth is, the longer irradiation wavelength provides the maximal O_2 concentration, starting from 418 nm for upper dermis layers to 600 nm at depth larger than 2.5 mm [3]. For the optimal O_2 generation in the whole dermis thickness, one should irradiate the skin surface at 575±5 nm [4].

References:

1. V.V. Barun, A.P. Ivanov, et al. “Method for Photodynamic Therapy of Oncologic Diseases” Patent No. 2438733 (RU) (2012).
2. V.V. Barun, A.P. Ivanov, S.D. Zakharov “Method for irradiation of skin surface and deep dermis layers under laser therapy” Patent Appl. No. a 20101717 (BY) (2010).
3. V.V. Barun, A.P. Ivanov, V.V. Tuchin, et al. “Method for local enhancement of molecular oxygen concentration in skin dermis” Patent Appl. No. 2011131602 (RU) (2011).
4. V.V. Barun, A.P. Ivanov, V.V. Tuchin et al. “Method for enhancement of molecular oxygen concentration in dermis of skin tissue” Patent Appl. No. 2011131640 (RU) (2011).

Paper B-O-2

LIGHT SCATTERING IN INVESTIGATION OF INTERACTION CHARGE MACROMOLECULES ENZYMES AND SOME METALS

K.V. Fedorova, M.A. Gurova, Zhang Xiaolei, G.P. Petrova

M.V. Lomonosov State University, Moscow, Russia

fedorova@physics.msu.ru

The toxic affect of heavy metals over the living organisms is known to arouse from the alternation of the course for biological reactions in cells. One of such violations appears to be the process of supramolecular structures formation, for example, the dipole protein nano-clusters in blood. This phenomenon can be well studied in the biological solutions, such as blood serum, or a widely adopted normal saline solution of enzymes.

Thus the important role in categorize heavy metals is played by following conditions: their high toxicity for live organisms in rather low concentration, and also ability to bioaccumulation. Almost all heavy metals, actively participate in biological processes, are a part some enzymes.

In this work was studied the effect of ions some metals (K^+, Na^+, Pb^{2+}, Fe^{3+}, Eu^{3+}) on enzymes (pepsin, collagenase, lyzosume, creatine kinase) in water solutions by different optical methods.

The results of our experiments has shown that charged macromolecules dynamic properties and radii of formed scattering particles in solutions essentially depend on net charge condition of enzymes and can be used for diagnostics and control.

Interaction of some proteins and enzymes carrying surface charges in solutions containing heavy metal ions results in the formation of large (nano sized) protein clusters. It was observed that the process of nano cluster formation begins at very low concentrations of heavy metal ions about PMC (maximum permission concentrations). That can explain their high toxicity for live organisms in rather low concentration and poisoning effect on enzymes and proteins.

The interaction of the metal ions with the charged surface of the enzyme in the solution is studied by the measurement of the light scattering coefficient, coefficient of translation diffusion along with the concentration variation of the former.

The nature of interaction enzyme macromolecules in case when the solution contains metal ions with a large ionic radius depends largely on dipole-dipole forces. Enzyme molecules may come extremely closely to one another to form a macromolecular complex-a dipole cluster

The nano-sized clusters form as a result of the phase transition when the Coulomb repulsion forces diminish and the pure dipole attraction forces take over.

The mass and radius of enzyme clusters forming in the solution increases by more than one order of magnitude as compared to the mass of a macromolecule and reaches its maximum near the isoelectric point of enzyme.

Cluster formation process can explain toxic influence of heavy metal ions at the very small concentration on the living organisms.

References:

1. W.L. Hubbell, H.M. McConnell, J. Am. Chem. Soc., Vol. 93, p. 314 (1971).
2. P. Debye, “Light scattering in solutions” J. Appl. Phys., Vol. 15, pp. 338–349 (1944).
3. G.P. Petrova, Yu.M. Petrusevich, D.I. Ten, Quantum Electron., Vol. 32, No. 10, p. 1–5 (2002).
4. G.P. Petrova, M.S. Ivanova, I.A. Sergeeva, T.N. Tichonova, K.V. Fedorova, “Diffusion processes in proteins and enzymes water solutions containing toxic heavy metals and visualization of appearing dipole nano structures by atomic force microscopy (AFM)”, PSFVIP-8 (Moscow, Russia, MSU, 21–25 August 2011), Proc. 8PSFVIP-117.

Paper B-O-3

SINGLET OXYGEN GENERATION BY METAL PHTHALOCYANINES ON THE NANOPARTICLES SURFACE

A.V. Ryabova[1], D.V. Pominova[1], A.I. Klimov[2], E.A. Luk'yanets[3], O.L. Kaliya[3], V.B. Loschenov[1]

[1]Prokhorov General Physics Institute RAS, Vavilova str. 38, Moscow 119991 , Russia
[2]Chemical Faculty of Lomonosov Moscow State University, Vorob'evy gory, 1-3, Moscow 119991, Russia
[3]State Scientific Center "Institute of Organic Intermediates and Dyes", Sadovaya str. 1-4, Moscow 123995, Russia

nastya.ryabova@gmail.com

Photodynamic therapy based on the use of the combination a photosensitizing drugs (PS), oxygen and light, can selectively damage the target tissue. To increase the generation of $^1O_2$ by PS at molecular oxygen physiological concentrations can be increased by placing the molecule of PS in close proximity of metal nanoparticles (Me-NPs) due to plasmon-induced increase of the triplet state transition oscillator strength [1]. The investigation of Me-NPs and PS combination properties initiated just recently, however, the possibility of creating NPs with enhanced antibacterial [2], and photodynamic effect [3] are shown. This paper presents the study of the $^1O_2$ generation by Al and Zn phthalocyanines (MePhc) and $^1O_2$ chemical quenching near the surface of silver, gold, iron oxide and silicon nanoparticles (NPs). The analysis of the MePhc behavior in aqueous solutions in comparison with MePhc precipitated (molecules adsorption due to Van-der-Waals force or electrostatic interactions) and conjugated (chemical covalent attaching the) on the surface of NPs was performed.

The definition of $^1O_2$ formation quantum yield ($\varphi\Delta$) by MePhc was carried out using a $^1O_2$ trap, ADMA [4]. For determining of the $^1O_2$ chemical quenching during irradiation was used previously developed in our laboratory spectroscopic method of oxygen content in the bioobject measuring by the hemoglobin oxygenation degree [5]. It is established that the studied NPs taken separately from MePhc have no photodynamic effect. Upon binding to the surface of NPs the MePhc absorption intensity is decreases, indicating that the additional dipole interaction between the NPs and the plane of the phthalocyanine ring is exist. Presumably, the MePhc molecules, adsorbed on the NPs surface and not involved in the light absorption, should not be involved in the $^1O_2$ generation.

For iron oxide and silicon NPs the MePhc photodynamic activity is decreased, probably due to too strong bounding with the surface of NPs, as well as absorption is decreased. However, the quantity of chemical quenching acts of $^1O_2$, generated by MePhc, bounding with MeNPs, was significantly higher in comparison with MePhc simple solutions.

Acknowledgements: This work was partially supported by the RFBR Grant № 12-02-12080-ofi-m.

References:

1. C. Geddes, K. Aslan, et al. "Noble metal nanostructures for metal-enhanced fluorescence", In: Review chapter for annual reviews in fluorescence (Plenum, NY, USA, 2004), p. 365.
2. N. Masilela, T. Nyokong, "The interaction of silver nanoparticles with low symmetry cysteinyl metallophthalocyanines and their antimicrobial effect" J. Photochem. Photobiol. A: Chemistry, Vol. 255, pp. 1–9 (2013).
3. L. de Melo, A. Gomes, S. Saska, at al. "Singlet oxygen generation enhanced by silver-pectin nanoparticles" J. Fluoresc. DOI 10.1007/s10895-012-1107-4 (2012).
4. N. Kuznetsova, N. Gretsova, O. Yuzhakova, at al. "New reagents for determination of the quantum yild in aqueous solutions" Russ. J. Gen Chem., Vol. 71, pp. 36–41 (2001).
5. A. Ryabova, A. Stratonnikov, V. Loschenov, "Laser spectroscopy technique for estimating the efficiency of photosensitisers in biological media" Quantum Electron., Vol. 36(6), pp. 562–568 (2006).

Paper B-O-4

RAMAN SPECTROSCOPY OF LUNG CANCER

Valery P. Zakharov[1], Ivan A. Bratchenko1, Oleg O. Myakinin[1], Dmitry V. Artemyev[1], Julia A. Khristophorova[1], Sergey V. Kozlov[2], Aleksandr A. Moryatov[2]

[1]*Radioengineering Department, Samara State Aerospace University, Moskovskoe Shosse 34, Samara 443086, Russia*

[2]*Samara Clinical Oncological Dispensary, Solnechnaya str. 50, Samara 443031, Russia*

zakharov@ssau.ru

Today in medicine acute problem of accurate cancer diagnosis. This problem takes into account lung tissues and lung tumors. The main problem in cancer detection is to determine exact tumor type. If malignant tumor was studied, than medicine stuff should provide appropriate treatment, otherwise healthy tissue was studied and no further treatment is needed. It is important to say that if malignant tumor is not treated appropriately or was missed by doctor as a healthy, it can lead to the patient's death. That's why it is very important to provide precise diagnose of cancerous tumors.

Fast and noninvasive diagnosis of human lung tissues is possible with usage of Raman spectroscopy (RS). This type of spectroscopy is very sensitive and can detect even the slightest changes of chemical composition that occur in tumors during growth.

RS system used in current experimental study contained Shamrock sr-303i spectrometer with DV420A-OE digital camera, RPB785 RS probe and LuxxMaster Raman Boxx laser (785nm, 200–300 mW).

Raman spectrums from different lung tissues (including healthy tissue, malignant and nonmalignant tumors) were used to identify the main chemical components of formations. Subsequent allocation of formations characteristics based on the Raman peaks intensities was performed. More than 30 human tissue samples were tested in this study *ex vivo* to determine if lung tumors diagnosis is possible with RS. This research was approved by the ethical committee of SEI HPE Samara State Medical University of Russian Health Ministry. For each tissue sample histological analysis for precise diagnosis was carried out.

It was found that different lung tissues have unique composition of intensities related to the lipid-specific and proteins bands peaks. Analysis of peaks features observed in the Raman spectrums resulted in the identification criteria for specificity determination of tumors in the healthy lung tissues. In the result it was fond that RS based diagnosis of lung tissues and tumors is more accurate than firs stage medicine stuff diagnosis.

Acknowledgements: This research was supported by the Federal Target Program "Research and development on priority directions of Russian scientific-technological complex for 2007-2013".

Paper B-O-5

SKIN CANCER DIAGNOSIS BY RAMAN SPECTROSCOPY AND OPTICAL COHERENCE TOMOGRAPHY

Ivan A. Bratchenko[1], Valery P. Zakharov[1], Oleg O. Myakinin[1], Dmitry V. Artemyev[1], Julia A. Khristophorova[1], Sergey V. Kozlov[2], Aleksandr A. Moryatov[2]

[1]*Radioengineering Department, Samara State Aerospace University, Moskovskoe Shosse 34, Samara 443086, Russia*

[2]*Samara Clinical Oncological Dispensary, Solnechnaya str. 50, Samara 443031, Russia*

ud_liche@mail.ru

Nowadays medical staff notes an increase number of different skin lesions appearing including benign and cancerous tumors. Optimal approach of these disease treatments requires precise determination of invasion borders in healthy skin and noninvasive disease specificity estimation. This requirement may be satisfied by using optical techniques. In this study we demonstrate joint usage of optical coherence tomography (OCT) and Raman spectroscopy (RS) for in vivo and ex vivo skin tumors diagnosis.

OCT setup was performed on the basis of a broadband superluminescent laser diode (840 ± 25 nm) at the source end, Michelson interferometer with 50/50 split ratio to the sample and reference arms, spectrometer with diffraction grating (1200 gr/mm) and CCD line scan camera (2048 pix, 29.3 kHz) at the detection end. OCT system allowed real-time obtaining of healthy skin and pathologies 3D images. Herewith OCT image resolution was 6–8 micrometers that let one accurately determine the invasion area and respectively a resection zone. RS system contained Shamrock sr-303i spectrometer with DV420A-OE digital camera, RPB785 RS probe and LuxxMaster Raman Boxx laser (785nm, 200–300 mW).

Raman spectrums from different tissues: melanoma, basal cell carcinoma, pigment nevi, keratosis, normal skin, were used to identify the main chemical components of formations. Subsequent allocation of formations characteristics based on the Raman peaks intensities was performed. More than 50 tissue samples were tested in this study by joint usage of OCT and RS for *in vivo* and *ex vivo* skin tumors diagnosis. This research was approved by the ethical committee of SEI HPE Samara State Medical University of Russian Health Ministry. For each tissue sample histological analysis for precise diagnosis was carried out.

It was found that different skin formations have unique composition of intensities related to the lipid-specific and amide I proteins bands peaks near 1270, 1310, 1459 and 1657 cm^{-1}. Analysis of peaks features observed in the Raman spectrum resulted in the identification criteria for specificity determination of tumors in the healthy skin. In melanoma diagnosis accuracy of developed method was 94.8%, and for the of basal cell carcinoma determination – 96%. These results are consistent with results of other authors, such as melanoma diagnostic accuracy in [1] was 87.5%, and in [2] was 92%.

Acknowledgements: This research was supported by the Federal Target Program “Research and development on priority directions of Russian scientific-technological complex for 2007-2013”.

References:

1. H. Zeng, “Real-time Raman spectroscopy for noninvasive in vivo skin analysis and diagnosis” New Developments in Biomedical Engineering, Vol. 24, pp. 455–474 (2010).
2. M. Gniadecka, “Melanoma diagnosis by Raman spectroscopy and neural networks: structure alterations in proteins and lipids in intact cancer tissue” J. Invest. Dermatol., Vol. 122, pp. 443–449 (2004).

Paper B-O-6

DETECTION OF HAZARDOUS CHEMICAL PRODUCTS IN SURGICAL SMOKE

A.M. Bratu[1], M. Petrus[1], C. Popa[1], C. Matei[1], M. Patachia[1], S. Banita[1], D.C. Dumitras[1]

National Institute for Laser, Plasma and Radiation Physics,
409 Atomistilor St., PO Box MG-36, 077125 Bucharest, Romania

e-mail:ana.magureanu@inflpr.ro

Lasers, high-frequency electroknives, drills, and ultrasonic scalpels are surgical instruments used in many types of procedures from wart removal to brain surgery. These are energy-based instruments and real sources of generating "surgical smoke" that pose chemical hazard and can impede surgical progress. Therefore, information on surgical smoke chemical composition is required to evaluate the potential hazard of the operating room personnel.

Surgical smoke contains various toxic chemicals, cell particles, viruses, and aerosols from tissues and blood [1]. The composition and toxicity associated with surgical smoke depend on a variety of factors such as the type of surgical procedure and device, nature of tissue, extent of tissue ablation, and duration of surgery [2, 3]. Both the visible and the odorous components of surgical smoke are toxic and present potential danger for operating room personnel. The possible effects of the chemicals include headaches, irritation and soreness of the eyes, nose and throat, hypoxia, nausea and vomiting, sneezing, weakness, dermatitis, cardiovascular dysfunction, anxiety, and even cancer [1].

The chemical composition of surgical smoke produced *in vitro* in our laboratory by CO_2 laser ablation of fresh animal tissue was investigated with laser photoacoustic spectroscopy (LPAS). The detected products were acetonitrile, acrolein, ammonia, benzene, ethylene, and toluene. Many of these substances are known to be dangerous [4, 5]. Exposure limits and possible health effects are presented when these substances exceed the permissible exposure limits (PEL) given for health organizations like OSHA, and recommended exposure limits (REL) given for health organizations like NIOSH.

We proved the presence of these toxic gases in the surgical smoke produced by laser tissue ablation at quite high levels compared with the exposure limits. Some of the concentrations are lower than the recommended values, but it has to consider the cumulative effect of all volatile compounds released during laser surgery, to which the influence of particles below 10 μm is added. Also, it should be stressed that through continuous exposure, the inhalation of surgical smoke becomes more harmful to the surgical team members.

References:

1. Yun Jo Chung, Sang Kyi Lee, Suk Hee Han, Chen Zhao, Myung Ki Kim, Seung Chul Park, Jong Kwan Park, "Harmful gases including carcinogens produced during transurethral resection of the prostate and vaporization" International Journal of Urology, Vol. 17, pp. 944–949 (2010).
2. Tjeerd de Boorder, Rudolf Verdaasdonk, John Klaessens, "The visualisation of surgical smoke produced by energy delivery devices: significance and effectiveness of evacuation systems", Proc. of SPIE, Vol. 6440, 6440R (2007).
3. W.L. Barrett, S.M. Garber, "Surgical smoke-a review of the literature" Business Briefing: Global Surgery, 1–7 (2004).
4. M. Petrus, C. Matei, M. Patachia, D.C. Dumitras, "Quantitative in vitro analysis of surgical smoke by laser photoacoustic spectroscopy" J. Optoelectr. Adv. Mat., Vol. 14(7-8), pp. 664–670 (2012).
5. K.J. Weld, S. Dryer, C.D. Ames, et al. "Analysis of surgical smoke produced by various energy-based instruments and effect on laparoscopic visibility" J. Endourology, Vol. 21, pp. 347–351 (2007).

Paper B-O-7

3D RECONSTRUCTION OF DEEPLY LOCATED MULTICOLOR UPCONVERSION NANOPARTICLE LABELS BY HIGH-RESOLUTION FLUORESCENCE DIFFUSE OPTICAL TOMOGRAPHY

E.V. Khaydukov[1], V.A. Semchishen[1], V.N. Seminogov[1], A.V. Nechaev[2], A.P. Popov[3], A.V. Bykov[3], V.V. Rocheva[1], A.A. Zvyagin[1], V.I. Sokolov[1], V.Ya. Panchenko[1]

[1]*Institute on Laser and Information Technologies of Russian Academy of Sciences, 1 Svyatoozerskaya St., Shatura, Moscow region, 140700, Russia*
[2]*Lomonosov Moscow University of Fine Chemical Technology, 86 Prospect Vernadskogo, Moscow, 119571, Russia*
[3]*Optoelectronics and Measurement Techniques Laboratory, University of Oulu, Erkki Koiso-Kanttilan katu 3, FI-90014, Oulu, Finland*

Khaydukov@mail.ru

Fluorescence diffuse optical tomography (FDOT) is an emerging biomedical imaging technique to localize deeply placed luminescent particles within biological tissues. However, utilization of this modality is strongly limited by its insufficient spatial resolution. We demonstrate that the current resolution of FDOT can be improved by using highly efficient rear-earth-metal-doped upconversion nanoparticles with nonlinear power-depend luminescence in combination with scanning fiber-optics detection, where the fiber bundle contains one illuminating and several collecting fibers in one tip.

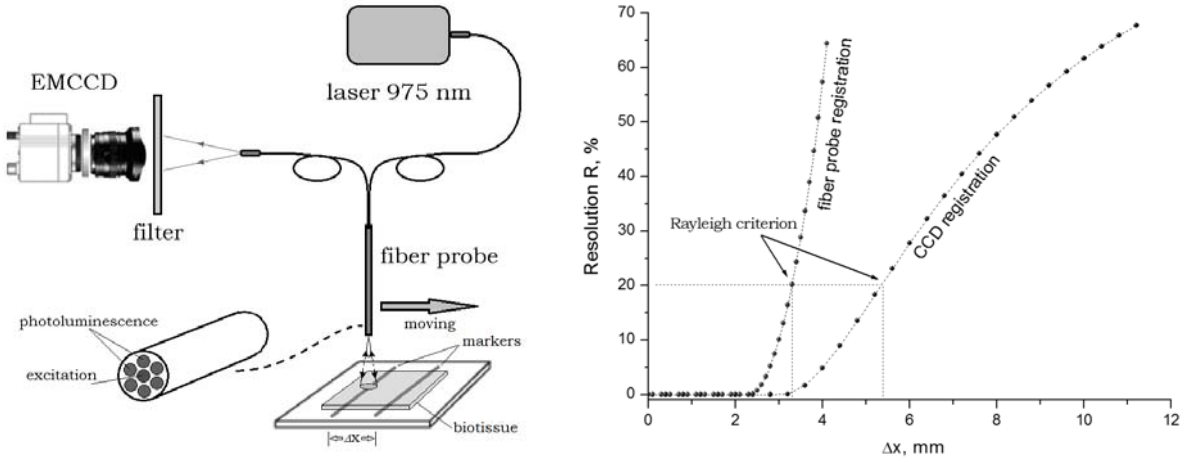

Fig. 1. A fiber-optic FDOT system (left). Comparison of the resolution limits achieved by a fiber-probe and a CCD-based registration techniques (right).

Hexagonal (β-phase) $NaYF_4$:Yb^{3+},Tm^{3+},Er^{3+} nanoparticles were synthesized in-house and utilized as contrast agents. The measured quantum yield of the luminescence in the visible and near-infrared spectral range excited by 975-nm light with intensity of 70 W/cm^2 exceeds 4%. The luminescent label comprised uniformly dispersed nanoparticles in a polymer matrix produced by a photo-polymerization method. The FDOT reconstruction experiments were carried out in a controlled environment using tissue-mimicking phantoms under excitation intensity well below the tissue-damage thresholds. The experiments show that the spatial resolution of the FDOT-reconstructed images can be significantly improved using a scanning fiber tip and overcome the current limits obtained by conventional CCD registration modalities.

Acknowledgements: The reported study was partially supported by RFBR, research project No. 12-02-31845mol_a, 13-02-01138A and by Tekes (FiDiPro project, No. 1027 21 2010).

Paper B-O-8

OPTICAL CHARACTERISTICS OF EYE AND COSTAL CARTILAGE TISSUES AND THEIR ALTERATIONS UNDER THE EFFECT OF NONDESTRUCTIVE 1.56-μm LASER RADIATION

A.V. Yuzhakov, A.P. Sviridov, O.I. Baum, E.M. Shcherbakov, E.N. Sobol

Institute on laser and information technologies, Russian Academy of Sciences, 2 Pionerskaya St., Troitsk 142092, Russia

yuzhalvas@gmail.com

This work is devoted to studies into optical properties of cornea and sclera of the eye and their alterations under the effect of 1.56-μm laser radiation. The laser settings corresponded to the laser treatment regimens used (1) to correct the shape of the cornea or cartilage to change the refraction of the eye or make an implant respectively[1, 2] and (2) to improve the hydraulic permeability of the sclera in glaucoma cases [1, 3]. We used a fiber-optical system to investigate the dynamics of the reflected and transmitted scattered laser radiation and a setup with a double integrating sphere to determine the optical properties of the ocular and cartilage tissues on the basis of the Monte-Carlo simulation of the propagation of light [4]. When the radiation characteristics corresponded to the treatment regimens for correcting the shape of the cornea or cartilage, no however noticeable changes were detected in its optical properties. When irradiating the sclera in conditions corresponding to the treatment regimens for improving its hydraulic permeability, the optical characteristics of the tissue showed definite. The results obtained as to the dynamics of the optical signals during the course of laser irradiation of the cornea, sclera and cartilage create prerequisites for designing test systems to be used with novel medical laser techniques for correcting visual abnormalities.

Acknowledgments: We are grateful for Russian Foundation for Basic Research funding of 12-02-31699 and 13-02-00435 projects.

References:

1. E.N. Sobol, “Method for Correcting Vision and a Device for its Implementation”, Eurasian Patent No. 011465, Iss. April 28 (2009).
2. A. Bolshunov, E. Sobol, S. Avetisov, O. Baum, V. Siplivy, A. Omelchenko, A. Fedorov, “A new method of eye refraction correction under non-ablative laser radiation”, Acta Ophthalmologica, Vol. 89, Iss. Suppl., p. 248 (2011).
3. O.I. Baum, E.N. Sobol, A.I. Omelchenko, E.M. Sherbakov, A.V. Bolchunov, “Effect of nondestructive laser radiation on water permeability of eye trabecula” Laser Physics Workshop (LPHYS’11), Saraevo, Bosnia and Gerzegovina, July 11–15 (2011).
4. L. Wang, S.L. Jacques, L. Zheng, “MCML – Monte-Carlo modeling of light transport in multi-layered tissues” Computer Methods Programs Biomed., No. 47, pp. 131–146 (1995).

Paper B-O-9

NOVEL MULTI-SPECTRAL IMAGING DEVICE FOR COMPLEX SKIN DIAGNOSTICS

Inga Saknite, Edgars Kviesis, Uldis Rubins, Oskars Rubenis,
Ilona Kuzmina, Amina Bekina, Janis Spigulis

Biophotonics Laboratory, Institute of Atomic Physics and Spectroscopy, University of Latvia, Raina Blvd 19, Riga, LV-1586, Latvia

inga.saknite@lu.lv

Nowadays, a non-invasive technique for assessment of different skin lesions is a must for medical doctors. For dermatologists, there are already quite a lot of different devices in the market that can be used for skin diagnostics, for example, a dermatoscope, *MelaFind*, *Siascope*. However, dermatologists' experience is that these devices are not completely trustworthy and precise, as well as most of them are very expensive.

In this study, a complex multi-spectral imaging device was developed and clinically tested. The main advantages of this device are: it is non-expensive, wireless; it gives chromophore maps, as well as different parameter values that are important for dermatologists for skin diagnostics. The second prototype of the device has been developed and tested.

The device is constructed as a cylinder that has all the electronic instalments in one half of it, but the other half consists of a ring of LEDs (365 nm, 450 nm, 530 nm, 650 nm, 940 nm, and white) with a simple RGB camera in the middle of it [1]. A memory card collects all data and can then be inserted into a PC for analysis of the data by software that has been developed and written in *Matlab*. It is then possible to analyse results of chromophore maps (bilirubin, hemoglobin), as well as maps of different parameters (erythema index, bilirubin index).

The second prototype was developed by taking into account problems with the first prototype, and the results are much better and more reliable. Results show that it is possible to acquire all the needed parameters for assessment of different skin lesions, for example, birthmarks, and for early diagnostics of melanoma.

Acknowledgements: This study was supported by the European Regional Development Fund, Grant #2010/0271/2DP/2.1.1.1.0/10/APIA/VIAA/030).

References:

1. D. Jakovels, J. Spigulis, L. Rogule, "RGB mapping of hemoglobin distribution in skin", Proc. SPIE. Vol. 8087, 80872B (2011).

Paper B-P-1

DESIGN OF OPTICAL TOOLS FOR DIAGNOSTICS AND THERAPY OF DENTINE CARIES

S.K. Dick[1], G.G Chistyakova[2], A.S. Terekh[1], A.V. Smirnov[1], N.I. Rosenik[2], M.M. Salimi Zadeh[1], V.V. Barun[1, 3]

[1]*Belarus State University of Informatics and Radioelectronics, 6 Brovka Str., 220013 Minsk, Belarus*
[2]*Belarus State Medical University, Dzerzhinskiy Av. 83, Minsk 220116, Belarus*
[3]*B.I. Stepanov Institute of Physics, Belarus National Academy of Sciences, 68 Skaryna Pr., 220072 Minsk, Belarus*

barun@dragon.bas-net.by

The presentation consists of two parts. The first one examines the hemodynamics of dental pulp at different stages of caries treatment. The speckle structure of light field reflected by a tooth is used as a tool for the investigations. A number of statistical parameters of the random light field were used as indicators of the changes in blood flow. Their variability as a function of the frequency of the Fourier transform of optical signals is studied. The second part is dedicated to the choice of a light source for photodynamic therapy (PDT) while one treats caries. Special attention is paid to the search of the optimal exposure power, wavelength, and exposure time of tooth tissues.

Hemodynamics study. The first step was the investigation of the speckles before and after the anesthesia. It is experimentally shown that the selected statistical parameters reflect the reduced blood flow during the anesthesia and their recovery after the procedure completed. The most sensitive parameter is the power of the Fourier spectrum. The second step was the study of speckle characteristics during the several other stages of caries treatment, namely before and after the preparation, after etching, after tooth filling, after irradiation, and after polishing. All the studied statistical parameters show the similar dynamics while treating caries. One can describe changes of blood flow through the pulp at all stages of the treatment by the following way: (*i*) there is observed an increased blood flow after the preparation, which is the response on the mechanical actions; (*ii*) blood flow sharply decreases after the etching, because the chemical acid action strongly depresses the hemodynamics; and (*iii*) after the tooth filling, irradiation, and polishing, the hemodynamics increases, blood flow gradually grows, but does not achieve the original level. The results obtained with using the speckles correlate reliably with data on the blood flow gathered by the Doppler method.

PDT tooth treatment. PDP methods can be used for removing cariogenic bacteria from damaged tooth tissues with the help of singlet oxygen. In comparison with usual antiseptic remedies, PDT provides a more vivid removal of pathogenic microorganisms from dentinal tubules that circle the carious cavity. When activating a photosensitizer (PS) with laser light, the heating of hard tooth tissues and pulp takes place. The temperature increase inside the pulp cell higher than some threshold causes microcirculation breakdown and finally leads to the loss of the pulp. With the purpose of development the methods of PDT while treating uncomplicated caries, one needs to define the maximum power and the duration of light exposure that are safe with accounting for the thermal parameters of the oral cavity. From all the considered modes of laser light action during PDT, the maximally safe should be assumed the irradiation by light power 50 mW, since the temperature rise in the tooth chamber remains tolerable. Under the irradiation by 150 mW laser power, the expose time should be limited to 379 s, and at 120 mW – to 415 s. When using a light emitting diode with wavelength 460 nm and light power 1000 mW, the expose time should be limited to 60 s.

Paper B-P-2

EVALUATION OF THE FRACTION OF POORLY DEFORMABLE RED CELLS IN DILUTE BLOOD SAMPLES *IN VITRO* BY MEANS OF LASER DIFFRACTOMETRY

A.E. Lugovtsov[1], A.V. Priezzhev[1], S.Yu. Nikitin[1], V.D. Ustinov[2], M.A. Kormacheva[1], V.B. Koshelev[3], O.E. Fadyukova[3], M.D. Lin[3]

[1]Physics Department and International Laser Center,
[2]Faculty of Computational Mathematics and Cybernetics and
[3]Faculty of Basic Medicineof M.V. Lomonosov Moscow State University,
Leninskye Gory 1, Moscow, 119991, Russia

anlug@bmp.ilc.edu.ru

One of the important characteristics of blood is the fraction of erythrocytes, which have a reduced ability to deform passing through thin capillaries (the fraction of poorly deformable erythrocytes). Laser diffractometry is one of the convenient, fast and relatively simple techniques for measuring the erythrocytes deformability in blood samples. This technique allows for quick evaluation of the mean deformability of the erythrocytes [1].

In this paper, we present a new method of evaluation of the fraction of poorly deformable cells in erythrocyte suspension. It is based on the model, in which the erythrocytes moving in the shear flow within the rheologic gap of the ektacytometer are considered as optically soft transparent elliptical disks [2]. Using this model we analytically calculated the light intensity distribution on the observation screen as well as the shapes of the isointensity lines in the vicinity of the central diffraction maximum of the diffraction pattern. We introduced the definition of isointensity line polar points as an intersection of this line with horizontal and vertical coordinate axes. Furthermore, we introduced the curvature radii of the isointensity line at the polar points. Coordinates of the polar points as well as the curvature radii of the isointensity line at the polar points can be determined from the experimental data obtained with laser diffractometry. As a result, we obtained a set of equations binding together the measured parameters of the diffraction pattern and the statistical characteristics of the erythrocyte suspension under study. Using these equations we developed an algorithm, which allows for evaluating the mean value of the shape parameter (a function of the relative elongation) of shear-elongated erythrocytes, the variance and the coefficient of asymmetry of erythrocyte shape parameter distribution on the basis of the laser ektacytometry data. For example, in the case of a bimodal ensemble, i.e. an ensemble, which contains cells of only two types in terms of their deformability, we can evaluate the fractions of cells of both types as well as the shapes of both components of the ensemble. Other types of erythrocytes ensembles were also considered.

Thus, in this work a new method of estimation of the fraction of poorly deformable erythrocytes in blood samples is proposed. The method is based on the analysis of the isointensity lines shapes arising at scattering of a laser beam on erythrocyte suspension in the ektacytometer. The algorithm efficiency was verified experimentally with blood samples containing different fractions of poorly deformable erythrocytes.

Acknowledgements: This work was partially supported by RFBR grants № 12-02-01329 and № 13-02-01372.

References:

1. M. Bessis, N. Mohandas, “A diffractometric method for the measurement of cellular deformability” Blood Cells, Vol. 1, pp. 307–313 (1975).
2. S.Yu. Nikitin, M.A. Kormacheva, A.V. Priezzhev, A.E. Lugovtsov, “Laser beam scattering on an inhomogeneous ensemble of elliptical discs modelling red blood cells in an ektacytometer” Quantum Electronics, Vol. 43(1), pp. 90–93 (2013).

Paper B-P-3

INITIALIZATION OF RADIOBIOLOGICAL STUDIES AT ROMANIAN HIGH POWER LASER FACILITIES

C. Matei, C. Popa, A.M. Bratu, M. Petrus, M. Patachia, S. Banita, I. Ivascu, D.C. Dumitras

Laser Department, National Institute for Laser, Plasma and Radiation Physics, 409 Atomistilor St., PO BOX MG-36, 077125 Magurele-Bucharest, Romania

consuela.matei@inflpr.ro

More than hundred years after the discovery of X-rays, different kinds of ionizing radiation are omnipresent in medicine, applied as well to clinical diagnostics as to cancer treatment.

Since 2000, when large high-power lasers operating at a few pulses per day demonstrated intense proton pulses with maximum energies in the range of 60 MeV [1], several groups made proposals concerning the therapeutic potential of laser-plasma-accelerated proton beams. Irrespective to its origin (classical accelerators or high power lasers), the application of radiation must rely on a precise dosimetric characterization and a detailed knowledge of the radiobiological effects induced in cancerous and normal tissue. A complete multi-stage process begins with *in vitro* irradiation experiments, which define the basic parameters to be used further in tissue and animal studies, and completes with clinical trials. However, the pulse properties of the proton beams obtained today by laser-plasma-acceleration are still far away from those commonly provided by medical accelerators. For proton therapy, proton beams with high energies (60–300 MeV) are needed, simultaneously accomplishing the condition of a high beam uniformity, monoenergetic selection, high repeatability and delivery of a required dose rate. Unfortunately, we are still at the threshold of 60 MeV proton energy, facing considerable problems with the beam repeatability and dose delivery.

In these circumstances, there is a tremendous need in accomplishing fundamental research studies with the aim of improving the properties of the laser produced proton beams, as well as characterizing the radiobiological effects on cells [2].

Based on the capabilities of the two facilities owned by the National Institute for Laser, Plasma and Radiation Physics, the 20 TW TEWALAS Facility (pulses of 25 fs duration with a 10 Hz repetition rate) and CETAL Facility (a main output of 1 PW, 25 fs, 0.1 Hz and an intermediate output of 40 TW, 25 fs and 10 Hz), we present an initial design of the setup to be firstly implemented in the TEWALAS Facility, then transferred to the CETAL. Aspects related to the production and acceleration of protons, the beam focusing and the energy selection methods, the dosimetry required at this stage, and the specific conditions imposed by the *in vitro* experiments will be discussed.

References:

1. R.A. Snavely et al., “Intense high-energy proton beams from petawatt-laser irradiation of solids” Phys. Rev. Lett., Vol. 85, pp. 2945–2948 (2000).
2. S.D. Kraft et al., “Dose-dependent biological damage of tumour cells by laser-accelerated proton beams” New Journal of Physics, Vol. 12, 0850031 (2010).

Paper B-P-4

CW DIFFUSE OPTICAL TOMOGRAPHY TESTING AND CALIBRATION ON FANTOMS

M. Patachia, C. Popa, S. Banita, C. Matei, A. Magureanu, M. Petrus, D.C. Dumitras

Department of Lasers, National Institute for Laser, Plasma and Radiation Physics, P.O. Box MG-36, 409 Atomistilor St., 077125, Bucharest, Romania

mihai.patachia@inflpr.ro

Abstract: Diffuse optical tomography (DOT) is a potential diagnostic tool for detecting abnormal growths in translucent soft tissues. Its principle is to use multiple movable light sources and detectors attached to the tissue surface to collect information on light attenuation, and to reconstruct the internal 3-D absorption and scattering distributions.

The development of optical imaging techniques, like that of any other medical diagnostic modality, has relied upon appropriate phantoms whose physical properties and geometries are matched to those of human tissues. Measurements on phantoms are used to evaluate the performance of systems and to validate the imaging algorithms.

Together with the reconstructions of the tissues structure, the calibration is the pivotal part of the data acquisition due to the variation in characteristics of each laser source, optical fibres, detectors, and optic elements. An accurate calibration is achieved in a homogeneous phantom. The work describes some methods to achieve homogeneous phantoms and how they are used to evaluate the performance of the system.

References:

1. D.C. Dumitraş, D.C. Duţu, C. Matei, A.M. Măgureanu, M. Paţachia, "Diffuse optical tomography (DOT) with serial approach" J. Optoelectron. Adv. Mater. – Symposia, Vol. 1, pp. 747–753 (2009).
2. M. Paţachia, D.C.A. Duţu, D.C. Dumitraş, "Blood oxygenation monitoring by diffuse optical tomography" Quantum Electronics, Vol. 40, pp. 1062–1066 (2010).
3. M. Patachia, "A simple continuous-wave diffuse optical tomography system for parametric investigation of different tissue phantoms" J. Optoelectron. Adv. Mater., Vol. 15(4), pp. 155–163 (2013).

Paper B-P-5

THE INTERACTION OF CESIUM WITH MODEL SOLUTIONS OF SERUM BY STATIC LIGHT SCATTERING (SLS)

I.A. Sergeeva, A.V. Komarova, V.V. Gibizova, G.P. Petrova

MSU, Faculty of Physics, GSP-1, 1-2 Leninskiye Gory, Moscow 119991, Russia

1sergeeva@physics.msu.ru

In this paper, using the methods of laser spectroscopy, studied the interaction of cesium ions with the model of serum samples of healthy and sick people with cancer.

Macromolecule proteins are unique to the study by the methods of molecular optics, because the size and weight of the protein macromolecules are strictly defined for each type of protein. The surface of the protein macromolecules is charged and has a large dipole moment - a few hundred Debye.

A detailed study of the scattered light properties provides information about the molecules structure and molecular systems. In experiments on SLS observed average (over time), the scattering intensity. The analysis of the angular and concentration dependence provides information on the size of the scattering centers: molecular weight and molecular interaction coefficient B.

Since the slope of the line connected to the slope, the coefficient of molecular interaction can be regarded as one of the main parameters for early detection of various diseases associated with components of blood serum.

Previously, we conducted research model solutions serum by SLS. The experiment received the concentration dependence of the scattering parameter cH/R90. The experimental results showed that, for healthy people dependent scattering parameter has a positive slope. For sick patients slope of the scattering parameter is negative.

In this work, it was found that the model solutions of blood serum with the addition of cesium ions sign of the intermolecular interaction does not change (positive slope remains the same), and model solutions in samples of blood serum - reversed (negative slope is positive).

Timely and accurate diagnosis of cancer at an early stage is the actual problem of modern medicine. In this connection, the use of heavy metals in model systems of blood serum, such as cesium, may serve as an additional indicator that increase the accuracy of detection of the tumor.

It is planned to carry out measurements on native serum samples.

Paper B-P-6

MAGNETITE NANOPARTICLES FOR LASER THERAPY AND DIAGNOSTICS OF CARTILAGE DISEASES

Y.M. Soshnikova[1,2], O.I. Baum[1], A.I. Omelchenko[1], S.G. Roman[3], N.A. Chebotareva[3], E.N. Sobol[1]

[1]*Institute on Laser & Information Technologies, Russian Academy of Sciences, Troitsk 142190, Russia*
[2]*Lomonosov Moscow State University, Department of Chemistry, Moscow 119992, Russia*
[3]*A.N. Bach Institute of Biochemistry, Moscow 119071, Russia*

Magnetic nanoparticles are becoming perspective materials for medical diagnostics and treatment of different diseases. They are considered to be used in magnetic resonance and optical tomography as contrast agents [1, 2]. Some of them are declared to be effective in drug delivery and cancer hyperthermia [3, 4]. Another possible application of magnetic nanoparticles is to use them as absorbers of laser radiation in laser diagnostics and treatment of degenerative cartilage. It is known that cartilage matrix contains pores and channels of different size depending on the tissue type, age and preliminary impact (including laser irradiation) [5]. The porous structure provides the tissue nutrition since cartilage matrix does not have blood vessels. Therefore small nanoparticles can penetrate in cartilage through the pores and channels its structure. According to laser treatment this will allow substantive decreasing the radiation power and avoiding the overheating of the tissue bulk by concentrating the energy selectively in the damaged area. Cartilage degradation always occurs in small local area which can not be diagnosed at early stages. The known diagnostic methods allow to resolve already large defects (about 1 mm) [6, 7]. Thus, the urgent problem is to study the possibility of magnetic nanoparticles to be applied in laser diagnostics of cartilage degradation at the very early stages by their impregnation in the tissue. Furthermore, the size of impregnated nanoparticles can indicate the damage degree.

The work is devoted to manufacturing and application of stabilized magnetite nanoparticles for laser therapy of cartilage. One of the most common problems is the agglomeration tendency of small magnetic nanoparticles. The penetration of large agglomerates and their massive accumulation in defects will result in overheating and necrosis of the cartilage during laser treatment. So, the stabilization of small magnetic nanoparticles by natural and accessible material is needed. At the present study we performed synthesis and stabilization of magnetite nanoparticles by polysaccharide and also investigated the ability to impregnate the nanoparticles into cartilage. The dispersions of synthesized magnetite particles were characterized by dynamic light scattering, analytical ultracentrifugation, transmission electron and atomic force microscopy methods. The optimal conditions for manufacturing stable nanoparticles were evaluated. The dispersions of magnetite nanoparticles demonstrated thermal stability (at least up to 70°C) and stability during their storage for at least one month period. It was shown that synthesized nanoparticles vary in size from 10 to 400 nm and the fraction of nanoparticles with small size can penetrate into healthy cartilage and thereby indicate the size of the channels in the cartilage structure. Defective cartilage contains large defects of about 1 μm, so it can be impregnated with large magnetite particles. The use of polydisperse nanoparticles will allow evaluating sizes of defects. We suppose that laser medical irradiation of the cartilage impregnated with nanoparticles will provide more local and dedicated treatment which will make the procedure more effective and safe.

References:

1. J. Chen, F. Wang, Y. Zhang, Ann. of Biomed. Eng., DOI: 10.1007/s10439-012-0621-5 (2012).
2. C.T. Xu, J. Axelsson, S. Andersson-Engels, Appl. Phys. Lett., Vol. 94, 251107 (2009).
3. W.H. De Jong, P.J.A. Borm, Int. J. Nanomed., Vol. 3(2), pp. 133–149 (2008).
4. A.P. Khandhar, R.M. Ferguson, K.M. Krishnana, J. Appl. Phys., Vol. 109, 07B310 (2011).
5. E. Sobol, A. Sviridov, A. Omelchenko, V. Bagratashvili, M. Kitai, S.E. Harding, Biotech. Gen. Eng. Rev., Vol. 17, pp. 553–578 (2000).
6. J.-J. Shyu, C.-H. Chan, M.-W. Hsiung, P.-N. Yang, H.-W. Chen, W.-C. Kuo, Prog. Electromagn. Res. PIER, Vol. 91, pp. 365–376 (2009).
7. M. Stolz, R. Gottardi, R. Raiteri, S. Miot, I. Martin, et al., Nat. Nanotech., Vol. 4, DOI: 10.1038/NNANO.2008.410 (2009).

Paper B-P-7

THE COMBINED ACTION OF LED BLUE (405 nm) LIGHT AND MAGNETIC Fe_3O_4 NANOPARTICLES ON MICROORGANISMS

Elena S. Tuchina[1], Kristina V. Kosina[1], Pavel O. Petrov[1], Vjacheslav I. Kochubey[2,3], Valery V. Tuchin[2,3,4]

[1]*Department of Biology, Saratov State University, Saratov, 410012, Russia*
[2]*Research-Educational Institute of Optics and Biophotonics, Saratov State University, Saratov, 410012, Russia*
[3]*Institute of Precise Mechanics and Control of Russian Academy of Sciences, Saratov, 410028, Russia*
[4]*Optoelectronics and Measurement Techniques Laboratory, Department of Electrical Engineering, University of Oulu, P.O. Box 4500, Oulu FIN-90014, Finland*

Iron oxide nanoparticles are widely used in chemical and biomedical research because of its photocatalytic and magnetic properties. The goal of this study was to evaluate the sensitivity of microorganisms to the action of LED blue (405 nm) light after treatment of their cells with Fe_3O_4 nanoparticles and Fe-nanocomposites with TiO_2 core.

The bacterial strains used in this study were *Staphylococcus aureus* 209 P meticillin-sensitive, *S. aureus* 54 meticillin-resistanse (standard strains), *S. simulans* and *S. hominis* (isolated from normal human skin). Cultures were grown on dense brain-heart infusion medium and incubated at 37°C.

As LED-light source with spectrum maxima at 405 nm providing corresponding power density of 70 mW/cm^2 were taken. The light exposure was ranged from 5 to 30 min. Fe_3O_4 nanoparticles with average size about 10 nm in concentration 0.01% were used.

The account of results was provided by calculation of colony forming units (CFU) in 24 hrs after light exposure.

Reduction of CFU number of *S. aureus* MS incubated with nanoparticles occurred in the range of 43 - 91%, for *S. aureus* MR – on 35–78%. The observed reduction of the CFU number of was not depending on the duration of light exposure. Using Fe_3O_4 nanoparticles and blue light led to a same, but more pronounced effect on *S. simulans*: after 10 min-exposure the reduction of CFU was on 72%, after 30 min – on 94%. Reduction of the CFU number of *S. hominis*, incubated with Fe_3O_4 nanoparticles, with variation of exposure time from 5 to 30 min occurred in the range of 47–95%.

SECTION D

Laser Diagnostics

Paper D-I-1

TIME-RESOLVED NON-LINEAR MAGNETO-OPTICS AS A TOOL TO STUDY SPATIALLY NON-UNIFORM NON-LOCAL ULTRAFAST SPIN DYNAMICS IN METALLIC MULTILAYERS

A. Melnikov

Fritz-Haber-Institut of the Max Planck Society, Faradayweg 4-6, 14195 Berlin, Germany

melnikov@fhi-berlin.mpg.de

The ultrafast spin dynamics, including that one induced by a transport of spin-polarized carriers, is a hot topic motivated by the fundamental interest in magnetic excitations and applications like spintronics and data storage. The understanding of elementary processes occurring on femtosecond time scales requires an experimental approach for investigation of ultrafast dynamics of highly excited states of solids. One well-established technique is the time-resolved magneto-optical Kerr (MOKE) and Faraday effects: excitation and detection by femtosecond laser pulses provides the time resolution approaching the time scale of interest. However, optically excited dynamics is spatially non-uniform, at least due to non-uniform excitation in strongly absorbing media, and this technique experiences a lack of spatial resolution. In metallic structures, owing to high carrier mobility, the dynamics of the excited state is essentially non-local being defined by the transport of laser-excited hot carriers (HC) which may be spin-polarized if excited in the exchange-split band structure of a ferromagnet. This again asks for high spatial resolution which is restricted to the "depth resolution" (along the normal-to-surface direction) in the case of multilayer structures with the in-plane translation symmetry.

Here we complement time-resolved MOKE, which probes the transient magnetization averaged over the optical penetration depth, by time-resolved magneto-induced optical second harmonic generation (mSHG) which is selectively sensitive to surfaces and (buried) interfaces and can probe transient spin polarization at interfaces. This is essential in the case of spin-polarized HC transport across a layered structure: (i) if there is a spin accumulation at an interface, it will be detectable by mSHG (but not by MOKE due to the averaging); (ii) if there is no spin accumulation, mSHG will monitor the spin polarization in the cross-section of the HC pulse, which is defined by the traversed interface at a given time, i.e. the interface "streaks" the HC packet. We have discussed recently such streaking for the case of spin transport by optically excited HC in Au/Fe/MgO(001) [1] where the Au layer is thick enough to block the mSHG signal from all interfaces except the Au surface and HC are excited in the Fe film (time-of-flight-like approach realized in a back pump-front probe scheme). In the general case, it is challenging to disentangle mSHG contributions from different interfaces. Here we discuss the dependence of mSHG response on the thickness of layers as an appropriate tool for that. We test our approach on Au/Fe/MgO(001) epitaxial bi-layers probed from the side of Fe film. By probing the Au surface in the back pump-front probe scheme, we demonstrate spin current pulses (SCP) of about 30 fs duration. These SCP are formed by HC generated in the Fe layer while they traverse the Au layer which works as spin-selective HC retarder. The spin dynamics excited by SCP in the Fe film is studied in Fe/Au/Fe/MgO(001) stacks. We demonstrate the control of HC-induced demagnetization timescale at the buried Fe/Au interface of the second Fe layer by manipulating the magnetization direction in the first Fe layer.

Acknowledgements: This study was carried out in collaboration with A. Alekhin, D. Bürstel, D. Diesing, V. Roddatis, T.O. Wehling, A.I. Lichtenstein, and U. Bovensiepen. Funding by the DFG through ME 3570/1 is gratefully acknowledged.

References:

1. A. Melnikov et al., Phys. Rev. Lett., Vol. 107, 076601 (2011).

Paper D-I-2

NONLINEAR-OPTICAL MICROSCOPY-SPECTROSCOPY OF FERROIC AND SEMICONDUCTOR NANOSTRUCTURES

E.D. Mishina

Moscow State Technical University of Radioengineering, Electronics and Automation, Vernadsky Av. 78, 119454 Moscow, Russia

mishina@mirea.ru

Nonlinear optical scanning microscopy based on the generation of the second harmonic generation (SHG) allows to explore the domain structure of ferroelectrics and multiferroics, effects of polarization switching and phase transitions. Nonlinear-optical spectroscopy, including additionally to SHG, two-photon luminescence is most effective in the study of semiconductor and organic materials when the excitonic or defect-induced transitions lie in the tuning range of the probe laser .

This paper discusses the possibilities and limitations of these techniques for the study of thin films and multilayer structures with ferroelectric and multiferroic properties as well as for the study of organic piezoelectric and semiconductor nanostructures.

Local polarization switching is studied in thin films and nanostructures based on $BaSrTiO_3$, the reasons for spatial inhomogeneity of switching are analyzed. In ferroelectric/ferromagnet (multiferroic) bilayer and multilayer planar nanostructures ferroelectric and magnetic phase transitions are studied, as well as influence on non-linear optical properties of the effect of electron tunneling through a ferroelectric.

In ZnO nanostructures both SHG and two-photon luminescence were studied. Two-photon 3D maps of the structures have been obtained. At room temperature the structures possess strong SHG and enhanced green TPL caused by defects of different origin.

Second harmonic generation and two-photon luminescence are investigated in the recently discovered biological ferroelectrics - peptide nanotubes (PNT) [1]. SHG microscopy method revealed a phase transition at 140°C. Below the phase transition PNT possess nonlinear susceptibility, comparable with this value in the non-linear optical crystals used in harmonic generators. Above the phase transition in the PNT an intense luminescence appears, showing strong enhancement with increasing excitation power.

The limits of spatial resolution of far-field two-photon microscopy in ferroic and semiconductor nanostructures are discussed. For semiconductor nanoparticles the stimulated emission depletion microscopy (STED) gives down to 70 nm resolution [2]. For nanostructures showing the high order nonlinearities (but not high harmonic generation), spatial resolution in visible can be enhanced by the square root of the nonlinearity order, which is about 200 nm that is not as high as for STED but still beyond the diffraction limit of far-field microscopy.

Acknowledgements: The work is supported by Russian Foundation for Basic Research and Ministry of Education and Science of RF.

References:

1. A. Kholkin, N. Amdursky, I. Bdikin, E. Gazit, G. Rosenman, “Strong piezoelectricity in bioinspired peptide nanotubes” ASC NANO, Vol. 4, pp. 610–614 (2010).
2. G. Moneron, S.W. Hell, “Two-photon excitation STED microscopy” Optics Express, Vol. 17, pp. 14567–14573 (2009).

Paper D-I-3

FAST RECORD OF WEAK ABSORPTION SPECTRA BY MODIFIED ICOS TECHNIQUE WITH THE HELP OF CAVITY REFLECTED BEAM

V. Nikolaev, V.N. Ochkin, S.N. Tskhai

P.N. Lebedev Physical Institute RAS, Leninski prospect 53, Moscow 119991, Russia

ochkin@sci.lebedev.ru

The problem of ICOS signal fluctuations is resulted from unstable coupling of a probe laser radiation with cavity modes. The way to suppress these intensity fluctuations by using the additional signal which is reflected from the cavity was provided in [1] (R-ICOS). Presently we studied this proposal in more details and applied it to measurements of methane concentration in the air.

In the present scheme the radiation of tunable diode laser near 1650 nm propagates through optical insulator and quartz plate splitter to the multipass 50 cm cavity. Mirrors reflection coefficients R = 0.8–0.99. A radiation transmitted by the cavity is detected in channel 1 and correspond to conventional ICOS signal. Additionally the part of radiation reflected from splitter is registered in the second (baseline) channel 2. Also the part of emission reflected from the cavity reflected again by the same plate in opposite to the channel 2 direction (channel 3).

The absorption coefficient of methane was measured with the help of the combination of all channels intensities and the regression technique was applied.

The methane absorption spectra ICOS and R-ICOS schemes are shown in the figure below. Both spectra are recorded during single frequency scan cycle of the laser radiation which takes about 5 ms and presented by 4096 point per scan with digital step of 1.25 μs.

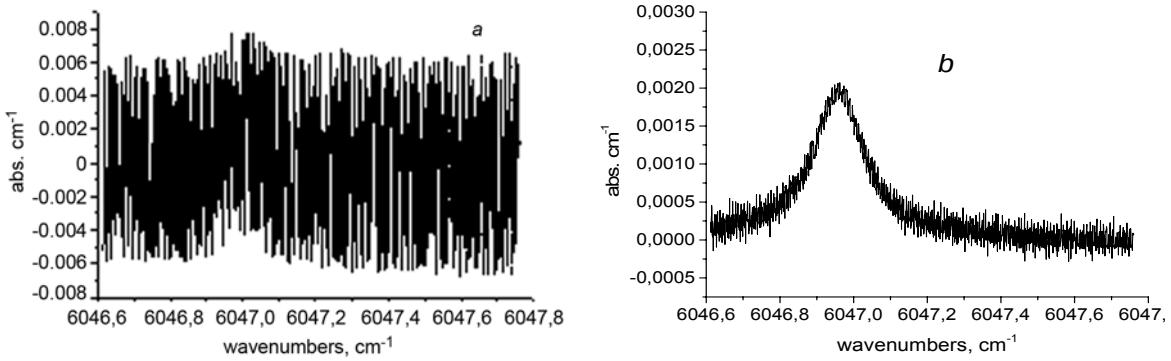

Spectra of methane: *a* – ICOS, *b* – R-ICOS. Mirrors reflectivity 0.8.

To estimate the absorption sensitivity and precision for both techniques at longer storage times an Allan variance plots have been used. As in case of fast measurements the precision of absorption coefficient for R-ICOS more than 10 times exceeds of that for ICOS.

Acknowledgements: Supported by the RFBR (grants 11-08-01127-a, 12-02-31100-MOL-A), Programs: Support of young scientists of RAS; Educational-Scientific Complex of the P.N. Lebedev Physical Institute of RAS; Fundamental Optical Spectroscopy and its Applications of the Department of Physical.

References:

1. I.V. Nikolaev, V.N. Ochkin, M.V. Spiridonov, S.N. Tskhai, “Methods of reference signal and phase shifts in the multipass laser schemes for the detection of trace gas impurities” Laser Phys., Vol. 21, pp. 2088–2093 (2011).

Paper D-I-4

OPTICAL PROPERTIES OF SILICON NANOWIRE ARRAYS

L.A. Golovan[1], K.V. Bunkov[1], K.A. Gonchar[1], V.Yu. Timoshenko[1], D.V. Petrov[2], M.N. Kulmas[3], V.A. Sivakov[3]

[1]*Physics Department, M.V. Lomonosov Moscow State University, Moscow 119991, Russia*
[2]*D.V. Skobeltsyn Nuclear Physics Institute, M.V. Lomonosov Moscow State University, Moscow 199991, Russia*
[3]*Institut für Photonische Technologien, Jena D-07745, Germany*

golovan@physics.msu.ru

Nowadays, silicon photonics has become a mainstream in optical and electronic engineering. In particular, arrays of silicon nanowires (SiNWs) consisting of crystalline silicon (c-Si) wires of 20–200 nm in diameter and of 1–200 μm in length are in the focus of the researchers' attention. SiNWs are ordered straight SiNWs, which demonstrate enhancement of spontaneous Raman scattering, coherent anti-Stokes Raman scattering and silicon interband photoluminescence (PL) efficiency in comparison with c-Si as well as visible PL caused by occurrence of Si nanocrystals at the SiNW walls. These features of SiNWs together with their extremely low (about 1%) total reflection in the visible range make this material very promising for various applications in photonics, photovoltaics and sensing.

SiNWs were formed by means of a metal-assisted chemical etching technique employing a two-stage chemical process: (1) the chemical deposition of silver nanoparticles (np-Ag) at the surface of c-Si wafer and (2) the macropore etching in c-Si with the help of np-Ag acting as catalysts. If it is necessary, np-Ag can be removed in nitric acid.

Experiments on Raman scattering were carried out with excitation at wavelengths of 488, 633, and 1064 nm. The TH experiments were done in reflection geometry with TH being pumped by Cr:forsterite laser (1250 nm, 80 fs, 2 nJ, 80 MHz).

Typically, the Raman scattering signals of SiNWs several times exceed corresponding signals from c-Si substrate. SiNW length of 1.5 μm is found to be enough to increase the Raman signal significantly. However, the ratio of Raman signal for SiNW I_{SiNW} and corresponding crystal substrate I_{wafer} strongly depends on the SiNW sizes, volume fraction, their order, and the excitation wavelength. For more ordered SiNW array I_{SiNW}/I_{wafer} increases with the decrease of excitation wavelength, whereas for less ordered sample it falls. Similar to the Raman scattering, the more ordered SiNW arrays exhibit TH signal exceeding one for c-Si substrate by one order of magnitude, whereas in the less ordered SiNW arrays do not demonstrate any TH signal rise. TH orientation dependences for SiNWs are totally different from the ones for c-Si.

Both the Raman scattering and TH efficiencies in SiNWs are determined by an interplay of the light scattering and absorption. Their actions are opposite: rise of the scattering efficiency results in increase of the photon lifetime in the medium, whereas the absorption reduces it. In the less ordered SiNWs effect of the light absorption is stronger than effect of the light scattering; as a result no light trapping takes place, whereas more ordered SiNWs allow the more effective light trapping and the rise of the Raman scattering and TH efficiencies.

Thus, the possibility to increase the Raman and TH signals in SiNWs more than order of magnitude in comparison with c-Si was demonstrated, with the efficiency of these processes strongly depending on the SiNW array structure.

Acknowledgements: This work was done at User Facility Centre of Moscow State University. This work was supported by RFBR grant No. 11-02-01087, Ministry of Education and Science of Russia and by BMBF grant.

Paper D-O-2

FEMTOSECOND LASER IN GAUGE BLOCK CALIBRATION

Z. Buchta, M. Čížek, V. Hucl, Š. Řeřucha, M. Šarbort, J. Lazar, O. Čip

Institute of Scientific Instruments, v.v.i., Academy of Sciences of the Czech Republic, Kralovopolska 147, 612 64 Brno, Czech Republic

buchta@isibrno.cz

This paper deals with using of mode-lock femtosecond laser for length measurement of gauge blocks. A novel principle for contactless gauge block measurement using a combination of low-coherence interferometry and laser interferometry is presented here. The experimental setup combines a Dowell interferometer and a Michelson interferometer to ensure a gauge block length determination with direct traceability to the primary length standard. This setup was designed for contactless complex gauge block analysis providing information about gauge block length, gauge block faces surface profile (e.g., indication of scratches) and by analysis of the interference fringes shape, also about the gauge block edge flatness distortion. The designed setup is supplemented by an automatic handling system designed for a set of 126 gauge blocks (0.5 to 100 mm) to allow the automatic contactless calibration of the complex gauge block set without a human operator.

Acknowledgements: This work was supported by Grant Agency of CR project GP102/09/P293 and partially by GAP102/11/P819 and GP102/10/1813, by Ministry of Industry and Commerce, project No. 2A-1TP1/127 and FR-TI2/705 and by Technology Agency of CR, project No. TA03010663. The background of the research was supported by the European Commission and Ministry of Education, Youth, and Sports of the Czech Republic project No. CZ.1.05/2.1.00/01.0017 and projects LC06007.

References:

1. T. Doiron, J. Beers, "The Gauge Block Handbook; NIST Monograph 180 with Corrections" 1-143 (1995).
2. J.E. Decker, J.R. Miles, A.A. Madej, R.F. Siemsen, K.J. Siemsen, S. de Bonth, K. Bustraan, S. Temple, J.R. Pekelsky, "Increasing the range of unambiguity in step-height measurement with multiple-wavelength interferometry – application to absolute long gauge block measurement" Appl. Opt., Vol. 42, pp. 5670–5678 (2003).
3. G. Bonsch, "Automatic gauge block measurement by phase stepping interferometry with three laser wavelength", Proc. SPIE, Vol. 4401, pp. 1–10 (2001).
4. V.M. Khavinson, "Ring interferometer for two-sided measurement of the absolute lengths of end standards" Appl. Opt., Vol. 38, pp. 126–136 (1999).
5. Y. Ishii, S. Seino, "New method for interferometric measurement of gauge blocks without wringing onto a platen" Metrologia, Vol. 35, pp. 67–73 (1998).
6. A. Abdelaty, A. Walkov, A. Abou-Zeid, R. Schodel, "PTB'S prototype of a double ended interferometer for measuring the length of gauge blocks" Proc. of the Simposio de Metrologia (Queretaro, Mexico, pp. 1–6, 2010).
7. M. Dobosz, O. Iwasinska-Kowalska, "A new method of non-contact gauge block calibration using a fringe-counting technique: Theory basis" Opt. Laser Tech., Vol. 42, pp. 141–148 (2010).
8. O. Iwasinska-Kowalska, M. Dobosz, "A new method of non-contact gauge block calibration using a fringe-counting technique: Experimental verification" Opt. Laser Tech., Vol. 42, pp. 149–155 (2010).
9. Z. Buchta, B. Mikel, J. Lazar, O. Čip, "White-light fringe detection based on novel light source and color CCD camera" Meas. Sci. Tech., Vol. 22, 094031 (2011).
10. E. Ikonen, J. Kauppinen, T. Korkolainen, J. Luukkainen, K. Riski, "Interferometric calibration of gauge blocks by using one stabilized laser and a white-light source" Appl. Opt., Vol. 30, pp. 4477–4478 (1991).
11. J.H. Dowell, "Improvements in or relating to interferometers for determination of length" British patent No. 555672 (1943).
12. B. Karlsson, G.C. Ribbing, "Optical constants and spectral selectivity of stainless steel and its oxides" J. Appl. Opt., Vol. 53, pp. 6340–6346 (1982).
13. O. Čip, F. Petrů, "A scale-linearization method for precise laser interferometry" Meas. Sci. Technol., Vol. 11, pp. 133–141 (2000).
14. O. Čip, Z. Buchta, F. Petrů, J. Lazar, "On-line monitoring of the refraction index of air for ultra-precise length measurement in the nano-world" Proc. of 8th IEEE Africon Conference, Windhoek, Namibia, Vol. 26–28, pp. 294–298 (2007).
15. J. Lazar, O. Čip, M. Čížek, J. Hrabina, Z. Buchta, "Suppression of air refractive index variation in high-resolution interferometry," Sensors, Vol. 11, pp. 7644–7655 (2011).
16. Z. Buchta, Š. Řeřucha, B. Mikel, M. Čížek, J. Lazar, O. Čip, "Novel principle of contactless gauge block calibration" Sensors, Vol. 12, pp. 3350–3358 (2012).
17. Z. Buchta, Š. Řeřucha, B. Mikel, M. Čížek, J. Lazar, O. Čip, "Novel principle of contactless gauge block measurement", Proc. SPIE, Vol. 8697, 86970D-1–86970D-7 (2012).
18. Š. Řeřucha, Z. Buchta, M. Šarbort, J. Lazar, O. Čip, "Detection of interference phase by digital computation of quadrature signals in homodyne laser interferometry" Sensors, Vol. 12, pp. 14095–14112 (2012).

Paper D-O-3

SHORT-RANGE SIX-AXIS INTERFEROMETER CONTROLLED POSITIONING FOR LOCAL PROBE MICROSCOPY

J. Lazar, J. Hrabina, Z. Buchta, O. Číp, M. Čížek, J. Oulehla

Institute of Scientific Instruments, v.v.i., Academy of Sciences of the Czech Republic, Královopolská 147, 612 64 Brno, Czech Republic

joe@isibrno.cz

We present a design of nanometrology measuring setup is part of a design of the national standard for nanometrology to be operated by the Czech Metrology Institute (CMI) in Brno, Czech Republic. The system uses a full six-axis interferometric measurement of the position of the sample holder with six independent interferometers. The concept of nanometrology system combining local probe microscopy and interferometric measuring and controlled positioning presented here represents one of a variety of possible approaches. A small range system based on a commercial nanopositioning stage driven by piezoelectric transducers with the overall range 200×200×10 μm was used. Due to the geometric configuration with a wide basis of the two units measuring in y-direction and the three measuring in z-direction the angle resolution of the whole setup goes down to tens of nanoradians and servo control of in all six axes of freedom allows to keep guidance errors below 100 nrad. Thermally compensated miniature interferometric units with fiber-optic light delivery and integrated homodyne detection system were developed especially for this system.

Acknowledgements: The authors wish to express thanks for support to the grant projects from the Grant Agency of CR, project GPP102/11/P820, Academy of Sciences of CR, project: RVO:68081731, Ministry of Education, Youth and Sports of CR, project: CZ.1.05/2.1.00/01.0017, European Social Fund and National Budget of the Czech Republic, project: CZ.1.07/2.4.00/31.0016 and Technology Agency of CR, projects: TA02010711, TE01020233.

References:

1. R.K. Leach, R. Boyd, T. Burke, H.U. Danzebrink, K. Dirscherl, T. Dziomba, A. Yacoot, "The European nanometrology landscape" Nanotechnology, Vol. 22(6) (2011).
2. U. Neuschaefer-Rube, M. Neugebauer, T. Dziomba, H.U. Danzebrink, L. Koenders, H. Bosse, "Recent developments of standards for 3D micro- and nanometrology" TM-Technisches Messen, Vol. 78(3), pp. 118–126 (2011).
3. J. Lazar, J. Hrabina, M. Sery, P. Klapetek, O. Cip, "Multiaxis interferometric displacement measurement for local probe microscopy" Central European Journal of Physics, Vol. 10(1), pp. 225–231 (2012).
4. G. Jager, E. Manske, T. Hausotte, H.J. Buchner, "Nano Measuring Machine for zero Abbe offset coordinate-measuring" Technisches Messen, Vol. 67(7-8), pp. 319–323 (2000).
5. J. Lazar, P. Klapetek, O. Cip, M. Cizek, M. Sery, "Local probe microscopy with interferometric monitoring of the stage nanopositioning" Measurement Science & Technology, Vol. 20(8) (2009).
6. J. Lazar, J. Hrabina, P. Jedlicka, O. Cip, "Absolute frequency shifts of iodine cells for laser stabilization" Metrologia, Vol. 46(5), pp. 450–456 (2009).
7. J. Hrabina, F. Petru, P. Jedlicka, O. Cip, J. Lazar, "Purity of iodine cells and optical frequency shift of iodine-stabilized He–Ne lasers" Optoelectronics and Advanced Materials-Rapid Communications, Vol. 1(5), pp. 202–206 (2007).

Paper D-O-4

MEASUREMENT OF SENSORS WITH FIBER BRAGG GRATINGS BY LASER INTERFEROMETER

Bretislav Mikel, Martin Cizek, Simon Rerucha, Ondrej Cip

Institute of Scientific Instruments, v.v.i., Academy of Sciences of the Czech Republic, Kralovopolska 147, 612 64 Brno, Czech Republic

mikel@isibrno.cz

We present method of measurement of fiber Bragg gratings (FBG) stretching by laser interferometer. We are oriented to research, development and to methodology of the production and application of FBGs. The elongation of FBGs can calculated from frequency drift of the Bragg resonance wavelength and from the change of the grating period during stretching. The inhomogeneity of optical fibers and of the FBGs can induce change of the grating period (Bragg resonance wavelength) of FBG which can be nonlinear with elongation of the optical fiber with FBG. Setup of the measurement of elongation of FBGs is in Fig. 1. The calibration of FBGs will be used for preparation and for the realization of the technology of measurement of shape deformation of concrete buildings.

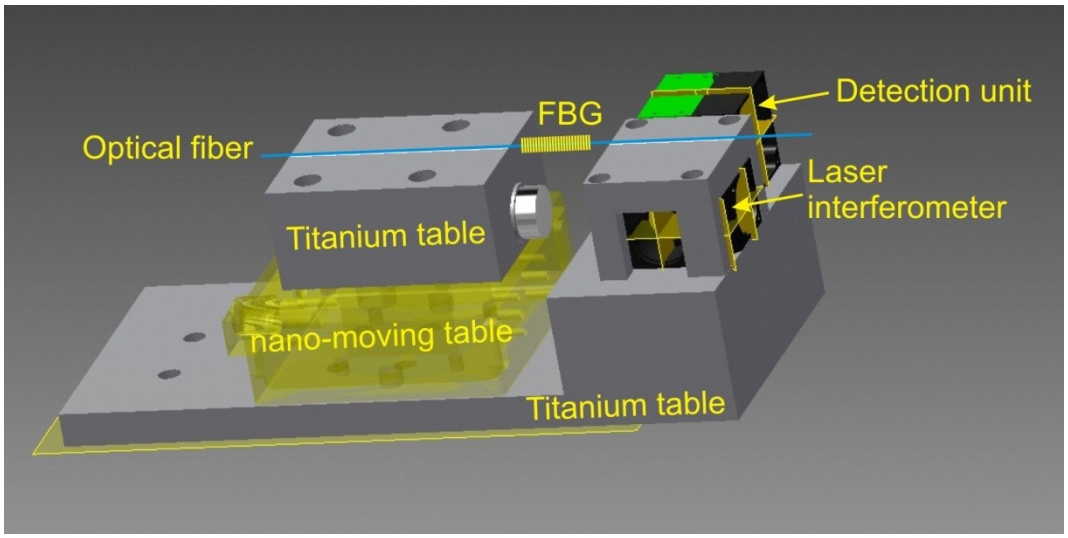

Fig. 1. Setup of the measurement of elongation of FBGs.

Keywords: fiber Bragg sensors, laser interferometry, optical spectrum analysis, fiber sensors.

Acknowledgements: The authors wish to express thanks for support to institutional support RVO:68081731, grant projects from the European Commission and Ministry of Education, Youth, and Sports of the Czech Republic, project No. CZ.1.05/2.1.00/01.0017 and Technology agency of the Czech Republic, projects No. TA01010995 and TA03010835.

Paper D-O-5

REMOTE MEASUREMENTS OF TROPOSPHERIC AEROSOL DISTRIBUTION BY A PORTABLE BACKSCATTER LIDAR

K.R. Allakhverdiev[1,2], M.F. Huseyinoglu1, A. Secgin[1], U. Cotuk[3]

[1]*TÜBİTAK Marmara Research Center, Materials Institute, P.O. Box 21, 41470 Gebze/Kocaeli, Turkey*
[2]*Azerbaijan National Academy of Aviation, Bina 25th km., Baku 1045, Azerbaijan*
[3]*Gebze Institute of Technology, Department of Physics, P.O. Box 141, Gebze/Kocaeli, Turkey*

fatih.huseyinoglu@tubitak.gov.tr

Aerosols have significant impact on the earth's radiation budget, however the uncertainty in the level of their understanding is relatively high. Light detection and ranging (lidar) technique has been a prominent tool in the increase of knowledge on aerosols for the past 20 years.

This presentation aims to show the possibility of using a backscatter lidar to measure the vertical distribution of tropospheric aerosols allowing to be able to make measurements at different locations.

A portable two wavelength backscatter lidar has been designed, developed and installed at TUBITAK MRC, KA09 Laser and Lidar Laboratory to study the vertical distribution of aerosols in 2012 and extensive measurements were taken during May to September 2013 in selected locations around Gebze region. The technical details of the lidar system are as follows. Transmitter is a Quantel Brilliant B Nd:YAG laser which emits 6 ns, 9 W average power pulses at 1064 nm and 5 ns, 4.5 W average power pulses at 532 nm wavelengths. The 8 mm beam is expanded to 40 mm by a homemade beam expander. Receiver is a 200 mm main mirror Cassegrain telescope with 200 cm focal length. Spectrum analyzer have 3 channels, 1064 nm elastic signal and 532 nm parallel and perpendicular polarization signals which are then converted to electrical signal by Hamamatsu photomultiplier tubes (PMT) and recorded by Licel Transient Recorder TR40-160. Custom made DataProcessing® software allows us to draw colormaps which show the vertical distribution of aerosol layers as seen in the Fig. 1 (please note that the colormaps are converted to black and white format).

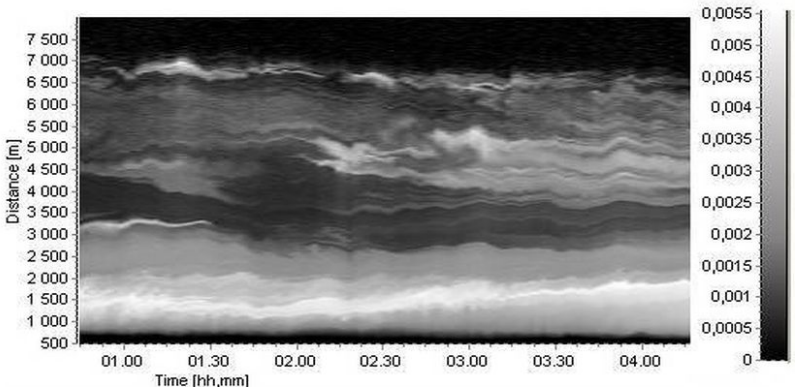

Figure 1. Backscatter colormap of aerosol layers over Gebze measured at 1064 nm for over a period of 4 hr at night. The axes can be described as follows: left axis is the distance in meters, right axis is the backscatter coefficient in m^{-1}, and the horizontal axis is time in hours. The measurement was realized at 20 degrees to the horizon, so the 7.000 m distance on the left axis corresponds to 2.394 m height.

Paper D-O-6

EFFICIENT LIGHT SCATTERING AND PHOTOLUMINESCENCE IN SILICON NANOPARTICLES FORMED VIA LASER ABLATION IN WATER, LIQUID NITROGEN AND HELIUM

S.V. Zabotnov[1], D.M. Zhigunov[1], F.V. Kashaev[1], P.D. Agrba[2], M.Yu. Kirillin[2], E.A. Sergeeva[2], L.A. Golovan[1], P.K. Kashkarov[1]

[1]M.V. Lomonosov Moscow State University, 1/2 Leninskie Gory, Moscow, 119991 Russia
[2]Institute of Applied Physics RAS, 46 Uljanov str., Nizhny Novgorod, 603950 Russia

zabotnov@physics.msu.ru

Nowadays ensembles of silicon nanoparticles produced by the laser ablation method are of special interest owing to possibility of their use as contrasting agents in the optical tomography [1] and photosensitizers in the photodynamic therapy [2]. However, currently the optical properties of such nanoparticles have not been studied fully yet.

The suspensions and powders of silicon nanoparticles produced by means of pico- and femtosecond laser ablation in water, liquid nitrogen and helium were studied by elastic and non-elastic light scattering and photoluminescence techniques.

The nanoparticles formed in water under picosecond laser irradiation vary in size from 2 to 200 nm accordingly microscopy analysis. The water suspensions with such nanoagglomerates were studied by spectrophotometry. Measurements of collimated transmission, total transmission and diffuse reflectance for silicon-water suspension allowed evaluation of scattering coefficient of the suspension as $\mu_s \sim 1$ cm^{-1} in the visible range at nanoparticle concentration of $n \sim 10^{13}$ cm^{-3}. Scattering was found to be sufficiently non-Rayleigh.

The obtained results allowing consider silicon nanoparticles as contrasting agents in the optical tomography. Pilot experiments on optical coherent tomography (OCT) imaging of a nanocrystal suspension drop on agar gel surface were performed. We observed significant increase in the OCT-signal from the areas of presence of nanocrystals.

The Raman scattering microscopy revealed crystalline phase (line 520.5 cm^{-1}) for nanoparticles formed both in helium and in liquid nitrogen. This result is especially important when nanoparticles have size less than 5 nm. The presence of such fractions was confirmed via microscopy analysis for both cases.

The photoluminescence spectroscopy of the silicon nanocrystal powders formed in liquid nitrogen and helium by the femtosecond laser irradiation revealed pronounced peaks at 750 nm (1.65 eV). This value is close to the energy of molecular oxygen transition from the $^3\Sigma$ state to the $^1\Sigma$ state (1.63 eV). Thus, the mentioned silicon nanocrystals can facilitate the production of singlet oxygen via energy transfer (under irradiation) to the oxygen molecules adsorbed on the surface.

Acknowledgements: This work was supported by Russian Foundation for Basic Research (projects 12-02-33033, 13-02-90424 and 11-02-01129).

References:

1. A. Krajnov, A. Mokeeva, E. Sergeeva, et al., "Nanoparticles as contrasting agents in diffuse optical spectroscopy", Proc. SPIE, Vol. 8699, 86990Q-1–86990Q-8 (2013).
2. D. Rioux, M. Laferriere, A. Douplik, et al., "Silicon nanoparticles produced by femtosecond laser ablation in water as novel contamination-free photosensitizers" J. Biomed. Opt., Vol. 142, 021010-1–021010-5 (2009).

Paper D-P-1

THE EVALUATION OF OVEREXERTION IN KANGOO JUMPS PROGRAM USING SPECTROSCOPIC MEASUREMENTS

C. Achim[1], M. Patachia[1], S. Banita[1,2], M. Petrus[1], A.M. Bratu[1], C. Matei[1], D.C. Dumitras[1,2]

[1]National Institute for Laser, Plasma and Radiation Physics, 409 Atomistilor St., PO Box MG-36, 077125 Bucharest, Romania

[2]University Politehnica of Bucharest, Faculty of Applied Sciences, Romania

cristina.achim@inflpr.ro

Abstract: Laser photoacoustic spectroscopy (LPAS) is growing quickly in its applications to real world problems (one of the problems is to prevent obesity) and it is a candidate technology for the breath analysis applications [1, 2].

Ongoing research is aim to investigate the evaluation of oxidative stress in females practicing Kangoo Jumps program.

Running is one of the earliest and simplest types of aerobic activity. The combination of science and technology has lead to the evolution of new forms of running. Kangoo Jumps boots are an example of a new technology that is continuing the evolution of this age-old activity and is defined to be the newest way to getting rid of stress. These boots are designed to dissipate the impact forces experienced through the ankles, knees, hips and back [2]. Due to the reduced impact of running with the use of the Kangoo Jumps, it is also hypothesized that subjects wearing running shoes will have a greater incidence of injury than those wearing Kangoo Jumps. The question that arises is, how effectively can subjects defend against the increased free radicals resulting from this type of aerobic? There has not been any literature published which has investigated the use of Kangoo Jumps for the risks of oxidative stress capacity [2].

Because it is not possible to directly measure free radicals in the body, we approach this question by measuring the by-products (breath ethylene) that result from free radical reactions.

Breath samples were collected and analyzed from 10 subjects (females) following an experimental set-up with a PA cell in an external configuration with a low power CO_2 laser. All measurements were done at 10P (14) line of a continuous wave CO_2 laser.

We found out that the mixture of exhaled breath in females after the Kangoo Jumps program contains low concentration of ethylene compared to exhaled breath of females before the start of exercise program. This result can give valuable information on the increased antioxidant defenses and may contribute to reduce the generation of pro-oxidants during and after Kangoo Jumps program.

References:

1. C. Popa, A. M. Bratu, C. Matei, R. Cernat, A. Popescu, D.C. Dumitras, Laser Physics, Vol. 21, p. 1336 (2011).
2. D. C. Dumitras, D. C. Dutu, C. Matei, R. Cernat, S. Banita, M. Patachia, A. M. Bratu, M. Petrus, C. Popa, Laser Physics, Vol. 21, p. 796 (2011).
3. http://kangooclubsouthbay.com/12-weeks.html
4. R.J. Bloomer, A.H. Goldfarb, Can. J. Appl. Physiol., Vol. 29, p. 245 (2004).

Paper D-P-2

SMALL DISPLACEMENT EVALUATION BY A HIGHLY-COHERENT TUNABLE LASER REFERENCED TO STABILIZED FEMTOSECOND COMB

Ondřej Čip, Radek Šmid, Jan Hrabina, Martin Čižek, Vaclav Hucl, Adam Lešundak, Miroslava Hola, Bohdan Růžička, Josef Lazar

Institute of Scientific Instruments, v.v.i., Academy of Sciences of the Czech Republic, Kralovopolska 147, 612 64 Brno, Czech Republic

ocip@isibrno.cz

The work describes the method for precise detection of length changes by a passive optical resonator working as a length sensor. The method is based on spectroscopy technique where a highly-coherent tuneable laser working at 1541 nm is locked to a selected mode of the optical resonator comb spectrum. Thus, the length change of the resonator is transformed to change of the optical frequency of the laser during the measuring process. The length of the resonator is kept by a spacer made from an ultra low expansion ceramic. If a temperature cycling of the spacer inserted in a vacuum chamber is done then the inspection of the coefficient of thermal expansion (CTE) of the ceramic is possible. The optical frequency of the tuneable laser identifies the length changes of the spacer during the temperature cycling. A precise detection of the optical frequency of the tuneable laser is required at kHz level. A down conversion processing must be applied to transfer the optical frequency to radiofrequency domain. Measurement of a beat-note signal between this laser and an optical frequency synthesizer – femtosecond comb solves this task well. In this case, the beat-note is detected with a period of repetition rate of the femtosecond comb laser. The described method is able to detect changes of the length in subnanometer level but with the range of micrometers. The work presents measured data of CTE and some records of measured beat-notes during the temperature cycling of the spacer.

Acknowledgements: The authors wish to express thanks for support to the grant project from the Grant Agency of CR, project GAP102/10/1813. The work uses an infrastructure funded by Academy of Sciences of CR, project: RVO:68081731, Ministry of Education, Youth and Sports of CR, project: CZ.1.05/2.1.00/01.0017, European Social Fund and National Budget of the Czech Republic, project: CZ.1.07/2.4.00/31.0016.

References:

1. O. Čip, F. Petrů, Z. Buchta, J. Lazar, "Small displacement measurements with subatomic resolution by beat frequency measurements" Meas. Sci. Technol., Vol. 18, pp. 2005–2013 (2007).
2. T. Udem, R. Holzwarth, M. Zimmermann, et al., "Optical frequency-comb generation and high-resolution laser spectroscopy" Topics in Applied Physics, Vol. 95, pp. 295–316 (2004).
3. H.R. Telle, G. Steinmeyer, A.E. Dunlop, J. Stenger, D.H. Sutter, U. Keller, "Carrierenvelope offset phase control: A novel concept for absolute optical frequency measurement and ultrashort pulse generation" Applied Physics B, Vol. 69, pp. 327–332 (1999).
4. R. Šmid, O. Čip, M. Čižek, B. Mikel, J. Lazar, "Conversion of stability of femtosecond mode-locked laser to optical cavity length" IEEE Transactions on Ultrasonics, Ferroelectrics and Frequency Control, Vol. 57(3), pp. 636–640 (2010).

Paper D-P-3

METHOD OF MEASUREMENT OF INTRAOCULAR LENSES OPTICAL CHARACTERISTICS

A.S. Goncharov, Y.V. Pankratova, N.G. Iroshnikov, A.V. Larichev

Faculty of Physics of M.V.Lomonosov Moscow State University, Leninskie Gory 1/2, Moscow 119991, Russia

goncharov@bk.ru

Visual acuity reduction caused by a cataract is the surgical indication for replacement of the crystalline lens with an intraocular lens (IOL) to restoration of visible light focusing on a retina. Today many types of IOL differing in a form, size, material of which they are made, weight, color, methods of fixing in an eye, etc. are used. For each patient must make an individual selection of the IOL with optimal optical performance.

The Shack-Hartmann method is most popular for an experimental evaluation of IOL optical characteristics. But the method can be inefficient for measurement of multifocal IOL. High gradients of the wavefront in transition areas between various optical force segments [1] lead to noticeable errors and therefore unreliable results. Increase lenslet density and use of Fourier-demodulation [2] is also difficult because in the transition areas may not be adiabatic condition [3]. A widely used algorithms using Fourier integration [4] are very sensitive to the boundary conditions and phase dislocations.

We have developed a new method for measuring the optical characteristics of the IOL. In particular, the ultradense lenslet for optical transformation was used. Demodulation was performed by filtration in spatial area with insignificant influence of aperture effects. Algorithms of digital segmentation were applied to allocation of areas with various optical characteristics.

We performed measurements on the eye model with the requirements of the international standard ISO11979-2. Comparative research of optical characteristics of the set of various types IOL was performed. The data on the evaluation of the IOL optical characteristics can be used in ophthalmology to describe, organize, developing new types of IOL and optimize individual patient selection.

Acknowledgements: This work was supported by the Russian Foundation for Basic Research (project No. 12-02-31265).

References:

1. J. Schwiegerling, E. DeHoog, “Problems testing diffractive intraocular lenses with Shack–Hartmann sensors” Applied Optics, Vol. 49, Issue 16, D62-D68 (2010).
2. C. Canovas, E. Ribak, “Comparison of Hartmann analysis methods” Applied Optics, Vol. 46, 1830-5 (2007).
3. Y. Carmon, E. Ribak, “Phase retrieval by demodulation of a Hartmann-Shack sensor” Optics Communications, Vol. 215, Issue 4–6, pp. 285–288 (2003).
4. A. Talmi, E. Ribak, “Direct demodulation of Hartmann-Shack patterns” J. Opt. Soc. Am. A, Vol. 21, pp. 632–639 (2004).

Paper D-P-4

TRANSLATION DIFFUSION COEFFICIENT FEATURES OF SERUM BLOOD MAIN PROTEINS IN MODEL SYSTEMS

I.M. Papok[1], G.P. Petrova[1], K.A. Anenkova[1], E.A. Papish[2]

[1]*Department of Molecular Physics, Faculty of Physics, Moscow State University, Moscow, 119991 Russia*
[2]*Department of Radiology, Russian Medical Academy of Postgraduate Education, Moscow, 125284 Russia*

petrova@phys.msu.ru

Abstract: Photon correlation spectroscopy was used to investigate the various dynamic processes in blood serum solution. These processes were induced by directional changes of the surface charges of macromolecules and its concentration in the solution. We suggest that the obtained associations between the translational diffusion coefficient value (Dt) and the medium pH value, as well as the protein concentration value, indicate the possibility of using the dynamic light scattering method for the effective diagnosis of widespread diseases, including cardiovascular pathology and cancers.

Keywords: bovine serum albumin, gamma globulin, bloodserum solution, photon correlation spectroscopy, dynamic light scattering, correlation function.

Significant changes of the translational diffusion coefficient values in the model solutions of blood serum were obtained by the use the photon correlation spectroscopy method. Results of our research indicate that the concentration dependences of translational diffusion coefficients measured for model [1] systems solution substantially differ between “healthy” and “sick” model samples. In particular, the pH dependence translational diffusion coefficient is characterized by minimum values of the coefficient in common isoelectric point of solutions. The dependence between the translational diffusion coefficient and the concentration value is characterized by alterations in the slope concentration dependence ratio. We believe that the method of dynamic light scattering could be applied as a diagnostic tool for the analysis of blood serum. It is important that the use of this method as a diagnostic tool is advantageous due to its very fast measurement speed (approximately 1 minute for one sample) and small requirement for serum. This approach may possibly be utilized for the early diagnosis of certain diseases, including cancer.

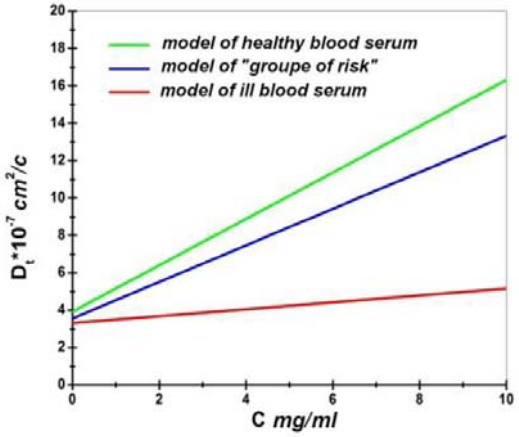

Fig. 1. The difference between concentration diffusion coefficient dependencies slope for model systems.

References:

1. Laser Physics, Vol. 19, No. 6, pp. 1303–1307 (2009).

Paper D-P-5

COMPUTATIONAL APPROACH TO INTERFERENCE PHASE DETECTION AND LINEARITY ERROR CORRECTION IN LASER INTERFEROMETRY

Simon Rerucha, Martin Sarbort, Zdenek Buchta, Ondrej Cip, Josef Lazar

Institute of Scientific Instruments of the ASCR, Kralovpolska 147, 61264 Brno, CZ

res@isibrno.cz

Although the laser interferometry represents the most precise class of techniques in the field of precise measurement of geometrical quantities, its wide use in measurement systems is still accompanied by many unresolved challenges. One of these challenges it the complexity of underlying optical systems that makes the interferometry systems very sensitive and expensive devices.

We present a novel approach to the interference phase detection in homodyne laser interferometry that aims at reduction of the optical complexity while the resolution is preserved. Our method employs a series of computational steps to infer a pair of signals in quadrature that allows to determine the interference phase with a sub-nanometre resolution from an interference signal from a non-polarising interferometer sampled by a single photodetector. The data processing covers a the phase detection as well as several error-correction and scale linearization techniques. The complexity trade-off is the use of laser beam with frequency modulation capability.

The method was experimentally evaluated on a Michelson interferometer-based free-space setup and its performance has been compared to a traditional homodyne detection method.The results indicate the method is a feasible alternative for the traditional homodyne detection since it performs with comparable accuracy (< 0.5nm standard deviation), especially where the optical setup complexity is principal issue and the modulation of laser beam is not a heavy burden, for instance in multi-axis measurement systems or laser diode based systems.

Acknowledgements: The authors wish to express thanks for the support of the GACR, project GAP102/10/1813, the research intent RVO: 68081731 and EU supported projects No. CZ.1.05/2.1.00/01.0017 and CZ.1.07/2.3.00/30.0054. Experimental tasks were supported by the Ministry of Industry and Commerce, projects FR-TI2/705 and FR-TI1/241.

References:

1. O. Cip, B. Mikel, J. Lazar, “Fast wavelength-scanning interferometry technique with derivative detection of quadrature signals - art. No. 61881F”, Proc. SPIE, Vol. 6188, F1881-F1881 (2006).
2. S. Rerucha, Z. Buchta, et al., “Detection of interference phase by digital computation of quadrature signals in homodyne laser interferometry”, Sensors, Vol. 12, pp. 14095–14112 (2012).
3. Z. Buchta, S. Rerucha, et al., “Novel Principle of Contactless Gauge Block Calibration”, Sensors, Vol. 12, pp. 3350–3358 (2012).
4. J. Lazar, M. Hola, et al., “Displacement interferometry with stabilization of wavelength in air” Optics Express, Vol. 20, pp. 27830–27837 (2012).
5. J. Hrabina, J. Lazar, et al., “Frequency noise properties of lasers for interferometry in nanometrology” Sensors, Vol. 13, pp. 2206–2219 (2013).

Paper D-P-6

THE NARROW-BAND TUNEABLE OPTICAL FILTER FOR BEAT-NOTE DETECTION BETWEEN SINGLE-FREQUENCY AND MODE-LOCKED LASER

Bohdan Růžička, Ondřej Číp, Radek Šmíd, Jan Hrabina, Martin Čížek, Václav Hucl, Adam Lešundák, Miroslava Holá, Josef Lazar, Břetislav Mikel

Institute of Scientific Instruments, v.v.i., Academy of Sciences of the Czech Republic, Královopolská 147, 612 64 Brno, Czech Republic

ruzicka@isibrno.cz

Some spectroscopic applications use an optical mixing of a single frequency tuneable laser and a femtosecond mode-locked laser when a precise value of the optical frequency of the tuneable laser has to be detected. The mode-locked laser has a broadband optical frequency spectrum which consists of thousands frequency modes (teeth). They are placed in an equidistant frequency spacing determined by a repetition frequency of femtosecond pulses, typically hundreds of MHz. When the optical mixing is done between this mode-locked laser and the single frequency one, the beat-note radiofrequency spectrum in the output of a photo detector is completely overloaded by many beat-notes came from mixing of the mode-locked laser modes themselves. This problem can be solved only by an optical filtering where frequency modes of the mode-locked laser farer from the single-frequency laser frequency are suppressed. Then only a small group of mode-locked laser modes is optically mixed between them. Our work presents an experimental setup with a fibre Bragg grating as the filter where only the narrow-band optical spectrum from the mode-locked laser is reflected to the beat-note processing with the single frequency laser. The grating has temperature control to change the reflecting optical frequency bandwidth to the desired value where the single-frequency laser operates. Examples of detected beat-notes are presented and evaluated.

Acknowledgements: The authors wish to express thanks for support to the grant project from the Grant Agency of CR, project GAP102/10/1813. The work uses an infrastructure funded by Academy of Sciences of CR, project: RVO:68081731, Ministry of Education, Youth and Sports of CR, project: CZ.1.05/2.1.00/01.0017, European Social Fund and National Budget of the Czech Republic, project: CZ.1.07/2.4.00/31.0016.

References:

1. T. Udem, R. Holzwarth, M. Zimmermann, et al., “Optical frequency-comb generation and high-resolution laser spectroscopy” Topics in Applied Physics, Vol. 95, pp. 295–316 (2004).
2. R. Šmíd, O. Číp, M. Čížek, B. Mikel, J. Lazar, “Conversion of stability of femtosecond mode-locked laser to optical cavity length” IEEE Transactions on Ultrasonics, Ferroelectrics and Frequency Control, Vol. 57(3), pp. 636–640 (2010).
3. H.R. Telle, G. Steinmeyer, A.E. Dunlop, J. Stenger, D.H. Sutter, U. Keller, “Carrier-envelope offset phase control: A novel concept for absolute optical frequency measurement and ultrashort pulse generation” Applied Physics B, Vol. 69, pp. 327–332 (1999).
4. O. Číp, F. Petrů, Z. Buchta, J. Lazar, “Small displacement measurements with subatomic resolution by beat frequency measurements” Meas. Sci. Technol., Vol. 18, pp. 2005–2013 (2007).

Paper D-P-7

MANIFESTATION OF DIFFRACTION EFFECTS IN MULTIBAND MULTIPIXEL DIAMOND-BASED PHOTODETECTORS

V.A. Shepelev, A.A. Altukhov, V.S. Feshchenko

Ltd "Industrial-Technological Center "UralAlmazInvest", 4 Ivana Franko st., Moscow, Russia

valq2006@rambler.ru

With the development of numerous applications of photodetectors, such as laser technologies, medicine and others, the problems of expansion of the photodetector spectral response, miniaturization of their sizes, increasing of the multipixel photodetector format, and reduction of the pixel sizes, assume an important significance. However, the increase in the number of photodetector individual spectral bands impedes the improvement of other parameters. This problem, as well as the problem of expanding the spectral range to the UV region, can be solved by designing and creation of a photodetector with a diamond [1] layer that is sensitive to the UV radiation. In the development of this photodetector the optical losses associated with the diffraction of the incident radiation should be taken into account.

A multiband multipixel photodetector is developed in "ITC "UralAlmazInvest" with applying of a 2a-type diamond crystal. Technology of the photodetector fabrication implies the layerwise detection of incident radiation of different spectral bands. The idea of the layerwise detection is widely applied in various multiband photodetectors due to relative availability of relevant semiconductor device fabrication planar technologies [2]. The electrode structure of multiband photodetectors is arranged for the signal registration in different photodetection bands. Resulting from the spacing of electrodes on different planes, diffraction of the detected radiation can be one of disadvantages of such multiband photodetectors. This drawback can play an important role in operation of imaging systems that are based on multiband photodetectors. Traditionally, an imaging system is segregated on independent optical and photo-electronic systems [3]. In fact, the optical system of a multiband imaging system is closely related to the individual photosensitive layers of a planar multiband photodetector.

Evaluation of the diffraction losses shows their low importance for the photodetectors developed by "ITC "UralAlmazInvest" with the following characteristics at a diamond plate of the 250-μm thickness: the pixel size and pitch are 20 and 30 μm, correspondingly, the long-wavelength edge of the spectral range is less than 1.2 μm. However, it should be noted that in general case of development of multipixel multiband photodetectors one has to model the diffraction losses with optimization of such photodetector parameters, as the thickness of a diamond plate, parameters of the pixel structure, and parameters of possible additionally-fabricated graphitized objects inside a diamond volume.

References:

1. V.S. Feshchenko, A.A. Altukhov, A.Yu. Mityagin, N.Kh. Talipov, V.A. Shepelev, "A 128×128 pixel ultraviolet photodetector based on a diamond sensor" Journal of Communications Technology and Electronics, Vol. 55, pp. 716–719 (2010).
2. A. Rogalski, "Recent progress in infrared detector technologies" Infrared Physics & Technology, Vol. 54, pp. 136–154 (2011).
3. I.P. Torshina, "Kompyuternoe modelirovanie optiko- elektronnyh sistem pervichnoy obrabotki informatsii". Moscow: Logos, 2009.

SECTION LM

Laser-Matter Interaction

Paper LM-I-1

BEYOND THE DIFFRACTION LIMIT: 3D NANOSTRUCTURING USING ULTRAFAST LASERS

M. Farsari

IESL-FORTH, N. Plastira 100, 70013, Heraklion, Crete, Greece

mfarsari@iesl.forth.gr

We present our most recent results into the fabrication of 3D nanostructures using Direct Laser Writing (DLW). These include:

1. The redox multiphoton polymerization of an organic-inorganic composite material, in which one of the components, a vanadium organometallic complex, also acts as a photoinitiator [1]. The composite employs multiphoton absorption to self-generate radicals by photo-induced reduction of the metal species from Vanadium (V) to Vanadium (IV) (Fig. 1a).

2. A new approach to hard tissue regeneration based on the mineralization of 3D scaffolds made using lasers [2]. To this end, we report the rational design of aspartatecontaining self-assembling peptides targeted for calcium binding. We further investigate the suitability of these peptides to support cell attachment and proliferation when coupled on a hybrid organic-inorganic structurable material (Fig. 1b).

3. Our investigations into the effect of porosity on pre-osteoblastic cell ingrowth of 3D biodegradable scaffolds fabricated by DLW [3]. The material we used is a purpose made photosensitive pre-polymer based on polylactide. We designed and fabricated complex, geometry-controlled 3D scaffolds with pore sizes ranging from 25 to 110 μm. We found a strong adhesion of the pre-osteoblastic cells from the first hours after seeding and a remarkable proliferation increase after 3 weeks and up to 8 weeks. Additionally, the PLA-based material indicated a 27% weight loss in six weeks, allowing enough time for the cells to develop a dense, 3D tissue matrix (Fig. 1c).

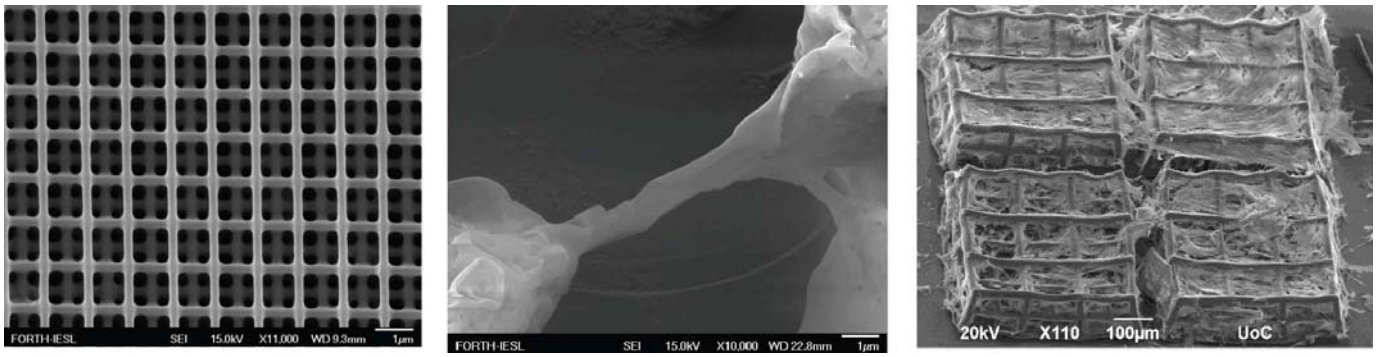

(a) (b) (c)

Figure 1. (a) 3D structures made by employing redox multiphoton polymerization. (b) Mineralized 3D scaffolds for bone tissue engineering. (c) Pre-osteoblastic cells on biodegradable scaffolds.

References:

1. E. Kabouraki et al., "Redox multiphoton polymerization for 3D nanofabrication", submitted.
2. K. Terzaki et al., "Mineralized self-assembled peptides on 3D laser-made scaffolds: A new route towards 'scaffold on scaffold' hard tissue engineering", submitted
3. P. Danilevicius et al., "The effect of porosity on cell ingrowth into 3D laser-fabricated biodegradable scaffolds for bone regeneration", submitted.

Paper LM-I-2

LASER MICROPRINTING OF LIQUIDS WITH SUB-PICOSECOND LASER PULSES

J.M. Fernández-Pradas, A. Patrascioiu, J.L. Morenza, P. Serra

Departament de Fisica Aplicada i Òptica, Universitat de Barcelona,
Marti i Franquès 1, 08028-Barcelona, Spain

jmfernandez@ub.edu

The laser printing of liquids through laser-induced forward transfer appeared as an alternative to the inkjet technique for the deposition of microdroplets with precision and control [1]. It allows the printing of liquids with a wide range of rheological properties and it requires little liquid engineering before the printing process. However, risks of material contamination and inhomogeneities in the deposited droplets arise from the step of preparing a liquid film precursor. These risks can be circumvented by directly transferring the microdroplets from a liquid reservoir.

Direct printing of the liquid from its reservoir can be done by strongly focusing a sub-picosecond laser pulse underneath the free surface of the liquid [2]. It has been demonstrated that there exists a focusing depth range which allows the deposition of well-defined, uniform microdroplets on the substrate [3]. Furthermore, very high degrees of reproducibility and resolution can be achieved.

Subsurface absorption of the laser radiation generates a cavitation bubble, which expansion and collapse promotes the formation of jets of liquid propagating away from the original surface (Fig. 1). In this way, the liquid can be gently deposited in the form of micrometric droplets on a substrate placed facing the liquid surface.

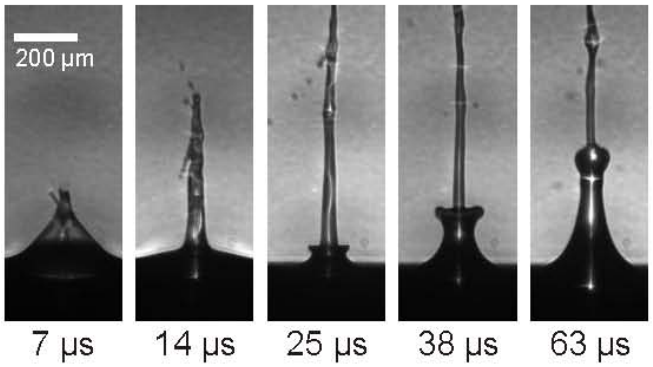

Figure 1 Time-resolved images of jets generated with sub-picosecond laser pulses.

Acknowledgements: This work is part of a research program funded by MCI of the Spanish Government (Projects MAT2010-15905 and CSD2008-00023), Fondo Europeo de Desarrollo Regional (FEDER), and by the European Commission (ICT: e-LIFT, Grant Agreement no. 247868)

References:

1. C.B.Arnold, P. Serra, A. Piqué, "Laser direct-write techniques for printing of complex material" MRS Bull., Vol. 32, pp. 23–31 (2007).
2. M. Duocastella, J.M. Fernández-Pradas, J.L. Morenza, D. Zafra, P. Serra, "Novel laser printing technique for miniaturized biosensors preparation" Sens. and Act. B, Vol. 145, pp. 596–600 (2010).
3. A. Patrascioiu, J.M. Fernández-Pradas, J.L. Morenza, P. Serra, "Microdroplets deposition through a film-free laser forward printing technique" App. Surf. Sci., Vol. 258, pp. 9412–9416 (2012).

Paper LM-I-3

DESIGN OF INTERFERENCE PATTERN USING COHERENT BEAMS

Yoshiki Nakata, Yoshiki Matsuba, Keiichi Murakawa, Noriaki Miyanaga

Osaka University, 2-6 Yamadaoka, Suita, Osaka, 565-0871 Japan

nakata-y@ile.osaka-u.ac.jp

A metamaterial consists of Meta-atoms in lattice has been fabricated by top-down methods such as lithography and ion beam figuring technique. On the other hand, we have been investigated the fabrication of nano-sized structures in lattice by interfering femtosecond laser technique. In the past experiments, a variety of metamaterials such as nanowhisker [3, 5], nanobump [3–5], MHA (metallic-hole array), nanodrop [3–5] have been fabricated. A shape of meta-atom reflect interference pattern, and it can be controlled by number of beam, phase and amplitude shift between the beams [1, 2]. Representative results will be presented.

(a) In the lower figure shows schematic illustrations of six beams correlation. (b) to (e) are the interference patterns with phase and amplitude shifts between the beams, which are explained in the illustration on each top. The six lower pictures are contour plots at different thresholds, where F_{th} is the ablation threshold and F_{max} is the highest fluence in an interference pattern (see right bottom in the figure). The wavelength and correlation angle are set to 785 nm and 14.6 degree. When a metal thin film target is processed by an interference pattern, gray region is ablated and black region remains. When phase shift π is applied to a beam, ladder pattern appears as shown in (b). It seems that periodic dots lie between lines, which corresponding to a metamaterial called "two-level cut-wire". In the case of (c) (i), double SRR (split-ring resonator) appears. (d) and (e) are cross and single SRR, respectively. We investigated combinations of interference parameters, and categorized the interference patterns into 21 patterns in the case of four beams correlation, and into 32 patterns in the case of six beams correlation [1, 2].

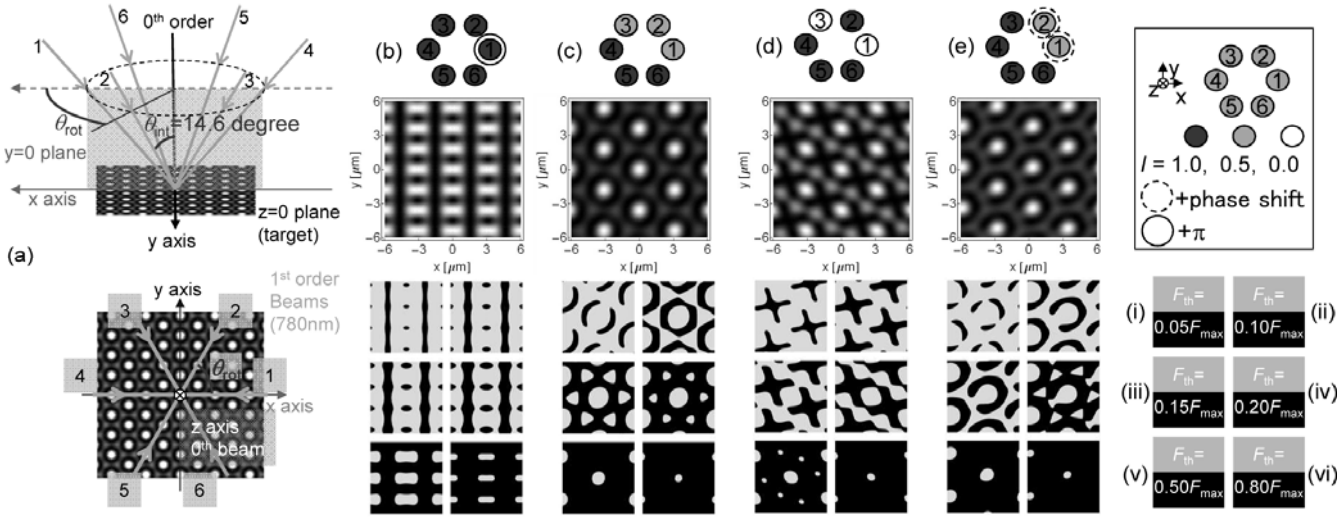

References:

1. Y. Nakata et al., "Design of interference using coherent beams configuring as a six-sided pyramid" Appl. Opt. Vol. 51, pp. 5004–5010 (2012).
2. Y. Nakata et al., "Designing of interference pattern in ultra-short pulse laser processing" Appl. Phys. A. (2012) [DOI: 10.1007/s00339-012-7239-1].
3. Y. Nakata et al., "Solid-liquid-solid process for forming free-standing gold nanowhisker superlattice by interfering femtosecond laser irradiation" Appl. Surf. Sci. Vol. 274, pp. 27–32 (2013).
4. Y. Nakata et al., "Nano-sized hollow bump array generated by single femtosecond laser pulse" Jpn. J. Appl. Phys. Vol. 42, pp. L1452–L1454 (2003).
5. Y. Nakata et al., "Generation of superfine structure smaller than 10 nm by interfering femtosecond laser processing", Proc. SPIE. 7920-10 (2011); Y. Nakata et al., "Frozen water drops in the nanoworld", SPIE newsroom. Published online, DOI: 10.1117/2.1200906.1708 (2009).

Paper LM-I-4

LOSSES OF ENERGY BY FS LASER RADIATION IN HIGHLY NONLINEAR MATERIAL (SILICON)

V.V. Kononenko

A.M. Prokhorov General Physics Institute, Moscow, Russia

vitali.kononenko@nsc.gpi.ru

For many years the necessity to develop devices for silicon-based photonics stimulates investigation of various techniques for silicon treatment and modification. In this work we have studied the reversible processes in silicon monocrystal bulk initiated by 250 fs laser irradiation. The wavelength of 1.2 μm of parametrically amplified light was chosen to exclude one-photon absorption.

High precision IR femtosecond interferometry has been used to measure the refractive index of changes in the irradiated zone. Using time series of interference images obtained in the experiments, we have reconstructed the laser pulse propagation and dynamics of the electron – hole plasma generated near the axis of a focused laser beam. Experimental data have been compared to relevant numerical simulation results obtained in a simple, two-photon absorption model. In order to measure the real beam intensity along the laser waist inside Si sample the original setup was developed.

Both experimental techniques have clearly revealed two features of fs pulse interaction with c:Si, which are quite important in terms of local light energy transfer inside the material bulk. Firstly, high intrinsic nonlinear (two-photon) absorption strongly limits light energy value that can be transfered and, consequently, deposited in material in the region of beam waist. It is shown that this effect is responsible for the observed anomalously high thresholds for damage of material structure. Secondly, inside silicon the strong filamentation has been found to hinder sharp light wave focusing that leads to poor energy localization in the beam waist. Two mechanisms that determine beam delocalization have been considered: strong kerr self-focusing and defocusing by e-h plasma filament which is featured by high transverse gradient of carriers density.

Acknowledgements: The authors acknowledge support from the Russian Foundation for Basic Research (Grant 13-02-00979).

Paper LM-I-5

LASER PRINTING OF METAL, SEMICONDUCTOR, AND DIELECTRIC NANOPARTICLE ARRAYS

B.N. Chichkov

Laser Zentrum Hannover e.V., Hollerithallee 8, 30419 Hannover, Germany

b.chichkov@lzh.de

I will report on our recent progress in the development of laser printing technologies for fabrication of complex nanoparticle structures. Fabrication, characterization, and sensing applications of the nanoparticle arrays will be demonstrated and discussed.

Paper LM-I-6

LASER THERMOCHEMICAL WRITING: INFLUENCE OF PHYSICAL PROCESSES ON RESOLUTION

V.P. Veiko[1], E.A. Shakhno[1], D.A. Sinev[1], M.V. Yarchuk[1], A.G. Poleshuk[2], V.P. Korolkov[2]

[1]*St.Petersburg State University of Information Technologies, Mechanics and Optics, 49 Kronverksky pr., 197101, St.Petersburg, Russia*

[2]*Institute of Automation & Electrometry Siberian Branch of Russian Academy of Sciences, 1 Acad. Koptjug pr., 630090, Novosibirsk, Russia*

veiko@lastech.ifmo.ru

The subject of the chapter is the thermochemical laser action (TLA), properly laser oxidation of the thin metal films. This subject was chosen because local laser oxidation of the thin metal films gives a unique opportunity to register an optical image on a thin films with a high resolution and without distortions specified for laser ablation [1]. The history of the invention of this method as well as it physics investigation is a quite typical for laser science field. From the other hand the unique high–tech application was developed based on TLA – it is the diffraction optical elements writing and special machine was created for these purposes – ring laser generator [2]. It permits to fabricate very complicated and specific DOE like null –corrector for the large (2 mirrors by 8.4 m diameter every) binocular telescope of Stuart observatory etc. Consecutively the possibilities to improve the spatial resolution of the thermochemical writing with the connection of the physical-chemical processes – short pulses action, thermochemical peaking, positive and negative feedbacks at the thermochemical action, diffusion less oxidation, structural changes, kinetic oxidation etc. [3, 4] are discussed.

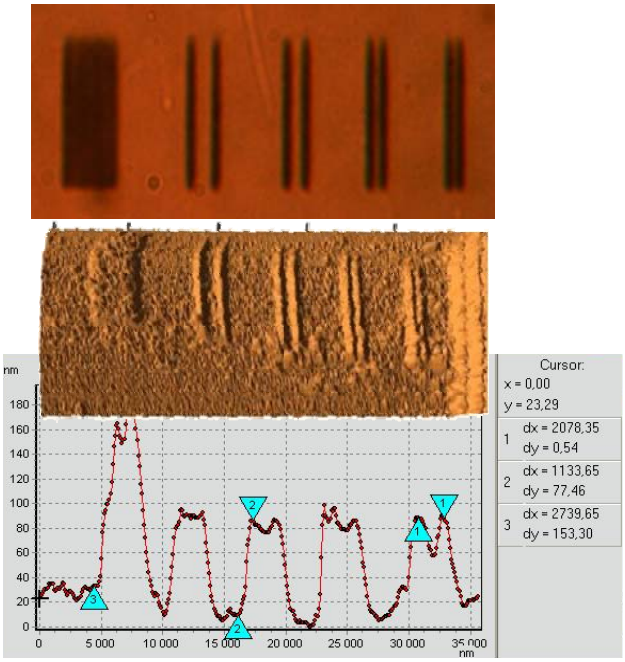

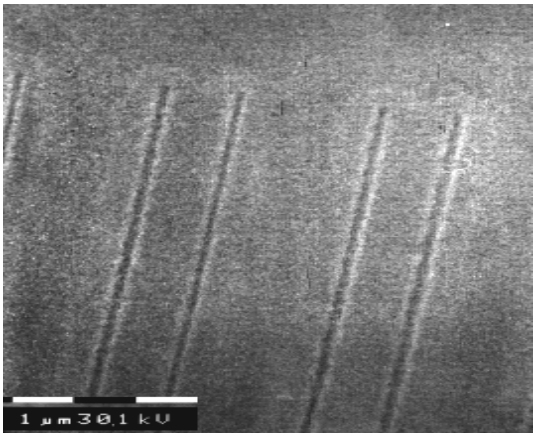

Electron photography of the surface area, with lines of width 200 nm and a period of 1.2 µm (up) and atomic–force microscopy image of similar sample (left)–*lines written by thermochemical technology at chromium film thickness of 50 nm.*

Acknowledgements: The work supported byRFBR Grants 12-02-00974 and 13-02-00033, Russian Federation President Grant for Leading Scientific School SS-619.2012.2 and Russian State Contract RSC № 14.B37.21.0144.

References:

1. V. Veiko, S. Metev, "Laser Assisted Microtechnology", Springer–Verlag, Heidelberg (1998).
2. A. Poleshchuk, "Techniques for formation of the surface profile of diffractive optical elements" Opt. Laser Eng. Vol. 29, No. 4–5, pp. 289–306 (1998).
3. V. Veiko, M. Yarchuk, A. Ivanov, "Diffusionless oxidation and structure modification of thin Cr films by the action of ultrashort laser pulses" Laser Phys. Vol. 22, No. 8, pp. 1310–1316 (2012).
4. V. Veiko, D. Sinev, E. Shakhno, A. Poleshchuk, A. Sametov, A. Sedukhin, "Peculiarities of multibeam laser thermochemical writing of diffraction microstructures" Comp. Opt. Vol. 36, No. 4, pp. 562–569 (2012).

Paper LM-I-7

EFFICIENT GLAA MICROWELDING BY DOUBLE-PULSE IRRAIATION OF FEMTOSECOND LASER

Koji Sugioka, Sizhu Wu, Katsumi Midorikawa

RIKEN, Wako, Saitama 351-0198, Japan

ksugioka@riken.jp

Efficient microwelding of glass substrates by irradiation by a double-pulse train of ultrafast laser pulses is demonstrated [1, 2]. The bonding strength of two photosensitive glass substrates welded by double-pulse irradiation was evaluated to be 22:9 MPa, which was approximately 22% greater than that of a sample prepared by conventional irradiation by a single-pulse train. Futher, we investigated dependence of delay time between 1st and 2nd pulse irradiation on the heat affected zone (HAZ) and the bonding strength (BS). Both HAZ and BS rapidly increased as the delay time increased from 0 ps to 12.5 ps, but they drastically decreased after 12.5 ps up to 30 ps. From 30 ps to 1–2 ns, they were almost saturated with a small peak at around 100 ps and were still larger than those for 0 ps. After 1–2 ns, they gradually decreased again, and finally both HAZ and BS at the delay time longer than 60 ns became smaller as compared with those for 0 ps. The rapid increase between 0 and 12.5 ps is responsible for individual control of each electron excitation process, i.e., multiphoton ionization or tunneling ionization by the 1st pulse followed by electron heating or avalanche ionization by the 2nd pulse. Namely, the 2nd pulse is efficiently absorbed by free electrons generated by 1st pulse, resulting in generation of higher-energy free electrons or more free electrons for efficient heating. The drastic decrease after 12.5 ps is ascribed to relaxation of the free electrons. The saturated but still higher HAZ and BS between 30 ps and 60 ns than those for 0 ps is due to the absorption of 2nd pulse by electrons trapped at the localized state such as self-trapped exciton. The pump-probe measurement of transient absorption supported these considerations. The detailed mechanism will be discussed based on electron excitation and relaxation processes.

References:

1. K. Sugioka, M. Iida, H. Takai, K. Micorikawa, “Efficient microwelding of glass substrates by ultrafast laser irradiation using a double-pulse train” Opt. Lett., Vol. 36, pp. 2734–2736 (2011).
2. S. Wu, D. Wu, J. Xu, Y. Hanada, R. Suganuma, H. Wang, T. Makimura, K. Sugioka, K. Midorikawa, “Characterization and mechanism of glass microwelding by double-pulse ultrafast laser irradiation” Opt. Express, Vol. 20, pp. 28893–28905 (2012).

Paper LM-I-8

FEMTOSECOND LASER SURFACE NANO- AND MICROFABRICATION AND APPLICATIONS

Andrey Ionin, Sergey Kudryashov, Sergey Makarov

Lebedev Physical Institute of Russian Academy of Sciences, 53 Leninsky pr., 119991 Moscow, Russia
aion@lebedev.ru

Surface nano- and micro-scale textures become more and more important bringing common materials new functionalities for tribological, optical (classical and metamaterial), solar energy and other applications. Femtosecond lasers have been proved to be very efficient in production of topological and chemical surface nano- and micro-textures.

This presentation provides an overview of our recent studies together with our Russian colleagues from the Belgorod State Univ (Belgorod), A.M. Prokhorov General Physics Institute of Russian Academy of Sciences (RAS)(Moscow), Institute of Automation and Electrometry, Siberian Branch of RAS (Novosibirsk) and A.N. Frumkin Institute of Physical Chemistry and Electrochemistry of RAS (Moscow) on femtosecond laser fabrication of nano- and micro-textures on surfaces of different materials (metals – Ti, Al, Au, Ni, steel; semiconductors – Si, GaAs, graphite; dielectrics – Al_2O_3, SiO_2) using Ti:Sapphire laser and Yb-doped fiber laser. Topographic and chemical surface characterization was performed by means of SEM and its EDS option.

Antireflective surface $\lambda/4$-layers in the form of surface diffraction gratings with sub-micron periods were fabricated directly on GaAs coupler (0.65 μm) and indirectly (through hot impressing of a Ni stamp with 0.47-μm grating) on PMMA optics surfaces, demonstrating their optical transmittance enhanced in IR range by tens percent. For a broad number of materials surface high-brightness colorizing diffraction gratings were produced via a new approach.

Hydrophilic surface nano- and micro-textures were produced on Ti surfaces being additionally modified by calcium hydroxyl appatite deposition, to provide their high biocompatibility to osteoblasts. In contrast, superhydrophobic surface nano- and microtextures were fabricated on dielectric and metal surfaces to make them self-cleaning.

Finally, nano- and micro-scale features were made on diverse material surfaces to work as cold electron emitters, totally absorbing targets for ultrastrong field laser physics, active elements for surface plasmonic optics, SERS substrates for nanophotonic sensing etc.

Acknowledgements: This research was supported by the Russian Foundation for Basic Research (Projects Nos. 11-02-01202-a, 11-08-01165-a, 12-02-13506 ofi-m-RA).

Paper LM-I-9

INVESTIGATION OF INTERFACE THERMAL RESISTANCE OF DIAMOND FILMS GROWN THROUGH LASER-ASSISTED COMBUSTION SYNTHESIS

J.-F. Silvain[1], T. Guillemet[1,3], J.L. Battaglia[2], A. Kusiak[2], A. Capella[2], J.M. Heintz[1], N. Chandra[4], Y.F. Lu[3]

[1]*Institut de Chimie de la Matière Condensée, ICMCB-CNRS, Université Bordeaux 1, Pessac, 33608, France*
[2]*Institut de Mécanique et Ingénierie, Dépt. TREFLE, Talence, 33400, France*
[3]*Department of Electrical Engineering,*
[4]*Department of Mechanical Engineering, University of Nebraska-Lincoln, Lincoln, NE 68588-0511*

Diamond films are attractive materials for passive applications in thermal management because of their high in-plane thermal conductivity and low thermal expansion coefficient. Although thermal conductivity of diamond films has been extensively investigated, there is still a need to evaluate the thermal resistance existing at interfaces between diamond films and engineering substrates such as silicon. Knowledge of the boundary thermal resistance is critical to a better understanding of the heat-transfer process occurring at the diamond film/substrate interface.

Diamond films were deposited on silicon and tungsten carbide substrates in open air through laser-assisted combustion synthesis. Laser-induced resonant excitation of ethylene molecules was achieved in the combustion process to promote diamond growth rate. In addition to microstructure study by scanning electron microscopy, Raman spectroscopy was used to analyze the phase purity and residual stress of the diamond films. High-purity diamond films were obtained through laser-assisted combustion synthesis. The levels of residual stress were in agreement with corresponding thermal expansion coefficients of diamond, silicon, and tungsten carbide. Diamond film purity increases while residual stress decreases with an increasing film thickness. Diamond films deposited on silicon substrates exhibit higher purity and lower residual stress than those deposited on tungsten carbide substrates.

Modulated infrared photo-thermal radiometry was employed to measure the thermal response of diamond films deposited on silicon substrates through laser-assisted combustion synthesis. The thermal resistance normal to the diamond/silicon interface was then estimated from the measurement of the phase and the amplitude of the thermal response. The diamond/silicon boundary resistance has previously been measured for diamond films grown through microwave-plasma assisted method. However no such data exists for the diamond films grown through laser-assisted combustion synthesis. Preliminary results show that the layered diamond/Si system exhibits an interfacial thermal resistance of about 2×10^{-8} $W\cdot K^{-1}$. The technique developed in this study enables a precise evaluation of the thermal resistance at the diamond/silicon interface and is promising for various thermal management applications of diamond thin-films in optics, electronics, or mechanics.

Keywords: combustion CVD diamond, silicon substrate, modulated infrared radiometry, interface, thermal boundary resistance.

Paper LM-I-10

DIRECT SURFACE NANOSTRUCTURING BY NS AND FS LASER PROCESSING

M. Sentis, Ph. Delaporte, D. Grojo, L. Charmasson, O. Utéza, N. Sanner

LP3 laboratory, CNRS - Aix-Marseille University, Campus de Luminy, 13288 Marseille, France

Sentis@LP3.univ-mrs.fr

Laser-matter interaction is a unique and simple approach to structure materials or locally modify their properties at the micro and nanoscale level [1]. Playing with the pulse duration and the laser wavelength, a broad range of materials and applications can be addressed. Direct irradiation of surfaces with laser beam through a standard optical beam setup allows an easy and fast structuration of these surfaces in the range of few micrometers. Nano-patterning of surfaces requires generally sophisticated approaches which are time consuming and need expensive technologies. In this presentation, two different approaches to achieve direct laser writing of nano-craters are described.

The first one is based on the irradiation with nanosecond laser pulses of materials through an array of dielectric nanospheres providing a unique opportunity to break the diffraction limit and to realize structures in the range of hundred of nanometers [2]. This simple, fast and low-cost near-field nanolithography technique will be presented and discussed, as well as its great potential. A specific study has been dedicated to the influence of the dispersion of the sphere diameter on the morphology of the ablation craters. This technique has been used for patterning of glass and silicon, as well as bi-layer substrates (metal on glass, SiO_2 on Si). In the latter case, the process leads to the formation of a nanoporous membrane which has been used to realize an array of gold nanodots on silicon [3].

The second one is based on the non linear interaction of ultrafast laser pulses with dielectrics. Surface ablation of fused silica is studied as a function of pulse duration (7–450 fs) and applied fluence ($F_{th} < F < 10\ F_{th}$, F_{th} being the ablation threshold fluence). We show that varying the pulse duration gives access to high selectivity (with resolution ~10 nm) for axial removal of matter but does not influence the transverse ablation selectivity, which only depends on the normalized applied fluence F/F_{th}. The ablation efficiency is shown to be inversely dependent to the pulse duration and saturates with respect to the applied fluence earlier at ultrashort pulse durations (≤30 fs). The deduced optimal fluence F_{opt} corresponding to the highest ablation efficiency for each pulse width defines two regimes of laser application. Below F_{opt}, the removed material depth can be accurately adjusted in a large range (~40–200 nm) as a function of the applied fluence and the morphology of the ablated pattern almost reproduces the Gaussian beam distribution. Above F_{opt}, the material removal depth tends to saturate and the morphology of the ablated pattern evolves to a top-hat distribution.

References:

1. A. Kabashin et al., “Nanofabrication with pulsed lasers” Nanoscale Res. Lett., Vol. 5, pp. 454–463 (2010).
2. D. Grojo et al. “Monitoring photonic nanojets from microsphere arrays by femtosecond laser ablation of thin films” Journal of Nanoscience and Nanotechnology, Vol. 11(10), pp. 9129–9135 (2011).
3. A. Pereira et al. “Laser-fabricated porous alumina membrane (LF-PAM) for the preparation of metal nanodot arrays” Small, Vol. 4, pp. 572–575 (2008).

Paper LM-I-11

PULSED LASER ABLATION OF COMPOUND SEMICONDUCTORS: VAPORIZATION MECHANISMS, CLUSTR GENERATION, EFFECTS OF METAL DOPING

A.V. Bulgakov[1,2], A.B. Evtushenko[1], Y.G. Shukhov[1], O.A. Bulgakova[1], V.P. Zhukov[3], M. Jadraque[4], M. Martin[4], N.M. Bulgakova[1,5]

[1]*Institute of Thermophysics SB RAS, 1 Lavrentyev Ave., 630090 Novosibirsk, Russia*
[2]*EaStCHEM, School of Chemistry, University of Edinburgh, EH9 3JJ, Scotland*
[3]*Institute of Computational Technologies SB RAS, 6 Lavrentyev Ave., 630090 Novosibirsk, Russia*
[4]*Instituto de Química Física "Rocasolano", CSIC, Serrno 119, 28006 Madrid, Spain*
[5]*Optoelectronics Research Center, University of Southampton, SO17 1BJ, United Kingdom*

bulgakov@itp.nsc.ru

Pulsed laser ablation (PLA) has proven to be an efficient and flexible method for synthesis of nanoclusters and nanostructures. However, controllable production of nanoclusters with desirable properties is still challenging, especially for multi-component materials when there is an additional parameter to control, cluster composition, which strongly affects cluster properties. This work is devoted to experimental and theoretical studies of nanosecond PLA of compound semiconductors (InP, ZnO, CdTe, Co-doped ZnS) important for various applications such as fabrication of solar cells and optoelectronic devices. Particular attention is given to characterization of the cluster formation process.

Detailed data on the ablation rate, the composition of the ablation plume and its expansion dynamics have been obtained as a function of laser fluence and wavelength. Neutral and cationic compound clusters of various stoichiometry have been produced in the gas phase and investigated using time-of-flight mass spectrometry. Analysis of the plume composition upon laser exposure has revealed congruent vaporization of ZnO while other studied materials exhibit a disproportional loss of the more volatile component. In addition, a delayed vaporization of phosphorus under InP ablation has been observed. The character of vaporization of semiconductors, congruent or incongruent, is found to affect strongly the composition of PLA-produced clusters. In particular, clusters observed under ZnO ablation are mainly stoichiometric whereas ablation of InP results in highly metal-rich clusters. Ablation of Co-doped semiconductors has been investigated in order to reveal synthesis ways for nanostructures with magnetic properties. The strongly non-equilibrium conditions inherent in PLA are shown to allow efficient generation of bimetallic thermodynamically stable clusters of different stoichiometry. Formation mechanisms of the observed clusters and possibilities to control their size and composition under PLA conditions are discussed.

Based on the analysis of abundances and velocities of the plume particles, we show that, depending on laser fluence, different mechanisms dominate in particle desorption/ablation from the irradiated surface. Two models have been developed to describe adequately the ablation process, electronic and thermal ones. The thermal model has been refined to account for material composition changing in a surface layer as a result of different volatility of the components. A model of non-thermal particle emission has been developed which assumes emission enhancement due to non-radiative recombination of the laser-induced *e–h* pairs. Modeling allows to get a deep insight into the complicated dynamics of melting and solidification processes of compound semiconductors.

Acknowledgements: This research is supported by the Marie Curie International Incoming Fellowship grant of the corresponding author, No. 302991, and by SB RAS, Integration Project No. 134.

Paper LM-I-12

CONTROLLED GROWTH OF ZnO NANOSTRUCTURED CRYSTALS BY NANOPARTICLE-ASSISTED PULSED LASER DEPOSITION AND THEIR LASING CHARACTERISTICS

Tatsuo Okada, Daisuke Nakamura, Tetsuya Shimogaki, Koto Okazaki, Hiroshi Ikenoue

Department of Electrical Engineering, Kyushu University, Fukuoka 819-0395, Japan

okada@ees.kyushu-u.ac.jp

ZnO is a II–VI wide band gap semiconductor with a direct band gap energy of 3.37 eV and a large exciton binding energy of 60 meV. It is abandon and bio-friendly materials. Low dimensional ZnO crystals such as nanowires, nanosheet and micro sphere and so on are especially attractive as the building blocks for the ultraviolet (UV) light emitting devices, because an optical function of the waveguide or the cavity can be realized self-organizing way without using the expensive and complicated micro-nano machining processes like optical lithography.

In this report, we present our recent progresses in the development of UV light emitting devices using the ZnO nanocrystals. A variety of low dimensional ZnO crystals is synthesized by the nanoparticles assisted pulsed laser deposition (NAPLD) [1] and the carbo-thermal method [2]. The synthesized crystals were characterized by a scanning electron microscope (SEM), a transmission electron microscope (TEM), the XPS analysis, the X-ray diffraction, a Raman spectroscopic system and the PL measurements. We have succeeded to achieve a patterned-growth on a ZnO buffer layed pre-patterned by the laser ablation. Using this method, we can grow patterned ZnO nanowalls on demand. Next, the lasing characteristics of the low dimensional ZnO crystals under optical excitation are described [3, 4]. Then we describe the laser processing, including laser annealing [5], laser doping for the realization of the *p*-type ZnO crystals.

Acknowledgements: A part of this work was supported by a Grant-in-Aid for Scientific Research from the Japan Society for the Promotion of Science (JSPS, No. 24656053) and Special Coordination Funds for Promoting Science and Technology from Japan Science and Technology Agency is also acknowledged.

References:

1. A.B. Hartant, X. Ning, Y. Nakata, T. Okada, Appl. Phys. A, Vol. 78, p. 299 (2004).
2. B.Q. Cao, K. Sakai, D. Nakamura, I.A. Palani, H.B. Gong, H.Y. Xu, M. Higashihata, T. Okada, J. Phys. Chem. C, Vol. 115, p. 1702 (2011).
3. K. Okazaki, D. Nakamura, M. Higashihata, P. Iyamperumal, T. Okada, Opt. Exp., Vol. 19, p. 20389 (2011).
4. K. Okazaki, T. Shimogaki, K. Fusazaki, M. Higashihata, D. Nakamura, T. Okada, Appl. Phys. Lett., Vol. 101, 211105 (2012).
5. T. Shimogaki, K. Okazaki, D. Nakamura, M. Higashihata, T. Asano, T. Okada, Opt. Exp., Vol. 20, p. 15247 (2012).

Paper LM-I-13

LASER-INDUCED NANOSTRUCTURED CLUSTERS: FUNCTIONALCAPABILITY FOR EXPERIMENTAL VERIFICATION OF MACROSCOPIC QUANTUM PHENOMENA

A. Antipov, S. Arakelian, S. Kutrovskaya, A. Kucherik, V. Prokoshev

Stoletov's Vladimir State University, Russia

arak@vlsu.ru

1. The main goal of our work is the laser-induced fabrication of nanostructured materials including the nano-and microclusters for control of electrical, optical and other properties for obtained structures. We showed an opportunity to select of particles in the sizes and weights and also, in topology distribution for some materials (carbon, Ni, PbTe, etc.).

   We used as well, a method of laser deposition metal (and/or oxide) nanoparticles from colloidal systems (LDPCS) to obtain the multilayered nanostructures with controlled topology including the fractal cluster structures (for Ni,Ag, PbTe, PbS et all) – see below the AFM-image figures (islet-like and spherical structures, microconnection of the particles).

2. In such a system can be two types of excitations, the configuration (structural) and the vibration (thermal), which are separated. An important parameter is, the definition of the surface energy, which characterizes the cluster energy and has a minimum for an optimal (hexagonal, in particular) structure. We will be interested in the question, how quantum phase transitions still appear in the some properties of macroscopic systems, located at finite temperature, for coupling particles (atoms) with a pair of interaction.

3. A correlated state for the system of nanoparticles occurs under conditions of «the energy trap» due to the surface effects, being the suppress factor for the temperature fluctuations for nanoparticles, organized in the cluster system.

4. The principal question to the quantum behavior development is, the estimation for effective mass for the de Broglie wavelength λ_B of a particle with mass m. E.g. for electrical transport properties of semiconductors the reduced coefficient for m is not more than 0.1, and results in the value $\lambda_B \geq 25$ nm, i.e. comparative with the cluster size. For quasi-particles with coupled states of different kind in collective phenomena the fact takes place, as well. So, nanoclusters can demonstrate the quantum behavior in some effects even for room temperature. The physically means that the characteristic energy ties more than the energy of thermal fluctuations, i.e. is not important in itself condition $T \rightarrow 0$, but the stability of the structure of the medium to the influence of temperature factors is a vital point. The fact is true for nonhomogenous structures with hollow structures under the particle tunnel effect development. For structures in the figures we demonstrated the superconductivity tendency to increase the electrical conductivity (in several times for our case) in comparison with homogenous sample, both at room temperature.

5. Such a generalization allows us to talk to nanoparticles on the conservation of correlation/coherence in cluster systems with dephasing length $l_{df} \sim \lambda_B$, also at high (room) temperature – analogue of the attraction between the atoms at low temperatures in the conditions of quantum states for condensed matter.

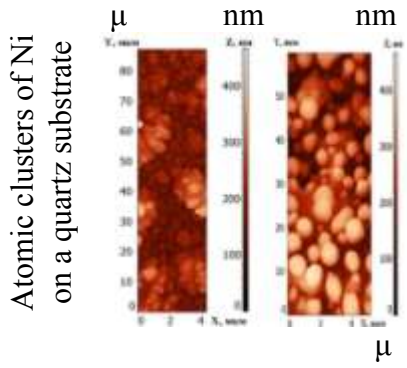

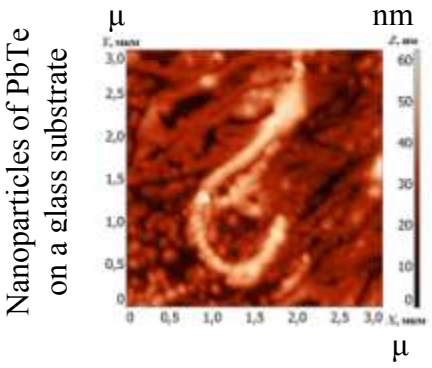

Paper LM-I-14

INTERACTION OF INTENSE FEMTOSECOND PULSES WITH LARGE MOLECULAR CLUSTERS: TOWARD BRIGHT X-RAY SOURCES

V.M. Gordienko[1], M.S. Dzhidzhoev[1], I.A. Zhvaniya[1], D.N. Trubnikov[2]

[1]*Physics Faculty and International Laser Center, M.V. Lomonosov Moscow State University, Russia*
[2]*Chemical Faculty, M.V. Lomonosov Moscow State University, Russia*

gord@phys.msu.ru

In recent years, the generation of hard (above 2 keV) characteristic X-ray radiation arising from the interaction of high intensity ($I > 10^{15}$ W cm^2) femtosecond laser radiation with cluster targets has been the subject of active investigations. Characteristic X-ray radiation contains information about the processes occurring in cluster nanoplasma and can be used for monitoring its physical properties. Besides it can be used for radiography of micro and nano-objects with high spatial and temporal resolution. All this applications require bright characteristic X-rays with high-contrast (the ratio of the K-line intensity to the continuum intensity) produced with high efficiency. It should be stressed that in cluster nanoplasma the X-rays can be generated with higher contrast as compared with X-ray emission from a solid-state plasma.

In our experiments we firstly observed an efficient generation (10^9 photons/J with energy conversion efficiency about 10^{-6}) of hard (2–4 keV) characteristic X-rays under the interaction of intense ($I \sim 10^{16}$ W/cm^2, $E = 5$ mJ) laser radiation with large molecular clusters (SF_6, CF_3I, CF_2Cl_2). It was obtained that at optimal experimental conditions the efficient X-ray generation is accompanied with the multifocal plasma filament formation. The multifocal structure of generated plasma filament can be used as a qualitative criterion for the optimization of control parameters. We have firstly observed generation of two X-ray lines corresponding to chlorine and argon (with efficiency of $3\cdot10^{-7}$ and $7\cdot10^{-8}$ correspondingly) as a result of adding to the mixture CF_2Cl_2–Ar (1:32) light carrier gas He. Adding of He to the mixture CF_2Cl_2–Ar leads to more efficient cooling of the mixture components that results in forming mixed clusters (containing from molecules CF_2Cl_2 and Ar atoms). The presence of mixed clusters is confirmed by the generation of X-ray lines that correspond to the both molecular and atomic gas.

Using the ternary mixtures is a promising way to create the source of multiline X-ray radiation with tunable line intensities, which can be controlled by changing the mixture concentration. The dual-energy X-ray source can be used for nanoscale material discrimination with temporal resolution. The dynamic of relative intensities of lines can provide information about the stability of mixed cluster formation.

In the presentation we will discuss the peculiarities of mixed clusters formation in the binary and ternary mixtures of molecules with carrier noble gases and hard X-ray lines (energy range 2–5 keV) generation under intense femtosecond laser excitation of these clusters.

Paper LM-I-15

FEMTOSECOND LASER PULSE TRAIN MICRO/NANO FABRICATION BASED ON ELECTRON DYNAMICS CONTROL: MODELING AND EXPERIMENTS

Lan Jiang[1], Cong Wang[1], Yanping Yuan[1], Xuesong Shi[1], Pengjun Liu[1], Dong Yu[1], Yong Feng Lu[2]

[1]Laser Micro/Nano Fabrication Laboratory, School of Mechanical Engineering, Beijing Institute of Technology, Beijing 100081, People's Republic of China
[2]Department of Electrical Engineering, University of Nebraska-Lincoln, Lincoln, NE 68588-0511, USA

jianglan@bit.edu.cn

An ultrafast (attosecond/femtosecond) laser pulse duration is shorter than many physical/chemical characteristic times, which makes it possible to manipulate/adjust/interfere electron dynamics such as excitations, ionizations, densities, and temperatures of electrons. This study proposes electron dynamics control (EDC) to change transient localized material properties and corresponding phase change mechanisms by shaping femtosecond pulse trains for micro/nano manufacturing. Based on our modeling predictions, our experiments results demonstrate that EDC can 1) enhance material removal rate and increase drilling aspect-ratio limit; 2) adjust the periods and orientations of submicrometer ripples; and 3) fabricate nanostructured substrates to obtain high enhancement in surface-enhanced Raman scattering.

Keywords: laser micro machining, modeling, electron dynamics control.

Paper LM-I-16

CONDUCTIVE CHANNEL FOR ENERGY TRANSMISSION

Victor V. Apollonov

A.M. Prokhorov General Physics Institute of RAS, Vavilov str. 38, Moscow 119991, Russia

vapollo@kapella.gpi.ru

For many years the attempts to create a super long conductive channels were taken in order to study the upper atmosphere and to settle special tasks, related to the energy transmission. There upon the program of creation of "Impulsar" represents a great interest, as this program in a combination with high-voltage high repetition rate electrical source can be useful to solve the above mentioned problems. It looks like as a some kind of "renaissance of N. Tesla ideas" for the days of high power lasers. The principle of conductive channel production can be shortly described as follows. The "Impulsar" - laser jet engine vehicle - propulsion take place under the influence of powerful high repetition rate pulse-periodic laser radiation. In the experiments the CO_2-laser and solid state Nd YAG laser systems had been used. Active impulse appears thanks to air breakdown (<30 km) or to the breakdown of ablated material on the board (>30 km), placed in the vicinity of the focusing mirror-acceptor of the breakdown waves. With each pulse of powerful laser the device rises up, leaving a bright and dense trace of products with high degree of ionization and metallization by conductive nano - particles due to the ablation process. Conductive dust plasma properties investigation in our experiments had been produced on the basis of two very effective approaches: high power laser controlled ablation of different materials and by electrical explosion of wire. Experimental and theoretical results of conductive canal modeling will be presented. The estimations show that with already experimentally demonstrated figures of specific thrust impulse the lower layers of the Ionosphere can be reached in several ten seconds that is enough to keep the high level of channel conductivity and stability with the help of high repetition rate high voltage generator. Some possible applications of new technology to prevent natural and human - induced disasters will be highlighted.

Paper LM-I-17

WAVELENGTH SWITCHABLE REMOTE LASER IN AIR

Y. Cheng[1], J. Yao[1], J. Ni[1], W. Chu[1], G. Li[1], H. Zhang[1], B. Zeng[1], C. Jing[1], H. Xie[1], Z. Xu[1], H. L. Xu[2], S.L. Chin[3]

[1]*State Key Laboratory of High Field Laser Physics, Chinese Academy of Sciences, Shanghai 201800, China*

[2]*State Key Laboratory on Integrated Optoelectronics, College of Electronic Science and Engineering, Jilin University, Changchun 130012, China*

[3]*Center for Optics, Photonics and Laser (COPL) & Department of Physics, Engineering Physics and Optics, Universite Laval, Quebec City, Qc G1V 0A6, Canada*

ya.cheng@siom.ac.cn

We report on our recent observation on amplification of harmonic-seeded radiation generated through femtosecond laser filamentation in air, which gives rise to laser-like narrow-bandwidth coherent emissions at wavelengths corresponding to transitions between different vibrational levels of the electronic $B^2\Sigma u^+$ and $X^2\Sigma g^+$ states of molecular nitrogen ions, as shown in Fig. 1 [1, 2]. This unusual phenomenon based on an "instantaneous" (e. g., within the interaction period of a ~100 fs laser pulse with the gaseous medium) establishment of a population inversed molecular ion system by strong field ionization seems to be universal as it occurs not only in nitrogen but also in carbon dioxide [3]. To understand the ultrafast pumping mechanism behind the lasing actions, we investigate the dynamics of population evolution of the excited molecular ions with a two-color pump-probe scheme [4, 5]. Our findings show that the coherent emissions originate from seed-injected amplification. Signature of molecular alignment has also been observed in the pump-probe measurements, which will be reported in the talk, too.

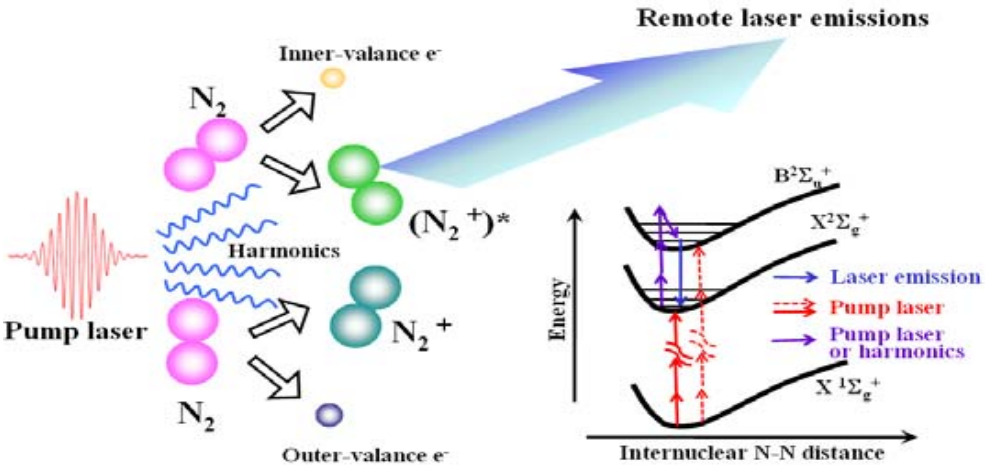

Fig. 1. Working mechanism of remote lasing driven by midinfrared laser pulses.

References:

1. J. Yao, B. Zeng, H. Xu, et al., "High-brightness switchable multiwavelength remote laser in air" Phys. Rev. A, Vol. 84, 051802(R) (2011).
2. J. Ni, W. Chu, H. Zhang, et al., "Harmonic-seeded remote laser emissions in N_2-Ar, N_2-Xe and N_2-Ne mixtures: a comparative study" Opt. Express, Vol. 20, pp. 20970–20979 (2012).
3. W. Chu, B. Zeng, J. Yao, et al., "Multiwavelength amplified harmonic emissions from carbon dioxide pumped by mid-infrared femtosecond laser pulses" Europhys. Lett., Vol. 97, 64004 (2012).
4. J. Yao, G. Li, C. Jing, et al., "Remote creation of coherent emissions in air with two-color ultrafast laser pulses" New J. Phys., Vol. 15, 023046 (2013).
5. J. Ni, W. Chu, C. Jing, et al., "Identification of the physical mechanism of generation of coherent N_2^+ emissions in air by femtosecond filament excitation" Opt. Express, Vol. 21, pp. 8746–8752 (2013).

Paper LM-I-18

TEMPERATURE ASPECTS FOR LASER IGNITION

E. Wintner[1], H. Kofler[2], F. Trawniczek[1]

[1]*Photonics Institute, Technische Universität Wien, Gusshausstrasse 27, A-1040 Wien, Austria*
[2]*BMW Motoren GmbH, Hinterbergerstrasse 2, A-4400 Steyr, Austria*

ernst.wintner@tuwien.ac.at

Non-resonant laser plasma ignition is the most likely candidate for a successful commercial system of laser ignition. A satisfying technical solution is achieved via a longitudinally diode-pumped passively Q-switched (Cr^{4+}:YAG) Nd^{3+}:YAG laser capable of emitting ~1 ns-pulses of at least 20 mJ [1, 2]. This type of solid-state laser confectioned in an engine-compatible form can be called a laser sparkplug. Early versions of this concept comprised a high-power diode pump laser (quasi-cw power >500 W @ 808 nm with ~500 µs duration) placed remote from the engine to avoid detrimental influences of temperature, vibrations, pollution etc. In this case only the solid-state laser is exposed to the elevated temperature in the vicinity of the cylinder walls (<100°C).

Recently, mainly cost-oriented considerations, but also technical advances, led to a change of concept from fiber-based remote pumping via edge emitter arrays to the use of newly devel-opped so-called power VCSELs. Thereby the symmetry of pump laser arrays is in the focus of attention: edge emitter arrays usually consist of one row of some 20 emitters (aperture around 1×5 µm) with ~50–100 µm periodicity, i.e. a very elongated arrangement of light sources. Collimation to form a round pump beam represents some challenge applying the laws of classical optics. Opposed to that, VCSELs are 2-dimensionally arranged (e.g. [3]). Hence the problem of collimation optics is much more relaxed. Additionally, direct mounting of the pump laser onto the laser sparkplug will improve simplicity and eventually cost, provided operation at elevated temperature due to direct mounting on the cylinder head of an engine can be tolerated.

The change of operation temperature has at least threefold impact on performance: the output power will be reduced; the lifetime of the device will shrink and the emission wavelength will become slightly longer. Mode characteristics might also vary, however this does not follow such a clear pattern. Typical specifications: changing from 20°C to 85°C @ 50 A current will result in a drop of the maximum output from ~50 W to ~25 W, i.e. to one half [3]! The lifetime of VCSELs can lie above 1 Mio. hours (corresponding to >100 yr) decreasing exponentially, however, with rising temperature [3]. This may lead to <1/10 of this time span for a realistic temperature rise still remaining sufficient.

Under engine-like operation conditions, the laser sparkplug will work at temperatures up to 120°C and hence the question of crystal temperature influence on laser performance had to be investigated [2]. A clear dependence of the Q-switched output pulse energy could be mea-sured in different open and monolithic set-ups. Consequences of this and other results will be discussed in more detail in the conference and proceedings papers.

References:

1. H. Kofler, E. Schwarz, E. Wintner, “Experimental development of a monolithic passively Q-switched diode-pumped Nd:YAG laser” Eur. Physical Journal D, Vol. 58, pp. 209–218 (2010).
2. H. Kofler, “Development of a laser spark plug and comparative testing”, PhD Thesis, Vienna University of Technology, 2009.
3. Introduction to vertical-cavity surface-emitting diode laser (VCSEL) technology: http://princetonoptronics.com/technology/technology.php

Paper LM-I-19

TOWARDS BETTER UNDERSTANDING OF ULTRAFAST LASER MODIFICATION OF TRANSPARENT SOLIDS: OPTO-THERMO-ELASTOPLASTIC MODELING

N.M. Bulgakova[1,2], V.P. Zhukov[3,4], Yu.P. Meshcheryakov[4]

[1]*Institute of Thermophysics SB RAS, 1 Lavrentyev Ave., 630090 Novosibirsk, Russia*
[2]*Optoelectronics Research Center, University of Southampton, SO17 1BJ, United Kingdom*
[3]*Institute of Computational Technologies SB RAS, 6 Lavrentyev Ave., 630090 Novosibirsk, Russia*
[4]*Novosibirsk State Technical University, 20 Karl Marx ave., 630073, Novosibirsk, Russia*
[5]*Design and Technology Branch of Lavrentyev Institute of Hydrodynamics SB RAS, Tereshkovoi street 29, 630090 Novosibirsk, Russia*

nbul@itp.nsc.ru

Femtosecond lasers are a powerful tool for modifying the structure and properties of transparent materials. Depending on material properties and irradiation conditions, a wide variety of modifications can be induced that gives rise to numerous technological applications based on 3D photonic structures in bulk optical materials. Among transparent materials, optical glasses are of prime importance for optoelectronics and photonics due to their relatively low cost, processability, and possibility of governing refractive index. The physics behind laser-induced glass modification is extremely rich and involves the multiplicity of the consecutive processes initiated by radiation absorption during the laser pulse and extending to millisecond time scales when the final structure becomes "frozen" in the glass matrix. While tremendous achievements have been made toward development laser-writing techniques, the physical mechanisms underlying glass modification have not been fully understood. However, controllable generation of desired modifications in transparent materials is impossible without deep understanding of the governing mechanisms of modifications.

In this work, the dynamics of ultrashort-laser-induced generation of free electron plasma inside bulk glass (fused silica as an example) is analyzed. The results of modeling are presented for typical glass modification regimes, obtained on the basis of the Maxwell equations supplemented with the equations describing electron plasma formation and the laser-induced electric current. We demonstrate that the model allows revealing important features of laser beam propagation in the regimes of dense electron plasma generation such as strong scattering up to complete displacing of light from the plasma region followed by beam refocusing, formation of periodic patterns in electron density distribution, anisotropy of laser energy absorption associated with the pulse front tilt. A controversial issue of the density level of electron plasma generated inside bulk glass by ultrashort laser pulses is discussed. The energy balance of excited matter is considered with introducing an "$E_e - n_e$" diagram matching the level of transient excitation with the maximum temperature of the glass matrix. From the simulation data on the geometry of the laser energy absorption zone, the glass temperature is mapped which may be foreseen at the end of electron – glass matrix relaxation. This, in turn, allows calculations of the laser-induced stress levels and making conclusions on the routes of glass modification. Based on the modeling results, we propose the mechanism responsible for the formation of volume nanogratings in a number of transparent solids under the action ultrashort laser pulses. Finally we address the question on which material properties favor nanograting imprinting into material matrix.

Acknowledgements: This research is supported by Marie Curie International Incoming Fellowship grant of the corresponding author, No. 272919, and by Russian Foundation for Basic Research, Grant No. 12-01-00510-a.

Paper LM-I-20

NONLINEAR ABSORPTION MECHANISMS IN ABLATION OF TRANSPARENT MATERIALS BY HIGH INTENSITY LASER PULSES

I.N. Zavestovskaya[1,2]

[1]*Institute of Quantum Radiophysics of P.N. Lebedev Physical Institute of RAS, Leninskiy prosp. 53, 119991 Moscow, Russia*
[2]*National Research Nuclear University "MEPhI", Kashirskoye shosse 31, 115409 Moscow, Russia*

zavest@sci.lebedev.ru

The processes of the nonlinear absorption and ablation of the transparent materials such as nitride semiconductor, sapphire and others under terawatt/cm^2-laser irradiation with ultrashort pulses are considered. The power consumption under the ablation process is described in terms of the nonlinear mechanism of the tunneling absorption.

Laser ablation of the TW/cm^2 range laser irradiation is suitable technique for processing and machining of transparent materials. A comparison of the ablation threshold has been performed for different transparent materials under very similar irradiation conditions. GaN epitaxial layers on the sapphire substrates, sapphire and silica-based glasses are tested [1, 2]. It was determined the laser-induced damage threshold (LIDS) and result shows the correlation of the LIDT with energy bandgap and other material characteristics. The threshold appears to grow as about third power of the energy bandgap.

The power consumption under the ablation process of transparent materials is described in terms of the induced absorption with an effective absorption coefficient of 2.5×10^4 cm^{-1}. The linear absorption in GaN at 400 nm is less than 100 cm^{-1}. It means that there is an effective nonlinear mechanism of the power irradiation absorption in the transparent frequency region at TW/cm^2-range of power density [2].

It is well known from the general theory of the nonlinear ionization of the atoms and solid materials that the character of the nonlinear ionization under a field action is determined as the intensity I as the irradiation frequency ω [3]. The important parameter of this theory is adiabaticity parameter γ. It was shown that if $\gamma << 1$ (high value of the laser power and the case of low frequencies) there is realized the tunneling mechanism of absorption in the electric field. For GaN $E_g \approx 3.43$ eV and for $I = 40$ TW/cm^2 $\gamma \sim$ ½ and $\omega = 10^{15}$ s^{-1}. It means that for the ablation processes in GaN at terrawatt laser power it is realized the tunneling mechanism of absorption. Using the dependencies of ω we was determined the LIDT dependence on E_g^3 which is in good agreement with experimental results. For other transparent materials parameter γ are much smaller than for GaN since the bandgap of GaN is the smallest one. In all the experimental results there realized the tunneling mechanism of ionization. The corresponding increasing of the absorption coefficient was determined. For GaN we had estimated α about 10^4 cm^{-1} that is in good agreement with the experimental results.

Acknowledgements: The work was supported by the Russian Academy of Science Grants (24P and 7OF) and Russian Foundation for Basic Research Grant 12-02-00761-a.

References:

1. P.G. Eliseev, H.-B. Sun, S. Juodkazis, et al. Jpn. J. Appl. Phys., Vol. 38, p. 839 (1999).
2. P.G. Eliseev, O.N. Krokhin, I.N. Zavestovskaya, Applied Surface Science, Vol. 248, p. 313 (2005).
3. L.V. Keldysh, JETF (USSR), Vol. 47, p. 1945 (1964).

Paper LM-I-21

PULSED LASER DEPOSITION OF MULTIFERROIC THIN FILMS

M. Martino[1], A,P. Caricato[1], C. Leo[1], G. Maruccio[1,2], A.G. Monteduro[2]

[1]*Università del Salento Dipartimento di Matematica e Fisica "Ennio De Giorgi", Via Arnesano 73100 Lecce ITALY*

[2]*NNL Istituto di Nanoscienze-CNR, Lecce, 73100, ITALY*

maurizio.martino@le.infn.it

Multiferroics are multifunctional materials presenting two or more ferroic (or antiferroic) orders, such as ferroelectricity, ferromagnetism etc. [1]. The complex transition metal oxide $BiFeO_3$ (BFO) is one of the most investigated magnetoelectric material for its perovskite crystal structure and its ordering temperatures. It is reported a G-type antiferromagnetic nature below the Neel temperature of $T_N = 643$ K and a ferroelectric ordering below $T_C = 1103$ K [2].

Here we report on the ceramic bulk target synthesis, the thin film deposition and structural, dielectric and magnetic characterization of BFO aiming the integration in spin devices. Structural characterizations, performed using FT-IR spectroscopy and X-Ray Diffraction, confirm the absence of any impurity phase in synthesized target.

BFO thin films (300nm) were deposited using Pulsed Laser Deposition (PLD) on Si substrates with a 5 μm SiO_2 top layer. A Lambda Physics 305i ArF excimer laser ($\lambda = 193$ nm, $\tau = 20$ ns) was used with an energy density of ≈2 J/cm^2 and a repetition rate of 10 Hz. The substrate was heated at 500 and 600°C. Samples were prepared by varying the oxygen atmosphere with 0.1, 0.5, and 1.0 Pa pressure. For dielectric constant measurements arrays of capacitors were fabricated in a cross bar architecture where the BFO film is sandwiched between two metal electrodes. The room temperature dielectric constant of BFO is found to decreases with increasing the oxygen pressure during the deposition. A large leakage current, probably due to oxygen vacancies or conductive impure phases, such as Bi_2O_3, was recorded, in agreement to literature results [3].

Due to magnetoelectric coupling BFO can play a key role in the development of spin devices in which the magnetic moment can be controlled electrically when an antiferromagnetic layer of BFO is in contact with a ferromagnetic one [4].

References:

1. W. Eerenstein, N.D. Mathur, J.F. Scott, "Multiferroic and magnetoelectric materials" Nature, Vol. 442, pp. 759–765 (2006).
2. J. Catalan, J.F. Scott, "Physics and applications of bismuth ferrite" Adv. Mater., Vol. 21, pp. 2463–2485 (2009).
3. L. You, N.T. Chua, K. Yao, L. Chen, J. Wang, "Influence of oxygen pressure on the ferroelectric properties of epitaxial $BiFeO_3$ thin films by pulsed laser deposition" Phys. Rev. B, Vol. 80, 024105 (2009).
4. Y.-H. Chu, L.W. Martin, M.B. Holcomb, M. Gajek, S.-J. Han, Q. He, N. Balke, C.-H. Yang, D. Lee, W. Hu, Q. Zhan, P.-L. Yang, A. Fraile-Rodrìguez, A. Scholl, S.X. Wang, R. Ramesh, "Electric-field control of local ferromagnetism using a magnetoelectric multiferroic" Nature Mater., pp. 7478–7482 (2008).

Paper LM-I-22

RESEARCH AND APPLICATION OF LASER SURFACE MODIFICATION AND REPAIRING ON TURBINE BLADES

Jianhua Yao[1], Zhong Ye[2], Hongwei Shen[3], Shimin Pan[4]

[1]Research Centre of Laser Processing Technology and Engineering, Zhejiang University of Technology, Hangzhou, 310014, China
[2]Hangzhou Steam Turbine Co., Ltd., Hangzhou, 310022, China
[3]Shanghai Electric Power Generation Equipment Co., Ltd., Shanghai, 200240, China
[4]Qingdao Jieneng Steam Turbine Group Co., Ltd., Qingdao, 266042, China

Steam turbine, as a key power equipment, plays an increasingly important role in many critical national economy fields, such as petroleum, chemical and light industry. As the main part of turbine, blades run at a high speed in the wet steam environment, which makes the leading edge of blade prone to cavitation and results in failure, even causes accidents for the turbine unit. Therefore, the anti-cavitation ability of the blade directly affects the efficiency and security of the steam turbine. As to various types of turbines and different working conditions, the different laser processing techniques, such as laser alloying, laser repairing and laser solid solution strengthening, were chosen to perform the modification and repairing on the surfaces of 2Cr13 and 17-4PH turbine blades in this paper. The microstructures, microhardness, residual stress, wear resistance, corrosion resistance and cavitations resistance before and after laser hardening were investigated respectively. The results show that, the laser alloying technology, which can replace the traditional flame hardening and induction hardening, is much safer and more reliable, makes the microhardness of the blade surface increase 1.8 times with respect to that of the substrate, and the cavitation resistance more than one time relative to that of the substrate. The laser cladding based on the DMD technology was used to repair the failed blade surface. There are no pores, cracks and other defects on the surface after laser cladding, the microhardness and wear resistance significantly improve as well. The further implementation of laser alloying on the repaired layer can get the surface with higher performances. So the technique can replace the traditional inlaid Stellite alloy technique. The laser solid solution strengthening technology was introduced to harden the precipitation hardened stainless steel blades. As the result, after the laser solution strengthening, the thickness of the laser hardened layer is more than 1.8 mm, the microhardness is more than 400HV0.2, and the cavitation resistance is more than one time from that of the substrate. The large deformation caused by the overall solution treatment and the insufficient hardening depth were solved. The three laser techniques performed on turbine blades have passed the installed tests in turbine manufactories, and the technology has been widely applied in turbine industry, which shows that the laser technology has extensive application prospect on the modification and repairing of turbine blades.

Paper LM-I-23

PULSED LASER COATING OF TEXTILE MATERIALS WITH ZNO THIN FILMS AND NANOPARTICLES: WETTING AND ANTIMICROBIAL PROPERTIES

Ion N. Mihailescu, Carmen Ristoscu

National Institute for Laser, Plasma and Radiation Physics, PO Box MG-54, RO-77125, Magurele, Ilfov, Romania

ion.mihailescu@inflpr.ro

Textile materials were coated with ZnO thin films or nanoparticles by pulsed laser deposition. The synthesized nanostructures were physico-chemically analyzed by X-ray diffraction, scanning electron microscopy, atomic force microscopy, contact angle measurements and microbiologically assessed by *in-vitro* tests. An increase of pulses number from 10 to 100 resulted in a drastic modification of the surface coating, from a dispersion of nanoparticles to uniform thin films that covered the fibers entirely.

Both ZnO nanoparticles and thin films deposited in 13 Pa Oxygen were hydrophilic, while the nanoparticles sputtered in vacuum (10^{-4} Pa) were hydrophobic and the thin films deposited in vacuum superhydrophobic. This radical modification of wetting behavior will be explained in terms of differences in nanostructure and surface electrical charging.

The textiles finished with nanoparticles and thin films in vacuum were antimicrobial, with 100% efficiency after 24 h against *Staphylococcus Aureus* and *Aspergilus Niger* colonies. However, in case of filamentous fungi recognized to be more resistant to ZnO, the efficiency of textiles finished with thin films dropped to 30%. To boost the activity against such microorganisms, we treated the textile surface with a hydrophobin secreted by *A. Nidulans* fungus. On its own, the hydrophobin was completely inefficient in stopping filamentous fungi colonies to spread, but in conjunction with ZnO thin films, they increased the efficiency up to ~95%. Moreover, these structures proved very resistant to washing. We accounted these ameliorations to the different growth orientation of ZnO crystallites in thin films deposited on textiles pretreated with hydrophobins.

These results can offer solutions for design in one step stable, superhydrophobic, antimicrobial textile surfaces, for large scale use in medical clothing.

Paper LM-I-24

SPATIAL COHERENCE DYNAMICS IN THE PROCESSES OF POLARITON CONDENSATE FORMATION AND DECAY IN A SEMICONDUCTOR MICROCAVITY

V.V. Belykh[1], D.A. Mylnikov[1], N.N. Sibeldin[1], V.D. Kulakovskii[2], C. Schneider[3], S. Höfling[3], M. Kamp[3], A. Forchel[3]

[1]P.N. Lebedev Physical Institute, Russian Academy of Sciences, Moscow 119991, Russia
[2]Institute of Solid State Physics, Russian Academy of Sciences, Chernogolovka 142432, Russia
[3]Technische Physik, Physikalisches Institut and Wilhelm Conrad Röntgen Research Center for Complex Material Systems, Universität Würzburg, D-97074 Würzburg, Germany

sibeldin@sci.lebedev.ru

One of the most attractive systems for studying Bose-Einstein condensation (BEC) is a polariton gas in a semiconductor microcavity (MC) with embedded quantum wells. Mixed exciton-photon states – polaritons possess bosonic statistics and in a MC have an extremely small effective mass ($\sim 10^{-4}$ of the free electron mass). These properties allow one to observe MC polariton BEC at high (up to the room) temperatures, which inspired considerable attention to this system in the last decade (see [1] for a review).

BEC is characterized by the macroscopic occupation of the ground state with wavevector $k = 0$ and the first order spatial coherence $g^{(1)}$ on the scale larger than thermal de Broglie wavelength. In the present work we studied the dynamics of the MC polariton BEC by monitoring the expansion of the spatial coherence [2] and evolution of polariton distribution in k-space. The sample was a GaAs-based MC with the quality factor $Q \approx 7000$, and it was excited by 3 ps laser pulses. The dynamics of spatial coherence was studied on the basis of Young's double slit experiment with different separations between the slits.

It was found that in the process of condensate formation the coherence expands with a constant velocity of about 10^8 cm/s. This velocity is mostly related to the rate of polariton relaxation into $k \approx 0$ states being $\sim 10^{10}$ times larger than the coherence expansion velocity in the Bose condensate of ultracold atoms. At the stage of condensate formation and decay, when the population of $k \approx 0$ states is not high (below $\sim 10^3$), spatial coherence is determined by the polariton momentum distribution. In this regime the measured dynamics of the coherence length is similar to that of $1/\Delta k$, where Δk is the width of polariton momentum distribution. On the other hand, in the range of maximal condensate density coherence is determined by the fluctuations of amplitude and phase of the condensate wavefunction which are not suppressed during the condensate lifetime. It was found that in the range of the condensate decay spatial coherence exceeds that in thermal equilibrium system. This effect is related to the large time required to reach equilibrium with respect to the time of the condensate decay that was confirmed by the direct measurements of polariton k-space distribution dynamics.

References:

1. "Exciton Polaritons in Microcavities", Springer Series in Solid-State Sciences, Vol. 172. Eds. D. Sanvitto and V. Timofeev. New York: Springer, 2012.
2. V.V. Belykh, N.N. Sibeldin, V.D. Kulakovskii, M.M. Glazov, M.A. Semina, C. Schneider, S. Höfling, M. Kamp, A. Forchel, "Coherence expansion and polariton condensate formation in a semiconductor microcavity" Phys. Rev. Lett., Vol. 110, 137402 (2013).

Paper LM-O-1

SPM PROBE-ASSISTED LASER NANOABLATION OF GRAPHITIC LAYERS

V.I. Konov, V.D. Frolov, P.A. Pivovarov, E.V. Zavedeev

A.M. Prokhorov General Physics Institute of RAS, 38 Vavilov str., 199991 Moscow, Russia

konov@nsc.gpi.ru

It has been shown that short-pulsed laser is an effective tool for ultra-precise surface structuring of diamond and diamond-like films. The amount of laser removed material can be as low as a few carbon atoms or clusters per pulse. That is why this regime was called nanoablation [1].

In the present work nanoablation of graphitic layers was studied for two cases: solely laser irradiation and combined with scanning probe microscopy (SPM) probe. The pulsed laser beam (τ = 7 ns, λ = 532 nm) was focused to the spot of 1 μm in diameter on the surface of crystal graphite either at the tip end (laser-probe ablation) or far away from the probe. Special cantilevers with sharp tips, operating in tapping mode, were used.

The dependence of the crater depth d for solely laser irradiation (total pulse number $N = 3 \cdot 10^4$) is presented in Fig. 1. Note that ablation rate can be as low as 10^{-3}–10^{-4} nm/pulse which correlates with the results obtained for diamond nanoablation. Second, there is a threshold laser fluence $E_{th} \approx$ 1–2 J/cm^2. For $E < E_{th}$ we observed strong dependence of ablation rate on fluence ($d \sim E^4$) while for higher $E > E_{th}$ the value of d grows with E almost linearly.

Interesting phenomena was found for Laser-Probe combination (see Fig. 2). In this case for $E \le E_{th}$ addition of SPM probe caused negligible variations in ablation rate. Only above E_{th} the probe action becomes important and leads to essential (up to about 2 times) growth of ablation rate for $E \approx$ 6–8 J/cm^2.

In our opinion, probe tip can strongly enhance laser field in close proximity on the sample surface. Possible mechanisms of graphite nanoablation below and above the critical laser fluence will be discussed.

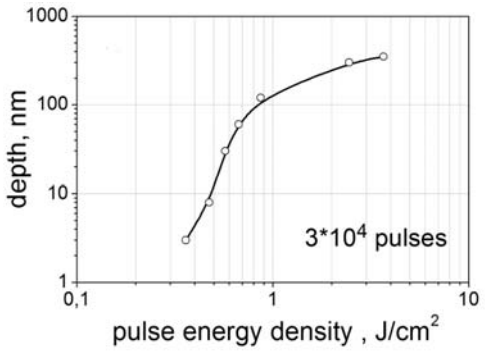

Fig. 1. Crater depth (d) v.s. pulse energy density (E) plot for free surface ablation.

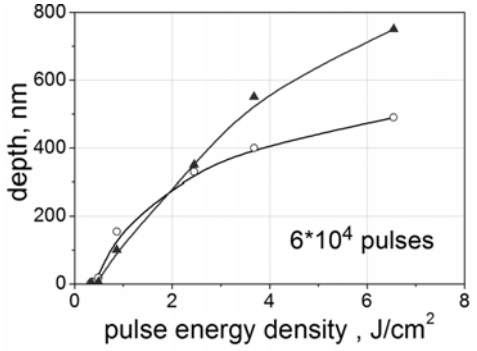

Fig.2. Comparative d–E plots for free surface (opened circles) and laser-probe (solid triangles) ablations

Acknowledgements: The work is supported by MES of Russia Grant 2012-1.2.1-12-000-2012-061 and Presidium of RAS grant in the frame of Program #24.

References:

1. V.I. Konov, “Laser in micro and nanoprocessing of diamond materials” Laser & Photon. Rev., Vol. 6, No. 6, pp. 739–766 (2012).

Paper LM-O-2

BIOFUNCTIONAL NANOPARTICLES GENERATION BY LASER ABLATION OF IRON IN LIQUID

A.I. Omelchenko[1], A.A. Serkov[2], A.V. Simakin[2], G.A. Shafeev[2]

[1]*Institute on Laser and Information Technologies, Troitsk, Moscow reg., Russia*
[2]*Wave Research Center, A.M. Prokhorov General Physics Institute, Moscow, Russia*

alexio@kmail.ru

In recent years, it is observed a high interest to use the biofunctional nanoparticles in laser medicine [1]. As a result of fabrication of biofunctional nanoparticles with the determined structure and properties, a new possibilities for engineering of tissues and cells have been opened in medicine. So, new applications of magnetic nanoparticles in laser diagnostics and healing cartilage damage have advance in orthopedics [2]. It is the results from a high permeability of the particles with the size of 5–10 nm in the dense cartilaginous matrix and high absorption of nanoparticles at the damage places on cartilage surface. Because of low vascular substance of cartilage (a pore size of 20–40 nm and no blood vessels) it has poor ability to repair damage. Laser irradiation of cartilage in no ablation mode and application of non-uniform magnetic field allow impregnating magnetite nanoparticles in the bulk of tissue. Photo-thermal effect of laser radiation on the nanoparticles localized at the damaged places of cartilage induces regeneration of tissue [3].

Magnetic nanoparticles of iron oxide have been obtained by the two methods: 1) direct generation of the nanoparticles in laser ablation of a bulk iron target in water; 2) chemical synthesis of the nanoparticles in co-precipitation process in the ferrous- and ferric chloride solutions. We compared physical and chemical property of the produced nanoparticles.

Laser-ablated iron oxide nanoparticles with a core-shell structure are mechanically stable, protected from corrosion, and have higher magnetic susceptibility. These properties are a little bit lower for chemical synthesized nanoparticles. Aqueous dispersions of the nanoparticles obtained by both methods were susceptible to agglomeration and sedimentation. By means of magnetic trap with axis-symmetric field, the nanoparticles with the size of 5–10 nm have been separated from their large agglomerates. Size distributions of nanoparticles in aqueous dispersions were analyzed by the measuring disk centrifuge. Magnetic susceptibility was measured by Faradey's technique.

Laser treatment of the nanoparticles in aqueous solutions of starch and PVP (stabilizer) is performed to produce stable colloids of magnetite. Kinetics of the total absorption spectra of the colloids has been measured. The agglomeration of nanoparticles of magnetite is revealed in the intact solution. Laser treatment makes these colloids stable without agglomeration and sedimentation for month's storage time. Chemical stability of these colloids is discussed.

Acknowledgements: Thanks to Russian Foundation for Basic Research for financial assistance Grant No. 11-08-00574a.

References:

1. A. Omelchenko "Biofunctional nanoparticles in laser medicine" Vestn. Yu. Univ., Vol. 21, pp. 40–50 (2011) [in Russian].
2. O. Baum, V. Golubev, A. Omelchenko, E. Sobol, A. Shekhter, "Advance of magnetic nanoparticles application in laser diagnostics and healing of cartilage damage", Proceedings of 3rd Eurasian Congress on Medical Physics and Engineering «Medical Physics-2010». Moscow, 21–25 June 2010. Vol. 3, pp. 222–224.
3. O. Baum, Yu. Soshnikova, A. Omelchenko, E. Sobol, "Nanoparticles for diagnostics and laser medical treatment of cartilage in orthopedics", Proc. SPIE, Vol. 8595. pp. 62–66 (2013).

Paper LM-O-3

INFLUENCE OF OXIDATION IN ULTRA SHORT LASER PULSE PROCESSING OF CFRP

Christian Freitag[1,2], M. Komlenok[3], T. Kononenko[3], R. Weber[2], V. Konov[3], T. Graf[2]

[1]*GSaME Graduate School of Excellence advanced Manufacturing Engineering, Nobelstr. 12, 70569 Stuttgart, Germany*
[2]*IFSW Institut für Strahlwerkzeuge, Pfaffenwaldring 43, 70569 Stuttgart, Germany*
[3]*GPI Prokhorov General Physics Institute, 38 Vavilov Str., 119991 Moscow, Russia*

christian.freitag@ifsw.uni-stuttgart.de

Laser processing of carbon fibre reinforced plastics (CFRP) is a challenging task due to the unique thermal properties of this material [1]. The structure of the compound can easily be damaged by thermal effects such as heat accumulation [2, 3]. To process CFRP with respect to high quality and productivity, adjusted process strategies have to be developed. The presented work addresses the question, whether specific oxidation of the carbon fibres can increase the productivity of the cutting process of CFRP.

Oxidation of Polyacrylnitril (PAN) based carbon fibres begins at temperatures of about 450°C with increasing oxidation rates for increasing temperatures [4]. When laser processing carbon fibres or CFRP, the material reaches sublimation temperature in the processing zone which is about 4000 K [5]. The object of the reported study was to investigate the significance of oxidation compared with material evaporation when processing CFRP with a high-repetition-rate picosecond laser system.

Nitrogen and oxygen have been used as process gases to ablate grooves in CFRP with different number of laser scans. Grooves ablated in air serve as a reference. By using nitrogen, the laser ablation process can be investigated without any oxidation effects. Parameters varied in the presented study were the distance of the nozzle from the surface and the gas flow. At the initial stages of the multi-pass cutting process of CFRP high ablation rates are achieved with every process gas. The observable effect of oxidation on the ablation rate at initial stages is negligible. In greater groove depths, the ablation rate is generally decreasing. In this stages of the multi-pass cutting process significantly higher ablation rates are achieved when using oxygen as a process gas compared to grooves ablated in nitrogen or in air. The highest enhancement in process efficiency is achieved with the highest gas flow. While through-cuts of the work piece were achieved when using oxygen, no through-cut was possible using air or nitrogen. To investigate the influence of the additional oxygen on the thermal damage of the material, the heat affected zone has been measured for each groove.

Acknowledgements: The authors would like to thank the Bundesministerium für Bildung und Forschung for the support of this work in the frame of the project ProCav.

References:

1. S.D. McIvor, M.I. Darby, G.H. Wostenholm, B. Yates, L. Banfield, R. King, A. Webb, “Thermal conductivity measurement of some glass fibre- and carbon fibre-reinforced plastics” Journal of Materials Science, Vol. 25, pp. 3127–3132 (1990).
2. R. Weber, C. Freitag, T. Kononenko, M. Hafner, V. Onuseit, P. Berger, T. Graf, “Short-pulse laser processing of CFRP” Physics Procedia, Vol. 39, pp. 137–146 (2012).
3. C. Freitag, V. Onuseit, R. Weber, T. Graf, “High-speed Observation of the heat flow in CFRP during laser processing” Physics Procedia, Vol. 39, pp. 171–178 (2012).
4. P. Morgan, “Carbon Fibres and their Composites”, 791 (2005).
5. H.B. Palmer, M. Shelef, Chemistry and Physics of Carbon (1968).

Paper LM-O-4

PERSPECTIVES OF FEMTOSECOND LASER INSCRIPTION IN MID-INFRARED PHOTONICS

Andrey Okhrimchuk[1,2], Mykhaylo Dubov[2], Vladimir Mezentsev[2]

[1]*Fiber Optics Research Center of RAS, 38 Vavilova Street, Moscow 119333, Russia*
[2]*Aston Institute of Photonic Technologies, Aston University, Birmingham B4 7ET*

a.okhrimchuk@aston.ac.uk

Femtosecond (fs) laser micro-modification enables a uniquely flexible method of sculpting of waveguides in various types of transparent materials, including glasses and crystals [1]. In particular, it offers a unique possibility for development of waveguiding structures in crystals suitable for Mid-IR applications. In this paper we discuss suitability of femtosecond writing in a range of Mid-IR materials, such as ZnSe, ZnS, $RbPb_2Cl_5$, Si, $LiNbO_3$ based on published papers and our own recent results.

The femtosecond written waveguides in crystals can be classified as Stress Induced Waveguides (SIW), Depressed Cladding Waveguides (DCW), and Directly Written Waveguides (DRW) [2]. Since negative modification of refractive index is predominantly obtained in the above mentioned as well as in most crystalline materials, we consider that only SIW and DCW types are suitable for Mid-IR applications. It has been recently demonstrated that DCW-type waveguiding structures exhibit low losses and provide great flexibility for near IR applications [3]. Design of this type appears to be the most attractive for Mid-IR devices since waveguide diameter scales independently on the diameter of the individual tracks. However direct exploitation of near IR geometries in Mid-IR range is inefficient primarily due considerable leakage losses nonlinearly increasing with wavelength. Meticulous shaping of a waveguide with depressed cladding is required to minimize leakage losses. We demonstrate examples of efficient low loss structures suitable e.g. for waveguide solid-state lasers and optical parametric oscillators operating in Mid-IR.

Acknowledgements: We acknowledge the support of the Leverhulme Trust (UK).

References:

1. R. Osellame, G. Cerullo, Roberta Ramponi (Eds), “Femtosecond Laser Micromachining: Photonic and Microfluidic Devices in Transparent Materials (Topics in Applied Physics)”, Springer, Heidelberg (2011).
2. A. Okhrimchuk, “Femtosecond Fabrication of Waveguides” in “Ion-Doped Laser Crystals in Coherence and Ultrashort Pulse Laser Emission”, F.J. Duarte (Ed.), InTech (2010); http://www.intechopen.com/articles/show/title/femtosecond-fabrication-of-waveguides-in-ion-doped-laser-crystals
3. A. Okhrimchuk, V. Mezentsev, A. Shestakov, I. Bennion, “Low loss depressed cladding waveguide inscribed in YAG:Nd single crystal by femtosecond laser pulses” Optics Express, Vol. 20, pp. 3832–3843 (2012).

Paper LM-O-5

DIRECT LASER WRITING WITH COMPLEX LIGHT IN TAILORED SILVER-CONTAINING PHOSPHATE GLASS

K. Mishchik[1], Y. Petit[1,2], E. Brasselet[1], I. Manek-Honninger[1], N. Marquestaut[1], A. Royon[1], T. Cardinal[2], L. Canioni[1]

[1]*Univ. Bordeaux, CNRS, LOMA, UMR 5798, 33400 Talence, France*
[2]*Univ. Bordeaux, CNRS, ICMCB, UPR 904, 33400 Pessac, France*

konstantin.mishchik@u-bordeaux1.fr

Femtosecond direct laser writing (DLW) in transparent dielectrics has revolutionized the field of laser applications, providing localized 3D material modifications with potential sizes below diffraction limit. This versatile technique appears as perfectly suitable for micro- and nanoscale 3D patterning of transparent materials towards the elaboration of new photonics elementary building blocks.

Combining DLW technique with the use of focused complex light field endowed with single or multiple optical phase singularities we demonstrate original vortex-assisted laser/matter interaction in a photosensitive silver-containing phosphate glass. Namely, original sub-wavelength spatial distributions of laser-induced linear and nonlinear optical properties are achieved. DLW was performed with a Ti:Sa amplified laser system (800 nm, 65 fs, 250 kHz) with tight focusing into the bulk of glass, leading to the localized production of Ag_m^{x+} silver clusters (with $m < 10$ the number of atoms and x the ionization degree), which provide a strong and broadband white fluorescence emission for near-UV excitation [1].

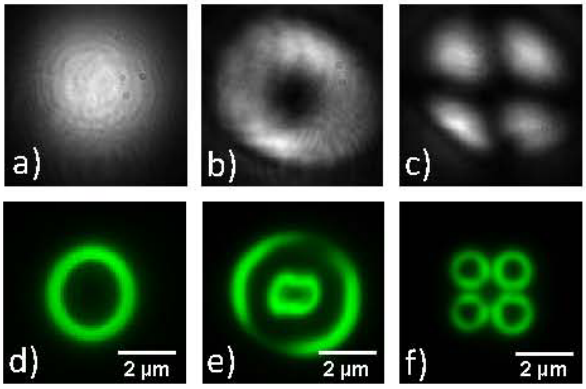

Fig. 1. Incident spatial intensity profiles of a) fundamental Gaussian beam, b) optical vortex beam with topological charge two, and c) optical quadrupole of single charge vortex. Corresponding laser-induced fluorescence patterns with d) annular, e) bi-annular, and f) quadrupole like geometries.

More precisely, here we demonstrate that our DLW process is driven by laser beam spatial intensity distribution, independently from its phase distribution. We also prove that our writing process is independent from both the magnitude and sign of topological charge of the optical vortex. For a Gaussian writing beam [Fig. 1a), d)], fluorescent silver clusters are arranged into a hollow pipe shape along the propagation axis, with wall thickness of about 100 nm. In contrast, tight focusing of spatially engineered light fields [2], here a charge two optical vortex beam and optical vortex quadrupole led to original fluorescence spatial distributions, namely bi-annular and quadrupole like fluorescence patterns, respectively. In addition, sub-wavelength silver cluster organization displays micro-structuring and potential future nanoscale structuring.

Correlative microscopy of fluorescent and second harmonic generation also showed the stable existence of a laser-induced buried static electric field being correlated to silver cluster profiles [3]. Such vortex-engineered electric field will be reported to be the root of silver cluster existence and stabilization. Vortex-assisted DLW thus appears as a very promising approach to tailor both fluorescent and SHG nonlinear responses below diffraction limit.

References:

1. A. Royon et al., Advanced Materials, Vol. 22, Iss. 46, pp. 5282–5286 (2010).
2. A. Desyatnikov et al., Optics Express, Vol. 18, Iss. 10, pp. 10848–10863 (2010).
3. G. Papon et al., to be submitted (2013).

Paper LM-O-6

FROM FEMTOSECONDS TO NANOSECONDS ENERGY TRANSFER DYNAMICS INDUCED BY INTENSE FEMTOSECOND LASER IN A BULK OF CRYSTALLINE DIELECTRICS

Fedor V. Potemkin, Vyacheslav M. Gordienko, Pavel M. Mikheev,
Evgeniy I. Mareev, Alexey A. Podshivalov

Faculty of Physics and International Laser Center Moscow State University, 119991, Russia

potemkin@automationlabs.ru

Abstract: We successively probed energy transfer stages after femtosecond laser excitation of a bulk of crystalline dielectrics from femtosecond to nanoseconds timescale. We observed a change in the frequency of THz phonons from 1.4 to 4.6 THz, quasi-resonantly excited by laser plasma oscillations under tight focusing (NA ~ 0.4) of intense femtosecond laser radiation in a bulk of quartz. In BaF2 a 15 ps time delay of the significant increase in the phonon wave amplitude was shown. In LiF the energy transfer between many phonon modes is clearly visible.

In our recent experiments [1, 2] we discussed preliminary results on energy transfer dynamics in a bulk of dielectrics after intense femtosecond laser pulse excitation. The experiments were carried out till time delays of about tens of picoseconds. In this work we focused on deep analysis of current results and extension to nanosecond time scales.

The key feature of our experiment is an extreme intensive laser pulse (~10^{13} W/cm^2), which exceeds the plasma formation threshold in a bulk of transparent solids, and a high-sensitivity version of pump-probe technique for time-resolved diagnosis, based on registration of a signal of third harmonic of the probe pulse [1, 2]. Radiation of Cr:forsterite laser system (λ = 1.24 μm, τ = 140 fs, E = 0.1–5 μJ with intensity contrast ~250) was employed. New opportunities related to time delay up to 2 ns increasing and using not only pump-probe technique but also shadowgraphy to analyze the initial stage of shock wave formation. We point out that in all our experiments the final stage of local energy deposition (NA ~ 0.4) into a bulk of solid is micromodification formation (Fig. 1).

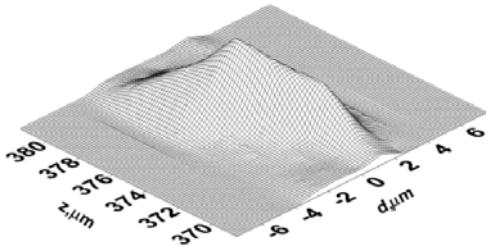

Fig. 1. Microdefect reconstruction based on third harmonic data

Current results mainly describe the dynamics of energy redistribution on time scale up to tens of picoseconds. Typical temporal behaviors of registered signals are sketched at Fig. 2.

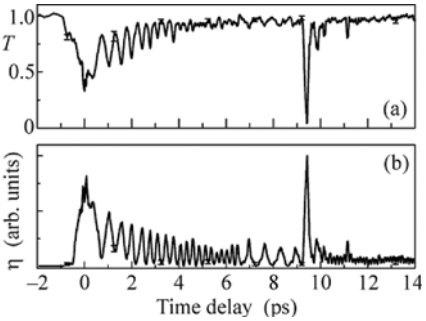

Fig. 2. Transmittance T and THG efficiency η of probe signal as a function of time delay for quartz at pump pulse energies of a) 2.7 μJ and b) 3.2 μJ. The number of experimental data points is 45000 per curve. Threshold of plasma formation is 3.0 μJ.

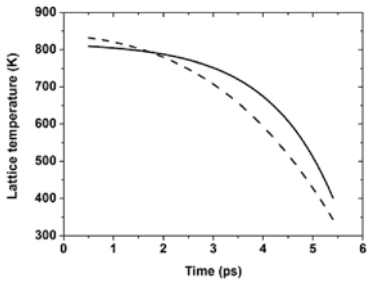

Fig. 3. Lattice temperature in quartz dynamics at pump energy 3.2 μJ (solid line) [10]. Dashed line is related to the modeling function $v(T) \sim (846–T)^{0.31}$

We obtained, that the energy transfer dynamics in quartz sample include three main regions: first is the coherent phonon (1.4–4.1 THz) quasi-resonant excitation by laser-induced plasma and further lattice cooling along with soft phonon mode A_1 147 cm^{-1} frequency changes from 1.4 to 4.6 THz (from 300 to 846 K, see Fig. 3), second one is the abrupt frequency change which possibly was related to fundamental phonon wave appearing due to second harmonic conversion efficiency decreasing in time and the last one is the most interesting threshold effect due to local bond breaking in interaction region.

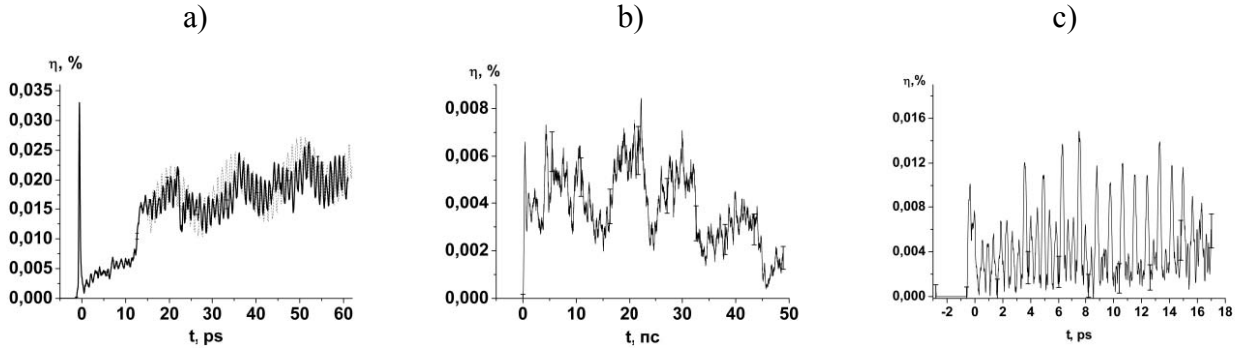

Fig. 4. The THG efficiency η of probe pulse in crystals: a) BaF_2 at pump pulse energy of 2 μJ, b) CaF_2 pump pulse energy of 4 μJ) LiF pump pulse energy of 3.6 μJ as a function of time delay between probe and pump pulses.

The excitation and relaxation dynamics of coherent phonons in fluorine-containing crystals was also investigated (Fig. 4). For the first time in the recorded signals of the third harmonic generated by probe pulse in BaF_2 and CaF_2 crystals the delays of the significant increase in phonon wave amplitude were observed. These delays are related to the time of energy transfer from electronic to phonon subsystem. In the LiF crystal the energy transfer between many phonon modes was observed, which is possibly related to the anharmonicity of the phonon waves.

On the base of experimental results, we propose a new mechanism of coherent phonon generation in transparent solids under plasma formation, so called quasi-resonant generation of coherent phonons by laser-induced plasma. First, the coherent phonon seed is formed via stimulated Raman scattering by front of pump pulse, then formed plasma absorbs a significant part of the laser pulse energy, and plasma energy is then quasi-resonantly transferred from free electrons to seeded coherent phonons. A quasi-resonant regime of energy transformation occurs due to the large amplitude coherent oscillations of ions which, in turn, lead to synchronous modulation of the dielectric band gap width. Such an effective energy transfer from plasma electrons to coherent phonons occurs in phase with coherent phonon oscillations at a minimal band gap width. Plasma dramatically influences the process of coherent phonons generation in crystals, including excitation and relaxation dynamics. By now our work is directed to probe the initial stage of shock wave formation, results will be coming soon. Till this time we established that for solids 2 ns time delay is not enough to visualize shock wave formation.

Acknowledgements: This research has been supported by the Russian Foundation for Basic Research (Project No. 11-02-01323-a) and partly by the M.V. Lomonosov Moscow State University Program of Development, Foundation for Assistance to Small Innovative Enterprises in the scientific and technological areas (program “UMNIK”).

References:

1. V.M. Gordienko, P.M. Mikheev, F.V. Potemkin, “Generation of coherent terahertz phonons by sharp focusing of a femtosecond laser beam in the bulk of crystalline insulators in a regime of plasma formation” JETP Lett., Vol. 92, pp. 553–558 (2010).
2. F.V. Potemkin, P.M. Mikheev, “Efficient generation of coherent THz phonons with a strong change in frequency excited by femtosecond laser plasma formed in a bulk of quartz” Eur. Phys. J. D, Vol. 66, No. 9, pp. 1–5 (2012).
3. R.R. Gattass, E. Mazur, “Femtosecond laser micromachining in transparent materials” Nature Photon. Vol. 2, p. 219 (2008).
4. T.E. Stevens, J. Kuhl, R. Merlin, “Coherent phonon generation and the two stimulated Raman tensors” Physical Review B, Vol. 65, 144304 (2002).

Paper LM-O-7

FABRICATION OF PHOTONIC STRUCTURES ON TiO_2 FILMS BY FEMTOSECOND LASER ABLATION

Iulia Anghel[1,2], Florin Jipa[1,2], Andreea Andrei[1], Razvan Dabu[1], Adrian Rizea[3], Marian Zamfirescu[1]

[1]*National Institute for Laser, Plasma and Radiation Physics, Atomistilor 409, 077125 Magurele, Romania*
[2]*University of Bucharest, Faculty of Physics, Atomistilor 405, 077125 Magurele, Romania*
[3]*S.C. IOEL S.A. (Prooptica group), Gh. Petrascu 67, 745081, Bucharest, Romania*

iulia.anghel@inflpr.ro

The photonic crystals (PhCs) introduced theoretically by Yablonovitch [1] and experimentally by John [2], have been in the past decade the subject of the multiple studies due to their unique electromagnetic properties and the advantage that they can be used in many optical devices, such as optical filters, waveguides, optical switches, chemical and biological sensors [3, 4]. PhCs are periodic optical structures consists of alternating regions with high and low refractive index at the scale of the order of the photon wavelength, forming the so called photonic band gap.

In this work we developed a photonic structure on TiO_2 thin films designed to show photonic band gap in the near-infrared, at the telecommunication wavelengths. The plane wave expansion method was used to compute the photonic band gap of the laser ablated structure. The impact of limited laser processing accuracy on the photonic band gap has been studied. The structure was produced by tightly focused femtosecond laser beam in multi-pulses ablation regime. A Ti:Sapphire CPA laser system with pulse duration of 200 fs and a focusing optics with numerical aperture NA = 0.5 was used to create the photonic structure. The resulting periodic structure has an estimated photonic band gap centred at 1.53 μm with a bandwidth of about 42 nm. The laser ablated pattern was characterized by Atomic Force Microscopy (AFM) (Fig. 1a).

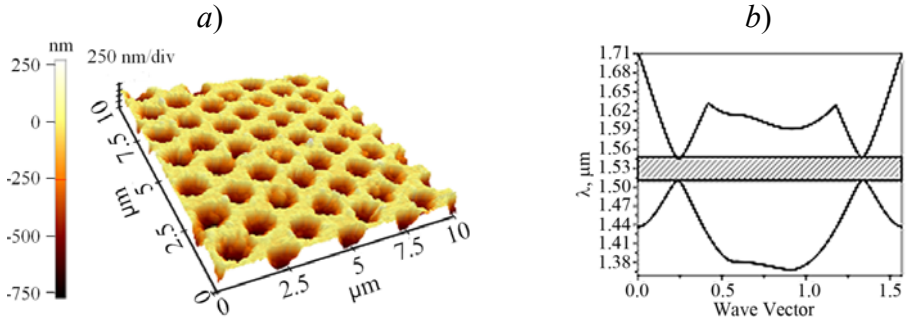

Figure 1. *a*) Photonic crystal structure produced by femtosecond laser ablation, *b*) photonic bands structure of the ablated structure.

References:

1. E. Yablonovitch, "Inhibited spontaneous emission in solid-state physics and electronics" Phys. Rev. Lett., Vol. 20, pp. 2059–2062 (1987).
2. S. John, "Strong localization of photons in certain disordered dielectric superlattices" Phys. Rev. Lett., Vol. 58, pp. 2486–2489 (1987)
3. C. López, "Materials aspects of photonic crystals", Adv. Mater., Vol. 15, pp. 1679–704 (2003).
4. J.D. Joannopoulos, R.D. Meade, J.N. Winn, "Photonic crystals – molding the flow of light", 2nd ed., Princeton Univ., Princeton, NJ (1995).

Paper LM-O-8

PERIODIC GROOVES IMPRINTED ON SILICON MATERIAL BY SINGLE PULSE LASER NEAR-FIELD ABLATION

Florin Jipa[1], Marian Zamfirescu[1], Iulia Anghel[1], Mihaela Filipescu[1], Adrian Dinescu[2], Razvan Dabu[1]

[1]National Institute for Laser Plasma and Radiation Physics, Magurele, Bucharest, Romania
[2]National Institute for Research and Development in Microtechnologies, Bucharest, Romania

florin.jipa@inflpr.ro

In the last few years, new characterization and processing methods which are based on the near-field effect were developed [1, 2]. Instead to use optical devices, such us microscope objective or lens systems, these methods use micro optical elements to focus the electromagnetic field. When the dimensions of these elements are comparable with the radiation wavelength, the electromagnetic field is focused in to a spot smaller than diffraction limit. Moreover, the intensity of the electromagnetic field which is produced in this spot increases several times.

Applying these effects for self-assembled colloidal particles, nano-patterns were produced on large surface in a single exposure step [3]. However, the pattern imprinted using this method is limited to nano-holes arranged in a hexagonal geometry. In order to overcame this limitation, we replaced the colloidal particles with transparent photopolymer mask. These masks can be produced in photoresist materials by laser direct writing approach, or other techniques, like e-beam lithography.

In this work, we present a theoretical and experimental study were photopolymer mask are used as focusing elements for near field ablation. The best mask parameters as well as the theoretic near-field distribution and intensification factor was computed by Finite-Difference Time Domain (FDTD) method.

To demonstrate the feasibility of this method, a silicon wafer was processed using a mask realized in PMMA positive photoresist through electron beam lithography. A single infrared femtosecond laser pulse was used to expose the photopolymer mask. Periodic grooves with dimensions under diffraction limit were produced on the silicon surface. The imprinted pattern was investigated with Atomic Force Microscopy (AFM).

References:

1. E. Betzig, J.K. Trautman, “Near-field optics: Microscopy, spectroscopy, and surface modification beyond the diffraction limit” Science, Vol. 257, No. 5067, pp. 189–195 (1992).
2. Y.-C. Tsai, R. Fardel, C.B. Arnold, “Nanopatterning on rough surfaces using optically trapped microspheres” Appl. Phys. Lett., Vol. 98, 233110 (2011).
3. N. Nedyalkov, T. Sakai, T. Miyanishi, M. Obara, “Near field distribution in two dimensionally arrayed gold nanoparticles on platinum substrate” Appl. Phys. Lett., Vol. 90, 123106 (2007).

Paper LM-O-9

LASER NANOSTRUCTURING OF THE PbX MATERIALS FOR THE SEMICONDUCTOR FILM TRANSPORT PROPERTIES CONTROL

A. Kucherik[1], A. Antipov[1], S. Arakelian[1], V. Emelianov[2], S. Zimin[3], S. Kutrovskaya[1], A. Makarov[1], A. Osipov[1]

[1]Vladimir State University named after Alexander and Nikolai Stoletovs, Gorkii st. 87, Vladimir 600000, Russia
[2]Lomonosov's Moscow State University, Moscow, Russia
[3]Yaroslavl State University named after P.G.Demidov, Russia

The method of producing semiconductor nanoparticles of lead chalcogenides with an average size of 5–50 nm by means of continuous laser radiation of a moderate intensity nearby infrared range (up to 10^6 W/cm^2) has been proposed in this paper. As it is shown in our papers the application of continuous laser radiation enables to initiate the nanostructuring of PbTe, PbSe, PbS semiconductors without specific demands to the environmental conditions. Radiation with 1.06 micrometers wavelength corresponds to a quantum of photon energy which considerably exceeds the width of a prohibited zone of semiconductors being used.

We studied solid-state laser modification of the surface of PbX semiconductor films selforganisation at photon energies above the band gap of the semiconductor. Experimental data were used to construct a model for defect deformation instability developing on the surface of an epitaxial film through strain-induced drift of laser-induced point defects. The model is capable of qualitatively describing the observed surface morphology and predicting the surface profile in laser modification experiments.

The method of laser ablation in liquids has been used for obtaining colloid systems; ethanol (C2H5OH) and glycerin (C3H5(OH)3) having been used as solvents.

The sizes of the particles obtained were determined by means of the particle size analyzer Horiba LB-550; the principle of its operation relying on the phenomenon of dynamic light scattering.

The paper represents the results of laser synthesis of semiconductor nanoparticles of lead chalcogenides. The method of laser evaporation in liquid was used for obtaining nanoparticles. The way proposed for obtaining nanoparticles under the action of continuous laser radiation has shown that nanoparticles can be quantum dots by their geometric properties. The method of drop deposition used for shaping a deposited layer consisting of quantum dots has been considered. It has been demonstrated that the given method enables to obtain structures with various morphology which depends on the substrate temperature. Later, optical and electro-physical properties of the obtained structures will be studied which is very important for their use in the devices of optoelectronics and photonics.

Paper LM-O-10

FEMTOSECOND LASER ABLATION OF METALS AND STRENGTHS OF CONDENCED STATE

S.I. Ashitkov[1], P.S. Komarov[1], M.B. Agranat[1], N.A. Inogamov[2], V.V. Zhakhovsky[3]

[1]*Joint Institute for High Temperatures of Russian Academy of Sciences, 13/19 Izhorskaya st., Moscow 125412, Russia*
[2]*Landau Institute for Theoretical Physics, Russian Academy of Sciences, Chernogolovka 142432, Russia*
[3]*Department of Physics, University of South Florida, Tampa, Florida 33620, USA*

Femtosecond ablation in metals with a different properties (aluminum, nickel) is studied. Time and spatial resolved interferometric technique was used to investigate the deformation dynamics of target surfaces with subpicosecond resolution. The experimental data on tensile strengths of metals in condenced state at extremely high strain rates of order 10^8–10^9 s^{-1} were obtained from the time evolution of surface velocity histories. In conjunction with experiment the dynamics of ablation were investigated by a combination of two-temperature hydrodynamic modeling and molecular dynamics simulations.

Approaching the ultimate shear and tensile strength of aluminum in experiments with femtosecond pulse laser

We studied the shock-wave phenomena generated by femtosecond laser pulses in aluminum films 0.5 to 1.2 μm in thickness. The free surface displacement as a function of time has been measured with femtosecond interferometric microscopy and converted into the free surface velocity histories. The relation between the shock front velocity and the particle velocity indicates the shock compression is elastic at least up to 13 GPa under these conditions. This is also confirmed by the small (≤1 ps) rise time of the shock waves. The data are in excellent agreement with dependence of apparent Hugoniot elastic limit on the wave propagation distance in the plate impact experiments. Shear stresses reached 3.4 GPa, which is close to estimated ultimate value for aluminum. The spall strength of aluminum at strain rates of about 10^9 s^{-1} is comparable with its "ideal" tensile strength and is in good agreement with molecular dynamics calculations.

Strength of metals in liquid and solid states at extremely high tension produced by femtosecond laser heating

We will discuss results of combined experimental and theoretical investigations of ablation and laser-driven shock-wave phenomena in metal films irradiated by femtosecond laser pulses. The femtosecond interferometric microscopy technique was used to make time-resolved measurements of optical properties as well as record the deformation dynamics at both the rear and frontal surfaces during initial two-temperature electron-ion relaxation and subsequent hydrodynamic expansion. In conjunction with experiment, the formation and propagation of strong tensile and compression waves were investigated by a combination of two-temperature hydrodynamic modeling and molecular dynamics simulations. The experimental tensile strengths of aluminum and nickel in solid and liquid states at extremely high strain rates in range 10^8–10^9 s^{-1} were obtained from the time evolution of rear and frontal surface velocities. Theoretical tensile strengths calculated by atomistic simulations of ablation and spallation using micron-sized films agree well with experiment. Elastic-plastic response of metallic films to shock compression investigated by both experiment and theory/modeling will also be discussed.

Paper LM-O-11

PROPAGATION OF LASER RADIATION THROUGH DIFFUSION FLAMES

A.V. Rodin, S.V. Gvozdev, A.F. Glova, V.Yu. Dubrovsky, S.T. Durmanov,
A.G. Krasiukov, A.Yu. Lysikov, G.V. Smirnov

State Research Center of Russian Federation "Troitsk Institute for Innovation and Fusion Research"
142190 Russia, Moscow, Troitsk, RSC TRINITI

rodin@triniti.ru

In recent years lasers are practically used for remote cutting of metal constructions of dangerous gas wells. Under these conditions there is no way for executing any quantitative measurements. Therefore, the only way to obtain the required information is to carry out laboratory experiments.

The phenomenological analysis of these processes was started in the TRINITI at the beginning of 90s in the previous century. During ground tests of the MLTC-50 complex (high-power CO_2-laser) several fragments of the gas armature were cut by a laser beam that passed through the flame area.

This work was devoted to experimentally investigating the absorption and scattering of laser radiation with the wave-length of about 1 μm under propagation through diffusion flames of aviation kerosene, ethanol and ethanol-kerosene mixtures. The radiation of a pulse repetition rate (PRR) Nd:YAG laser (λ = 1.06 μm, the half-amplitude pulse duration is τ = 130 μs, the pulse-repetition rate is f = 1–50 Hz, the highest pulse energy E_{max} = 0.5 J) or a CW ytterbium fibre (YB) laser (λ = 1.07 μm, the peak power is 4 kW) was collimated into the practically parallel beam. This radiation was then directed through the flame area to radiation detectors. Part of the radiation scattered by a small flame segment was separated out to measure the radiation power in dependence on the scattering angle.

Power measurements of the Nd:YAG laser radiation scattered by the flame were made under the beam propagation through the yellow part of the kerosene flame of 4.5 cm in length. The distance between the beam axis and the kerosene cell edge was h = 2 cm. The average radiation power at the flame input was equal to 2.5 W. The measurements were made under the various scattering angles: 70°, 90° and 110°. Our experiments showed that the scattering was anisotropic and the fraction of the radiation scattered by the diffusion flame of the aviation kerosene was as low as about ~0.23%.

We compared the measured absorption coefficients α for the PRR Nd:YAG laser radiation with the data for the CW fibre laser and the same h for the kerosene flame. The radiation intensities at the flame input were approximately the same and corresponded to the intensities usually used for the remote cutting of metals by the CW laser radiation. The absorption coefficient for the CW laser radiation, as well as for the case of the PRR laser radiation, decreased with the increase in the flame length. However, when the intensities and lengths for both lasers were close, the absorption coefficient for the CW laser radiation was considerably higher than that for the PRR laser. The greater α for the CW laser radiation is due to the fact that the average temperature of the in-flame heated particles is higher under the additional CW radiation heating than under the repetition rate radiation heating. As a consequence, the density of radiation-absorbing combustion products is higher, which leads to greater α.

So the radiation absorption coefficient of this flame depends on the flame length, radiation intensity, laser operation mode and flame area through which the radiation propagates. The absorption of radiation with the intensity of 10^3–10^4 W·cm^{-2} in the flame depends on the fuel type and can vary within a wide range.

Paper LM-O-12

CORRELATION ANALYSIS OF DATA OF MULTI-CHANNEL PYROMETER IN GAS –ASSISTED LASER CUTTING TECHNOLOGY: DIFFERENCE BETWEEN CUTTING USING CO2-LASER AND FIBER LASER

Alexander V. Dubrov, Yury N. Zavalov, Vladimir D. Dubrov

Institute on Laser and Information Technology of Russia Academy of Science, Shatura, Moscow Region, Russia

dubrovav@gmail.com

The gas-assisted laser cutting of samples of mild steel with a thickness of 3 mm was monitored: the time depended behavior of the melt temperature was measured along the cutting front by multichannel pyrometer as described in [1]. The CO_2 laser of 1500 W and Ytterbium-doped fiber laser of 1800 W were used. Temperature pulsations in five regions of cutting front spaced about 0.6 mm and with average size of 0.1 mm were measured simultaneously; the cutting parameters: cutting velocity and pressure of assisted gas (oxygen) were varied in different tests.

The cross-correlation functions of signals from adjacent channels were calculated based on technique described in [2]. The delays of the temperature inhomogeneities travel from one region of view to another will be presented. This technique was also repeated with filtered temperature data. Pre-filtration was performed of temperature fluctuations in each channel: the entire range of temperature spectrum was divided into six octaves: 62 Hz–125 Hz, … 1 kHz–2 kHz, 2 kHz–4 kHz. The delays of the travel of "filtered" temperature inhomogeneities were calculated too. Thus, the velocity of temperature inhomogeneities displacement and its spectral components were determined. Spectral components of the velocity is determined here as velocity of displacement of temperature inhomogeneities that repeated in a narrow range of frequency.

It is shown that this technique allows determining not only the surface velocity of the melt flow, but also the speed of inertial waves [3]. These data were obtained for a range of cutting speed and pressure of assistant gas (oxygen). So it is proven experimentally that differences (V^+–V_m) and (V_m–V^-) are varied with increasing of the cutting parameters: cutting speed and oxygen pressure. It is known that differences remain largely a function of surface-tension component in phase with the wave slope and local gas pressure as well as Weber number of the melt flow [4]. The decreasing of differences specified above with increasing cutting speed in the case of fiber laser may be explained [5], by larger angle of cutting front compared with the case of CO_2 laser cutting.

Acknowledgements: The reported study was partially supported by RFBR, research project No. 13-08-00987.

References:

1. A.V. Dubrov, Y.N. Zavalov, V.D. Dubrov, et al., "Spectrum of temperature pulsations of the melt in gas-assisted cutting with fiber laser" Opt. Eng., Vol. 51, 094301 (2012).
2. A.M. Yaglom, "Correlation theory of stationary and related random functions", Vol. 1–2. New York: Springer-Verlag, 1987.
3. G.B. Whitham, "Linear and Nonlinear Waves", John Wiley & Sons, 1974.
4. K. Chen, Y.L. Yao, "Striation formation and melt removal in the laser cutting process" J. of Manufacturing Systems, Vol. 18, pp. 43–53 (1999).
5. M. Vicanek, G. Simon, H.M. Urbassek, I. Decker, "Hydrodynamical instability of melt flow in laser cutting" J. of Physics D: Appl. Phys., Vol. 20, pp. 140–145 (1987).

Paper LM-O-13

DEVELOPMENT OF METHODS OF CREATION AND RESEARCH NANOSTRUCTURES ON THE BASIS OF ZnO(Co) AND Mn_XSi_{1-x} WITH CONTROLLED MAGNETIC AND ELECTRIC PROPERTIES

O.A. Novodvorsky[1], A.A. Lotin[1], D.A. Zuev[1], O.D. Khramova[1], A.V. Shorokhova[1], L.S. Parshina, B.A. Aronzon[2], V.V. Rylkov[2], M.A. Pankov[2]

[1]*Institute on Laser and Information Technologies of RAS, 140700 Shatura, Russia*
[2]*National Research Centre, Kurchatov Institute, 123182 Moscow, Russia*

onov@mail.ru

The thin films ZnO(Co) and Mn_xSi_{1-x} have been received by a method of a pulse laser deposition (PLD) with the direction of a energy spectrum of ions low-temperature plasmas. For working off of technology of production nanostructural ferromagnetic semiconductor materials detailed researches of their composition and structural features by methods of X-ray photoelectronic spectroscopy and the X-ray diffraction analysis were made. The technology of creation of compounds of $Si_{1-x}Mn_x$ with the high content of manganese is developed for the first time.

The modified method of a PLD on the crossed beams which allows to direct energy of deposited particles in the wide range is developed. Samples of $Zn_{1-x}Co_xO$ were received by a PLD with use of sapphire (0001) substrates at a temperature of 500°C in the oxygen atmosphere at different pressure. Concentration of cobalt in films changed from 0.1 to 45 at.%, varied thickness of films (60–130 nm). The limit of solubility of cobalt in $Zn_{1-x}Co_xO$ films with wurtzite structure up 35 at.% is reached. Strong hysteresis dependence of longitudinal resistance Rxx on a field B directed perpendicularly of the film surface for $Zn_{1-x}Co_xO$ films with of $d = 60$ nm thickness was observed. Field dependence of longitudinal resistance of Rxx (B) for $Zn_{1-x}Co_xO$ film ($x = 0.2$) thickness of $d = 60$ nm shows that the magnetoresistance is negative. Resistance is maximum at magnetization $M = 0$, i.e. in the field of H = Hc, where Hc – coercive force, and decreases at parallel orientation of the magnetic moments of nanoclusters. Such behavior of a magnetoresistance (MR) is inherent in granular metals in the conditions of spin-dependent dispersion of carriers of a charge when size MR is proportional to M2. Such anisotropy enhances ferromagnetism of films and is important for application of magnetic semiconductor films in spintronics.

For the first time $Si_{1-x}Mn_x$ 55–70 nm thick films with the various maintenance of Mn ($x = 0.44$–0.6) are received by PLD method with use of separation of besieged particles on speed. For the first time possibility of creation of films of $Si_{1-x}Mn_x$ on structure close to MnSi silicide (x ~ 0.5), possessing ferromagnetics is shown at temperatures above 300 K [1]. It is shown that in nonstoichiometric alloys of $Si_{1-x}Mn_x$ at $x = 0.52$–0.55 temperature of Curie can reach 500 K, and the abnormal effect of the Hall at $T = 300$ K for these films is nearly 5 times higher, than for $Si_{1-x}Mn_x$ films at $x \sim 0.35$ [2].

Acknowledgements: This work was supported by the Ministry of education and science of the Russian Federation (grant no.24.08.12.8391) and by the Russian Foundation for Basic Research (project nos. 12_02_33022 mol_a_ved, 12_07_00301a, 12_08_00642a.

References:

1. V.V. Rylkov, S.N. Nikolaev, K.Yu. Chernoglazov, B.A. Aronzon, K.I. Maslakov, V.V. Tugushev, E.T. Kulatov, I.A. Likhachev, E.M. Pashaev, A.S. Semisalova, N.S. Perov, A.B. Granovskii, E.A. Gan'shina, O.A. Novodvorskii, O.D. Khramova, E.V. Khaidukov, V.Ya. Panchenko, "High temperature ferromagnetism in $Si_{1-x}Mn_x$ ($x > 0.5$) nonstoichiometric alloys" Pis'ma v Zhurnal Eksperimental'noi i Teoreticheskoi Fiziki, Vol. 96, No. 4, pp. 272–280 (2012).
2. S.N. Nikolaev, V.V. Ryl'kov, B.A. Aronzon, K.I. Maslakov, I.A. Likhachev, E.M. Pashaev, K.Yu. Chernoglazov, A.S. Semisalova, N.S. Perov, V.A. Kul'bachinskii, O.A. Novodvorskii, A.V. Shorokhova, O.D. Khramova, E.V. Khaydukov, V.Ya. Panchenko, "High temperature ferromagnetism of $Si_{1-x}Mn_x$ films fabricated by laser deposition using the droplet velocity separation technique" Semiconductors, Vol. 46, No. 12, pp.1511–1518 (2012).

Paper LM-P-1

THE THIN FILM SYNTHESIS AND DEPOSITION OF NANOSTRUCTURES FROM COLLOIDAL SYSTEMS BY LASER BEAMS

A. Antipov, D. Bukharov, A. Kucherik, S. Kutrovskaya, D. Nogtev, A. Makarov

Vladimir State University named after Alexander and Nikolai Stoletovs, Gorkii str. 87, Vladimir 600000, Russia

Formation of metal coverings on a surface of various materials the important applied task. Use of laser radiation stimulates process of deposition and allows controlling morphology of a deposited layer. Thickness and width of the deposited layer can be varied from hundred nanometers to tens micron that allows to carry out selective deposition on a surface of the any form.

In this work colloidal is produce from liquid phase (ethanol, glycerin etc) and metal nanoparticles (the size less to 100nm). Varying parameters of a laser radiation and quantity of scans of a laser spot on the surface, it is possible to obtain deposited layer of various width and a thickness.

Investigation of deposited layers by raster electron microscopy, atom force microscopy and X-ray spectroscopy with FIB-profiling have shown that the deposition layer forming without damage of initial surface. For investigation process of depositing the model of laser heating and particles diffusion are developed. This model demonstrate the dependence of morphologies properties deposited layer from initial relief of surface.

In the given work the method of formation nanostructured films and covers is offered. This method realized on base method of Laser Deposition of Metals from Solutions (LDMS) at action of laser pulse-periodical radiation on colloidal systems. Offered method allows controlling process of particles deposition and allowing forming different structures along a trajectory of moving a laser beam. Properties of the deposition layer depend on a material of a colloidal solution used at preparation and properties of substrate.

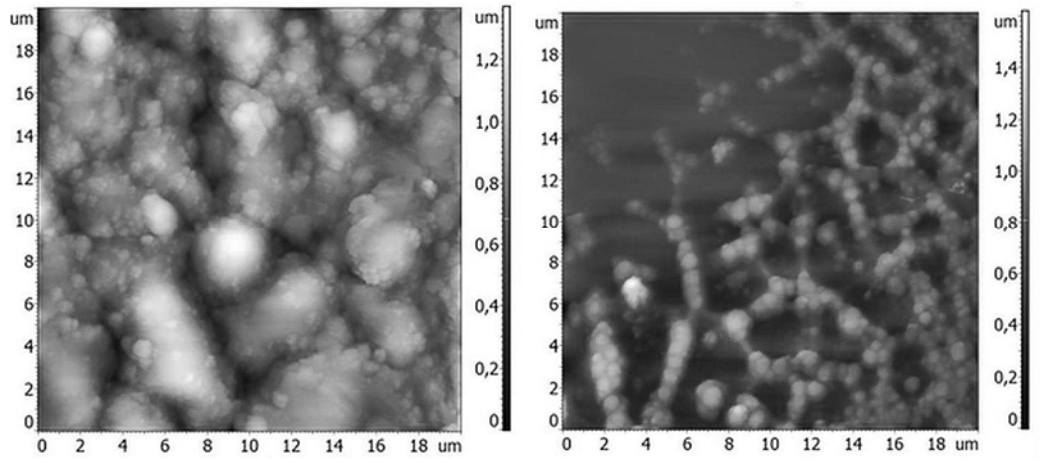

a) b)

Laser deposition of nickel nanoparticles on a solid substrate surface placed into a colloid solution: AFM images of the deposition area on the copper substrate surface (a) and on the surface of a glass substrate (b).

Paper LM-P-2

PLD GROWN THIN FILMS STOICHIOMETRY AND STRUCTURE STUDY

V.M. Brendel[1], T.F. Yagafarov[1], S.V. Garnov[1], V.A. Terechin[2], U.A. Trutnev[2]

[1]*Prokhorov General Physics Institute, Russian Academy of Sciences, Vavilov Str., 38, Moscow 119991, Russia*

[2]*FSUE RFNC - VNIIEF, Mira ave. 37, Sarov 607188, Nizhny Novgorod region*

vadim-boss@mail.ru

Dielectric and semiconducting films on metal substrate are good candidates for photocathodes, which can withstand exposure to air [1]. Initially we used PLD technique to produce CsI, CsBr thin films on copper substrate and measured quantum yield of such photocathodes [2]. In this work we decide to carefully investigate stoichiometry and structure of PLD films. GaAs is chosen as promising material for durable photocathodes [3].

We have made thin films of CsI, CsBr and GaAs on dielectric substrates (glass). The films were made by pulse laser deposition with Nd:YAG electro-optically Q-switched laser. The laser parameters: wavelength 1064 nm, pulse duration – 20 ns, the maximum pulse energy – 1000 mJ, the maximum frequency – 20 Hz. Coating was carried out in a vacuum chamber with oil-free evacuation to 10^{-5} mbar. Coatings were deposited for 2 hours (20 Hz) at various temperatures of substrate: room temperature, 500°C, 1000°C. The laser pulse energy was minimal, but one in which the target ablation occurred. During the deposition process was performed manually adjust the focus of the laser spot on the target.

After production samples were transferred to stoichiometry and film structure study by X-ray diffraction analysis and scanning electron microscopy. We found that the stoichiometry of CsI and CsBr is ideally coincides with the initial state of target. GaAs films have increased Ga content in all our samples, including specially produced samples on Cu substrate. All films are polycrystalline with spherical clusters (Figs. 1 and 2). Increase of substrate temperature leads to increase coating density in all cases.

We attribute stoichiometry breach with the fact that constituent elements of the GaAs crystal are light weight. After ablation Ga and As lose their bindings and fly away. Especially this can be demonstrated on big droplets on film, which has 45% at. % Ga and only 17% at. (spectrum 1 on Fig. 3).

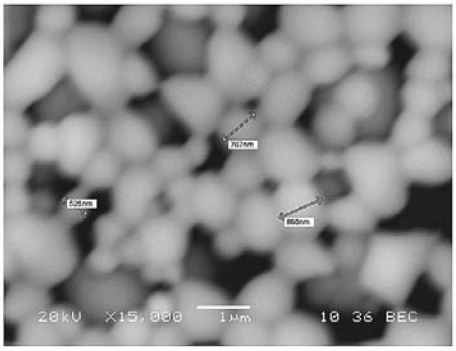

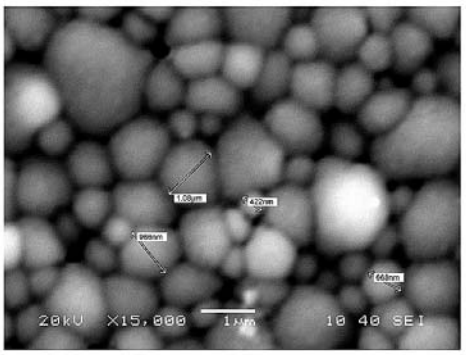

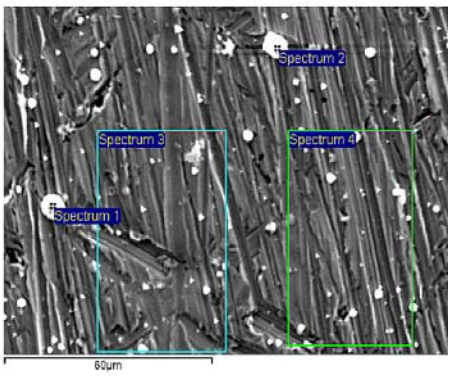

Fig. 1. CsBr film on glass (room temp). **Fig. 2.** CsI film on glass (room temp). **Fig. 3.** GaAs film on Cu (room temp).

References:

1. A.F. Byzylyckov, Gas photodetectors with solid photocathode's. Physics of elementary particles and atomic nuclei. 3th ed., pp. 813–870 (2008).
2. V. Brendel et al. "Fabrication of alkali halide UV photocathodes by pulsed laser deposition" Quantum Electronics, Vol. 42 (12), pp. 1128–1132 (2012).
3. W. E. Spicer, A. Herrera-Gomez, "Modern theory and applications of photocathodes", SLAC-PUB-6306, SLAC/SSRL-0042 (1993).

Paper LM-P-3

DYNAMIC ADAPTATION SHOCK-CAPTURING METHOD FOR GASDYNAMIC PROBLEMS

P.V. Breslavskii

Keldysh Institute of Applied Mathematics Russian Academy of Sciences,
Miusskaya sq., 4, Moscow, 125047, Russia

vim@modhef.ru

Dynamic adaptation method applied to gas dynamics problems was considered earlier [1]. Shock and contact discontinues occurrence is the main problem to gain acceptable numerical solutions for gas-dynamics equations. The existing techniques for solving gas dynamics problems can be divided into two groups: explicit front tracking methods and shock capturing methods. When physical statement doesn't require explicit boundary tracking the shockcapturing methods become more convenient. The artificial viscosity technique is used in this paper as shock-captured method.

The adaptation function used in this paper is determined by the condition that the grid point is quasi-uniform and is concentrated in the steep-gradient regions simultaneously. The features of the dynamic adaptation shock-capturing method are demonstrated using two tests: SOD problem [2], and Woodward-Colella problem.

SOD problem numerical solutions for N = 100 are shown on the figure: a – WENO3, b – WENO5, c – MUSCL, d - dynamic adaptation shock-capturing method.

Acknowledgements: The work was partially supported by RFBR Grants Nos. 13-07-00597, 12-07-00436.

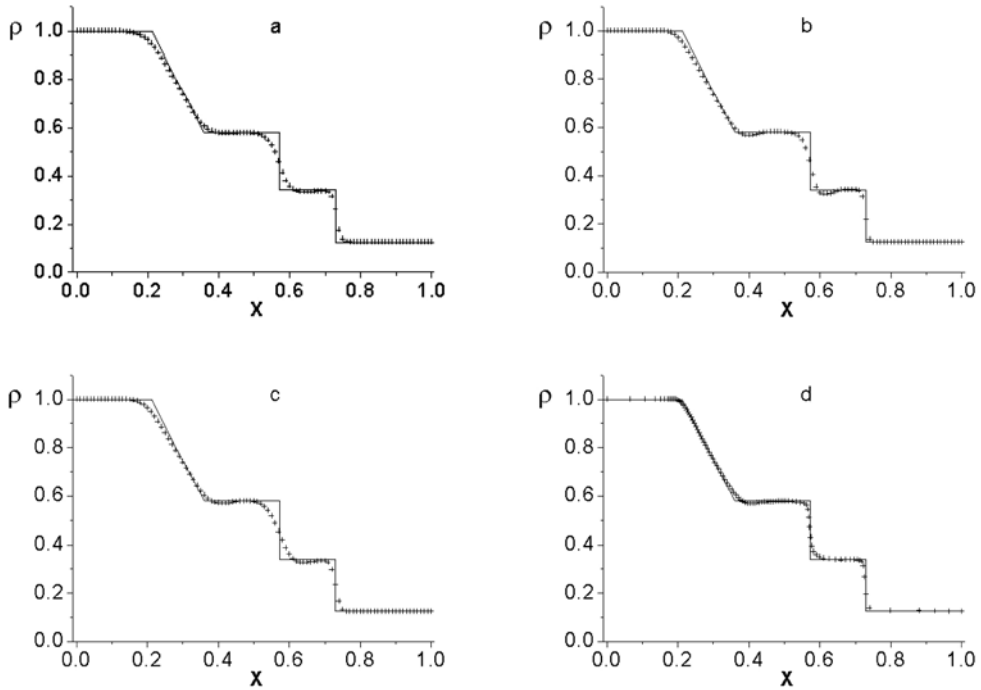

References:

1. P.V. Breslavskii, V.I. Mazhukin, "Dynamically adapted grids for interacting discontinuous solutions" Comp. Math. and Math. Phys., Vol. 47, N 4, pp. 687–706 (2007).
2. E.F. Toro, "Riemann solvers and numerical methods for fluid dynamics", 2nd ed., Springer (1999).

Paper LM-P-4

USING MULTI-CHANNEL PYROMETER TO RESEARCH FEATURES OF MELT FLOW IN TECHNOLOGY OF CO_2 LASER CUTTING WITH AUXILIARY GAS

Alexander V. Dubrov, Yury N. Zavalov, Vladimir D. Dubrov,

Institute on Laser and Information Technology of Russia Academy of Science, Shatura, Moscow Region, Russia

dubrovav@gmail.com

The time depended behavior of the melt temperature on the cutting front was studied while oxygen-assisted cutting of metal sheets with CO_2-laser. The temperature was measured by multichannel pyrometer described in [1], discretization time was 0.062 ms. The temperature was taken from five local regions in upper part of the cutting front with distance about 0.6 mm between each other.

Low-carbon steel sheets with thickness of 6 and 10 mm was used. Cutting parameters and assisted gas pressure was varied in experiments with deviation from "optimal conditions". The cutting speed of 10 mm steel was much less than melting velocity (Vm is about 0.03 m/s), while for 6 mm steel the cutting speed was 0.025–0.04 m/s.

Then the cross-correlation, [2], was calculated based on measured multichannel data and so the delays of the temperature inhomogeneities travel from one view region to another along the cutting front was obtained. Knowing the distance between view regions one can get the dependences of melt surface velocity on cutting speed and assisted gas pressure.

The calculation was performed but taking into account that two inertial waves are also present on the cutting front: one with a larger velocity and second with a smaller than velocity of the melt surface [3]. Obtained so melt depth estimation is in well accordance with calculated data from [4]. The analysis of obtained spectral dependences of sweep velocity of temperature inhomogeneities is performed and results are discussed.

Acknowledgements: The reported study was partially supported by RFBR, research project No. 13-08-00987.

References:

1. A.V. Dubrov et al., "Application of optical pyrometry for on-line monitoring in laser-cutting technologies" Appl. Phys. B. Lasers and Optics, Vol. 105(3), pp. 537–543 (2011).
2. A.M. Yaglom, Correlation theory of stationary and related random functions. Vol. 1–2. New York: Springer-Verlag, 1987.
3. N. Andritsos, T.J. Hanratty, "Interfacial instabilities caused by air flow" Int. J.Multiphase Flow, Vol. 13, pp. 583–603 (1987).
4. K. Chen, Y.L. Yao, V. Modi, "Gas Dynamic Effects on Laser Cut Quality" J. Manufacturing Processes, Vol. 3, pp. 38–49 (2001).

Paper LM-P-5

MATHEMATICAL SIMULATION OF RADIATION ACCELERATED OUTFLOWS

M.P. Galanin, V.V. Lukin, V.M. Chechetkin, K.L. Shapovalov

Keldysh Institute for Applied Mathematics of RAS, Miusskaya sq., 4, Moscow, Russia

galan@keldysh.ru

The RMHD model for formation of astrophysical jet outflow from the vicinity of a compact object surrounded by a thin accretion disk and immersed into the nebula of a galactic plasma is considered.

The numerical methods for solving the systems of magnetic hydrodynamics (MHD) equations and radiation transport equation in two-dimensional axis - symmetrical statement on triangular unstructured grid were developed. The numerical algorithms are based on division by physical processes and include a difference scheme for the MHD system and discrete directions method for radiation transfer equation.

The numerical methods were implemented as a software system designed for high performance systems with shared memory, including systems with graphical accelerators. Parallel implementation of RKDG method for solution of two-dimensional equations of ideal magnetic hydrodynamics on triangular unstructured grids was considered. The software complex was built with the MPI and OpenMP technologies. The algorithms for monotonization and divergence – free reconstruction of magnetic field are presented. They allow getting physically adequate results with high order accuracy. The results of test calculations and obtained from parallel technologies values of computation accelerations are discussed.

The modeling results show the formation of the accelerating channel and acceleration of jet plasma up to 1/5 luminal speed and comply with the available observation data. Computations are performed on a KIAM K-100 cluster.

The processes of creation and development of magneto-rotational instability of near – star plasma disc were investigated. The results show that instability leads to withdraw of the angular momentum on the periphery of the disk and the accretion on a star.

Acknowledgements: The investigation is partially supported by RFBR (projects 12-01-00109, 12-01-31193, 12-02-12096, 12-02-00687), grant of President of Russian Federation for state support of leading scientific schools of RF (project NSH-1434.2012.2).

Paper LM-P-6

INTERACTION OF SURFACE PLASMON POLARITON PULSES AT THE SURFACE OF DIELECTRIC WITH KERR NONLINEARITY

D.O. Ignatyeva, A.P. Sukhorukov

Lomonosov Moscow State University, Leninskie Gory, 1, bld. 2, Moscow 199991, Russia

ignatyeva@physics.msu.ru

This work is devoted to the analysis of the phenomenon of the nonlinear interaction of two surface plasmon polariton (SPP) pulses at the interfaces of noble metal and the dielectric with cubic nonlinearity. Using such interaction one can control the propagation dynamics of the signal pulse via the modulation of the intensity of the pump pulse. Similar method based on the phenomenon analogous to the total internal reflection of light implemented in the time domain was proposed in [1] for the bulk optical pulses. In contrast to ordinary crystals or optical fibers plasmonic systems can provide more efficient methods of light control due to the high energy concentration in SPP wave near the metal-dielectric interface [2]. Therefore the efficiency of the various nonlinear interactions of surface waves is higher that the interaction of the bulk waves (see, for example, [3]). Plasmonic systems are also characterized by the high frequency dispersion so that the distance required for the nonlinear interaction of the two pulses of different frequency is shortened. At the same time we should take into account that the propagation distance of SPP is very small (about 100 μm in the optical frequency range).

We analyze the propagation dynamics of the pump and the signal SPP pulses taking into account dispersion, cubic nonlinearity of the dielectric, losses in metal, group velocity dispersion and the interaction between the SPP pulses. Strong pump SPP pulse induces the inhomogeneity of the dielectric permittivity moving with the group velocity of the pulse. Weak signal SPP pulse of a different frequency propagates at the same interface with a certain initial delay. Due to the group velocity dispersion it reaches the pump SPP. The interaction of the pulses is studied both by the numerical solution of the derived slowly varying amplitude equations and by the analytical description of the SPP trajectory using the eikonal method.

We found that under certain conditions if the pump SPP intensity is rather high the signal SPP pulse is “reflected” from the induced inhomogeneity. It means that initially propagating with higher group velocity signal SPP pulse slows down by the pump and continues travelling behind the pump SPP. This “reflection” is followed with the spectral shift of the signal SPP. At the same time if the intensity of the pump SPP pulse is below the critical value the signal SPP propagates through the pump in a usual way and runs ahead due to the difference of the group velocities of pulses. Optimal duration of the signal and pump SPP pulses required for the implementation in such system is about 50 fs.

Therefore the intensity of the SPP pump pulse determines the delay and the relative position of the signal SPP pulse.

References:

1. V.E. Lobanov, A.P. Sukhorukov, “Total reflection, frequency, and velocity tuning in optical pulse collision in nonlinear dispersive media” Phys. Rev. A, Vol. 82, 033809 (2010).
2. S.A. Maier, “Plasmonics: Fundamentals and Applications”, Springer (2007).
3. D.O. Ignatyeva, A.P. Sukhorukov, “Plasmon beams interaction at interface between metal and dielectric with saturable Kerr nonlinearity” Appl. Phys. A, Vol. 109, pp. 813–818 (2012).

Paper LM-P-7

OPTICAL PROPERTIES OF PLASMONIC NANOSTRUCTURES WITH MAGNETIC CONSTITUENTS

A.N. Kalish[1], V.I. Belotelov[1], A.K. Zvezdin[2]

[1]*Lomonosov Moscow State University, Leninskie Gory 1 2, Moscow 119991, Russia*
[2]*Prokhorov General Physics Institute of RAS, Vavilova str. 38, Moscow 119991, Russia*

kalish@physics.msu.ru

Magneto-optics is one of the most attractive fields of photonics as magneto-optical effects provide efficient management of light properties [1]. Nanostructuring offers significant enhancement of magneto-optical effects. In particular, we suggest the plasmonic magnetic heterostructure shown in Fig. 1. Depending on the magnetization direction various effects related to either polarization or intensity emerge.

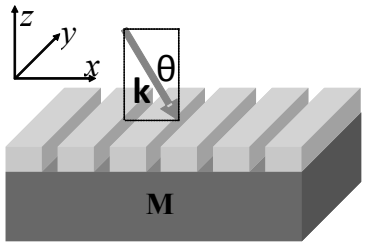

Fig. 1. Magnetoplasmonic crystal under consideration and the incidence configuration. The metallic grating is deposited on a smooth magnetic dielectric layer.

We develop the original approach for the theoretical study of magneto-optical response of such heterostructure based on analysis of eigenmodes and S-matrix properties. The eigenmodes of the structure play a crucial role both in the near-field and in the far-field magneto-optical response because their properties are dependent on magnetization. That leads to resonant features in spectra of magneto-optical effects observed both in reflected and in transmitted light. Our analysis reveals that excitation of eigenmodes leads to either significant enhancement of conventional effects or emergence of quite novel phenomena originating solely from nanostructuring.

If magnetization is directed along *y*-axis the transverse Kerr effect gets resonantly enhanced by 3 orders of magnitude in comparison with bulk magnetic media [2]. Magnetization directed along *z*-axis is favorable for the Faraday effect observation. The Faraday effect also gets resonantly increased by an order of magnitude at the eigenmodes excitation [3]. Finally, if magnetization is directed along *x*-axis a novel intensity effect emerges that cannot occur in smooth films. At this the intensity modulation can reach 100% and more [4].

References:

1. M. Inoue, M. Levy, A.V. Baryshev (ed.), “Magnetophotonics: From Theory to Applications”, Springer (2013).
2. V.I. Belotelov, I.A. Akimov, M. Pohl, V.A. Kotov, S. Kasture, A.S. Vengurlekar, Achanta Venu Gopal, D.R. Yakovlev, A.K. Zvezdin, M. Bayer, “Enhanced magneto-optical effects in magnetoplasmonic crystals” Nature Nanotechn. Vol. 6, pp. 370–376 (2011).
3. J.Y.Chin, T. Steinle, T. Wehlus, D. Dregely, T. Weiss, V.I. Belotelov, B. Stritzker, H. Giessen, “Nonreciprocal plasmonics enables giant enhancement of thin-film faraday rotation” Nature Comm. Vol. 4, p. 1599(1–6) (2013).
4. V.I. Belotelov, L.E. Kreilkamp, I.A. Akimov, A.N. Kalish, D.A. Bykov, S. Kasture, V.J. Yallapragada, Achanta Venu Gopal, A.M. Grishin, S.I. Khartsev, M. Nur-E-Alam, M. Vasiliev, L.L. Doskolovich, D.R. Yakovlev, K. Alameh, A.K. Zvezdin, M. Bayer, “Plasmon mediated magneto-optical transparency” Nature Comm. (accepted).

Paper LM-P-8

TWO PARAMETRIC SCALING LAW AND FIGURES OF MERIT FOR REVERSE SATURABLE ABSORPTION OF FUNCTIONAL DYES

L.M. Koldunov[1], M.F. Koldunov[2]

[1]*Moscow Institute of Physics and Technology (State University), 9, Institutskiy lane, Dolgoprudny, Moscow Region, 141700*

[2]*A.M.Prokhorov General Physics Institute Russian Academy of Sciences, 38 Vavilova St., Moscow, 119991*

lenia-laboratory@yandex.ru

The reverse saturable absorption investigation of functional organic dyes is stimulated by the practical aims of nonlinear laser elements development, for example Q-switch and optical limiter. It is very important to find figures of merit for the functional dyes to develop these elements. In this paper we give a ground to the two-parametric scaling law describing the functional dyes reverse saturable absorption. This law depicts the experimental data very well as it is demonstrated in figure below.

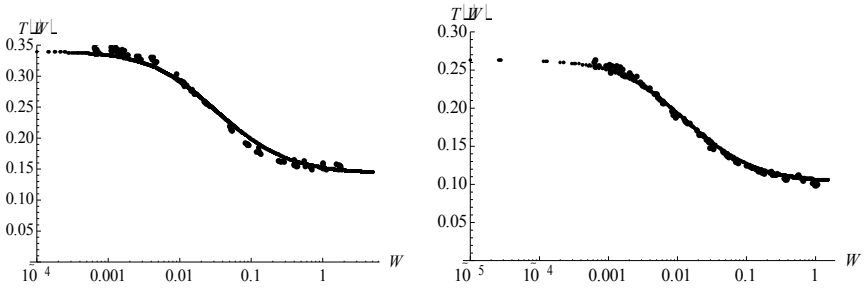

Transmission (T) is versus energy density (W). The left plot is zinc porphyrin in ethyl acetate and right plot in nano porous glass – polymer composite. Solid line is the experimental date approximation by scaling low. Points are experimental data [1].

We show that the parameters of this scaling law are the adequate figure of merits for the reverse saturable absorption of functional dyes. They are presented in terms of the functional dyes characteristics (cross sections, relaxation times and so on) and permit to forecast the quality of the functional dyes.

References:

1. S.M. Dolotov, L.M. Koldunov, et al., "Nonlinear absorption of laser radiation by zinc and lead phthalocyanines and zinc porphyrin in a nanoporous-glass/polymer" Quantum Electron., Vol. 42, pp. 39–43 (2012).

Paper LM-P-9

MELTING AND EVAPORATION OF SILICON BY A PICOSECOND LASER PULSE

O.N. Koroleva[1], A.V. Mazhukin[2]

[1]*Moscow University for Humanities*
[2]*Keldysh Institute of Applied Mathematics of RAS*

koroleva.on@mail.ru

Pulsed laser irradiation is now one of the most widely used materials-processing tools, including semiconductor. From the semiconductor materials most widely used in instrumentation is silicon. This material is one of the most perspective for thin-film nanotechnology.

A detailed study of the dynamics of the processes taking place in the area of radiation and which result in surface modification, including an analysis of the processes of heating, melting and evaporation is necessary for the development of new technologies of surface laser processing of semiconductors and to optimize the available.

In this paper by means of mathematical modeling methods we consider the dynamics of melting and evaporation processes of the silicon plate under the influence of a picoseconds laser irradiation of various intensities with the wavelength of. The laser pulse duration was varied in the range of 10^{-12}–3.5×10^{-11} with a radiation intensity – in the range of 10^{9}–10^{10} W/cm^2. The mathematical description of the dynamics of phase transformations carried out within the multi-phase version of the Stefan problem for the nonstationary one-dimensional statement of the problem. Application of the Dynamic Adaptation method to the numerical solution of partial differential equations allowed to determine the space-time distribution of temperature fields, to explicitly distinguish the position of the moving of interfaces, the velocity of its movement, the lifetime of the melt and the thickness of melted and vaporized layers.

Time profiles of the laser irradiation, the temperature on the target surface, velocity of melting and evaporation fronts for the irradiation intensity $G = 5\times10^{9}$ W/cm^2 and pulse duration $\tau = 3.5$ ps are shown in Figs. 1 and 2.

Acknowledgements: The work was partially supported by RFBR grants №№ 13-07-00597, 12-07-00436.

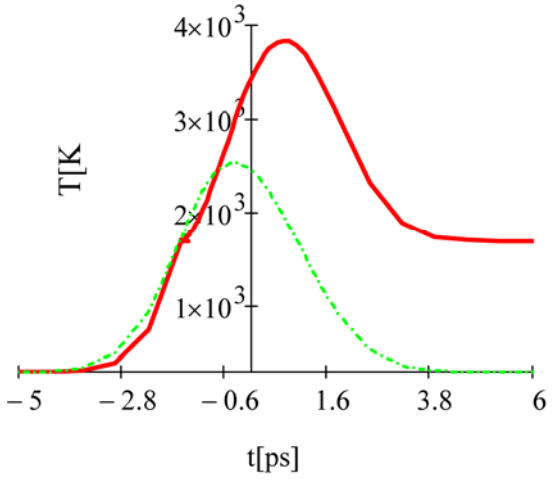

Fig. 1. The time dependence of the temperature on the target surface.

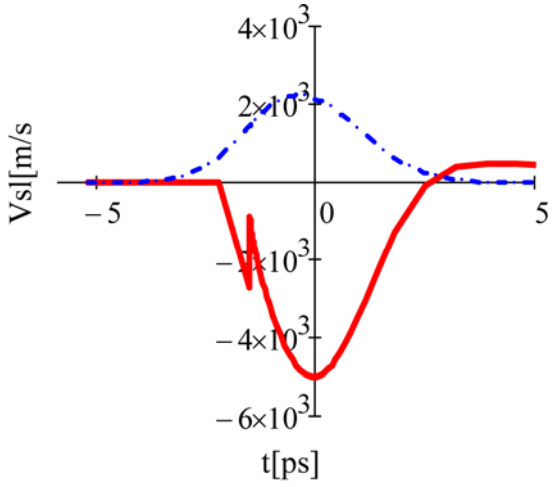

Fig. 2. Velocity of the melting front.

Paper LM-P-10

BV ABSORPTION BAND INFLUENCE ON NONLINEAR ABSORPTION IN $^{Bu}Pc_2Dy$

V.I. Krasovskii[1,2], A.B. Karpo[1], A.V. Zasedatelev[2], V.E. Pushkarev[3,4], L.G. Tomilova[3,4]

[1]*A.M.Prokhorov General Physics Institute of RAS, 38 Vavilov St., Moscow 119991, Russia*
[2]*National research nuclear university MEPhI, 31 Kashirskoye shosse, Moscow 115409, Russia*
[3]*Department of Chemistry, M.V. Lomonosov Moscow State University, 1 Leninskie Gory, Moscow 119991, Russia*
[4]*Institute of Physiologically Active Compounds of RAS, 1, Severny proezd, Chernogolovka 142432, Moscow Region, Russia*

The photophysical properties and nonlinear absorption of butyl substituted dysprosium bisphthalocyanine in the tetrahydrofurane (THF) solution was studied. Z-scan measurements were carried out using the open aperture z-scan technique with the pulsed laser light of 532 nm wavelength and pulse duration of 350 ps. The luminescence measurements revealed that at such excitation wavelength two absorption bands, Q and BV, are affected by the incident light. Therefore, we determined in what proportion these bands are excited under such illumination. To accomplish this we evaluated absorption cross-sections at 532 nm relating to each of the two considered transitions. Also, the lifetimes of these excited states were determined using TCSPC technique. Theoretical model treating BV- and Q- excitation channels as parallel and independent was proposed. Employing this approach we showed that these two channels compete with each other, where the one relating to BV-transition saturates and the other relating to the Q-transition leads to the strong reverse state absorption causing optical limiting.

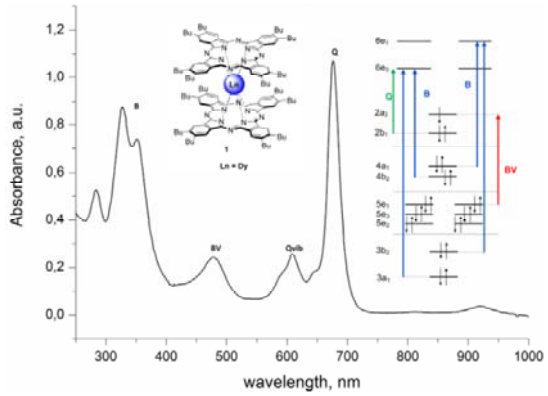

Fig. 1. Uv/Vis absorption spectrum of $^{Bu}Pc_2Dy$. Inset shows the electron transition scheme [2].

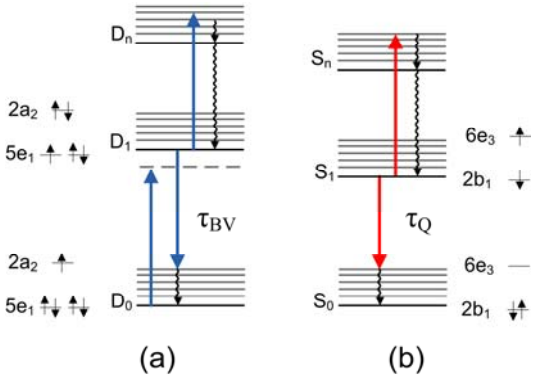

Fig. 2. Diagram of excitation and relaxation processes under illumination at 532 nm depicting two channels of absorption, due to BV absorption (a) and due to Q absorption (b).

References:

1. V. Pushkarev, A. Ivanov, I. Zhukov, E. Shulishov, Y. Tomilov, Russ. Chem. Bull., Int. Ed., Vol. 53, pp. 554–560 (2004).
2. A. B. Karpo, V.E. Pushkarev, V.I. Krasovskii, L.G. Tomilova, Chem. Phys. Lett., Vol. 554, pp. 155–158 (2012).

Paper LM-P-11

LASER FORMATION AND DEPOSITION OF BIMETALLIC Au/Ag CLUSTERS

A. Kucherik, A. Antipov, S. Arakelian, S. Kutrovskaya

Vladimir State University named after Alexander and Nikolai Stoletovs,
Gorkii str. 87, Vladimir 600000, Russia

Nanostructures of noble metal nanoparticles are promising to create optoelectronic devices with controllable properties. Bimetallic structures have improved physical and chemical stability and selectivity compared with isometric structures. The bimetallic complex is related to change the optical properties, in particular transmission and absorption, depending on the structure. Separate direction of controlling the optical properties of such nanostructures formation of clusters with variable morphology.

In this work, a method for the formation of bimetallic clusters on the surface of an optically transparent media is offered. Noble metal nanoparticles obtained by laser ablation targets of gold and silver, placed in glycerin. In this task use a continuous laser beam of moderate intensity (λ = 1.06 μm, $I \sim 10^6$ W/cm^2). Particle sizes in generated colloidal solution were determined using the particle size analyzer by dynamic light scattering and made approximately 8 nm.

For the cluster formation the method of laser deposition of nanoparticle from colloidal systems was used. Nanosecond laser pulses (λ = 1.06 μm, $E \sim 1$ J/cm^2) were applied. The prepared colloidal solution was deposited on a cold substrate (glass polished K-8) with a thin layer. As a result, the local laser effects on the colloidal solution on the surface of the substrate is deposited bimetallic clusters along the path of the beam. After the deposition of the morphological properties of the clusters were investigated using atomic force and scanning electron microscopy. The change of the absorption spectrum of the resulting structures, depending on the concentration of gold and silver nanoparticles in the colloidal solution was shown.

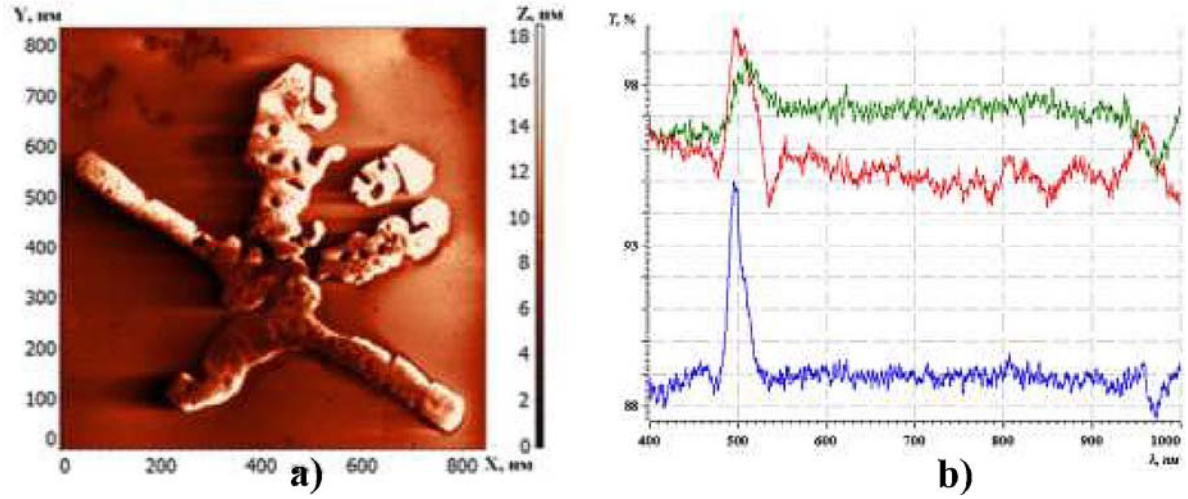

Fig. 1. a) The AFM image of Au-Ag clusters on the glass substrate, the concentration of particles 1:1; b) Changing the transmission spectrum of the clusters: blue- only Au, greenonly Ag, red – Au/Ag.

Paper LM-P-12

GENERATION OF COHERENT ULTRASHORT X-RAY BEAMS IN LASER INTERACTION WITH NANOFILMS

Victor V. Kulagin[1], Vladimir A. Cherepenin [2], Vladimir N. Kornienko[2]

[1]*Sternberg Astronomical Institute of Lomonosov Moscow State University, Moscow, Russia*
[2]*Institute of Radioengineering and Electronics of RAS, Moscow, Russia*

victorvkulagin@yandex.ru

Coherent ultrashort x-ray pulses can be generated through Thomson backscattering of a probe laser pulse off a relativistic electron mirror [1]. In this case, parameters of X-ray pulse, such as amplitude, frequency, envelope, phase, etc., can be controlled easily. In this presentation, we consider problems, which should be solved for experimental realization of this idea: shaping of the laser pulse front, generation of relativistic electron mirror and back reflection of a probe laser pulse off such a mirror.

An idea for synchronous acceleration of electrons from a nanofilm with a superintense nonadiabatic laser pulse was considered in [2]. For a nonadiabatic laser pulse of relativistic amplitude incident normally at the nanofilm, all electrons can be expelled simultaneously out of the nanofilm in the longitudinal direction (along the laser beam axis) due to the action of the longitudinal component of the Lorentz force. As a result, a relativistic electron mirror can be formed - an electron bunch with diameter of several micrometers and thickness of several nanometers or less. Accelerating laser pulse should be relativistic with amplitude exceeding some threshold, which is determined by material and thickness of the nanofilm, besides the front of the laser pulse should be sharp enough.

We consider laser pulse front shaping using plasma layers with thickness of about laser wavelength or more. Such layers allow fully suppressing the part of the laser pulse with small amplitude, and the transmitted pulse maximal amplitude can be about that of the incoming laser pulse. Then, we studied numerically characteristics for relativistic electron mirrors generated with shaped pulses. It was shown that, for a nanofilm with a thickness of several nanometers, a lifetime of relativistic electron mirror can be tens of femtoseconds with good homogeneity and with momenta spread of no more than 1–2%.

At last, the reflections of the counter-propagating probe laser pulses off generated relativistic electron mirrors were investigated. It was shown that a single coherent X-ray pulse with duration of less than 100 as, wavelength of ten nanometers or less and power of several hundreds of gigawatts can be generated. Characteristics for X-ray pulses were investigated such as dependence of the reflected pulse parameters on amplitude and duration of the probe pulse, nanofilm thickness and electron density, etc. It was shown that if the relativistic electron mirror stays in the field of accelerating pulse during interaction with the probe pulse, a reflection coefficient of the mirror and a frequency up-shift coefficient for the probe pulse do not depend on the amplitude of the probe pulse up to that of the accelerating pulse.

Acknowledgements: This work was supported by Russian Foundation for Basic Research (grants 12-02-92702-IND_a, 13-02-01398_a, and 13-02-12233-ofi-m-2013).

References:

1. V.V. Kulagin et al., “Generation of relativistic electron mirrors and frequency upconversion in laser–plasma interactions” Appl. Phys. Lett., Vol. 85, pp. 3322–3324 (2004).
2. V.V. Kulagin et. al, “Theoretical investigation of controlled generation of a dense attosecond relativistic electron bunch from the interaction of an ultrashort laser pulse with a nanofilm” Phys. Rev. Lett., Vol. 99, 124801 (2007).

Paper LM-P-13

TRANSFER PHENOMENA AND PHASE TRANSITIONS IN SYSTEMS WITH NANO-OBJECTS IN RESONANCE RADIATION FIELD

V.V. Levdansky[1], J. Smolik[2], V. Zdimal[2]

[1]Heat and Mass Transfer Institute NASB, 15 P. Brovka St., 220072 Minsk, Belarus,
[2]Institute of Chemical Process Fundamentals AS CR, v.v.i., Rozvojova 135,
165 02 Prague 6, Czech Republic,

vlev5@yahoo.com

Transfer phenomena in systems with nano-objects under the effect of resonance radiation are of interest for many branches of nanotechnology. Resonance (e.g. laser) radiation can excite gas molecules and accordingly change the character of the interaction between gas molecules and a condensed phase. The possibility to affect surface processes by resonance radiation allows one to change a number of phenomena occurring in aerosol systems with nanoparticles and porous bodies with nanoscale pores. The paper deals with a theoretical study of transfer processes and phase transitions in systems with nanoscale objects under the effect of resonance radiation. It is shown that resonance radiation can induce the resulting mass flux in porous membranes with nanoscale pores in initially equilibrium (before the effect of radiation) systems. The influence of resonance radiation on the growth rate of nanoscale aerosol particles is also considered.

Resonance radiation can excite both the vapor molecules and molecules of a foreign (buffer) adsorbable gas that is present in the system. This can lead to a change in phase transitions and mass transfer in the systems with nanoscale objects. It is shown that excitation of foreign gas molecules leading to a decrease in the sticking coefficient and adsorption time of these molecules (and correspondingly to a decrease in the concentration of adsorbed molecules of a foreign gas on the interphase boundary), depending on the parameters of the system, can both increase and decrease the rate of condensational growth of the aerosol nanoparticle and the resulting flux of molecules on the interphase boundary of the evaporating concave hemispherical meniscus located in the nanoscale cylindrical capillary. It is also shown that a change in the concentration of adsorbed molecules of a foreign gas on the nano-object surface in the field of resonance radiation can induce the resulting flux of vapor molecules on the interphase boundary in the initially equilibrium systems. The values of the critical (equilibrium) size of the above-mentioned nano-objects with consideration of foreign gas adsorption on the interphase boundary and the effect of resonance radiation are obtained.

Acknowledgements: The work was partially supported by GAAVCR (project IAA200760905) and by BRFFI (project T12R-018).

Paper LM-P-14

MODELING OF THE PROCESS OF HOMOGENEOUS MELTING OF ALUMINUM

V.I. Mazhukin, M.M. Demin, A.V. Shapranov

Institute of Mathematical Modeling of RAS, 4a Miusskaya sqr., 125047 Moscow, Russia

vim@modhef.ru

The problem of heating of Aluminum target by an ultra-short laser pulse is considered within the framework of one-dimensional hydrodynamic two-temperature model with explicit tracking of interphase fronts. [1]. The pulse duration is 0.1 ps, absorbed fluence 0.055 J/cm^2. A method of calculation of volume melting is suggested by means of introduction of nuclei –the new liquid phases into the superheated solid phase. These new phases have moving boundaries where usual surface melting conditions are written. The same equations of two-temperature hydrodynamics are solved within the new phases. Such nuclei are introduced every time when certain maximum superheating margin is reached. Depending on the particular laser action regime, the total number of such nuclei in every moment of time can be up to 10–20. The efficiency of the dynamic adaptation method was confirmed for such statements of the problem. As a result of analysis of different previously published theoretical estimates [2, 3] for the value of the maximum superheating and estimates from the calculations using the method of molecular dynamics, we have chosen the temperature value for the nucleus introduction criterion to be $1.4T_m(P)$. For comparison, we also investigate the process of volume melting for other maximum values of superheating, 1.2 and 1.6 $T_m(P)$. The figure shows an example of current and average volume melting speed for the value of superheating of 1.4.

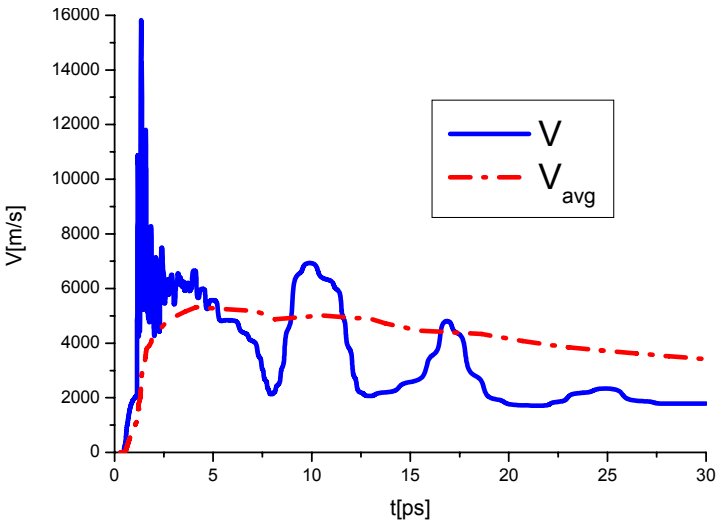

References:

1. V.I. Mazhukin, A.V. Mazhukin, M.M. Demin, A.V. Shapranov, The dynamics of the surface treatment of metals by ultra-short high-power laser pulses. Surface Modification Technologies XXVI (SMT 26). Eds T.S. Sudarshan, M. Jeandin, V. Firdirici, Vol. 26, pp. 557–566 (2013).
2. S.-N. Luo et al., “Maximum superheating and undercooling: Systematics, molecular dynamics simulations, and dynamic experiments” Phys. Rev. B, Vol. 68, 134206 (2003).
3. K. Lu, Y. Li, “Homogeneous nucleation catastrophe as a kinetic stability limit for superheated crystal” Phys. Rev. Lett., Vol. 80, p. 4474 (1998).

Paper LM-P-15

THEORETICAL ANALYSIS OF THERMAL STRESSES ON PULSED LASER IRRADIATION OF THIN FILMS UNDER CONDITIONS OF MICROBUMP FORMATION AND NONVAPORIZATION FORWARD TRANSFER

Yu.P. Meshcheryakov[1], M.V. Shugaev[2], T. Mattle[3], T. Lippert[3], N.M. Bulgakova[4,5]

[1]*Design and Technology Branch of Lavrentyev Institute of Hydrodynamics SB RAS, Tereshkovoi street 29, 630090 Novosibirsk, Russia*
[2]*Department of Materials Science and Engineering, University of Virginia, 395 McCormick Road, Charlottesville, Virginia 22904-4745, USA*
[3]*Paul Scherrer Institut, General Energy Research Department, 5232 Villigen PSI, Switzerland*
[4]*Institute of Thermophysics SB RAS, 1 Lavrentyev Ave., 630090 Novosibirsk, Russia*
[5]*Optoelectronics Research Center, University of Southampton, SO17 1BJ, United Kingdom*

ura@kti-git.nsc.ru

In this work we present a theoretical analysis of the processes in thin solid films irradiated by short and ultrashort laser pulses in the regimes of film structuring and laser-induced forward transfer. The regimes are considered at which vaporization of the film materials is insignificant and film dynamics is governed mainly by mechanical processes. Thermoelastoplastic modeling has been performed for a model film in one- and two-dimensional geometries. A method has been proposed to estimate the height of microbumps produced by nanosecond laser irradiation of solid films. Contrary to femtosecond laser pulses, in nanosecond pulse regimes, stress waves across the film are weak and cannot induce film damage. The main role in laser-induced dynamics of irradiated films is played by radial thermal stresses which lead to the formation of a bending wave propagating along the film and drawing the film matter to the center of the irradiation spot. The bending wave dynamics depends on hardness of the substrate underlying the film. The causes of the receiver substrate damage sometimes observed upon laser-induced forward transfer in the scheme of the direct contact between the film and the receiver are discussed.

Paper LM-P-16

THE NANOCLUSTERS AND MICRON-SIZED PERIODIC STRUCTURES CREATION AT THE SURFACE OF THE CRYSTAL AND AMORPHOUS SILICA BY RESONANT CO_2 LASER IRRADIATION

A.F. Mukhamedgalieva[1], A.M. Bondar[1], I.M. Shvedov[1], M.A. Kononov[2], V.B. Laptev[3], N.N. Novikova[3]

[1]*Moscow State Mining University, Leninsky prospect 6, 119991, Moscow, Russia*
[2]*Institute of General Physics, Russian Academy of Sciences, Vavilov street 38, 119991, Moscow. Russia*
[3]*Institute of Spectroscopy, Russian Academy of Sciences, 142190, Moscow, Troitsk, Russia*

anel-mggu@mail.ru

The formation of nanoclasters and micrometer sized periodical structures at the surface of silica (crystal quartz and fused quartz) by action of pulsed CO_2 laser radiation (pulse energy of 1 J, pulse time of 70 ns) have been investigated. The samples was irradiated by CO_2 laser in two regimes – single-mode (fluency of 40 J/cm^2) and multi-mode (fluency of 48 J/cm^2) and with two laser frequency – 975 and 1076 cm^{-1}.

The images of laser spots by means of the high resolution optical microscop and atomic force microscop have been made. The infrared (IR) reflection spectra and luminescence spectra of irradiated surface also have been recorded. It has been observed that by laser action on the surface of samples two kind of structures have appeared – periodical micron-sized structures with the period length close to wave length of CO_2 laser irradiation and nanoclusters with size close to 50–100 nm. Micron-sized structures have appeared by laser action with more low fluency – 5.2 J/cm^2 and single-mode laser action, whereas nanostructures have appeared by more high fluency – 7–10 J/cm^2. It has been observed that the relief depth of the periodic structures depends on laser pulses number.The maximal highness of nanoclusters at the resonant frequency of laser (1076 cm^{-1}) has been observed. We believe that these nanoclusters consist mainly of silicon atoms that confirm the luminescence spectra of irradiated sample.

The IR reflection spectra for irradiated samples show the enhancement of reflectance in the region of laser frequency with the band width of 20 cm^{-1} for crystal quartz. More high enhancements have been found at the frequency of 1076 cm^{-1}. It has established that the reflectance enhancement has an accumulating character, namely, dependence of this ones on the number of laser pulses incident upon the samples take place.

We can made some conclusion. 1) The periodical micro-and nano-structures in a crystal and amorphous silica have appeared because of interference of incident waves and surface waves induced by incident waves in resonant absorption media. That structures arise because of the increase of ablation velocity at the maxims of standing waves. 2) Cumulative properties of periodical structures formation show us that the mainly ablation processes take place by laser action on silica surface. 3) Dependence of relief depth from frequency of laser action shows that microstructure formation connects with the resonant interaction of CO_2 laser radiation with silicates. Intensive ablation in maxims of standing waves connects with the breaking of covalent oxygen – silicon bonds in region of laser action frequency what can be proved by IR spectra of irradiated samples [1].

References:

1. A. Mukhamedgalieva, A. Bondar, “Laser-induced selective sublimation from silicates”, Proc. SPIE, Vol. 2118-33, pp. 224–226 (1994).

Paper LM-P-17

DIRECT LASER-WRITING IN PHOTOSENSITIVE GLASSES: CORRELATIVE MICROSCOPY OF FLUORESCENT SILVER CLUSTERS AND THE ASSOCIATED SPACE CHARGE SEPARATION

Y. Petit[1,2], G. Papon[1], K. Mishchik[1], A. Royon[1], K. Bourhis[2], N. Marquestaut[1], Y. Deshayes[1,4], M. Dussauze[3], V. Rodriguez[3], T. Cardinal[2], and L. Canioni[1]

[1]*LOMA, UMR 5798 CNRS, Universite de Bordeaux, 351 Cours de la Liberation, F-33405 Talence, France*
[2]*ICMCB, UPR 9048 CNRS, Universite de Bordeaux, Avenue du Dr. Schweitzer, F-33608 Pessac, France*
[3]*ISM, UMR 5255 CNRS, Universite de Bordeaux, 351 cours de la Liberation, Talence, F-33405, France*
[4]*IMS, UMR 5218 CNRS, Universite de Bordeaux, 351 cours de la Liberation, Talence, F-33405, France*

yannick.petit@u-bordeaux1.fr

Direct-Laser Writing (DLW)

Innovative photonics developments require the multi-scale structuring of transparent composite materials, from the 100 nm mesoscopic scale to macroscopic scale, to provide the elementary bricks of tomorrow's optical components [1]. DLW with tightly focused high repetition rate femtosecond (fs) lasers, has already demonstrated its high applicative potential, thanks to its possibility to locally engineer 3-dimensionnal (3D) structure modifications in prepared glass, as *e.g.* fluorescent clusters production [1]. DLW gives access to promising optical contrasts in both localized linear and nonlinear optical properties, as well as in potential meta-properties resulting from the global 3D architecture of laser-induced modifications.

Fluorescent silver clusters and space charge distributions

Silver containing zinc phosphate glasses are good candidates for DLW. We have demonstrated that 3D structuring in this glass by fs laser irradiation at the TW/cm^2 level, leads to remarkable fluorescence and electric field induced SHG (EFISHG) emissions from the structured zone. We used fluorescence and non-linear induced properties as contrast mechanism for high potential 3D high-density data storage [2–6].

Here, we report on the correlative microscopy imaging of both fluorescence and EFISHG emission properties of structured lines induced by DLW in a prepared glass at the voxel of a focused fs laser. We show a clear spatial correlation between these two emissions, even if they lead to significantly different profiles. While fluorescence emission is associated to silver cluster production, EFISHG is related to the space charge distribution induced by the silver cluster creation.

We have already studied spatial and spectral aspects to characterize these optical structures. However, the full understanding of their formation remains challenging under laser irradiation, especially the space charge distribution resulting from the spatial distribution of silver clusters at the edge of the structuring laser beam. We believe further work including both experimental and numerical aspects could better incorporate the rich physical phenomena (multi-photon processes, cumulative effects and local heating, heat diffusion, photo-chemical reactivity and chemical diffusions of species), to explain such structure formation in order to improve the control of the resulting properties.

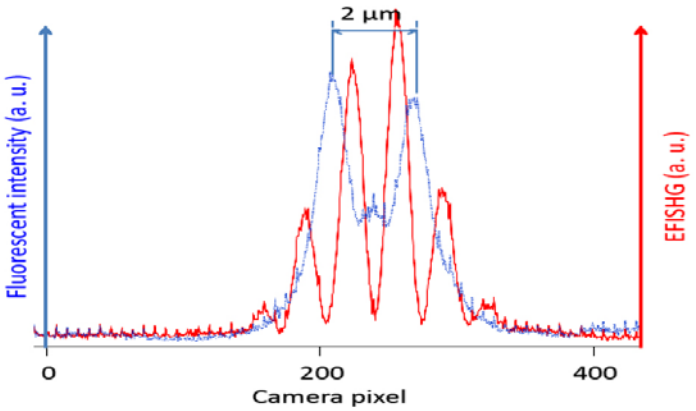

Figure. Overlapped emissions of fluorescence (blue) excited by a 405 nm laser diode, and EFISHG (red) of a 1030 nm fs laser beam, from a laser-induced linear structure (with sub-micron domain walls) in a photosensitive glass, showing correlated but distinct spatial distributions.

References:

1. A. Royon et al., “Femtosecond laser induced photochemistry in tailored materials” Optical Material Express, Vol. 1(5), pp. 866–882 (2011).
2. M. Bellec et al., “3D patterning at the nanoscale of fluorescent emitters in glass” J. Phys. Chem. C, Vol. 114, 15584 (2010).
3. A. Royon et al., “Silver clusters embedded in glass as a perennial high capacity optical recording medium” Adv. Mat., Vol. 22, pp. 5282–5286 (2010).
4. M. Bellec et al., “Beat the diffraction limit in 3D direct laser writing in photosensitive glass” Optics Express, Vol. 17(12), pp. 10304–10318 (2009).
5. L. Canioni et al., “Three-dimensional optical data storage using third-harmonic generation in silver zinc phosphate glass” Opt. Lett. Vol. 33, p. 360 (2008).
6. J. Choi et al., “Three-dimensional direct femtosecond laser writing of second-order nonlinearities in glass” Optics Letters, Vol. 37(6), pp. 1029–1031 (2012).

Paper LM-P-18

STUDY OF THE STRESS-STRAIN STATE IN GLASS-CARBON PLATES AFTER ULTRAFAST LASER PROCESSING

T.N. Sokolova, Yu.V. Chebotarevsky, E.L. Surmenko, A.V. Konyushin, I.A. Popov, D.A. Bessonov

Gagarin Saratov State Technical University, 77 Polytechnicheskaya st., 410054, Saratov, Russia

sokolova@pribor-t.ru

When using ultrafast lasers in micromachining processes it is necessary to account the possible negative effects that occur in the processing of brittle materials. Removing material from the surface in cold ablation process caused by laser light, in such a short period of time with such a high rate, it creates the area of high pressure in the interaction zone that could cause a microdamage of brittle materials.

To study the stress-strain state arising in brittle materials under the influence of ultrafast lasers, the following physical-mathematical model of the process was formulated [1]. As a measure of the mechanical action of laser radiation on the processed material in cold ablation the reactive force was taken. The force occurs after an outflow of a certain volume of substance from the surface of the object being processed in a single pulse:

$$F = \rho \frac{\Delta \upsilon}{\Delta t} u,$$

where u – speed of the substance outflow; υ – volume of substance, being removed in one laser pulse; Δt – duration of the substance outflow from the laser-matter interaction zone; ρ – density of substance; t – time. When studying picosecond laser-matter interaction the Coulomb explosion was taken into account which accompanied by the formation of a surface plasma cloud, $u = 10^5$ m/s; speed of the substance outflow assumed constant because of the ultrashort interaction.

As a mechanical reaction of the treated glass-carbon substrate a back pressure generated by the reactive force was considered. Brittle materials suffer plastic deformation, as a rule, only in the areas of high-temperature heating. Hence, in case of picosecond treatment in cold ablation process the material, from a mechanical point of view, was seen as a perfectly elastic up to its destruction. From a geometrical point of view, the processed object was presented in the form of a thin rectangular plate.

The intensity of stresses arising in the glass-carbon plate was taken as a parameter allowing estimation the strength of the plate. On the base of the calculated results, the modes of surface picosecond laser structuring were chosen for glass-carbon field-emission cathodes [2].

Acknowledgements: The study was supported by The Ministry of education and science of Russian Federation, project 14.B37.21.0746.

References:

1. Yu. Chebotarevsky, “Building a Simulation Model to Study the Stress-State of Local Heated Brittle Non-Metallic Materials with Consideration of Plastic Deformation” University Scientific Digest: Mechanics of Deformable Media, Vol. 9, pp. 49–59 (1985).
2. T. Sokolova, A. Konyushin, E.L. Surmenko, et al., “Laser technologies and modern equipment in manufacture of autoemissive cathodes from monolithic glass-carbon” Vacuum Technics and Technology, Vol. 21, pp. 95–98 (2011).

Paper LM-P-19

MODELING OF THIN FILM EXPLOSIVE BOILING – HEATING RATE EFFECT

V.I. Mazhukin[1], A.V. Shapranov[1], A.A. Samokhin[2], A.Yu. Ivochkin[2]

[1]*Keldysh Institute of Applied Mathematics, RAS, Moscow, Russia*
[2]*A.M. Prokhorov General Physics Institute, RAS, Moscow, Russia*

asam40@mail.ru

The explosive boiling process of thin (~50 nm) liquid film is investigated in the framework of molecular dynamics simulation in the case of homogeneous sub-nanosecond heating with different rates. Problem formulation and calculation details are presented elsewhere. The results of calculations show that at these conditions the surface evaporation process considerably affects the explosive boiling picture due to surface vaporization cooling and formation of non-homogeneous (convex) spatial temperature distribution in the homogeneously heated film.

At low heating rate (2 K/ps) the film, which is initially in equilibrium with its saturated vapor at 6400 K, attains steady state temperature distribution with maximum temperature ~6600 K = $0.87T_C$, where T_C ~ 7600 K is critical temperature of the film liquid. At higher rate of heating (4 K/ps) explosive boiling process begins at T ~ 7000 K = $0.92T_C$ and t ~ 300 ps from start of the heating which results in cavity formation between two fragments of the film moving in opposite direction. This movement is due to vapor pressure rather than inertial effect as it is in the case of spallation. Maximum pressure value at the beginning of explosive boiling estimated from the fragment acceleration is about 400 atm and velocity grows up to about 450 m/s at t = 700 ps when cavity dimension is about 200 nm as compared with fragment thickness ~ 20 nm. The fragments temperature T during this time interval diminishes from 7000 to 6600 K. If the heating rate is greater than 10 K/ps then no cavity formation is observed and film density distribution is relatively smooth in accordance with picture of supercritical expansion. Pressure estimation in the central part of the film based on its particle velocity distribution shows that the pressure value rapidly reaches and exceeds critical pressure of the film liquid (1.4 kbar). Fragmentation picture at heating rate ~ 10 K/ps is different from supercritical expansion and explosive boiling regimes and may be probably referred as spinodal decomposition where density fluctuations grow with no pronounced interphase boundary formation.

Acknowledgements: The work was partially supported by RFBR grant № 13-02-01129, Grant № 13-07-00597.

Paper LM-P-20

UV-INDUCED HOLOGRAPHIC GRATING INSCRIPTION INTO POLYMER MATRIX WITH EMBEDDED SILICON NANOPARTICLES

A.G. Savelyev, E.V. Khaydukov, K.V. Khaydukov, N.V. Marusin, S.I. Molchanova, M.M. Nazarov, V.N. Seminogov, V.I. Sokolov, V.Ya. Panchenko

Institute on Laser and Information Technologies of the Russian Academy of Sciences, Sviatoozerskaya str. 1, Shatura 140700, Moscow reg., Russia

A.G.Savelyev@gmail.com

We developed a technique for embedding silicon nanoparticles into the polymer matrix. Silicon nanoparticles have a higher refractive index than polymer. Therefore, the refractive index of the composition can be modified in a wide range by changing the concentration of nanoparticles.

We utilized interferometric technique at the wavelength of He-Cd laser (325 nm) to fabricate holographic 1D and 2D gratings in the composite material made of photopolymer and 10 nm Si nanoparticles. Silicon nanoparticles migrated in the UV-curable polymer during UV exposure (see Fig. 1). Thus, doped and undoped regions were produced [1]. The modulation of the refractive index had a high accuracy. The achieved period of holographic grating is in the range from 500 nm up to 10μm.

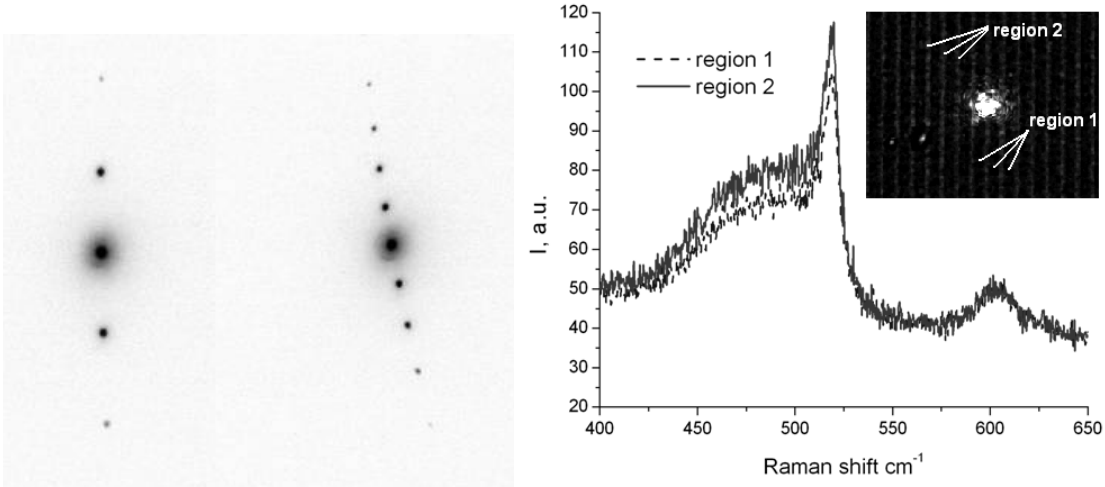

Fig. 1. Diffraction patterns from fabricated gratings at 632.8 nm wavelength (left). Raman probe of doped and undoped grating regions (right).

Acknowledgements: The reported study was partially supported by RFBR, research projects No 12-02-31773 мол_а, 12-07-31223 мол_а, 13-02-01371 а, and 13-07-00976 а, grant of the President of Russian Federation for the state support of young Russian scientists МК-6798.2013.9.

References:

1. N. Suzuki, Y. Tomita, T. Kojima, “Holographic recording in TiO_2 nanoparticle-dispersed methacrylate photopolymer films” Appl. Phys. Letters, Vol. 81, pp. 4121–4123 (2002).

Paper LM-P-21

METHOD OF OVERLAPPING BLIND HOLES FOR STRUCTURING OF A SURFACE

T.N. Sokolova, Yu.V. Chebotarevsky, E.L. Surmenko, A.V. Konyushin, I.A. Popov, D.A. Bessonov

Gagarin Saratov State Technical University, 77 Polytechnicheskaya st., 410054, Saratov, Russia

sokolova@pribor-t.ru

The process of laser structuring is widely used in brittle material processing, especially in glass-phase and ceramic treatment. There is a traditional approach to structuring of the surface - the linear scanning. Parallel and perpendicular lines with a choice of the minimum distance between them are engraved on the surface. The density of peaks on the surface is determined by the number of grid lines. At the intersections of the lines there are long grooves in the direction in which the last lines are patterned (Fig. 1a). We suggest another technological solution - the formation of the surface structure by overlapping blind holes. The scheme is presented in Fig. 1b.

In both cases, there is single-mode laser radiation; that is, the intensity distribution in the beam cross-section is close to Gaussian. As shown in Fig. 1b, the overlapping blind holes technique allows the density of the emitting structures to be increased. If the number of peaks obtained by linear scanning over a certain area is N^2, then the number of peaks obtained by the second method is $N^2 + (N–1)^2$ in the same area.

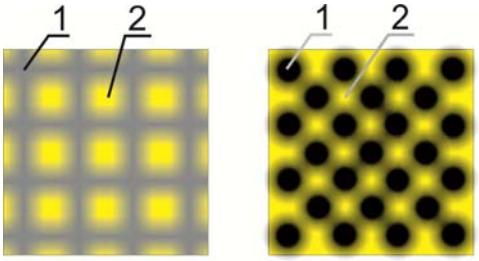

Figure 1. Schemes of the surface treatment. a) Linear scan. Dark lines labeled 1 are cut lines; yellow squares labeled 2 are peaks. b) Overlapping blind holes. Dark points labeled 1 are holes; yellow dots labeled 2 are peaks.

The appearance of the surface structure differs depending on the time of interaction, intensity, pulse repetition rate, and average laser power. In this work we discuss the structures obtained with two modes: 1) diode-pumped Nd:YAG-laser setup, 50 ns pulse duration, 0.8 W average power, and 5 kHz pulse repetition rate, a height of peaks 10 μm; 2) with the same system and power of 1.0 W and a pulse repetition rate of 10 kHz, a height of peaks 20 μm.

Acknowledgements: The study was supported by the Ministry of education and science of Russian Federation, project 14.B37.21.0746.

Paper LM-P-22

LIBS-ESTIMATION OF DIFFUSION OF ELEMENTS IN INTRAOSSEOUS IMPLANTS COATING

T.N. Sokolova, E.L. Surmenko, D.A. Bessonov, I.P. Melnikova

Gagarin Saratov State Technical University, 77 Polytechnicheskaya st., 410054, Saratov, Russia

surmenko@yandex.ru

A new type of bioactive coating of dental implants was tested. The mentioned coating is a special two-layer film «boehmite (AlO(OH)) + hydroxyapatite ($Ca_{10}(OH)_2(PO_4)_6$)» deposited on titanium substrate at different time, temperature, chemical and other modes. The mutual influence of these parameters makes the resulting coatings differ to each other. The diffusion of aluminum into the hydroxyapatite layer and into the substrate determines the properties of the coating, including transplantability.

The penetration of boehmite into the hydroxyapatite layer and the substrate was characterized by means of laser induced breakdown spectroscopy (LIBS). The diffusion in substrate was observed layer-by-layer way with the aid of scanning sampling – four times from the same sampling path. Seventeen samples obtained in different modes were studied with the same equipment and parameters.

The experimental set-up is based on Q-switched Nd:YAG laser (λ = 1.06 μm). Pulse repetition rate is 25 Hz. Power density in a monopulse mode reaches 10^{10}–10^{12} W/cm^2. Focus spot size is about 10 μm. Limit of element detection is 10^{-10} g; relative limit of detection is 0.001%. Registration of spectra is implemented by diffraction spectrograph and CCD camera.

It was found out that the layer of bioactive coating is less friable in the case of deposition on massive titanium without powder titanium interlayer. Besides, some combinations of parameters of deposition cause unexpected effect – increasing the proportion of aluminum in depth. Some other trends and their comparative analysis are presented in the work.

Acknowledgements: The study was supported by The Ministry of education and science of Russian Federation, project 14.B37.21.0746.

Paper LM-P-23

ANALYSIS OF LASER ABLATION OF KEVLAR

O.G. Tsarkova, V.B. Tsvetkov, S.V. Garnov

[1]Prokhorov General Physics Institute of RAS, ul. Vavilova 38, Moscow, 119991 Russia

olga@kapella.gpi.ru

Due to the unique combination of high tensile strength, low density, thermal and chemical stability Kevlar fiber is widely used for a manufacturing of the construction materials especially in the products to ensure personal safety. The studies of the protection properties of Kevlar (or the similar materials) under laser radiation are topical.

From the references [1-5] it is known that radiation of continuous 0.1–1 kW power CO_2-laser, focused in the area diameter of the order of hundreds of microns [1, 2], is successfully used for cutting Kevlar laminate.

The results of numerical modeling while using the code KARAT (description of the methods of calculation is given in [6]) under the influence of the CW laser radiation demonstrated good agreement with the experiments [1, 2], despite the lack of data on the temperature dependences of the optical characteristics of the material in the infrared range. The unknown values of the effective absorptivity can be estimated on the basis of the cost of the laser energy on the destruction of the substance.

At the thermal Kevlar decomposition carbon is formed and it is not oxidized completely at 10^7–10^8 K/s speeds of laser heating, so the soot is deposited on the surface of the material [1, 2]. We suggest that there are a significant shading of the laser radiation for the decomposition time and a decrease in the effective absorptivity of the surface. As a result the periodic structures on walls of the crater during the cutting Kevlar laminate are obtained.

In addition, the numerical simulation of laser heating using the experimental data of [1–5], approximated to the temperature of decomposition of Kevlar, leads to the conclusion to consider IR-radiation transmission through the sample.

The studied evaluation of the optical characteristics of the material at the analysis of experimental data [1–5] and numerical simulation [6] allows to estimate the heating rates, temperature gradients, as well as the resistance of Kevlar to the CW IR-laser radiation at some kilowatts power in the laser beam area ~1cm^2 for ~1 s duration of exposure.

References:

1. “Laser cutting of Kevlar laminates”, BDX-613-1877, Unclassified Topical Report prep. by R. VanCleave, D/861, PDO 6985051, The Bendix Corp. Kansas City Division (1977).
2. D. Doyle, J. Kokosa, “The laser cutting of kevlar: a study of the chemical by products”, Materials and Manufacturing Processes, Vol. 5, Iss. 4 (1990).
3. “Kevlar 49 Data Manual”, E.I. Du Pont de Nemours & Co. Inc. (1989).
4. “Kevlar Aramid fiber. Technical guide”, DuPont, Advanced Fiber Systems, Customer Inquiry Center, Richmond. H-77848 4/00, Web Address: www.kevlar.com
5. J. Grunlan, K. Rajagopal, J. Reddy, “Performance characterization of polyimide-carbon fiber composites for future hypersonic vehicles”, Texas Engineering Experiment Station, Final Report to Air Force Office of Scientific Research, FA9550-07-1-0285 (2010).
6. O. Tsarkova, A. Rukhadze, V. Tarakanov, V. Tsvetkov, S. Garnov, V. Nazarenko, P. Nosatenko, B. Vyskubenko, “Estimation of the absorptivity of a constructive material at unknown losses in ablation plume during laser ablation” Physics of Wave Phenomena. Vol. 20, No. 1, pp. 18–23 (2012).

Paper LM-P-24

LASER ABLATION OF A CONSTRUCTIVE MATERIAL – ESTIMATION OF UNKNOWN CHARACTERISTICS OF THE MATERIAL AND THE ABLATION PLUME

O.G. Tsarkova, V.B. Tsvetkov, A.A. Rukhadze, S.V. Garnov

[1]*Prokhorov General Physics Institute of RAS, ul. Vavilova 38, Moscow, 119991 Russia*

olga@kapella.gpi.ru

The analysis of the action of laser radiation (λ = 1.3 μm) with a power density of about 3 kW/cm^2 and a duration of about 1 s on the carbon silicon carbide composite material (CSCM) sample is carried out.

In the experiments the functions of the temperature versus the exposure time were measured for the front surface (with using the micropyrometer) and the back surface (with using the W-W-Re thermocouples). The numerical modeling of the sample temperature fields by means of the KARAT code is carried out and the experimental data being measured under the laser heating of the CSCM samples are compared with the modeling results.

It was shown that the plume formed above the face side not only significantly limits the laser flux on the sample decreasing the effective absorptivity of the sample. Moreover, the plume also reduces the thermal flux from the surface catching by the pyrometer objective. So the pyrometer fixes a lower temperature than the true temperature of the sample surface.

As the results of the analysis for unknown optical characteristics of the sample and the plume:

- the irradiative heat exchange between the plume and the sample are estimated including the light scattering by the plume;
- energy losses in the plume are estimated and the main reason for the screening of the laser radiation is identified;
- the temperature dependence of the effective absorptivity (i.e., the fraction of the laser radiation actually absorbed by the sample, with allowance for the loss in the plume) is determined;
- the temperature functions of the true absorptivity of the sample are estimated;
- the distribution of particles in the plume, as well as their sizes and mass fractions are estimated;
- the particle concentrations are calculated;
- the velocities of the emitted particles from the irradiated surface of CSCM sample are estimated;
- it is found that the burning of ablation products can be accompanied by the ionization of atoms in the plume;
- the significant influence of the silicon content and the porosity at the ablation of the sample is found.

References:

1. O. Tsarkova, A. Rukhadze, V. Tarakanov, V. Tsvetkov, S. Garnov, V. Nazarenko, P. Nosatenko, B. Vyskubenko, “Estimation of the absorptivity of a constructive material at unknown losses in ablation plume during laser ablation” Physics of Wave Phenomena. Vol. 20, No. 1, pp. 18–23 (2012).
2. O. Tsarkova, V. Tsvetkov, A. Rukhadze, S. Garnov, V. Nazarenko, P. Nosatenko, “Analysis of the sizes and number of microparticles in the ablation plume, which attenuates laser radiation during ablation of a constructive material” Physics of Wave Phenomena, Vol. 20, No. 1, pp. 24–34 (2012).

Paper LM-P-25

NUMERICAL SIMULATION OF FS LASER PULSE PROPAGATION THROUGH BULK SILICON

E.V. Zavedeev, V.V. Kononenko, V.I. Konov, P.A. Pivovarov

A.M. Prokhorov General Physics Institute of RAS, 119991, Moscow, Vavilov Str., 38

dodeskoden@gmail.com

A number of recently published papers demonstrated method of local structure modification inside transparent materials by means of nonlinear absorption of fs laser pulses (e.g. [1]). Silicon is able to transform its structure from crystalline to amorphous [2]. Thus one have a hypothetical possibility to use this method for making microstructures inside c-Si volume.

Experiments made in our group [3] revealed two specific features of tightly focused fs pulse propagation (λ = 1.2 μm, τ = 250 fs, energy up to 100 μJ) through crystalline silicon. The first is high energy losses before focus, the second is formation of long (>1 mm) light filament. The energy losses can be well described by simple mathematical model that takes into account only one nonlinear effect: two-photon absorption (TPA). For better understanding of processes that lead to filamentation, numerical solution of electromagnetic wave equation wave coupled with continuity equation for the free-carrier density was done. We used wave equation with nonlinear terms written for slowly varying envelope in paraxial approximation. Simulation results are in qualitative agreement with experimental femtosecond interferometry data.

Optical Kerr effect, TPA and plasma defocusing are causes of laser pulse filamentation. Influence of other effects on pulse propagation is considered.

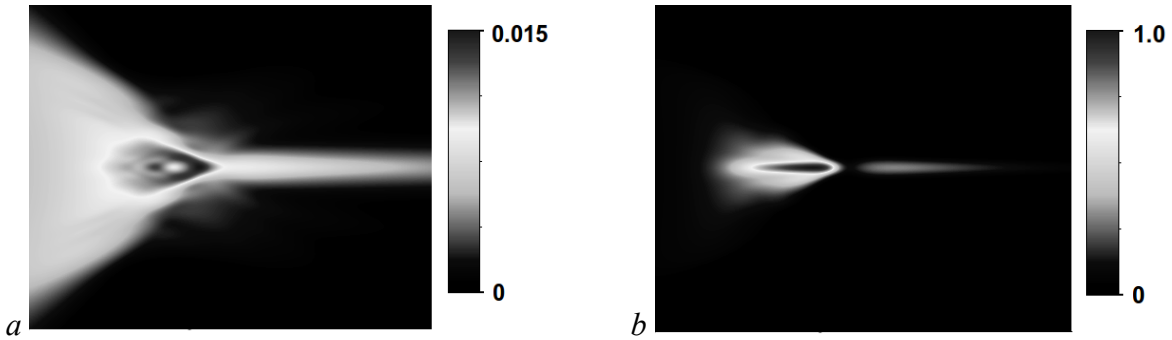

Fig. 1. Simulation of 2 μJ laser pulse propagation through silicon: *a*) fluence map (J/cm^2); *b*) photo-induced free-carrier density map (10^{19}/cm^3). Map size is 2.5×0.08 mm.

Acknowledgements: present study was supported by Russian Foundation for Basic Research (grant № 12-02-31437 mol_a)**.**

References:

1. S. Juodkazis, K. Nishimura, H. Misawa, T. Ebisui, R. Waki, S. Matsuo, T. Okada, “Control over the crystalline state of sapphire” Adv. Mater., Vol. 18, pp. 1361–1364 (2006).
2. D.R. Clarke, M.C. Kroll, P.D. Kirchner, R.F. Cook, “Amorphization and conductivity of silicon and germanium induced by indentation” Phys. Rev. Lett., Vol. 60, pp. 2156–2159 (1988).
3. V.V. Kononenko, V.V. Konov, E.M. Dianov, “Delocalization of femtosecond radiation in silicon” Optics Letters, Vol. 37, Iss. 16, pp. 3369–3371 (2012).

Paper LM-P-26

ABSORPTION INSTABILITY AS A POSSIBLE REASON OF GRATING FORMATION UPON PROPAGATION OF FEMTOSECOND LASER PULSES IN GLASSES

V.P. Zhukov[1,2], N.M. Bulgakova[3,4]

[1]*Institute of Computational Technologies SB RAS, 6 Lavrentyev Ave., 630090 Novosibirsk, Russia*
[2]*Novosibirsk State Technical University, 20 Karl Marx ave., 630073, Novosibirsk, Russia*
[3]*Institute of Thermophysics SB RAS, 1 Lavrentyev Ave., 630090 Novosibirsk, Russia*
[4]*Optoelectronics Research Center, University of Southampton, SO17 1BJ, United Kingdom*

zukov@ict.nsc.ru

Femtosecond-laser-induced modification of transparent solids is a powerful tool for technological applications based on 3D photonic structures. In spite of impressive achievements in development novel fs-laser-writing applications, rich physics of the modification phenomenon is not fully understood. To get insight into modification processes, we have developed a 2D (axially-symmetric) model describing laser beam propagation through transparent solids, based on non-linear Maxwell's (NLM) equations. The model accounts for the Kerr effect, photo-ionization, frequency dispersion of dielectric permittivity, and plasma hydrodynamics with laser-induced electron acceleration and avalanche. Material excitation dynamics has been studied numerically for the fused silica case in a wide range of irradiation parameters. The simulations show that, at large numerical apertures, relatively long laser pulse durations, and in a certain range of laser energies, laser energy absorption becomes unstable. It appears in the form of free electron density perturbations with a characteristic size of order of the laser wavelength. Although the observed absorption instability develops under the irradiation conditions when axial symmetry of the laser energy absorption is violated, it has been found that the instability is a physical phenomenon but not an artifact of axial symmetry breaking in our 2D model. This was verified by simulating the exact 2D NLM problem of "laser knife" whose data also showed the absorption instability at the same range of irradiation parameters. Remarkable is that the volumetric nanomirror structures (nanogratings) are formed under the irradiation conditions characteristic for instability development.

We propose the mechanism of nanograting formation. The absorption instability leads to free electron density perturbations with spatial dimension of laser wavelength and with a tendency to violate axial symmetry towards an elongated geometry. Due to the glass memory effects conditioned by defect formation, the subsequent laser pulses propagate in disturbed medium, thus enhancing perturbation of electron density distribution in the laser-affected region with further tendency of forming an elongated structure with 2D features. As a result of many pulses, the electron density perturbation transforms into a sliced (nanograting) structure.

Acknowledgements: This research is supported by Russian Foundation for Basic Research (project No. 12-01-00510-a). NMB acknowledges Marie Curie International Incoming Fellowship, No. 272919.

SECTION LS

Laser Systems

Paper LS-I-1

HIGH ENERGY ND:GLASS LASERS WITH INCREASED REPETITION RATE

E.A. Khazanov, A.A. Kuzmin, A.A. Shaykin

Institute of Applied Physics, 46 Ulyanov street, Nizhny Novgorod 603950, Russia

khazanov@appl.sci-nnov.ru

Nd:glass is widely used in petawatt lasers as an active media or as a pump for either a sapphire crystal or a parametric amplifier of chirped pulses. The main advantage of Nd:glass is a possibility to store a large amount of energy. However, a relatively low thermal conductivity of glass noticeably limits the repetition rate of laser pulses. Nowadays creation of multipetawatt facilities with a pulse repetition rate of about 1 shot per 1 minute or less is an urgent problem. According to the modern state of laser technology using Nd:glass is the only one way to reach this goal. Notice that using Nd:YAG active medium except glass allowed to achieve 1 PW at 1 Hz. But this result can not be significantly improved because of a small value of the stored energy in Nd:YAG. The development of a multipetawatt region requires using Nd:glass amplifiers with hundreds Joules of stored energy.

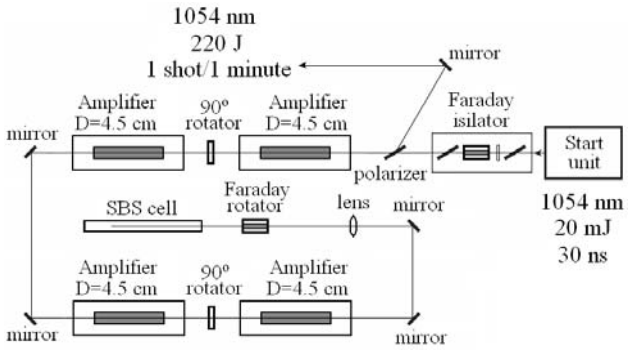

Fig. 1. Laser layout

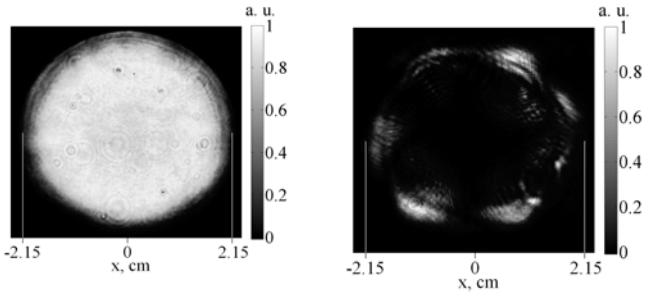

Fig. 2. Output (left) and depolarized (right) beams

We have constructed a prototype of a pumping laser for Ti:Sa multipetawatt laser facility that operatse at 0.02 Hz of repetition rate. Laser layout is shown in Fig. 1. Start unit was based on Nd:YLF laser operating at 1054 nm wavelength. 20 mJ-energy, 30 ns-duration pulse passed through Faraday isolator and a polarizer and was injected to the four double-pass four Nd:glass rods (25 cm long and 4.5 cm in diameter) with phase conjugate mirror based on Stimulated Brillouin Scattering (SBS). Due to threshold nature of the mirror there was no self-excitation of the amplifier line even though total double-pass gain was 1.3×10^6. Due to 90-degree rotators and Faraday rotator placed before SBS-mirror the polarization distortions were reduced from 25% to below 0.5% (see Fig. 2).

Output beam (see Fig. 2) energy was 220 J and beam quality was close to the diffraction limit. Pulse shape was very close to the input pulse shape with 30 ns pulse duration. Output parameters of the laser can be easily multiplied by using several power channels in parallel.

Paper LS-I-2

PROGRESS IN ALKALI LASERS RESEARCH AND DEVELOPMENT

B.V. Zhdanov

US Air Force Academy, Laser and Optics Research Center, 2354 Fairchild Dr., Ste. 2A31, USAF Academy, CO 80840, USA

boris.zhdanov.ctr@usafa.edu

Alkali vapor lasers are under extensive research and development during the last several years because of their potential for scaling to high powers while keeping a good beam quality. In addition, a possibility of using efficient diode lasers for pumping of alkali vapors promises high total wall plug efficiency for Diode Pumped Alkali Laser (DPAL). Since the first DPAL demonstration with output power of 130 mW in 2005 [1], a significant progress in this field was achieved. The output power of about 1 kW in continuous wave (CW) operation with optical efficiency close to 50% was recently demonstrated for Cs DPAL [2]. Also, the DPALs based on other alkali metals (Rubidium and Potassium) were also demonstrated [3, 4].

In spite of these significant achievements, there are still several problems in DPAL power scaling exist that must be addressed. Among them are the thermal [5] and photoionization [6] issues that become important even at several tens of watts CW power level.

In this talk, we discuss main achievements in the field of DPAL research and development, different problems in DPAL power scaling and possible ways to mitigate them.

References:

1. T. Ehrenreich, B. Zhdanov, T. Takekoshi, S. P. Phipps, R. J. Knize, "Diode Pumped Cesium Laser" Electron. Lett., Vol. 41(7), pp. 47–48 (2005).
2. A.V. Bogachev, S.G. Garanin, A.M. Dudov, V.A. Yeroshenko, S.M. Kulikov, G.T. Mikaelian, V.A. Panarin, V.O. Pautov, A.V. Rus, S.A. Sukharev, "Diode-pumped caesium vapour laser with closed-cycle laser-active medium circulation" Quantum Electron.,
   Vol. 42(2), pp. 95–98 (2012).
3. J. Zweiback, W. Krupke, "28 W average power hydrocarbon-free rubidium diode pumped alkali laser" Opt. Exp., Vol. 18(2), pp. 1444–1449 (2010).
4. B.V. Zhdanov, M.K. Shaffer, R.J. Knize, "Demonstration of a diode pumped continuous wave potassium laser", Proc. SPIE, Vol. 7915. pp. 791506-1–791506-6 (2011).
5. B.V. Zhdanov, J. Sell, R.J. Knize, "Multiple laser diode array pumped Cs laser with 48 W output power" Electron. Lett., Vol. 44(9), pp. 582–583 (2008).
6. R.J. Knize, B.V. Zhdanov, M.K. Shaffer, "Photoionization in alkali lasers" Opt. Exp., Vol. 19(8), pp. 7894–7902 (2011).

Paper LS-I-3

RECENT LASER RESULTS OBTAINED WITH Yb^{3+} AND Nd^{3+} DOPED FLUORIDE LASER CRYSTALS

W. Bolanos[1], A. Benayad[1], G. Brasse[1], P. Camy[1], J.L. Doualan[1], A. Braud[1], R. Moncorgé[1], F. Druon[2], P. Georges[2], D. Descamps[3], E. Cormier[3], L. Su[4], J. Xu[4]

[1]*Centre de recherche sur les Ions, les Materiaux et la Photonique (CIMAP), UMR CNRS-CEA-ENSICaen/Universite de Caen, 6 Blvd Ml. Juin, 14050 Caen, France*
[2]*Laboratoire Charles Fabry (LCFIO), UMR CNRS/Universite Paris-Sud, Palaiseau, France*
[3]*Centre Lasers Intenses et Applications (CELIA), UMR CNRS-CEA/Universite de Bordeaux, France*
[4]*Shanghai Institute of Ceramics, Chinese Academy of Sciences, Shanghai, China*

richard.moncorge@ensicaen.fr

Yb^{3+} doped CaF_2 is now one of the most intensively studied laser materials for the future high intensity and short-pulse laser chains. Among other developments, it enters now as an efficient and scalable diode-pumped laser amplifier medium in important laser programs such as ILE-APOLLON in France and PENELOPE in Germany. It is also studied, in conjunction with especially developed high brightness pump sources, to produce more energetic laser oscillators with higher repetition rates [1].

Yb^{3+} doped $LiYF_4$ is also a laser system which has been proved to be able to produce fairly high laser powers [2]. However, its implementation as a bulk material is somewhat reduced owing to a pump wavelength which is less favorable than in the case of CaF_2 and of a more complicated crystal growth which prevents developments on a large scale. As a matter of fact, it seems much more promising for compact and efficient laser systems such as laser waveguides built from undoped substrates and Yb^{3+} crystalline layers grown by using the LPE (liquid phase epitaxy) technique.

On the other hand, CaF_2 doped with Nd^{3+} ions was forgotten for a long time as system laser because of a very detrimental concentration quenching effect resulting from the clustering of the Nd^{3+} active ions which kills its emission efficiency. A hope appeared, however, towards the end of the 90s, by codoping the material with "buffer" (non-optically active) ions such as Y^{3+} or La^{3+} with the intention of "breaking" the clusters and of improving the emission efficiency by restricting the energy transfers between the ions; but these first tries were not really conclusive as much as the utilized optical pumping was provided by a flash-lamp and that the laser performance remained very modest [3]. The idea therefore germinated to study the spectroscopic properties and the laser performance of CaF_2 crystals doped with Nd^{3+} and co-doped with Y^{3+} [4] or Lu^{3+} as a function of the co-dopant concentrations more carefully, and by pumping the crystals around 800 nm with a Ti:sapphire or a fiber-coupled laser diode.

Therefore, two types of results will be presented (i) the short pulse and/or the high power laser performance of Yb^{3+} doped CaF_2 and $LiYF_4$ crystals in the form of bulk crystals and waveguides, (ii) the spectroscopic properties and the laser characteristics of Nd^{3+} doped CaF_2 crystals co-doped with buffer ions like Y^{3+} and Lu^{3+}.

References:

1. G. Machinet, P. Sevillano, F. Guichard, R. Dubrasquet, P. Camy, J.L. Doualan, R. Moncorgé, P. Georges, F. Druon, D. Descamps, E. Cormier, Opt. Lett., (2013).
2. L.E. Zapata, D. J. Ripin, T. Y. Fan, Opt. Lett., Vol. 35, p. 1854 (2010).
3. J. Fernandez, A. Oleaga, J. Azkargorta, I. Iparraguirre, R. Balda, M. Voda, A. A. Kaminskii, Opt. Mater., Vol. 13, p. 9 (1999).
4. B. Su, Q. G. Wang, H. J. Li, G. Brasse, P. Camy, J.L. Doualan, A. Braud, R. Moncorgé, Y.Y. Zhan, L.H. Zheng, X.B. Qian, J. Xu, Laser Phys. Lett. (2013).

Paper LS-I-4

DEVELOPMENT OF HIGH-ENERGY MID-INFRARED PARAMETRIC SOURCES USING STRUCTURED NONLINEAR MATERIALS

V. Pasiskevicius, C. Canalias, F. Laurell, N. Thilmann, A. Zukauskas

Royal Institute of Technology, KTH, Roslagstullsbacken 21, 10691 Stockholm, Sweden

vp@laserphysics.kth.se

Nanosecond pulses with energies of the order of 100 mJ and tunable in the near and mid-infrared are of interest for applications such as spectroscopy, remote sensing, biology and medicine, and material processing. Optical parametric oscillators (OPOs) pumped by well-established, efficient lasers operating at 1 μm offer a simple and reliable way to generate such pulses. Quasi-phase matched (QPM) nonlinear materials in high energy OPOs provide definite advantages, such as noncritical phase matching for any chosen signal-idler pair, a large acceptance angle and the possibility to use the highest nonlinear coefficients. These advantages of QPM can be achieved in the ferroelectric oxide crystals $KTiOPO_4$ (KTP), $LiNbO_3$ and $LiTaO_3$ structured by using the electric field poling technique. High-energy parametric devices require large-aperture QPM crystals in order to mitigate optical damage. Moreover the homogeneity of the QPM structure is of paramount importance.

Fabricating large aperture periodically poled crystals in any of the above-mentioned materials is challenging In thick samples even a small domain broadening can lead to merging of the domains, overall resulting in a spatially inhomogeneous QPM grating. Periodically poled Mg:$LiNbO_3$ and Mg:$LiTaO_3$ with thicknesses of up to 5 mm along the polar axis have been recently reported [1]. However, the periodic domain structures were limited in homogeneity due to duty cycle variations, domain broadening and domain merging throughout the crystal thickness.

KTP isomorphs are considered to be one of the best materials for frequency conversion in the visible, near- and mid-infrared spectral regions down to 4 μm owing to their good mechanical and thermal properties, as well as high nonlinearity and high damage threshold. Periodically poled structures in KTP and isomorphic $RbTiOAsO_4$ (RTA) crystals with a thickness of up to 3 mm have been reported previously [2]. RTA, however, is not readily available from commercial vendors. In flux-grown KTP the high ionic conductivity, the inhomogeneous stoichiometry over a single wafer and a poor wafer-to-wafer consistency makes large-aperture poling a complicated process even for 3-mm thick samples.

Here we demonstrate that the above-mentioned limitations of KTP can be overcome by employing Rb:KTP [3]. Consistent periodic poling of this material over a crystal thickness of 5 mm has been achieved. These crystals were employed in a 1064 nm pumped OPO and OPA setups for high-energy pumping of cascaded parametric downconversion source operating around 6 μm.

References:

1. H. Ishizuki, T. Taira, "High-energy quasi-phase-matched optical parametric oscillation in a periodically poled MgO:$LiNbO_3$ device with a 5 mm × 5 mm aperture" Opt. Lett., Vol. 30, pp. 2918–2920 (2005).
2. M. Peltz, U. Bäder, A. Borsutzky, R. Wallenstein, J. Hellström, H. Karlsson, V. Pasiskevicius, F. Laurell, "Optical parametric oscillators for high pulse energy and high average power operation based on large aperture periodically poled KTP and RTA" Appl. Phys. B, Vol. 73, pp. 663–670 (2001).
3. A. Zukauskas, N. Thilmann, V. Pasiskevicius, F. Laurell, C. Canalias, "5 mm thick periodically poled Rb-doped KTP for high energy optical parametric frequency conversion" Opt. Mat. Exp., Vol. 1, pp. 201–206 (2011).

Paper LS-I-5

A_3B_5 NANOSTRUCTURES FOR NEAR-INFRARED LASERS

N.N. Rubtsova[1], A.A. Kovalyov[1], V.V. Preobrazhenski[1], M.A. Putyato[1], B.R. Semyagin[1], T.S. Shamirzaev[1], G.M. Borisov[1], O.V. Buganov[2], S.A. Tikhomirov[2], V.E. Kisel'[3], N.V. Kuleshov[3], S.V. Kuril'chik[3]

[1]*A.V. Rzhanov Institute of Semiconductor Physics of Siberian Branch of Russian Academy of Sciences, 13 acad. Lavrentyev pr., Novosibirsk, 630090, Russia*

[2]*B.I. Stepanov Institute of Physics, National Academy of Sciences of Belarus, 68, Nezavisimosti ave., Minsk, 220072, Belarus*

[3]*Institute for Optical Materials and Technologies, Belarusian National Technical University, 65, Nezavisimosti ave., Build. 17, Minsk, 220013, Belarus*

rubtsova@isp.nsc.ru

Infrared lasers operating in the mode-locking regime in the near infrared region are of great interest for various applications. The most suitable way to get the self-mode-locking in compact low-gain solid-state lasers is to use the semiconductor saturable absorber (SA). Further expansion for femtosecond laser spectral range is possible due to second harmonic generation (SHG).

This report represents our experience in the design, manufacturing and testing of saturable absorbers and second harmonic generation elements based on semiconductor A_3B_5 nano-structures. The questions under consideration are: methods of hetero-structures characterization [1], all-in-one semiconductor laser mirror with saturable absorption and groupdelay dispersion compensation [2], UV laser modification of saturable absorber recovery time [3], nano-structured fast SA with low optical loss for near-infrared femtosecond laser[4], A_3B_5 nano-structures for SHG of femtosecond near-infrared lasers.

Acknowledgements: Support of Russian Foundation for Basic Research Grant 12-02-00327a is acknowledged.

References:

1. A.A. Kovalyov, M.A. Putyato, V.V. Preobrazhenskii, O.P. Pchelyakov, N.N. Rubtsova, Laser Phys., Vol. 17, p. 478 (2007).
2. N.N. Rubtsova, N.V. Kuleshov, V.E. Kisel', A.A. Kovalyov, S.V. Kurilchik, V.V. Preobrazhenski, M.A. Putyato, O.P. Pchelyakov, T.S. Shamirzaev, Laser Phys., Vol. 19, p. 285 (2009).
3. N.N. Rubtsova, N.V. Kuleshov, V.E. Kisel', S.A. Kochubei, A.A. Kovalyov, S.V. Kurilchik, V.V. Preobrazhenskii, M.A. Putyato, O.P. Pchelyakov, T.S. Shamirzaev, Laser Phys., Vol. 20, p. 1262 (2010).
4. A.A. Kovalyov, V.V. Preobrazhenskii, M.A. Putyato, O.P. Pchelyakov, N.N. Rubtsova, B.R. Semyagin, V.E. Kisel', S.V. Kuril'chik, N.V. Kuleshov, Laser Phys. Lett., Vol. 8, p. 431 (2011).

Paper LS-I-6

OPTICALLY MODULATED HYBRID SILICON-VANADIUM DIOXIDE RING RESONATORS

R. Haglund[1], J.D. Ryckman[2], J. Nag[2], R.E. Marvel[2], P. Markov[2], S.M. Weiss[2]

[1]*Department of Physics and Astronomy, Vanderbilt University, Nashville, TN 37235-1807*
[2]*United States Air Force Office of Scientific Research*

The constantly increasing need for more rapid data communication — both on-chip and device-to-device — continues to motivate the search for higher speed, all-optical modulators that are compatible with silicon technology. In this paper, I describe our recent progress in achieving GHz-speed optical switching in hybrid ring resonators embodying vanadium dioxide as the switching element, with switching energies less than 1 pJ per bit. The femtosecond switching time of the insulator-to-metal transition in this material has long attracted attention; however, the much slower metal-to-insulator transition (on a time scale of a few nano-seconds) has seemed like a significant obstacle. However, recent experiments both on vanadium dioxide thin films and on hybrid ring resonators suggest that it may be possible to circumvent this obstacle by femto-second-laser-induced transient metallization without triggering the reversible, but slow, structural phase transition from the monoclinic insulating phase to the tetragonal metallic state.

Paper LS-I-7

GENERATION OF TUNABLE FEMTOSECOND PULSES IN THE VUV BY SECOND AND THIRD ORDER NONLINEAR INTERACTION

M. Beutler[1], M. Ghotbi[1], P. Trabs[1], V. Petrov[1], U.K. Sapaeev[1], F. Noack[1], A.S. Aleksandrovsky[2], A.M. Vyunishev[2], A.I. Zaitsev[2], N.V. Radionov[2]

[1]*Max Born Institute for Nonlinear Optics and Short Pulse Spectroscopy, Berlin, Germany*
[2]*Institute of Physics, Russian and Siberian Federal University, Krasnoyarsk, Russia*

noack@mbi-berlin.de

Ultrashort light pulses with photon energies between 6.2–12.4 eV are an ideal tool for studies of ultrafast processes in small molecules and clusters because many of them can be ionized by a single photon in this wavelength range between 100–200 nm, being a part of the so called vacuum ultraviolet (VUV). Although by free electron lasers now a device is available that also can directly generate femtosecond light pulses in this wavelength range, there is still a demand for small and flexible sources of ultrashort light in the VUV.

We will give an overview of our investigations of various approaches to generate and measure tunable vacuum ultraviolet (VUV) pulses with duration less than 100 fs. In detail we will discuss collinear [1] as well as noncollinear [2] four wave mixing (FWM) in a gas cell. We will show that pulse energies up to 2 μJ and pulse durations of less than 20 fs are attainable [3]. In order to achieve the very short VUV pulse duration in the interaction zone of a time resolved experiment we demonstrated that by controlling the chirp of the pulses interacting for the VUV generation one has a tool to adjust the chirp of the emitted pulses.

To get real tunable VUV pulses we combined optical parametric generation with the FWM process. Because of the broad bandwidth of the parametric conversion in BIBO we could achieve pulses with less than 50 fs duration [4].

Based on a numerical model we will show that one of the main limitations of the FWM processes in rare gas is the multiphoton absorption of the generated VUV pulse and will discuss approaches to overcome this limit.

Finally we will present our first results based on second harmonic generation in randomly layered Strontium Tetraborate (SBO) [5]. The layers with a thickness between 0.1 and 100 μm are oppositely poled, allowing an enhancement of the conversion by a process comparable to quasi phase matching. With about 4×10^{-5} the SHG conversion is several orders of magnitude higher than in a coherence length of a crystal without the layer structure and comparable to typical values for high harmonic generation.

References:

1. M. Beutler, M. Ghotbi, F. Noack, I.V. Hertel, “Generation of sub-50 fs vacuum UV pulses by four-wave-mixing in argon” Opt. Lett., Vol. 35, p. 1491 (2010).
2. M. Ghotbi, M. Beutler, F. Noack, “Generation of 2.5 μJ vacuum ultraviolet pulses with sub-50 fs duration by noncollinear four-wave mixing in argon” Opt. Lett., Vol. 35, p. 3492 (2010).
3. M. Ghotbi, P. Trabs, M. Beutler, “Generation of high-energy, sub-20-fs pulses in the deep ultraviolet by using spectral broadening during filamentation in argon” Opt. Lett., Vol. 36, p. 463 (2011).
4. M. Ghotbi, P. Trabs, M. Beutler, F. Noack, “Generation of tunable-sub-45 femtosecond pulses by noncollinear four-wave mixing” Opt. Lett., Vol. 38, p. 468 (2013).
5. A.S. Aleksandrovsky, A.M. Vyunishev, A.I. Zaitsev, “Applications of random nonlinear photonic crystals based on strontium tetraborate” Crystals, Vol. 2, pp. 1393–1409 (2012).

Paper LS-I-8

RECENT PROGRESS IN THE RAPID PRODUCTION OF ACTIVE FIBERS BY THE GRANULATED SILICA METHOD COMBINED WITH SOL-GEL TECHNOLOGY

Valerio Romano[1,2], Dereje Etissa[2], Manuel Ryser[2], Thomas Feurer[2], Woojin Shin[3]

[1]*Institute of Applied Physics, University of Bern, Sidlerstrasse 5, 3012 Bern, Switzerland*
[2]*ALPS Institute, Bern University of Applied Sciences, Pestalozzistrasse 20, 3400 Bern, Switzerland*
[3]*APRI, GIST, 1 Oryong-dong, Buk-gu, Gwangju 500-712, Republic of Korea*

valerio.romano@iap.unibe.ch

The granulated silica method (GSM) is one of the most versatile ways to produce preforms for optical fibers. It offers the possibility to easily adapt the structure of a fiber to one's requirements, e.g. to produce microstructured optical fibers circumventing the limits on geometrical symmetry imposed by mCVD (for standard fibers) or by the stack and draw technique (for microstructured fibers). It further allows to mix the fiber preform elements (core rods, capillaries, granulated silica) such as to obtain virtually any fiber structure. In the past, we used this technique for the first time to produce passive large solid core photonic crystal fibers.

With the introduction of rare earth, transition metals and aluminum oxides the full potential of GSM for the production of photonic waveguide components and active optical fibers was deployed [1, 2].

The disturbing scattering losses encountered mainly at high dopant levels were significantly reduced by iterative milling and CO_2-laser remelting. When directly drawing the assembled preforms to fibers (without prior vitrification) losses in the range of 0.35 dB/m at 633 nm were measured. In recent studies we have improved this figure to about 0.2 dB/m at 633 nm by vitrifying the preforms before drawing by the use of a laser based moving small zone heating technique. We found that a considerable part of the scattering is due to Rayleigh scattering, so that this attenuation value is well below 0.1 dB/m in the near infrared (eg at 1030 nm, a wavelength of interest for Ytterbium activated fibers).

Current work aims at further improving the granulated silica method by producing the starting granulated material by the sol-gel technique. The key benefits of this additional step are the increase in homogeneity of the material at higher dopant levels as well as the eased co-doping with phosphor oxide, which is done at the liquid stage in the early stage of sol-gel production process. Apart from mitigating photodarkening, the introduction of phosphor oxide jointly with aluminum oxide allows to precisely control the refractive indices of cladding and core materials. This allows to obtain very small index contrasts of the order of 10^{-4}, which is a key point for producing large mode step index fibers. Further, the the indices of the passive cladding and the active core can be easily matched. This is difficult to obtain with other methods and is required to produce microstructured fibers such as PCFs or leakage channel fibers.

Acknowledgements: This work was supported by the Swiss National Science Foundation, SNSF, and the Swiss Commission for Technology and Innovation, CTI in different projects.

References:

1. R. Renner-Erny, L. Di Labio, W. Luthy, "A novel technique for active fibre production" Opt. Mater., Vol. 29, p. 919 (2007).
2. M. Neff, V. Romano, W. Luthy, "Metal-doped fibres for broadband emission: Fabrication with granulated oxides" Opt. Mater., Vol. 31, p. 247 (2008).

Paper LS-I-9

PASSIVE COHERENT BEAM COMBINING OF Yb-DOPED FIBER AMPLIFIER ARRAY WITH INJECTION-LOCKED SEED SOURCE

Jun Zhou, Yifeng Yang, Man Hu, Bing He, Yunfeng Qi, Houkang Liu

Shanghai Key Laboratory of All Solid-State Laser and Applied Techniques,
Shanghai Institute of Optics and Fine Mechanics, Chinese Academy of Sciences, Shanghai 201800, China

junzhousd@siom.ac.cn

Coherent beam combining (CBC) of fiber laser and amplifiers has created an interest to scale fiber lasers to high power levels [1] and overcome the limits set by nonlinear optical process of single fibers [2].Passive CBC with all-optical feedback loop is simple in design and operation, which has experienced a continuous improvement in recent years [3]. A seed laser is necessary for the fiber amplifier chains in passive CBC [3]. In order to improve the visibility of the pattern when the phase locking is achieved, the seed laser is always turned off. Unfortunately, the amplifiers may be damaged by self-oscillations with no seed laser. As a result, the protection of the amplifier chains and the improvement of the visibility of the far-field interference pattern becomes a dilemma.

In this letter, we demonstrated a passive CBC of four Yb-doped fiber amplifier chains with injection-locked seed laser. An Yb-doped injection-locked fiber laser as the seed source, and a two-dimensional four Yb-doped fiber amplifier chains passive CBC system is established to verify its function and stability (Fig. 1). The phase locking of four separate laser beams is achieved. The visibility of the far-field interference pattern with the total output of 20 W is 89.3% when the 1064 nm seed laser is on. The seed laser extinguished when the pump power of the injection-locked fiber laser is lower than the upper bound, and then the visibility of the phase-locked far-field pattern is improved up to 91.5% (20 W total CBC output power). Far-field interference pattern of four independent beams is shown in Fig. 2.

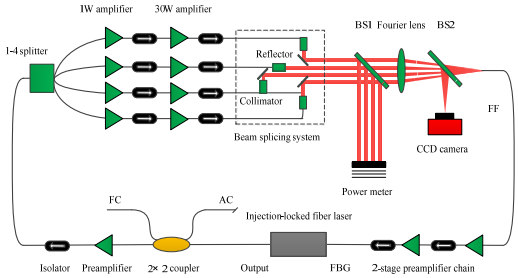

Fig. 1. Experimental apparatus of the passive beam combination of four Yb-doped fiber amplifier chains with injection-locked fiber laser seed source.

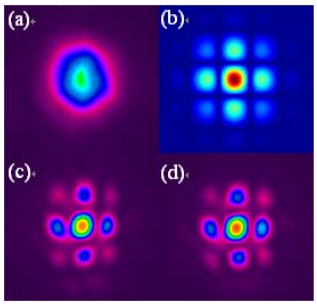

Fig. 2. Far-field interference pattern of four independent beams (a) far-field pattern in an open loop, (b) calculated far-field phase-locked pattern, (c) far-field phase-locked pattern with 1064 nm seed laser on. (d) far-field phase-locked pattern with seed laser off.

Acknowledgements: This work was supported in part by the National Natural Science Foundation of China (No. 60908011).

References:

1. N.R.V. Zandt, R.J. Bartell, et al., Opt. Eng., Vol. 51, 104301 (2012).
2. B. He, Q. Lou, W. Wang, J. Zhou, et al., Appl. Phys. Lett., Vol. 92, 251115 (2008).
3. H. Liu, Y. Xue, Z. Li, B. He, et al., Chin. Phys. Lett., Vol. 29, 044204 (2012).

Paper LS-I-10

SUBWAVELENGTH FOCUSING OF LASER LIGHT BY MICROOPTICS DEVICES

V.A. Soifer, V.V. Kotlyar, S.N. Khonina

Image Processing Systems Institute of the Russian Academy of Sciences, Samara, 443001, Russia

ipsi@smr.ru

The diffraction phenomenon, which was previously considered as a restrictive factor in optics, has currently become a fundamental basis for creating novel optical components and advanced information technologies. Since the 19-th century, the diffraction limit (DL), which can be defined as full-width half-maximum of the Airy disk size, was considered to be unbreakable in optics: FWHM = $0.51\lambda/NA$, where λ is incident wavelength, NA is the numerical aperture. Recent studies have shown that the DL can be broken. For instance, with use of an annular aperture or radially polarized light [1] it becomes possible to break the DL through enhancing the depth of focus and decreasing the energy efficiency. In this case, the focal spot size is equal to the Bessel beam's diameter of FWHM = $0.36\lambda/NA$. Using diffractive optical elements, the light energy can be redistributed to a side lobe, forming a bright ring around the focus. In this way, by decreasing the energy coming to it, the focal spot size can be made smaller than the DL. This phenomenon is termed super-oscillation [2]. By focusing light near the material surface (of refractive index n) using gradient-index or diffractive optics, it becomes possible not only to attain an n-fold increase in resolution but also to break the DL due to constructive interference of the surface waves (solid-state immersion [3]).

In this study, we discuss particular realizations of optical elements and devices that enable one to break the DL. By way of illustration, a planar binary photonic crystal lens that approximates the gradient-index hyperbolic secant lens with $n(x) = n_0 \operatorname{ch}^{-1}(ax)$, where n_0 is the refractive index on the lens optical axis and a is the lens parameter that defines its focal length, can focus light near its surface into a focal spot of intensity FWHM = 0.31λ [4]. Another example is associated with focusing light by means of a zone plate (ZP). A binary ZP was realized in an electron resist for wavelength 532 nm. The ZP has $NA = 0.996$. The focal spot size is FWHM = $(0.42 \pm 0.02)\lambda$ [5]. We also analyze the focusing of laser vortex beams that are generated with a binary spiral microaxicon of period 560 nm ($NA = 0.95$). The smaller dimension of an elliptic focal spot is FWHM = 0.36λ [6].

References:

1. R. Dorn, S. Quabis, G. Leuchs, "Sharper focus for a radially polarized light beam" Phys. Rev. Lett., Vol. 91, 233901 (2003).
2. F.M. Huang, N. Zheludev, Y. Chen, F.J. Garcia de Abajo, "Focusing of light by a nanohole array" Appl. Phys. Lett., Vol. 90, 091119 (2007).
3. K. Karrai, X. Lorenz, L. Novotny, "Enchanced reflectivity contrast in confocal solid immersion lens microscopy" Appl. Phys. Lett., Vol. 77, pp. 3459–3461 (2000).
4. M.I. Kotlyar, Y.R. Traindaphilov, A.A. Kovalev, V.A. Soifer, M.V. Kotlyar, L. O'Faolain, "Photonic crystal lens for coupling two waveguides" Appl. Opt., Vol. 48, pp. 3722–3730 (2009).
5. V.V. Kotlyar, S.S. Stafeev, Y. Liu, L. O'Faolain, A.A. Kovalev, "Analysis of the shape of a subwavelength focal spot for the linearly polarized light" Appl. Opt., Vol. 52, pp. 330–339 (2013).
6. S.N. Khonina, D.A. Savel'ev, I.A. Pustovoy, P.G. Serafimovich, "Diffraction at binary microaxicons in the near field" J. Opt. Techn., Vol. 79, pp. 626–631 (2012).

Paper LS-I-11

A SLOW (FIBER FUSE EFFECT) AND FAST (DETONATION-LIKE) MODES OF OPTICAL DISCHARGE PROPAGATION IN SILICA-BASED FIBERS

I.A. Bufetov, E.M. Dianov

Fiber Optics Research Center, Russian Academy of Sciences, 38 Vavilov str., 119333 Moscow, Russia

iabuf@fo.gpi.ru

The propagation of an optical discharge in an optical fiber was first observed in 1987 (25 years ago) and was called catastrophic damage or the fiber fuse effect (see [1] and references therein). At the laser radiation intensities ≥1MW/cm^2, the optical discharge front moves towards the laser radiation in the optical fiber with a velocity of several meters per second. In this case, the propagation mechanism is similar to the optical-discharge propagation in gases in the slow combustion mode. The traces of discharge propagation especially after the abrupt power shutdown are very freaky (see Fig. 1). We know that when the laser radiation intensity in gases increases, the slow-combustion mode changes to the light-detonation mode already at light intensity of ≈5 MW/cm^2 [2]. Experiments with two order of magnitude higher light intensities in a silica fiber core have shown that in this case we observe instead of fiber fuse quite different physical phenomenon very similar to detonation wave. The propagation velocity of another type of optical discharge reaches 3 km/s (at laser power levels of ~1 kW). But this is only half of the sound velocity in silica. The low and fast optical discharges are essential processes limiting the laser power in fibers. They have to be taken into account both for high capacity fiber communication systems and high power fiber lasers.

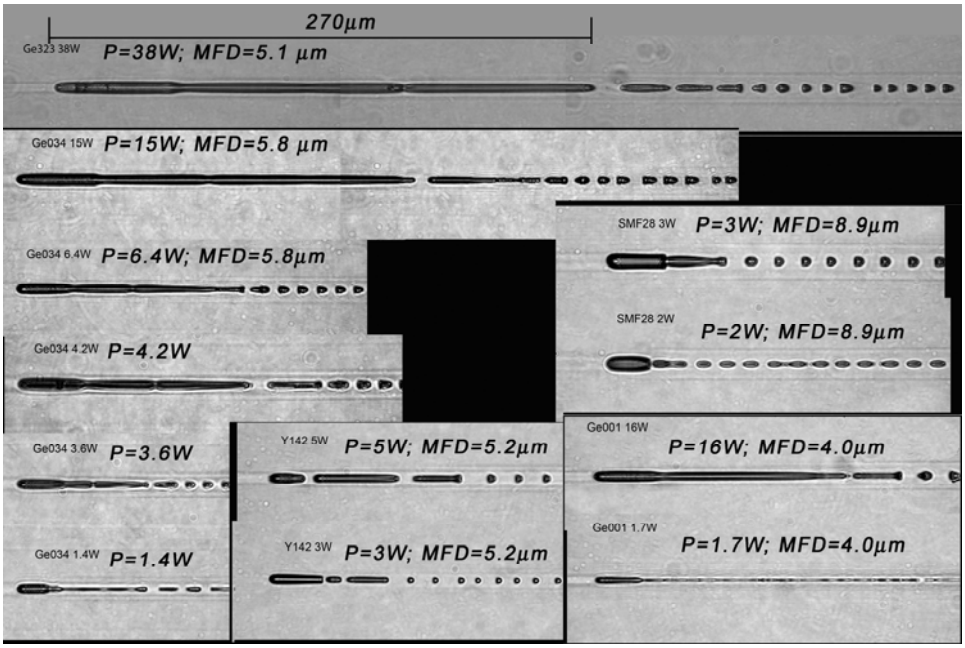

Fig. 1. Breakpoints of the optical discharge propagation after abrupt power shutdown. Laser light propagated from the left to the right. The scale is the same for all pictures. The laser power (λ = 1058 nm) in the core before shutdown and mode field diameter are indicated near each trace. Traces are shown here for fibers of 5 different types.

References:

1. R. Kashyap, "The Fiber Fuse – from a curious effect to a critical issue: A 25th year retrospective" Optics Express, Vol. 21, pp. 6422–6441 (2013).
2. I.A. Bufetov, V.B. Fedorov, V.K. Fomin, "Propagaption of an optical flame along a tube" Combustion, Explosion and Shock Waves, Vol. 22(3), pp. 274–284 (1986).

Paper LS-I-12

APPLICATION OF ULTRASHORT LASER PULSES IN OPTICAL METROLOGY

Aladar Czitrovszky, Lenard Vamos, Attila Kerekes, Attila Nagy, Daniel Oszetzky

Wigner Research Centre for Physics, Institute for Solid State Physics and Optics, Budapest, P. O. Box 49, H-1525

czitrovszky.aladar@wigner.mta.hu

The modern laser systems can generate ultrashort light pulses in femtosecond pulse regime having at the same time TW–PW power. These ultrashort laser pulses, differing in many respects even from short - ps - laser pulses, can be successfully applied in surgery, biology, nonlinear optics, material processing, micro-machinery, 3D waveguide writing, plasmonics, etc. In many application their negligible thermal- and at the same time considerable damage-effect can give us certain advantages [1, 2].

After giving an overview of the application of such ultrashort pulses in the above mentioned fields, in the presentation we will emphasize on metrological aspects - e.g. determination of the damage threshold of different optical layers, optical materials and holographic elements (gratings, mirrors, beam splitters, birefringent crystals, etc.), where different ionization phenomena are dominating on femtosecond time scale on different band-gap materials.

Another application is the generation of white light continuum (WLG) having wide spectral range, short pulse duration. These pulses are widely used in pump-probe measurements - different kinds of time-resolved laser spectroscopy (transient-absorption spectroscopy, time-resolved fluorescence spectroscopy, time resolved photoemission spectroscopy, etc.).

The statistical properties of plasmons generated by femtosecond pulses were also studied and intensity–intensity correlations were determined for light signals stemming from the spontaneous decay of surface plasmon oscillations, generated in the Kretschmann geometry. Non-classical photon statistics and the transition from antibunching to bunching of the electron counts have been found experimentally and analysed on a new theoretical basis [3].

The above mentioned methods, techniques and experiments would help the successful development and realization of the Extreme Light Infrastructure - ELI ALPS - BEAMLINE - PHOTONUCLEAR laser facilities, which will be the biggest laser projects in Europe.

Acknowledgement: The authors are acknowledge the support of the KTIA_AIK_12-1-2012-0019 and TET_10-1-2011-0725 projects.

References:

1. H. Lubatschowski et al. “Application of ultrashort laser pulses for intrastromal refractive surgery” Graefe’s Archive for Clinical and Experimental Ophthalmology, Vol. 238(1), pp. 33–39 (2000).
2. M. Sawa et al. “Application of femtosecond ultrashort pulse laser to photodynamic therapy mediated by indocyanine green” British Journal of Ophthalmology, Vol. 88(6), pp. 826–831 (2004).
3. Varro, Sandor, et al. “Hanbury Brown–Twiss type correlations with surface plasmon light” J. Mod. Opt., Vol. 58(21), pp. 2049–2057 (2011).

Paper LS-I-13

MID IR SUPERCONTINUUM GENERATION IN SILICA BASED FIBERS

A.S. Kurkov, V.A.Kamynin, Ya.E. Sadovnikova

A.M. Prokhorov General Physics Institute of RAS, Moscow, Russia

kurkov@kapella.gpi.ru

Supercontinuum generation beyond 2 μm is interesting due to the potential application in spectroscopy, atmospheric analysis, medicine, etc. As a rule, to generate supercontinuum in this spectral range special fibers are applied. The main disadvantage of such sources is the bad compatibility with standard communication fiber technology. In this paper we demonstrate a possibility to obtain the Mid IR supercontinuum in the silica based fibers.

Cladding pumped Q-switched Er-doped fiber laser was used as the pump source. Q-switching was realized by emplacement of a self-saturable absorber based on a Tm-doped fiber. Lasing wavelength was of 1.59 μm, maximum output power was near 1 W with repetition rate of 4.4 kHz and pulse duration of 35 ns. Pulse energy of 0.21 mJ and peak power of 6 kW can be estimated.

As an active medium we have used several samples of the standard fibers, fiber doped by germanium oxide with molar concentration of 70%. Also we have tested Ho-doped fiber amplifier pumped at 1125 nm and Tm-doped fiber amplifier pumped at 1200 nm.

In the standard telecommunication fibers we have obtained the supercontinuum from 1600 to 2400 nm with the average power up to 0.85 W. Spectral variations of the intensity was less than several dB. Spectrum is limited by the optical losses which sharply grow in this spectral range. Typical fiber length was of approximately of 10 m.

In germanium fiber nonlinear factor is higher and losses in this spectral range are less, than in conventional optical fibers. As a result the application of heavily germanium doped fiber allowed us to obtain the supercontinuum up to 2700 nm. Average output power as high as 0.49 W was measured. Intensity variation in the range of 1.6–2.7 μm was much less than one decade. Fiber length was of 7 m.

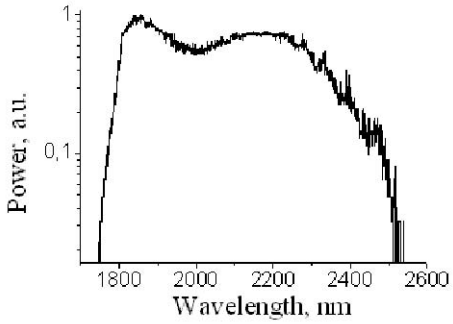

Fig. 1. Supercontinuum spectra obtained in thulium-doped fiber amplifier.

In the Ho-doped amplifier it was possible to observe the efficient supercontinuum generation in the range of 2.0–2.5 μm with the strong depletion of the emission at the shorter wavelength. Very flat spectrum was observed in the range of 2.20–2.42 nm where power variation is less than 20%. The maximum average power was measured as 0.35 W for the pump power at 1125 nm of 5.6 W. Total output pulse energy is 0.1 mJ with spectral density 10 W/nm.

In the Tm-doped fiber amplifier we have obtained the flat spectrum (–5 dB level) from 1900 to 2400 nm. It was caused by broadening of two fluorescence bands due to nonlinear interaction (Fig. 1). First band (1700–2000 nm) is caused by amplification of at the transition $^3F_4 \rightarrow {}^3H_6$ and the second band with the maximum at 2.4 μm. Therefore there is reason to believe the existence of the optical transition $^3H_4 \rightarrow {}^3H_5$ in the Tm-doped silica based fibers.

All-fiber source of supercontinuum with long-wavelength limit near 2.7 μm was demonstrated. To enhance supercontinuum in the certain spectral ranges Ho-and Tm-doped amplifier can be applied.

Paper LS-O-1

FREQUENCY-DOMAIN FLUORESCENCE LIFETIME MICROSCOPY (FLIM) AND POLAR-PLOT ANALYSIS OF GALLIUM SELENIDE

K.R. Allakhverdiev[1,2], S. Zahner[3], L. Kador[3], E.Yu. Salaev[4], M.F. Huseyinoglu[1]

[1]*TÜBİTAK Marmara Research Center, Materials Institute, P.K. 21, 41470 Gebze/Kocaeli, Turkey*
[2]*Azerbaijan National Academy of Aviation, Bina 25th km., Baku 1045, Azerbaijan*
[3]*University of Bayreuth, Institute of Physics and Bayreuther Institut für Makromolekülforschung (BIMF), 95440 Bayreuth, Germany*
[4]*Institute of Physics, Azerbaijan Academy of Science, 370073 Baku, Azerbaijan*

kerim.allahverdi@tubitak.gov.tr

Photoluminescence lifetimes can be measured in the frequency domain by exciting the sample with amplitude-modulated cw laser light. Fluorescence lifetimes in the nanosecond range require modulation frequencies of several ten MHz. The non-zero lifetime of the excited state leads to a phase shift (φ) of the fluorescence emission and a decrease of its modulation amplitude (M) with respect to the excitation, and it can be determined from both of these effects. The corresponding lifetime values ("phase lifetime" τ_φ and "amplitude lifetime" τ_M) are only identical, if the fluorescence decay is single-exponential.

An informative graphical representation of fluorescence lifetime data is the polar-plot or phasor approach which corresponds to the Cole-Cole plot in dielectric spectroscopy. It consists in plotting $M \sin \varphi$ versus $M \cos \varphi$. For single-exponential fluorescence decay, the data points are located on a semi-circle with radius 0.5 and center point (0.5; 0); for bi- or multi-exponential decay, they lie within the semi-circle. Also more complex relaxation behavior such as Förster resonance energy transfer (FRET) can be identified from polar-plot data.

We performed frequency-domain fluorescence lifetime imaging microscopy on gallium selenide (GaSe) single crystals. GaSe is a chalcogenide semiconductor which consists of thin layers bound by weak (mainly van der Waals) forces. The excitation source was a frequency-doubled solid-state laser at λ = 532 nm which was amplitude-modulated between 25 and 50 MHz. The polar-plot analysis revealed the following effects:

1. Different spots on the crystals exhibit very different fluorescence lifetimes and relaxation behavior. This indicates a high concentration of local defects, which probably results from the low rigidity of the material and the weak forces between its layers.
2. Most data points in the polar plot are located *outside* the semi-circle. This behavior is quite uncommon and has its origin in the nearly quadratic dependence of the fluorescence signal on excitation intensity.
3. In addition, the polar-plot data form loop-like structures which indicate the presence of a donor-acceptor-type energy transfer process between (at least) two emissive states. We tentatively interpret these states as the edge of the conduction band and Wannier excitons. Two consecutive absorption processes involving the excitons are probably the origin of the nonlinear intensity dependence of the fluorescence signal.

Paper LS-O-2

SPECTROSCOPY AND LASING CHARACTERISTICS OF TM:SC_2SiO_5 CRYSTAL

V.A. Mikhaylov, Yu.D. Zavartsev, A.I. Zagumennyi, Yu.L. Kalachev,
S.A. Kutovoi, I.A. Shcherbakov

A.M. Prokhorov General Physics Institute, RAS, 38 Vavilov str., 119991 Moscow, Russia

mihailov@kapella.gpi.ru

Biaxial 5% Tm:Sc_2SiO_5 (Tm:SSO) optical quality laser crystal for lasing in 2 μm range have been grown by the Czochralski method. Laser active element was cut out in the form of a cube with 3.5 mm edge. The uncoated polished plane-parallel faces of the cubic crystal were oriented along crystallographic orientations (100), (010). Active element was cooled by a contact with copper heat sink.

Tm:SSO crystal was pumped either at 795 nm ($^3H_6$–$^3H_4$ transition) by laser diode or 1678 nm ($^3H_6$–$^3F_4$ transition) by a Raman shifted Erbium fiber laser (RSEFL) at 1678 nm.

Absorption, luminescence and lasing spectra for (100) and (010) oriented Tm:SSO crystals were investigated.

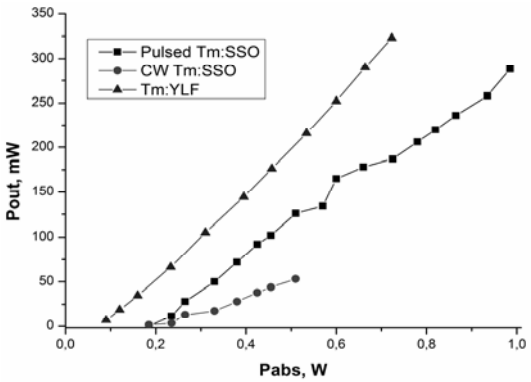

Fig. 1. Output power vs. absorbed pump power

The hemispherical laser resonator was formed by a flat mirror and 52 mm radius of output coupler with 97% reflectivity.

The best Tm:SSO laser efficiencies (total ~30% and slope ~42%) were reached at RSEFL pumping and (100) crystal laser orientation (Fig. 1). Tm:SSO laser demonstrates efficiencies which are comparable with efficiency of high quality commercially available Tm:YLF crystal under the same experimental conditions. Efficiency of RSEFL pumping essentially exceeds efficiency of diode pumping of Tm:SSO laser.

The temperature dependence of Tm:SSO laser efficiency was measured.

The further improvement of both slope and total laser efficiencies is possible on the base of improvement of crystal quality of active element by reduction of internal crystal impurities.

Acknowledgements: This work was supported by the Russian government in the frame of Program of RAS № III.8.

References:

1. Yu.D. Zavartsev, A.I. Zagumennyi, Yu.L. Kalachev, S.A. Kutovoi, V.A. Mikhaylov, I.A. Shcherbakov, "The study of Tm:Sc_2SiO_5 crystal pumped at 1678 nm", Book of abstracts ALT'12 conference (Thun, Switzerland), p. 123 (2012).

Paper LS-O-3

ACTIVE MEDIA FORMATION IN VANADATE LASERS

A.A. Sirotkin, V.I. Vlasov, A.I. Zagumennyi, Yu.D. Zavartsev, S.A. Kutovoi, I.A. Shcherbakov

Prokhorov General Physics Institute of the Russian Academy of Sciences,
119991, 38 Vavilov str., Moscow, Russia

saa@kapella.gpi.ru

Here, we present laser sources based on a novel methods control of spectral parameters in diode-pumped vanadate lasers.

Nd:$GdVO_4$, Nd:$GdVO_4$ and mixed Nd:$Y_xGd_{1-x}VO_4$, Nd:$Y_xSc_{1-x}VO_4$ vanadat are an excellent laser crystals. This crystals are ideal laser host materials for the flash-lamp and diode pumped solid state lasers as its good physical, optical and mechanical properties. The *a*-cut (σ-polarization) and *c*-cut neodymium-doped vanadate crystals are efficient active media and have a considerable potential to produce new laser possibilities [1–3].

Spectroscopic and lasing properties of Nd:YVO_4, Nd:$GdVO_4$ and mixed Nd:$YxGd_{1-x}VO_4$, Nd:$YxSc_{1-x}VO_4$ crystals were investigated. We have experimentally investigate, for the first time as far as we know, angular dependences of the luminescence intensity of Stark transitions in vanadate crystals. The frequency shift and redistribution of the luminescence intensity of Stark transitions are observed.

We have shown that lasers with nonselective resonator based on *a*-cut for π- and σ- polarized vanadate crystals) work at difference wavelengths. The different wavelength for π- and σ- polarizations allows creating two-color lasers with orthogonal polarization, which is important for the conversion to terahertz spectral range using the GaSe nonlinear optical crystals as convertor for example.

Two-color lasing has been obtained in the *a*-cut (π- and σ-polarization), *variable*-cut and *c*-cut vanadate crystals at the spectral lines separated by 2.3, 3.2 and 3.8 nm with parallel and orthogonal polarization. QW, mode-locking and Q-switching regimes with passive and active acoustic-optical modulators were realised for two-color lasers.

The grazing incidence multipass amplifier based on 1 at.% c-cut Nd:YVO_4 slab (dimensions: 20 mm × 5 mm × 2 mm) was used for the amplifier two-color radiation with parallel and orthogonal polarization.

We suggest using combinations of two different vanadate crystals or mixed vanadates for creation active media with new parameters.

We have experimentally investigated the operation of diode-pumped passively *Q*-switched *variable*-cut (θ = var, φ = 0) Nd:YVO_4, Nd:$GdVO_4$ lasers with Cr^{4+}:YAG saturable absorber and compared their relative advantages and drawbacks. The best passively *Q*-switched performance obtained in our experiments is from the *variable*-cut (θ = 25°, φ = 0) laser, which gives the narrowest pulse of 2.5 ns with the highest peak power of 10.3 kW.

References:

1. V.I. Vlasov, S.V. Garnov, Yu.D. Zavartsev, A.I. Zagumennyi, S.A. Kutovoi, A.A. Sirotkin, I.A. Shcherbakov, “New lasers based on c-cut vanadat crystal” Quantum Electronics, Vol. 37, p. 938 (2007).
2. A.A. Sirotkin, V.I. Vlasov, A.I. Zagumennyi, Yu.D. Zavartsev, S.A. Kutovoi, “Vanadate lasers with σ-polarised radiation” Quantum Electronics, Vol. 41(7), pp. 584–589 (2011).
3. A.A. Sirotkin, S.V. Garnov, V.I. Vlasov, A.I. Zagumennyi, Yu.D. Zavartsev, S.A. Kutovoi, I.A. Shcherbakov, “Two-frequency vanadate lasers with mutually parallel and orthogonal polarisations of radiation” Quantum Electronics, Vol. 42, p. 420 (2012).

Paper LS-O-4

DEVELOPMENT OF ISO 21254 COMPLIANT SEMI-AUTOMATIC LIDT STATION IN THE FRAME OF HILASE PROJECT

Jan Vanda[1], Roman Svabek[1], Michal Chyla[1], Vaclav Skoda[2]

[1]HiLASE Project, Institute of Physics of the ASCR, Na Slovance 2, 18221, Prague, Czech Republic
[2]Crytur ltd. Palackeho 175, 51101 Turnov, Czech Republic

Vandaj@fzu.cz

Laser induced damage threshold is a key parameter for all components in high-power laser system, that establishing limits of maximum achievable energy, and consequently average power. Currently, more powerful laser systems are built to meet the need of evolving technology. To provide reliable and stable laser sources, desirable both in academic and industrial area, components of such sources has to be tested and meet certain quality criteria. Utilizing of gathered knowledge and state-of-the-art then allows construction of compact devices in applied research, which can reach substantial output powers and energy densities.

Together with laser system, LIDT station [1] offers necessary background for components reliability testing and for overall high power lasers development. One of the main goals of application program in HiLASE [2] project is to remove deficit of reliable, test-and-go facility for industry and applied research, and provide valuable workplaces allowing fast set-up and exposure variety of samples. Within this scope, HiLASE project is developing three kW class thin-disk laser lines, delivering 1–2 ps pulses of energy up to 1 J with repetition rate of 1 kHz and Gaussian beam diameter 15 mm, and one multislab system delivering 2–10 ns pulses of energy 100 J with repetition rate up to 10 Hz and square beam with size 45 mm.

Following paper presents results of LIDT test of novel, high damage threshold broadband mirrors, intended to use in laser system built within the HiLASE project. Also advanced LIDT test station design in compliance with ISO 21254 standards series, fully computer controlled, which will use HiLASE laser as source is described.

Acknowledgements: This work benefitted from the support of the Czech Republic's Ministry of Education, Youth and Sports to the HiLASE (CZ.1.05/2.1.00/01.0027) and DPSSLasers (CZ.1.07/2.3.00/20.0143) projects.

References:

1. J. Vanda, L. Gemini, R. Svabek, T. Mocek, G. Cherieaux, "Advanced LIDT testing station in the frame of the HiLASE Project", Proc. SPIE, Vol. 8530, 85301D-1–85301D-9 (2012).
2. M. Smrz, P. Severova, T. Mocek, "Design and modeling of kW-class thin-disk lasers", Proc. SPIE, Vol. 8235, 82350R-1–82350R-8 (2012).

Paper LS-O-5

COLLINEAR PHASE-MATCHED FOUR-WAVE MIXING GENERATION OF RAMAN RADIATION COMPONENTS IN THE CALCITE PARAMETRIC RAMAN LASER

S.N. Smetanin[1], A.S. Shurygin[2], A.V. Fedin[2]

[1]Research Center for Laser Materials and Technologies of Prokhorov General Physics, Institute of the Russian Academy of Sciences, 38 Vavilov Str., 119991 Moscow, Russia
[2]Kovrov State Technological Academy, 19 Mayakovsky Str., 601910 Kovrov, Russia

ssmetanin@bk.ru

There is currently great interest in solid-state lasers with stimulated Raman scattering (SRS) that provide a Stokes-shifted output. An important issue in the case of crystalline Raman lasers is the ability to ensure efficient generation of higher order Stokes Raman components and anti-Stokes waves. In the case of high-order Stokes SRS generation, a considerable increase in pump intensity (limited by the optical damage threshold of the crystal) is necessary, which would entail a drop in Raman gain coefficient with an increase in the wavelength of Stokes Raman components. In the case of anti-Stokes wave generation through SRS, the phase matching condition for four-wave mixing of Raman radiation components should be satisfied, which is prevented by refractive index dispersion if the mixing waves propagated collinearly. The parametric Raman anti-Stokes laser generation at tilted pumping of the Raman laser cavity satisfying vectorial phase matching of four-wave mixing was studied for the first time in [1].

When the phase matching condition is satisfied, parametric four-wave mixing not only ensures anti-Stokes wave generation through SRS, but also enables a substantial reduction in higher order Stokes SRS generation thresholds [2]. In [3], the original method of exact satisfaction of four-wave mixing phase matching through biharmonically pumped single-pass SRS of orthogonally polarized waves in calcite was proposed and realized. In [4], it was shown that the phase matching conditions for partially degenerate and nondegenerate collinear four-wave mixing of several Raman radiation components are exactly satisfied in certain directions of different birefringent Raman-active crystals upon interaction between orthogonally polarized waves at single wave pumping.

In this work, the possibilities of collinear four-wave mixing generation of Raman radiation components in birefringent Raman-active crystals at satisfaction of phase matching conditions of several types differing by combination of polarization vectors of mixed waves are studied. Low-threshold four-wave mixing generation in the calcite parametric Raman laser with collinear (longitudinal) pumping of the Raman laser cavity satisfying theoretically determined phase matching condition $\mathbf{k}_0 - \mathbf{k}_1 = \mathbf{k}_1 - \mathbf{k}_2$ of partially degenerate four-wave mixing of the laser pump radiation (wave vector $\mathbf{k}_0$) with the first (wave vector $\mathbf{k}_1$) and second (wave vector $\mathbf{k}_2$) Stokes Raman radiation components is experimentally realized.

References:

1. A.Z. Grasiuk, L.L. Losev, A.P. Lutsenko, S.N. Sazonov, “Parametric Raman anti-Stokes laser” Quantum. Electron., Vol. 20, pp. 1153–1155 (1990).
2. T.T. Basiev, S.N. Smetanin, A.S. Shurygin, A.V. Fedin, “Parametric coupling of frequency components at stimulated Raman scattering in solids” Phys.-Usp., Vol. 53, pp. 611–617 (2010).
3. J.A. Giordmaine, W. Kaiser, “Light scattering by coherently driven lattice vibrations” Phys. Rev., Vol. 144, pp. 676–688 (1966).
4. S.N. Smetanin, T.T. Basiev, “Phase matching of four-wave interactions of SRS components in birefringent SRS-active crystals” Quantum Elecrton., Vol. 42, pp. 224–227 (2012).

Paper LS-O-6

ELECTRIC-DISCHARGE LASER WITH ELECTROHYDRODYNAMIC CIRCULATION SYSTEM

V.A. Yamshchikov, Yu.A. Zheleznov, M.V. Malashin, S.V. Nebogatkin, I.E. Rebrov, Yu.V. Khomich

Institute for electrophysics and electric power RAS,
18 Dvortzovaya nab., Sankt-Peterburg 191186, Russia

yamschikov52@mail.ru

Dielectric barrier discharge (DBD) can form the electrohydrodynamic (EHD) flow which may be used in circulation system of electric-discharge lasers [1]. Circulation systems based on DBD have no moving parts. They do not create vibrations and they are silent in work. From traditional lasers with electromechanical fan it differs by simplicity, compactness and reliability. In present work we investigate high-power electric-discharge laser with electrohydrodynamic gas circulation system.

Investigations were based on high-power N_2-laser [2]. Laser has discharge volume 2 cm·2 cm·50 cm = 100 cm^3. When circulation system contain electromechanical fan the energy of radiation pulses (λ = 337 nm) was equal to W = 3 mJ with repetition rate up to 150 Hz. In modified version the fan was removed from laser chamber (LG) and replaced by electric-discharge device for EHD flow. Figure shows the schematic cross-sectional laser chamber with EHD circulation system.

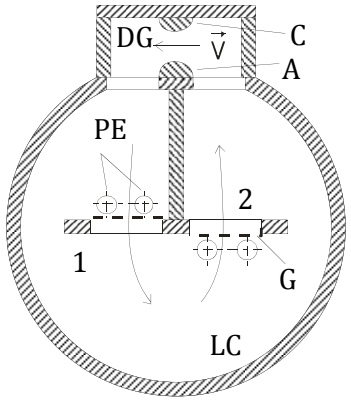

The scheme contains two cascades 1 and 2. In [1] there were desribed the operation and main characteristics of separate pumping unit. Plasma ion emitters (PE) were feeded by periodic voltage of 12 kV with frequency up to 25 kHz. The constant voltage up to 20 kV was applied to the grid (G). Flow velocity V in a discharge gap (DG) exceeds of 5 m/s. If one cascade operates the energy maximum of W = 3 mJ is reached at frequency of 50 Hz. When two cascades operate the same energy is maintained at frequency up to 100 Hz. This demonstrates the scalability of the flux and possibility of increasing the pulse repetition rate by increasing the number of pumping cascades.

Acknowledgements: This work was supported by RFBR, grant № 12-08-33045.

References:

1. S.I. Moshkunov, S.V. Nebogatkin, I.E. Rebrov, V.Yu. Khomich, V.Ya. Yamshchikov, “Gas mixture circulation system in lasers using a high-frequency barrier discharge” Quant. Electronics, Vol. 41(12), pp. 1093–1097 (2011).
2. V. Apollonov, V. Yamshchikov, “Efficiency of an electric-discharge N_2 laser” Quant. Electronics, Vol. 27(6), pp. 469–472 (1997).

Paper LS-O-7

AN ALTERNATIVE METHOD FOR THE COMPENSATION OF LASER BEAM SPATIAL DISTORTIONS BASED ON COMPUTER GENERATED HOLOGRAMS

Laura Ionel

National Institute for Laser, Plasma and Radiation Physics, Laser Department, Atomistilor Str. 409, P. O. Box MG-36, 077125 Magurele-Bucharest, Romania

laura.ionel@inflpr.ro

A fast and accurate method for the compensation of spatial distortions of the laser beam intensity profiles based on computer generated holograms (CGHs) is presented. Considering the optical beam path from a CW laser source, we simulated the aberrated intensity distribution in case of user-induced misalignments in the optical setup using a numerical ray-tracing model. This numerically modeled setup is based on two spherical mirrors which are responsible with the spatial distortions introduced in the optical system due to a fine user-induced misalignment. To correct this aberrated intensity profile, an iterative code based on the Gerchberg-Saxton algorithm (GSA) was used to design CGHs for a spatial light modulator. In order to experimentally verify our numerical intensity profile correction method, two cases were investigated: the correction of the distorted intensity distribution with the aim to improve the laser beam spot profile and the achievement of a desired diffraction intensity pattern in a logo. For both cases, a specific optical setup based on two spatial light modulators was built. Thus, we created a compact and easily-implementable optical system to correct the distorted intensity profiles of the laser beam. The results are relevant for different applications with needs of high quality laser beam profile.

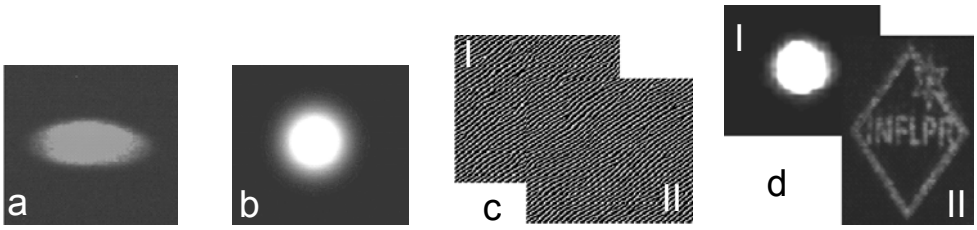

Fig. 1. Correction of the laser beam intensity profile: (a) laser wavefront after the first SLM; (b) ideal Gaussian beam profile - desired pattern in the image plan; (c) associated computer generated holograms addressed on the second SLM in order to correct the aberrated beam intensity profile (d I) and to generate high quality logo diffraction patterns (d II).

Acknowledgements: This work was supported by National Authority for Scientific Research, Project LAPLAS3.

References:

1. L. Ionel, C.P. Cristescu, Opt. Adv. Mater. Rapid Commun., Vol. 5(9), pp. 906–910 (2011).
2. L. Ionel, C.P. Cristescu, F. Jipa, M. Enculescu, M. Radoiu, R. Dabu, M. Zamfirescu, M. Ulmeanu, Opt. Adv. Mater. Rapid Commun., Vol. 4(11), pp. 1920–1924 (2010).
3. D. Ursescu, L. Ionel, J. Opt. Adv. Mater., Vol. 4(1), pp. 662–666 (2009).

Paper LS-O-8

SELF-MIXING LASER DIODE VIBROMETER FOR VERY LOW FREQUENCY APPLICATIONS

Giuseppe Martini[1], Enrico Randone[2], Silvano Donati[1]

[1]*University of Pavia, Via Ferrata 1, I-27100 Pavia, Italy*
[2]*Arkedos S.r.l.- Pavia site, via Ferrata 1, I-27100 Pavia, Italy*

martini@ieee.org

Introduction: Optical vibrometer based on Laser Diode Self-Mix Interferometry (SMI) is the elective choice in non-invasive vibration monitoring. We present an instrument aimed at measurement of small amplitude (10 nm < s < 1 μm) vibrations at very low frequency, below 10^{-3} Hz. Intended application is *in situ* vibration monitoring of artwork, e.g. during 3D surface topography aimed at indentification of the original piece to counteract forgery of the artwork, or to prevent or detect theft during transportation before/after an exhibition. In the intended application, long term stability and glitch-free operation are required. The proposed vibrometer exploits the fringe-lock configuration, and the advantages offered by the presence of the feedback loop. In previous design with AC feedback only, glitches were observed because of fringe lock loss due to wavelength fluctuation induced by temperature fluctuation, even with TEC control of the Laser Diode temperature.

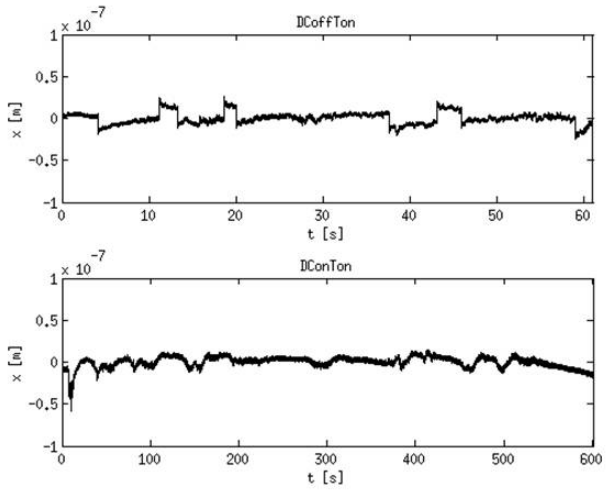

Fig. 1. Typical signal with AC feedback only (upper) and with DC loop added (lower); LD temperature is controlled by TEC in both cases.

Instrument description and results: Basically, in SMI [1] a returned field $E_R \exp(j\varphi(t))$ is added to unperturbed cavity field E_0, generates amplitude (AM) and frequency (FM) modulation of the lasing field. Intensity modulation is easily read by the power monitor photodiode as a interferometric signal $I = I_0(1+F(\varphi(t)))$, where the actual form of $F(\varphi(t))$ depends on physical parameters of the LD and on the ratio E_R/E_0, i.e. the injection level. At low injection level, $F(\varphi(t))$ is the usual cosine and become distorted at higher injection level. In a proper regime of injection, $F(\varphi(t))$ becomes sawtooth, allowing development of the fringe-lock vibrometer [2]. Usually, AC coupled feedback loop is employed. Our improved design uses, in addition to the usual AC coupled loop for signal extraction, a separate DC loop to improve long-term stability of the system. Long term measurements of a rigid set-up on top of a vibration isolation honeycomb table are shown in Fig. 1. The glitches seen with open DC loop arises from the wavelength drift due to temperature fluctuation ($d\lambda/dT$ = 0.65 nm/K), and vanishes when DC loop is closed, allowing long term acquisition lasting up to 10 minutes and longer.

References:

1. S. Donati, "Developing self-mixing interferometry for instrumentation and measurements" Laser Photonics Rev., Vol. 6, pp. 393–417(2012) (DOI: 10.1002/ lpor.201100002).
2. G. Giuliani, S. Bozzi-Pietra, S. Donati, "Self-mixing laser diode vibrometer" Meas. Sci. Technol. Vol. 14**,** pp. 24–32 (2003) (DOI: 10.1088/0957-0233/14/1/304).

Paper LS-P-1

INVESTIGATION OF INFRARED BISMUTH FLUORESCENCE IN $ZnWO_4$ CRYSTALS

O.K. Alimov, M.E. Doroshenko, L.I. Ivleva, A.G. Papashvili, I.S. Voronina, V.V. Osiko

Prokhorov General Physics Institute RAS, Vavilov Str. 38, Moscow, Russia

olim@lst.gpi.ru

New Bi doped $ZnWO_4$:1.48wt.%Bi_2O_3 crystals were synthesized using Czochralski technique and IR bismuth fluorescence in as grown crystals was investigated. Under 532 nm excitation intensive IR fluorescence of Bi ions in $ZnWO_4$ crystals was observed. The measured decay curves in IR spectral region have demonstrated well pronounced double exponential shape as could be seen in Fig. 1. As follows from the figure the decay curves are well fitted by a sum of two exponentials with short (about 1 μs) and long (about 6 μs) lifetimes which could be assigned to two different types of Bi optical centers. Fig. 1 also demonstrates that the contribution of different Bi optical centers to overall fluorescence varies strongly for different wavelengths. The significant difference in the fluorescence lifetime allowed to measure a time resolved fluorescence spectrum of $ZnWO_4$:Bi crystal under 532 nm excitation shown in Fig. 2 with time delays for two presented fluorescence spectra chosen according to measured lifetimes for two Bi ions optical centers.

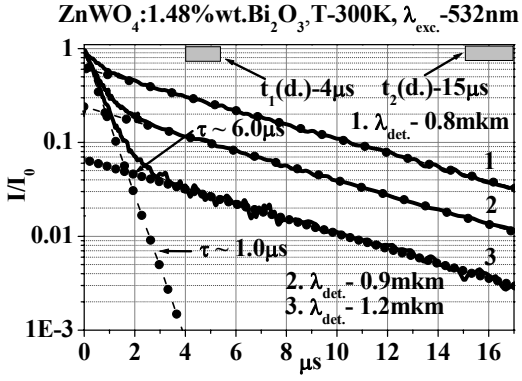

Fig. 1. Double exponential decay curves for $ZnWO_4$:Bi crystal under 532 nm excitation.

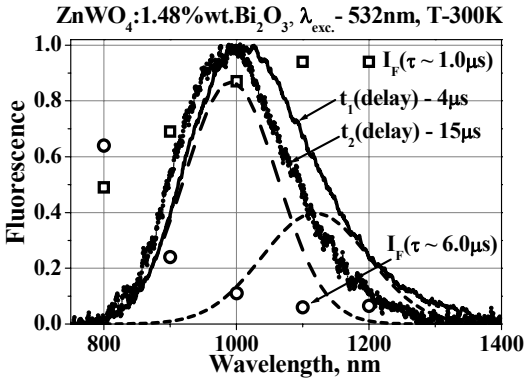

Fig. 2. Time resolved fluorescence spectra of $ZnWO_4$:Bi crystal under 532 nm excitation.

As could be seen from Fig. 2 the spectral maximum position and width of the fluorescence spectra are changed with time delay. As follows from the figure for short delay time of 4 μs broad fluorescence peaking at ~1000 nm was observed while increasing delay to 15 μs results in shift of IR fluorescence maximum towards shorter wavelengths and narrowing of the fluorescence spectrum. As could be also seen from Fig. 2 the time resolved fluorescence spectrum for 4 μs delay in $ZnWO_4$:Bi crystal could be well decomposed into two Gaussian shape lines peaking at ~1100 nm and ~1000 nm the latter having very similar shape with fluorescence spectrum measured for 15 μs delay. To determine the two Bi optical centers contribution to the overall IR fluorescence the decay curves were measured at a number of wavelengths and the amplitudes for two components are plotted in Fig. 2 by hollow dots (square – short and circle – long component, respectively).

Thus intensive IR fluorescence in as grown Bi doped $ZnWO_4$ crystals was observed and analyzed. The IR fluorescence was suggested to be a product of two different Bi ions optical centers fluorescence with long ~6 μs (maximum at 1000 nm) and short ~1 μs (maximum at 1100 nm) lifetimes. IR fluorescence behavior for other excitation wavelengths and temperatures was also investigated and will be presented.

Paper LS-P-2

APPLICATION OF DIGITAL SIGNAL PROCESSING IN LOCKING OF CW LASERS ON OPTICAL FREQUENCY COMBS

Martin Čižek, Ondřej Čip, Radek Šmid, Jan Hrabina, Břetislav Mikel, Josef Lazar

Institute of Scientific Instruments of the ASCR, Kralovopolska 147, 612 64 Brno, CZ

cizek@isibrno.cz

In cases when it is needed to lock the optical frequency of a CW laser such as a DFB diode laser to a precise metrological reference [1, 2] a possible way is to utilize a setup where an optical frequency comb is used for transferring the stability of a radio frequency (RF) normal (GPS-disciplined oscillator, H-maser, etc.) to the optical domain.

Such system takes the signal generated by the RF standard (usually 10 MHz or 100 MHz) as a reference and stabilizes the repetition (f_{rep}) and offset (f_{ceo}) frequencies of the comb contained in the RF output of the f-2f interferometer [3]. In the next level, the frequency of a beat note (f_{beat}) between the tunable DFB diode laser and a selected component of the comb spectrum is locked to the same RF standard. As a result, we get a diode laser with optical frequency derived directly from a stable RF reference. These control loops are usually built around analog electronic circuits processing the output signals from fast photodetectors. The presented work describes a different approach based on digital signal processing and software-defined radio algorithms used for processing the f-2f and beat-note signals.

The measurements of f_{rep}, f_{ceo} and f_{beat} were analyzed by means of calculating Allan deviations for times ranging up to 10 000 s. The digital system is able to stabilize the 100 MHz repetition frequency with absolute deviations observed in mHz. The offset frequency stabilized at 10.7 MHz center exhibits fluctuations in kHz order. In case of f_{beat} stabilized at 5 MHz offset from a comb spectrum component, the observed fluctuations were in 0.1 kHz order of magnitude. Observed stabilities in the RF domain result in the overall performance of the complete system in the optical domain where it is able to stabilize a diode laser with optical frequency stability in the 10^{-11} order.

Acknowledgements: This work was supported mainly by Grant Agency of CR project No. GAP102/11/P819 and GP102/10/1813. The pilot set-up of the method was partially funded by Technology Agency of the Czech Republic, project No. TA01010995. The background of the research was supported by the European Commission and Ministry of Education, Youth, and Sports of the Czech Republic project No. CZ.1.05/2.1.00/01. The presentation of the work was supported by the European Commission and Ministry of Education, Youth, and Sports of the Czech Republic project No. CZ.1.07/2.4.00/31.0016.

References:

1. O. Cip, R. Smid, M. Cizek, Z. Buchta, J. Lazar, "Study of the thermal stability of Zerodur glass ceramics suitable for a scanning probe microscope frame" Central European Journal of Physics, Vol. 10(2), pp. 447–453 (2012).
2. R. Smid, M. Cizek, Z. Buchta, J. Lazar, O. Cip, "Evaluation of Fabry-Perot cavity length by the stabilized optical frequency comb and acetylene absorption", Joint Conference of the Ieee International Frequency Control Symposium/European Frequency and Time Forum Proceedings, pp. 345–348 (2011).
3. M. Bellini, T.W. Hansch, "Phase-locked white-light continuum pulses: toward a universal optical frequency-comb synthesizer" Optics Letters, Vol. 25(14), pp. 1049–1051 (2000).

Paper LS-P-3

160-W SINGLE-FREQUENCY LASER BASED ON ACTIVE TAPERED DOUBLE-CLAD FIBER AMPLIFIER

S.A. Filatova[1], A.I. Trikshev[1], A.S. Kurkov[1], V.B Tsvetkov[1], J. Kertulla[2], V. Filippov[2], Yu.K. Chamorovskiy[3], O.G. Okhotnikov[2]

[1]*Prokhorov General Physics Institute of the Russian Academy of Sciences, Vavilov Str. 38, 119991, Moscow, Russia*
[2]*Optoelectronics Research Centre, Tampere University of Technology, P.O. BOX 692, 33101 Tampere, Finland*
[3]*Institute of Radio Engineering and Electronics of the Russian Academy of Sciences, Mokhovaya 11, bld. 7, 125009, Moscow, Russia*

S.Simus@mail.ru

The main factor limiting the output power of fiber lasers is the influence of nonlinear effects: stimulated Raman scattering (SRS), stimulated Brillouin scattering (SBS), etc. To obtain high power densities, it is proposed to sum coherently radiations from several sources [1]. A generally accepted approach is to use a narrow-band master oscillator and several cascades of fiber amplifiers [2].

In this study, we present a two stage high-power amplifier using ytterbium-doped GTWave fiber in the first stage and tapered ytterbium-doped fiber concept in the second stage. The T-DCF approach takes advantage of the large mode volume combined with good beam quality and utilizes cost-effective low-brightness end pumping.

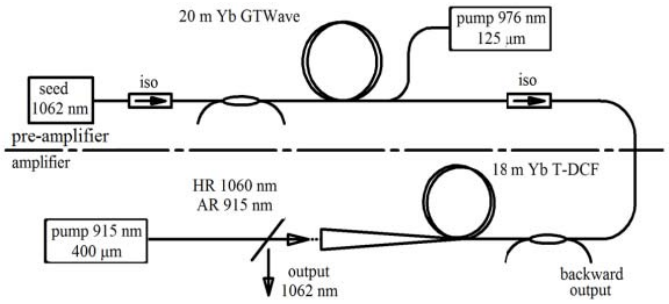

Fig. 1. Experimental setup.

The seed laser and two-stage power amplifier studied here are shown in Fig. 1. We used a 1062 nm, 20 mW single-frequency semiconductor laser as a master oscillator. The first stage is a Yb-multicore fiber amplifier. The active fiber has an absorption coefficient of 0.8 dB/m at 975 nm pump wavelength and a length of 20-meter is used in this stage. The first stage can boost the output power to 3 W then pumped 7.5 W. The TDCF amplifier was 18 m long and had a tapering ratio of T~6 with core/cladding diameters of 44 μm/700 μm and 7.5 μm/120 μm in the wide end and narrow end, respectively. The fiber was coiled with 15 cm radius and freespace pumped with a 915 nm fiber-coupled diode laser using collimating and focusing lenses, and a dichroic mirror. Pump absorption in the T-DCF was measured to be 15 dB. The output end face was angle cleaved to ~7° to suppress feed-back. An additional cladding mode stripper was placed at the narrow end of the taper to block 915 nm pump light unabsorbed in the amplifier. A 10% tap coupler was spliced between the isolator and the CMS to monitor backward-propagating signal.

The useful single-frequency signal is about 130 W at maximum output power of 160 W. The slope efficiency was 61.4%. The maximum backward power is 0.3 W. Maximum achievable gain was about 40 dB. Lasing linewidth was less than 3 MHz. Beam quality factor is 1.05/1.2 (for two orthogonal axes).

References:

1. G.D. Goodno, H. Komine, S.J. McNaught, S.B. Weiss, S. Redmond, W. Long, R. Simpson, E.C. Cheung, D. Howland, P. Epp, M. Weber, M. McClellan, J. Sollee , H. Injeyan, Opt. Lett., Vol. 31, p. 1247 (2006).
2. X. Dong, H. Xiao, P. Zhou, X. Wang, Y. Ma, J. Leng, X. Xu, Z. Liu, Laser Phys., Vol. 21, p. 1108 (2011).

Paper LS-P-4

POSITION SENSING WITH STANDING WAVE DETECTION WITHIN A PASSIVE FABRY–PEROT CAVITY

M. Holá, J. Hrabina, O. Číp, J. Oulehla, J. Lazar

Institute of Scientific Instruments, v.v.i., Academy of Sciences of the Czech Republic, Královopolská 147, 612 64 Brno, Czech Republic

hola@isibrno.cz

We present a measuring technique for displacement and position sensing over a limited range with detection of standing-wave pattern inside of a passive Fabry-Perot cavity. The concept considers locking of the laser optical frequency and the length of the Fabry-Perot cavity in resonance. Fixing the length of the cavity to e.g. a highly stable mechanical reference allows to stabilize wavelength of the laser in air and thus to eliminate especially the faster fluctuations of refractive index of air due to air flow and inhomogeneities. Sensing of the interference maxima and minima within the cavity along the beam axis has been tested and proven with a low loss photoresistive photodetector based on a thin polycrystalline silicon layer. Reduction of losses was achieved thanks to a design as an optimized set of interference layers acting as an antireflection coating. The principle is demonstrated on an experimental setup.

Acknowledgements: The authors wish to express thanks for support to the grant projects from the Grant Agency of CR, project GPP102/11/P820, Academy of Sciences of CR, project: RVO:68081731, Ministry of Education, Youth and Sports of CR, project: CZ.1.05/2.1.00/01.0017, European Social Fund and National Budget of the Czech Republic, project: CZ.1.07/2.4.00/31.0016 and Technology Agency of CR, projects: TA02010711, TE01020233.

References:

1. G.D. Rovera, F. Ducos, J.J. Zondy, O. Acef, J.P. Wallerand, J.C. Knight, P.S. Russell, “Absolute frequency measurement of an I-2 stabilized Nd:YAG optical frequency standard” Meas. Sci. Technol. Vol. 13(6), 918-922 (2002).
2. Doloca, N. R., Meiners-Hagen, K., Wedde, M., Pollinger, F., and Abou-Zeid, A., “Absolute distance measurement system using a femtosecond laser as a modulator” Meas. Sci. Technol., Vol. 21, 115302 (2010).
3. G. Bartl, M. Krystek, A. Nicolaus, W. Giardini, “Interferometric determination of the topographies of absolute sphere radii using the sphere interferometer of PTB” Meas. Sci. Technol., Vol. 21, 115101 (2010).
4. J. Lazar, O. Číp, M. Čížek, J. Hrabina, Z. Buchta, “Suppression of air refractive index variations in high-resolution interferometry” Sensors, Vol. 11, pp. 7644–7655 (2011).
5. R. Šmíd, O. Číp, J. Lazar, “Precise length etalon controlled by stabilized frequency comb” Meas. Sci. Technol., Vol. 8, pp. 114–117 (2008).
6. J. Lazar, M. Holá, O. Číp, M. Čížek, J. Hrabina, Z. Buchta, “Refractive index compensation in over-determined interferometric systems” Sensors, Vol. 12, pp. 14084–14094 (2012).
7. J. Lazar, M. Holá, O. Číp, M. Čížek, J. Hrabina, Z. Buchta, “Displacement interferometry with stabilization of wavelength in air” Opt. Express, Vol. 20(25), 27830 (2012).

Paper LS-P-5

LASER FREQUENCY STANDARDS BASED ON IODINE ABSORPTION CELLS FILLED TO SATURATION PRESSURE

Jan Hrabina, Miroslava Holá, Josef Lazar, Ondřej Číp

Institute of Scientific Instruments, v.v.i., Academy of Sciences of the Czech Republic, Královopolská 147, 612 64 Brno, Czech Republic

hrabina@isibrno.cz

The contribution is oriented towards frequency stabilization of frequency-doubled Nd:YAG lasers for nanometrology through spectroscopy in molecular iodine. We designed and manufactured a series of new type of iodine absorption cells and tested the frequency stability of the laser stabilized with these cells. The set of starved iodine cells does not need a cold finger for stabilization of the pressure of the absorbing media due to the saturation pressure of iodine is defined during the iodine filling process. A second part of the contribution is focused to absorption cells made of borosilicate glass instead of traditionally used fused silica. Absorption cells prepared by these two approaches were used for frequency stabilization of Nd:YAG laser by the linear and saturation spectroscopy in different environmental conditions and resulted frequency stability was compared to commonly used laser standard based on quartz silica glass cell. The achievable hyperfine transitions linewidths were studied in detail.

Acknowledgements: The authors wish to express thanks for support to the grant projects from the Grant Agency of CR, project GPP102/11/P820, Academy of Sciences of CR, project: RVO:68081731, Ministry of Education, Youth and Sports of CR, project: CZ.1.05/2.1.00/01.0017, European Social Fund and National Budget of the Czech Republic, project: CZ.1.07/2.4.00/31.0016 and Technology Agency of CR, projects: TA02010711, TA0101995, TE01020233.

References:

1. H. Salami et al., "A molecular iodine atlas in ascii format" J. Mol. Spectrosc., Vol. 233(1), pp. 157–159 (2005).
2. K. Nyholm et al., "Frequency stabilization of a diode-pumped Nd:YAG laser at 532 nm to iodine by using third-harmonic technique" IEEE T. Instrum. Meas., Vol. 52(2), pp. 284–287 (2003).
3. J. Hrabina et al., "Purity of iodine cells and optical frequency shift of iodine-stabilized He-Ne lasers" J. Optoelectron. Adv. M., Vol. 1(5), pp. 202–206 (2007).
4. G. D. Rovera et al., "Absolute frequency measurement of an I-2 stabilized Nd:YAG optical frequency standard" Meas. Sci. Technol., Vol. 13(6), pp. 918–922 (2002).
5. J. Lazar et al., "Absolute frequency shifts of iodine cells for laser stabilization" Metrol., Vol. 46(5), pp. 450–456 (2009).
6. J. Hrabina et al., "Frequency noise properties of lasers for interferometry in nanometrology" Sensors, Vol. 13(2), pp. 2206–2219 (2013).
7. J. Hrabina et al., "Investigation of short-term amplitude and frequency fluctuations of lasers for interferometry" Meas. Sci. Rev., Vol. 13(2), pp. 63–69 (2013).
8. L. S. Ma et al., "Absolute frequency measurement of molecular iodine lines at 514.7 nm, interrogated by a frequency-doubled Yb-doped fibre laser" Metrol., Vol. 43(3), pp. 294–298 (2006).
9. J. Hrabina et al.,. "Methods for measurement and verification of purity of iodine cells for laser frequency stabilization" Meas. Sci. Rev., Vol. 8(5), pp. 118–121 (2008).
10. J. Hrabina et al., "Multidimensional interferometric tool for the local probe microscopy nanometrology", Meas. Sci. Technol., Vol. 22(9) (2011).
11. J. Hrabina et al., "AFM nanometrology interferometric system with the compensation of angle errors", Optical Measurement Systems for Industrial Inspection, Vol. 7, p. 8082 (2011).

Paper LS-P-6

GROWTH AND PROPERTIES OF RAMAN-ACTIVE $SrMoO_4:Pr^{3+}$ CRYSTAL

I.S. Voronina, E.E. Dunaeva, A.V. Nekhoroshikh, L.I. Ivleva, P.G. Zverev, M.E. Doroshenko

A.M. Prokhorov General Physics Institute of Russian Academy of Sciences

ivleva@lst.gpi.ru

The use of the Stimulated Raman Scattering (SRS) of laser radiation in crystalline materials is an efficient way to design spectrally positioned laser sources. Scheelite type $SrMoO_4$ crystal is the promising SRS material having congruently melting composition and holding no phase transition in temperature region from room temperature to the melting point. Introduction of rear-earth impurity dopants into the matrix allows to combine laser and nonlinear features in the same optical element.

In this work the results on the growth technique, spectral and luminescence characteristics of Pr^{3+} ions in $SrMoO_4$ Raman crystals are presented. The samples of $SrMoO_4$ crystal doped with praseodymium were grown by Czochralski method from the 100 cm^3 Pt crucible in the air. The impurity was introduced in the form of PrNbO4 in the concentration range from 0.1 till 3.0 wt.% in the melt. Search for the optimal growth conditions such as thermal cell construction, volume crystallization rate, growth and annealing regimes was carried out and optically homogeneous single crystals with diameter 25 mm and 90 mm length were obtained. Absence of light scattering centers, growth striations and refractive index inhomogeneities was approved by methods of optical microscopy and dynamic holography. The spectral emission analysis of $SrMoO_4$:$PrNbO_4$ (3.0 wt.%) sample showed that the Sr–Mo ratio corresponded to a stoichiometric composition and the value of effective segregation coefficient of Pr^{3+} ions for it was found to be 0.85.

Absorption spectra of $SrMoO_4:Pr^{3+}$ crystals revealed a number of absorption peaks in the visible spectral range that corresponded to $^3H_4$–$^3P_0$, $^3P_1$, $^1I_6$, $^3P_2$, $^1D_2$ transitions. The maximal absorption was observed at 449 nm that well corresponds to the emission band of blue GaN laser diodes. Fig. 1 shows linear dependence of absorption coefficient at 449 nm with respect to concentration of Pr^{3+} ions. The fluorescence spectrum (Fig. 2) exhibited intense optical transition at 646 nm under laser diode excitation.

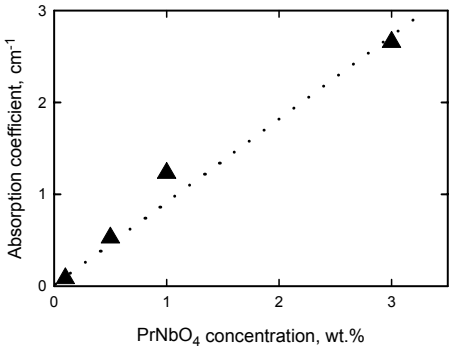

Fig. 1. Absorption of $SrMoO_4:Pr^{3+}$ crystals at 449 nm.

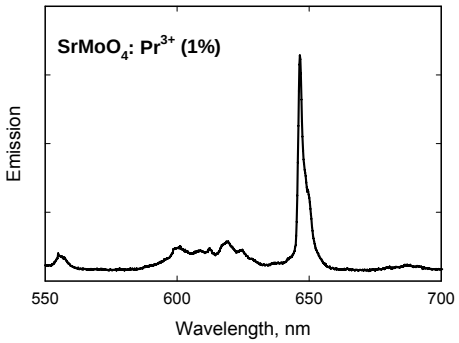

Fig. 2. Emission spectrum of $SrMoO_4:Pr^{3+}$ under laser diode excitation.

The radiation lifetime was measured under excitation with second harmonic of pulsed tunable $LiF:F^{2+}$ color center laser (450 nm). The lifetime was reduced from 1.5 μs to 1.25 μs for $SrMoO_4$:$PrNbO_4$ samples with the increase of $PrNbO_4$ concentration from 0.5 to 3 wt.%. The suitability of this material for simultaneous laser and SRS oscillation will be discussed.

Paper LS-P-7

GENERATION THE LONGITUDINAL COMPONENT OF ELECTRIC FIELD ON THE OPTICAL AXIS USING ASYMMETRIC BINARY AXICONS ILLUMINATED BY LINEARLY AND CIRCULARLY POLARIZED BEAMS

Svetlana N. Khonina

Image Processing Systems Institute of the Russian Academy of Sciences, Samara, 443001, Russia

khonina@smr.ru

The axicon is known to generate a zero-order Bessel beam with the central spot size for intensity FWHM = 0.36λ/NA [1–4], which is 37% smaller than the Airy disk produced with a similar numerical aperture (NA) lens. However, that results have been obtained for the radially polarized incident beams. Although a great number of intra- and extra-cavity schemes have been proposed for generating radially polarized beams, all of them either make the optical setup rather sophisticated or require costly devices.

If the incident beam is linearly polarized (as in most lasers), a decrease in the focal spot size is hindered by the contribution of the strong longitudinal component of electric field which energy is concentrated in the side lobes. A linearly polarized laser beam can rather easily be transformed into a circularly polarized beam, which retains a circular symmetry even when being sharply focused. The resulting focal spot is also widened owing to a ring contribution of the longitudinal component.

It is possible to redistribute the longitudinal component into the central part of the focal spot using incident beams with a linear or vortex phase singularity [5, 6]. A similar result can be obtained with use of a bi-axicon and spiral binary axicon [7].

An analytical and numerical study of the diffraction of linearly and circularly polarized laser beams by three types of binary diffractive axicons (axisymmetric, spiral and bi-axicon) is performed. The numerical simulation was based on the plane wave expansion method with regard for the Fresnel transmission coefficients and the finite-difference time-domain method.

Generation of on-axis light spot with considerable longitudinal component is significant for applications such as microscopy, high-resolution metrology, electron acceleration, and material processing.

References:

1. V.P. Kalosha, I. Golub, “Toward the subdiffraction focusing limit of optical superresolution” Opt. Lett., Vol. 32, pp. 3540–3542 (2007).
2. T. Grosjean, D. Courjon, “Smallest focal spots” Opt. Comm., Vol. 272, pp. 314–319 (2007).
3. V.V. Kotlyar, A.A. Kovalev, S.S. Stafeev, “Sharp focus area of radially-polarized Gaussian beam propagation through an axicon” Progress In Electromagnetic Research C, Vol. 5, pp. 35–43 (2008).
4. S.N. Khonina, N.L. Kazanskiy, A.V. Ustinov, S.G. Volotovskiy, “The lensacon: Nonparaxial effects” J. Opt. Technol., Vol. 78 (11), pp. 724–729 (2011).
5. S.N. Khonina, S.G. Volotovsky, “Controlling the contribution of the electric field components to the focus of a high-aperture lens using binary phase structures” J. Opt. Soc. Am. A, Vol.27, No.10, pp. 2188–2197 (2010).
6. S.N. Khonina, “Simple phase optical elements for narrowing of a focal spot in high-numerical-aperture conditions” Optical Engineering, Vol. 52(9), 091711-7pp (2013).
7. S.N. Khonina, D.V. Nesterenko, A.A. Morozov, R.V. Skidanov, V.A. Soifer, “Narrowing of a light spot at diffraction of linearly-polarized beam on binary asymmetric axicons” Optical Memory and Neural Networks (Information Optics), Vol. 21(1), pp. 17–26 (2012).

Paper LS-P-8

LUMINESCENT PROPERTIES OF LANTHANUM–GALLIUM TANTALATE CRYSTALS

N.S. Kozlova[1], I.S. Didenko[1], A.P.Kozlova[1], N.A. Siminel[1], A.V. Siminel[2]

[1]*National University of Science and Technology "MISIS", Leninskiy prospekt 4, Moscow, Russia*
[2]*Institute of Applied Physics of the Academy of Sciences of Moldova, Chisinau, Republic of Moldova*

Lanthanum – gallium tantalate crystals $La_3Ta_{0.5}Ga_{5.5}O_{14}$ (langatate, LGT) are regarded as a perspective laser material. However, due to the lack of optical quality of LGT crystals such application hasn't been developed, therefore the luminescent properties of these crystals are slightly investigated. At the present time significant improvement of crystal quality opens an ability to use LGT crystals for lasers.

Thereby the main purpose of this paper is the complex investigation of the influence of single crystal obtaining conditions (the growth atmosphere) on luminescent properties of LGT crystals.

In this study, we performed experiments with langatate crystals produced by the company Fomos-Materials. The space group of symmetry is P321.The crystals were grown by the Czochralski method in iridium crucibles in an Ar atmosphere and in a mixture of argon and oxygen (Ar +(2%) O_2) and (Ar +(~0.5%) O_2). Polar cut samples were used. All samples were investigated with methods of optical spectroscopy, diffuse reflection spectroscopy, optical microscopy, atomic force microscopy, X-ray photoelectron spectroscopy [1].

The first obtained luminescence of langatate single crystals are investigated. The luminescence was excited with third harmonic of YAG:Nd^{3+} laser with energy of 2 mJ.

Wide emission spectra were observed with a maximum at ~450 nm. Registered lifetimes of the luminescence on different wavelengths are up 5 to 8 ms. Occurrence of individual peaks at 3.1 and 2.9 eV are probably connected with formation of oxygen vacancies at different sites of lattice.

Decrease of oxygen concentration in the growth atmosphere of crystals leads to the considerable changing of their optical and luminescent characteristics. Crystals grown in an Ar atmosphere are almost colorless, while those grown in an (Ar + O_2) atmosphere are of bright orange color [2]. The luminescent intensity decreases with increasing of oxygen concentration in the growth atmosphere. It indicates the activization of oxygen centres formation.

References:

1. O.A. Buzanov, I.S. Didenko, N.S. Kozlova, A.P. Kozlova, E.A. Skrylyova, N.A. Siminel. "The influence of isothermal annealing on optic parameters of lanthanum–gallium tantalate crystals" Izvestiya Vysshih Uchebnyh Zavedeniy. Materialy Elektronnoi Tekhniki (Materials of Electronic Technics), № 1, pp. 22–25 (2012) [in Russian].
2. O.A. Buzanov, E.V. Zabelina, N.S. Kozlova, "Optical properties of lanthanum–gallium tantalate at different growth and post-growth treatment conditions" Crystallography Reports, Vol. 52, № 4, pp. 691–696 (2007).

Paper LS-P-9

ZrO_2–Y_2O_3–Tm_2O_3 AND ZrO_2–Y_2O_3–Ho_2O_3 CRYSTALS AS ACTIVE MEDIUM FOR LASERS OF TWO-MICRON SPECTRAL REGION

M.A. Borik[1], A.V. Kulebyakin[1], E.E. Lomonova[1], P.A. Ryabochkina[2], S.N. Ushakov[1], A.N. Chabushkin[2]

[1]*A.M. Prokhorov General Physics Institute of the Russian Academy of Sciences, Moscow, Russia*
[2]*N.P. Ogarev Mordovian State University, Saransk, Russia*

kulebyakin@lst.gpi.ru
ryabochkina@freemail.mrsu.ru

Yttrium-stabilized zirconia crystals activated with rare earth ions have a disordered structure. The absorption and luminescence spectra of rare-earth ions in the crystals are inhomogeneously broadened. The wide luminescence bands of rare-earth ions in these crystals provide potential possibility of receiving on their basis of the tunable lasing and realization of a mode-locking regime.

In this paper results of studying of the spectral-luminescence characteristics of yttriumstabilized zirconia crystals activated with Tm^{3+} and Ho^{3+} ions are presented. The crystals were grown by directional crystallization technique with direct RF-heating in the cold container (skull melting).

Lasing at the $^3F_4 \rightarrow {}^3H_6$ transition of Tm^{3+} ions in diode-pumped ZrO_2 — 12 mol% Y_2O_3 — 2 mol% Tm_2O_3 crystals is obtained for the first time (Fig. 1). The lasing wavelength is 2046 nm.

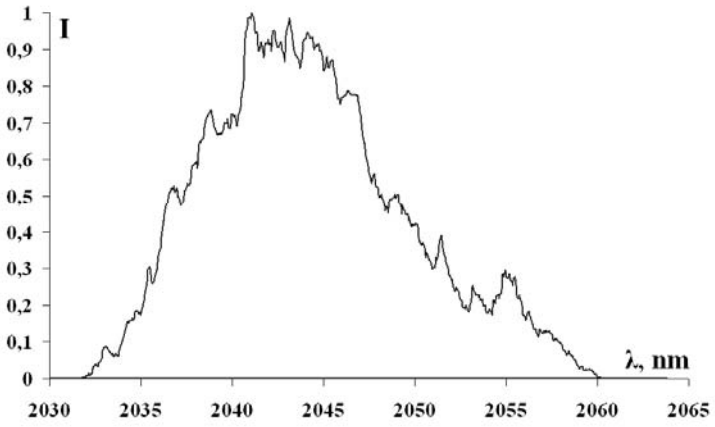

Fig. 1. Lasing spectra of Tm^{3+} ions for the $^3F_4 \rightarrow {}^3H_6$ transition in ZrO_2 — 12 mol% Y_2O_3 — 2 mol% Tm_2O_3 crystals at T = 300 K

The spectral dependence of the gain cross section for the $^5I_7 \rightarrow {}^5I_8$ laser transition of Ho^{3+} ions in ZrO_2 — 13.6 mol% Y_2O_3 — 0.4 mol% Ho_2O_3 crystals shows that the gain range for the transition of Ho^{3+} ions in ZrO_2–Y_2O_3–Ho_2O_3 crystals corresponds to the wavelength range of 2120–2350 nm.

Acknowledgements: The work was supported by the federal targeted program "Scientific and Pedagogical Personnel of Innovative Russia (2009–2013)", state contract no. 14.740.11.0071.

Paper LS-P-10

MOLYBDATE CRYSTALS AS HOST FOR DOWNCONVERSION MATERIALS

D.A. Lis[1], K.A. Subbotin[1], E.V. Zharikov[1,2], O.B. Petrova[2], I.V. Stepanova[2]

[1]*A.M. Prokhorov General Physics Institute of the Russian Academy of Sciences, Vavilov Str. 38, 119991 Moscow, Russia*

[2]*D.I. Mendeleyev University of Chemical Technology of Russia, Miusskaya sq. 9, 125047 Moscow, Russia*

lisdenis@lsk.gpi.ru

Photovoltaic cells are an important source of "green" and renewable energy and attract attention of researchers all over the world. Currently, their wide commercial application is limited due to its relatively low efficiency. The average efficiency of industrial silicon solar cells is now less, than 20%. The energy gap in Si solar cells is approximately 1.12 eV, which is equivalent to the photon with a wavelength of 1.1 μm. Thus, the significant part of the solar energy absorption is spent on the thermalization of charge carriers, generated by the absorption of high-energy photons. If we could able to split one high-energy photon with energy higher than 2.24 eV (wavelength less, than 550 nm) on two low-energy photons (down-conversion, DC), the efficiency of the solar cell will significantly be increased. Another additional way is to use the up-conversion mechanism to employ the infrared part (wavelength more than 1.1 μm) of the spectrum. It is shown, that the use in the solar cell unit the up- and downconversion materials can increase its efficiency to 50%.

So, the materials, which convert the high-energy part of the solar spectrum into the near-infrared (NIR) wavelength region attract attention due to its potential application in solar energy industry. Rare earth ions with abundant energy levels are being actively studied as good candidates for DC materials. As such DC materials recently studied the systems of RE–Yb^{3+} (RE = Tm^{3+}, Ce^{3+}, Pr^{3+}, Tb^{3+}, Eu^{2+}), where the energy of the excitation is transferred from sensitizer ion to Yb ion. Another way is the using of self-sensitizing material, e.g. molybdates that have strong absorption in UV region and could transfer the excitation energy from the host-lattice to the Yb ions. The strong absorption band in UV region is due to excitation from the filled oxygen 2p levels in the valence band to empty Mo 4d levels of the conduction band.

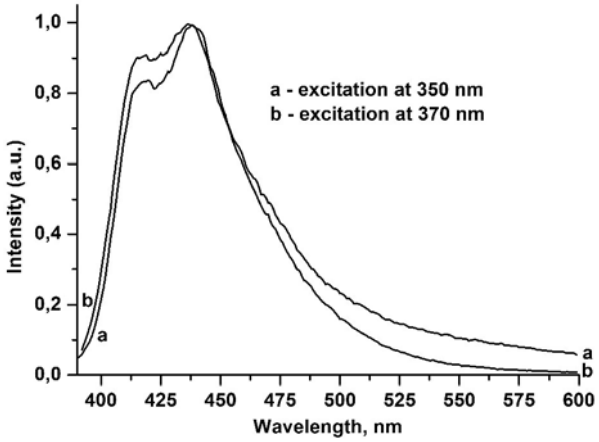

Fig. 1. Normalized fluorescence spectra of NGM crystal.

This paper presents the first results of our research of $NaGd(MoO_4)_2$ crystal as a material for down-conversion. The fluorescence spectra are shown in Fig. 1. Under the excitation of UV light, a broad emission centered at 435 nm was observed.

To show the energy transfer from molybdate to Yb^{3+} ions, the concentration series of single crystals of disordered double sodium gadolinium molybdate $NaGd(MoO_4)_2$ (NGM) doped with Yb ions (0.5, 3, 20%) was grown and is under investigation now.

Paper LS-P-11

XEROGELS OF INORGANIC FLUORIDE: SYNTHESIS AND STUDY

M.N. Mayakova[1], P.P. Fedorov[1], S.V. Kuznetsov[1], V.V. Voronov[1], K.N. Boldyrev[2], O.V. Karban[3]

[1]*Prokhorov General Physics Institute RAS, Vavilov str. 38, 119991 Moscow, Russia*
[2]*Institute for Spectroscopy RAS, Fizicheskaya str. 5, Moscow, Troitsk 142190, Russia*
[3]*Physical-Technical Institute of the Ural Branch of the RAS, Kirov str. 132, Izhevsk, Udmurt Republic, 426000, Russia*

mn.mayakova@gmail.com

Recently interest in synthesis and study of nanofluorides increased significantly due to specific features of nanodisperse compounds. Luminescence properties of nanopowders change in comparison with parameters of bulk materials because of an interaction between radiation and surface layer of nanoparticles. This enables designing a new generation of luminescent materials and scintillators. Fluoride nanopowders with complex compositions are used for different biomedical applications. Nanopowders also can be used as precursors for preparation of laser ceramics and single crystals.

In this work, unique monolithic optically transparent fluoride xerogels with rare earth elements were obtained using aqueous solutions technique. Morphology and characteristics of these samples were studied. It was found that they consist of agglomerated nanoparticles and water solutions.

Our investigations by SEM, AFM, and TEM has shown that the obtained transparent xerogels have a hierarchical structural organization. Primary nanoparticles have a size 20–30 nm, and they agglomerate into bigger particles of about 100 nm witch form so-called “Skeleton” with multiple cavities and channels. The synthesized xerogels are not found in the nature. XRD phase analysis of the samples has revealed submicron heterogeneous system containing solid crystalline phase and adsorbed hydrate layer which stabilize the overall structure. Optical transparency of these samples gives a possibility to build a new type of optical materials.

Infrared transmittance spectra with heating the sample were measured in the temperature range 25–460°C using a vacuum sample chamber. Detailed temperature dependence of the transmission spectra demonstrated a decrease of intense water bands at 275–350°C. A further heating up to 425°C and, then, a cooling down to 20 °C in a vacuum chamber did not markedly change the spectra. However, after a brief contact with atmosphere, the sample rapidly absorbs the atmospheric water vapors, and in 20 minutes, as is evident from the spectra, it received about one third of the water lost during the heating. This result may indicate decisive role of water in the structure of the investigated object.

Acknowledgements: authors thanks R.P. Ermakov, A.E. Baranchikov, O.V. Uvarov for their help in carrying out the work.

Paper LS-P-12

COMPACT CONTINUOUS-WAVE INTRACAVITY OPTICAL PARAMETRIC OSCILLATOR PUMPED BY A VERTICAL EXTERNAL CAVITY SURFACE-EMITTING LASER

M.Yu. Morozov, Yu.A. Morozov

Kotelnikov Institute of RadioEngineering & Electronics (Saratov Branch), Russ. Acad. Sci., 38 Zeleonaya str., Saratov, Russia

mikkym@mail.ru

Continuous-wave optical parametric oscillators (OPOs) being of narrow linewidth and widely tunable devices are almost ideally suitable for high-resolution spectroscopic applications in near- and mid-infrared ranges [1]. The principle of OPO's operation is based on dividing the energy of photon of highest energy (the pump) into two lower energy photons (denoted the signal and idler). Such a frequency down-conversion appears as one, two or all three involved optical fields are resonant and threshold of a parametric interaction is reached. Now, the sing-ly-resonant OPOs (SROs) with one wave resonating (most usually, the signal wave) have only found a widespread implementation. The SROs, however, require tens-of-watt pumping lasers in order to overcome the threshold. One of the routes to diminish the threshold is to place an SRO within a high-finesse cavity of a pumping laser. In particular, such the intracavity SRO (ICSRO) was demonstrated with a neodymium laser (Nd:YAG) [2]. Unfortunately, ICSROs pumped by neodymium lasers appear to show pronounced relaxation oscillations of output wave intensity. To eliminate this disadvantage the pumping of the ICSRO by a semiconductor vertical external cavity surface-emitting laser (VECSEL) has been proposed recently [3].

We propose and analyze a novel type of a compact ICSRO pumped by a VECSEL. Unlike to the ICSRO presented in [3], we have usage of the common cavity both for the pumping laser and the signal down-converted wave. When doing so we suppose that the normalized differ-ence between the pump and the signal wavelengths doesn't exceed about ten percents. Be-sides, frequency selective elements, e.g. Fabry–Perot etalons or birefringent tuners have been removed from the cavity, thus taking advantage of maximal compactness and simplicity of the construction. The total length of our ICSRO's plano-concave cavity with a nonlinear crystal of quasi-phase-matched GaAs inserted is just about 10 mm. According to the findings of A. Garnache et al. [4], a VECSEL itself shows single-frequency operation without intracavity eta-lons provided the cavity is quite short (about 10–20 mm). These observations allows us to ex-pect a single-mode operation of the proposed ICSRO.

The detailed description of the ICSRO and the results of numerical analysis will be presented.

Acknowledgements: This study was supported by RFBR grant No.12-02-31888-mol_a.

References:

1. F. Tittel, D. Richter, A. Fried, "Mid-infrared laser applications in spectroscopy", in Solid-state mid-infrared laser sources. Eds. T. Sorokina, K. L. Vodopyanov, Springer-Verlag, Berlin–Heidelberg (2003).
2. D. Stothard, M. Ebrahimzadeh, M. Dunn, "Low pump threshold, continuous-wave, singly resonant, optical parametric oscillator" Opt. Lett., Vol. 23, pp. 1895–1897 (1998).
3. D. Stothard, J. Hopkins, D. Burns, M. Dunn, "Stable, continuous-wave, intracavity, opical parametric oscillator pumped by a semiconductor disk laser (VECSEL)", Opt. Express, Vol. 17, pp. 10648–10658 (2009).
4. A. Garnache, A. Ouvrard, D. Romanini, "Single-frequency operation of external-cavity VCSELs: non-linear multimode temporal dynamics and quantum limit" Opt. Express, Vol. 15, pp. 9403–9417 (2007).

Paper LS-P-13

LEAD-BARIUM FLUOROBORATE GLASSES AND TRANSPARENT GLASS-CERAMICS DOPED WITH Nd^{3+} OR Er^{3+}

O.B. Petrova[1], T.S. Sevostjanova[1], D.A.Lis[2], A.V. Khomyakov[1]

[1]*D. Mendeleyev University of Chemical Technology of Russia*
[2]*Prokhorov General Physics Institute, Russian Academy of Sciences*

petrova@proriv.ru

Oxyfluoride glass-ceramics is widely researched as host materials for active optical ions because they not only have comparatively low phonon energies which corresponding to fluoride crystals, but also high chemical and mechanical stabilities related to oxide glasses. By heat-treatment made closely to the crystallization temperature of oxyfluoride glasses, oxyfluoride glass-ceramics can be obtained, in which fluoride crystallites are dispersed in the oxide glass matrix. In lead fluoroborate and barium fluoroborate systems it's possible to get glasses doping by RE [1–4]. Heat treatment of glasses in PbF_2–PbO–B_2O_3 system results to separation of two crystalline phases: orthorhombic α-PbF_2 and cubic β-PbF_2. β-PbF_2 phase can effectively included RE [2, 3]. In BaF_2–BaO–B_2O_3 glasses there is separation of only one crystalline phase: cubic BaF_2, but it does not include RE^{3+} [4].

In this work, we have synthesized combined lead-barium fluoroborate glasses doped with 1 mol. % of RE (RE = Nd^{3+} or Er^{3+}) and have studied their properties and the possibility of modifying the glasses by heat treatment at the temperatures above the glass transition (T_g) as well as the possibility of using these glasses as the matrix for glass ceramic material contained cubic fluoride crystal phases. Such materials are perspective for using at laser optics.

Glasses in system PbF_2 (BaF_2) – BaO (PbO) – B_2O_3 with different ratio of components ($25PbF_2$–$25BaO$–$50B_2O_3$, $25BaF_2$–$25PbO$–$50B_2O_3$, $20PbF_2$–$30BaO$–$50B_2O_3$, $30BaF_2$–$20PbO$–$50B_2O_3$) doped with NdF_3 or ErF_3 were synthesized at 850–900°C for 1 hour in corundum crucibles. The glasses were prepared with casting. We investigated the influence of the source of fluorine (BaF_2 or PbF_2) on properties of glasses and crystallization. Glass transition temperatures, density, refractive index, microhardness, the limit of elasticity glasses were measured.

According to the XRD analysis heat treatment leads to mixed fluoride $Pb_xBa_{1-x}F_2$-phase crystallization, but when the fluorine is doped into glass as BaF_2 – x = 0.02–0.04, and as PbF_2 – x = 0.4–0.5. According to the luminescence spectra, Nd^{3+} is effectively included in the crystalline phase.

References:

1. G. Dantelle, M. Mortier, G. Patriarche, D. Vivien, "Er^{3+}-doped PbF_2: Comparison between nanocrystals in glass-ceramics and bulk single crystals" J. Sol. St. Chem., Vol. 179, pp. 1995–2003 (2006).
2. W.A. Pisarski, T. Goryczka, J. Pisarska, W. Ryba-Romanowski, "Er-doped lead borate glasses and transparent glass ceramics for near-infrared luminescence and up-conversion applications" J. Phys. Chem. B, Vol. 111, pp. 2415–2757 (2007).
3. O.B. Petrova, A.V. Popov, V.E. Shukshin Y.K. Voron'ko, "Activated by ions Nd^{3+} lead fluoroborate glass and transparent glass-crystalline materials based on them" Opt. Jour., Vol. 78, pp. 30–35 (2011).
4. K. Biswas, A.D. Sontakke, R. Sen, K. Annapurna, "Luminescence properties of dual valence Eu doped nano-crystalline BaF_2 embedded glass-ceramics and observation of $Eu^{2+} \rightarrow Eu^{3+}$ energy transfer" J. Fluoresc., Vol. 22, pp. 745–752 (2012).

Paper LS-P-14

COMPOSITE LASER FIBER WITH Yb, Er CO-DOPED PHOSPHATE GLASS CORE AND SILICA CLADDING

Ya.E. Sadovnikova[1], B.I. Denker[1], B.I. Galagan[1], V.A. Kamynin[1], A.S. Kurkov[1], S.L. Semenov[2], S.E. Sverchkov[1], V.V. Velmiskin[2], E.M. Dianov[2]

[1]A.M. Prokhorov General Physics Institute of RAS, Vavilov str. 38, Moscow 119991, Russia
[2]Fiber Optics Research Center of RAS, Vavilov str. 38, Moscow 119333, Russia

snegovij@pochta.ru

The standard silica-based Er, Yb co-doped fiber amplifiers (EDFAs) have doping level limitations and thus limited gain per unit length. On the contrary phosphate glass can contain high concentrations of lanthanide ions. It is also a unique laser host that provides high efficiency of energy transfer from Yb ions to the upper laser level of Er ions and efficient lasing at ~1.5 μm under pumping into Yb absorption band. This paper describes laser action in a multimode fiber with neodymium-doped phosphate glass core and silica cladding. The fiber perform was made by melting the components of the phosphate glass in a silica tube.

In the present investigation the fiber fabrication process was started not from raw chemicals but from the well-dehydrated Yb–Er laser glass. To minimize the inevitable mechanical stress between the phosphate and silica components in the fiber perform and the fiber itself we have chosen for the composite fiber the glass SELG Yb–Er laser glass with the lowest available room-temperature thermal expansion 7.2×10^{-6} K^{-1}.

To pump Er–Yb doped fiber we applied Yb-doped fiber laser emitting at 1064 nm with the maximum power of 4 W. As one could see, output fiber of 1064 nm source was spliced with high-reflective fiber Bragg grating, and then the grating was spliced with Er–Yb fiber. It should be noted that this Bragg grating was written on SMF fiber with 9 um core diameter that corresponds to core diameter of the Er–Yb fiber. So splice losses at the last case were about 3 dB. Cavity of the Er–Yb laser was closed by the high- reflective Bragg grating with the resonance wavelength that 1535 nm and cleaved output end. The length of Er–Yb fiber in the cavity was of 0.9 m.

One can see that the oscillation wavelength is of 1535 nm that corresponds to the resonance wavelength of the Bragg grating. The maximum of output power of 130 mW was measured. Efficiency slope can be estimated as 4%. Relatively small value of the efficiency can be explained by the high background losses and losses on splice connection. To increase the lasing efficiency a length of the cavity should be shorten. That can be achieved due to the active ions concentration increasing and/or due to optimization of the pumping wavelength.

For the first time an optical fiber with Yb, Er co-doped phosphate glass core in a silica cladding was fabricated and tested. 1.54 μm laser action was demonstrated under 1.06 μm pumping into Yb absorption band.

References:

1. M. Lange, E. Bryant, M. Myers, J. Myers, R. Wu, C. Hardy, “High Gain Short Length Phosphate Glass Erbium-Doped Fiber Amplifier Material”, OSA , Optical Fiber Communications Conference Proceedings, March, pp.17-22 (2001).
2. I.A. Bufetov, S.L. Semjonov, A.F. Kosolapov, M.A. Mel’kumov, V.V. Dudin, B.I. Galagan, B.I. Denker, V.V. Osiko, S.E. Sverchkov, E.M. Dianov, “Ytterbium fibre laser with a heavily Yb^{3+}-doped glass fibre core” Quantum Electronics, Vol. 36(3), pp. 198–191 (2006).
3. B. Denker, B. Galagan, V. Osiko, S. Sverchkov, “Peculiarities of energy storage and relaxation in Yb–Er glasses with enhanced Er content”, Advanced Solid State Lasers’2001 Technical Digest, pp. 389–394 (2001).

Paper LS-P-15

TUNABLE TWO-FREQUENCY σ-POLARIZED ND:YVO_4–YVO_4 LASER

S.P. Sadovskiy, A.A. Sirotkin, S.V. Garnov

A.M. Prokhorov General Physics Institute, Russian Academy of Sciences,
Vavilova str. 38, Moscow 119991, Russia

spsadovskiy@gmail.com

The two-frequency nanosecond and picoseconds laser pulses can be efficiently converted in terahertz emitters and nonlinear optical crystals [1-3]. The general aim of our research is to obtain two-frequency emission with ps-pulse duration on vanadate crystal under longitudinal diode pump. The scheme of laser setup to demonstrate the capabilities of laser double-wavelength tuning is shown in Fig. 1. As active laser elements, we used the a-cut composite Nd:YVO_4–YVO_4. As a selecting element, we used an intracavity Fabry–Perot cavity standard [4] made of a YAG crystal in the form of a plane-parallel plates about 80, 97, 130, 270 μm thick. In this work, we proposed and realized a promising method of wavelength tuning for the a-cut (σ-polarization) YVO_4: Nd:YVO_4 crystal. Realized restructuring difference wavelengths in the range of 1.2 to 4.4 nm. Fig. 2 shows the output spectrum of the laser radiation at entry to the cavity FP standards in continuous generation. A stable two-frequency lasing at the $^4F_{3/2}$–$^4I_{11/2}$ transition of the neodymium ion in YVO_4:Nd:YVO_4 crystals is obtained in the cw regime, acousto-optic Q-switched regime, active acousto-optic mode-locked regime.

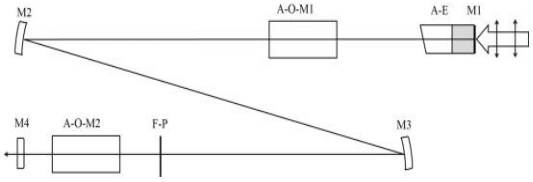

Fig. 1. Scheme of the laser. M1- mirror deposited on the A-E, A-E – active element, A-O-M1,2 – acousto-optic modulators, M2,3 – spherical mirrors=340mm, F–P – Fabry–Perot cavity standard, M4 – output mirror.

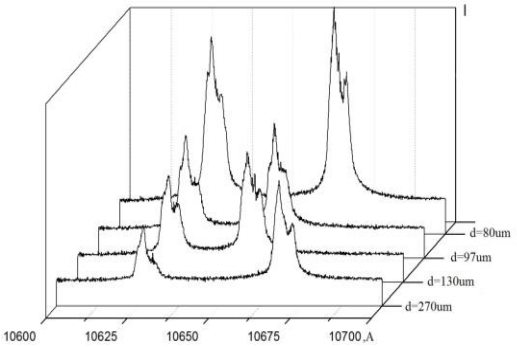

Fig. 2. Dual-frequency spectrum of the radiation Nd: YVO_4-YVO_4-laser FP thickness 80, 97, 130, and 290 um, respectively.

References:

1. U. Willer, R. Wilk, W. Schippers, S. Bottger, D. Nodop, T. Schossig, W. Schade, M. Mikulics, M. Koch, M. Walther, H. Niemann, B.G. Uttler, "A novel THz source based on a two-color Nd:LSB microchip-laser and a LT-GaAsSb photomixer" Appl. Phys. B, Vol. 87, p. 13 (2007).
2. P. Zhao, S. Ragam, Y.J. Ding, I.B. Zotova, "Compact and portable terahertz source by mixing two frequencies generated simultaneously by a single solid-state laser" Optics Letters, Vol. 35, p. 23 (2010).
3. A. Sato, K. Imai, K. Kawase, H. Minamide, S. Wada, H. Ito, "Narrow-linewidth operation of a compact THz-wave parametric generator system" Optics Communications, Vol. 207, p. 353 (2002).
4. V.I. Vlasov, S.V. Garnov, Yu.D. Zavartsev, A.I. Zagumennyi, S.A. Kutovoi, A.A. Sirotkin, I.A. Shcherbakov, "New possibilities of neodymium-doped vanadate crystals as active media for diode-pumped lasers" Quantum Electronics, Vol. 37, p. 938 (2007).

Paper LS-P-16

THE HIGH PEAK POWER PASSIVELY Q-SWITCHED YVO_4–Nd^{3+}:YVO_4 LASERS FOR MEDICINE APPLICATIONS

A.A. Sirotkin

Prokhorov General Physics Institute of the Russian Academy of Sciences,
Vavilov 38, Moscow 119991, Russia
Advanced Energy Technologies LTD 107045, Sretensky bul 7/1/8, Moscow, Russia

saa@kapella.gpi.ru

We present UV laser sources for medicine application based on a novel methods control of spectral parameters in diode-pumped vanadate lasers.

We have investigate polarization and angular dependences of the luminescence intensity of Stark transitions in of Nd:YVO_4, Nd:$GdVO_4$ and mixed Nd:$Y_xGd_{1-x}VO_4$, Nd:$Y_xSc_{1-x}VO_4$ vanadate crystals. The frequency shift and redistribution of the luminescence intensity of Stark transitions are observed.

It is known, that too large emission cross-section of with *a*-cut π-polarized vanadate crystals is a shortcoming for Q-switched lasers, because it limits their energy-storage capacity, leading to smaller pulse energies. Usual methods to avoid this drawback are to use *c*-cut vanadat crystals [1], mixed vanadates Nd:$Gd_xY_{1-x}VO_4$ [2] or *a*-cut (σ-polarization) vanadat crystals [3, 4]. However wavelengths of *c*-cut and *a*-cut σ-polarized vanadate crystals distinct from *a*-cut π-polarized emission. In addition *c*-cut vanadate crystals have nonpolarised radiation.

Using angular dependences of the luminescence intensity of Stark transitions in vanadate crystals we can to create active media with different coefficients of gain and wavelengths.

Variable-cut composite YVO_4–Nd^{3+}:YVO_4 ($\theta = 25°$, $\varphi = 0$) crystal have stimulated emission cross-section value are comparable to one *c*-cut or *a*-cut (σ-polarization) vanadate crystals. It has the polarized radiation, Moreover wavelength of radiation coincide with *a*-cut π-polarized emission. It allows creating effective master oscillator-amplifier systems.

Laser operation under different angles of cut were investigated for composite YVO_4–Nd^{3+}:YVO_4. Cr^{4+}:YAG saturable absorber with initial transmission 65% and 80% oriented with their normal along the (111)-crystal axis, were used as the passive Q switch.

We have shown experimentally that the variable-cut ($\theta = 25°$, $\varphi = 0$) YVO_4–Nd^{3+}:YVO_4-laser could have good passively Q-switched performance, which gives the narrowest pulse of 2.5 ns with the highest peak power of 13 kW.

The average power of visible and UV radiation up to 210 and 9 mW has been obtained in the case of extracavity conversion of the laser radiation in crystals PPLN and BBO, respectively.

We have demonstrated a low-cost, compact, high-efficiency passively Q-switched UV-VIS-IR laser medicine systems based on the variable-cut YVO_4–Nd_3:YVO_4-laser with Cr^{4+}:YAG saturable absorber crystal.

References:

1. Y.F. Chen, Y.P. Lan, “Comparison between c-cut and a-cut Nd:YVO4 lasers passively Q-switched with a Cr^{4+}:YAG saturable absorber” Appl. Phys. B, Vol. 74, p. 415 (2002).
2. J. Liu, Zh. Wang, X. Meng, Z. Shao, B. Ozygus, A. Ding, H. Weber, “Improvement of passive Q-switching performance reached with a new Nd-doped mixed vanadate crystal Nd:$Gd_{0.64}Y_{0.36}VO_4$” Opt. Lett., Vol. 28, p. 2330 (2003).
3. A. Agnesi, S. Dell’acqua, “High-peak-power diode-pumped passively *Q*-switched Nd:YVO_4 laser” Appl. Phys. B, Vol. 76, pp. 351–354 (2003).
4. A.A. Sirotkin, V.I. Vlasov, A.I. Zagumennyi, Yu.D. Zavartsev, S.A. Kutovoi, “Vanadate lasers with σ-polarised radiation” Quantum Electronics, Vol. 41(7), p. 584 (2011).

Paper LS-P-17

INVESTIGATION OF LASER OSCILLATION SPECTRA IN THE F_2^-:LiF CRYSTAL AT LOW TEMPERATURE

A.G. Papashvili, S.N. Smetanin, V.A. Konyushkin, M.E. Doroshenko

Research Center for Laser Materials and Technologies of Prokhorov General Physics, Institute of the Russian Academy of Sciences, 38 Vavilov Str., 119991, Moscow, Russia

E-mail: ssmetanin@bk.ru

The F_2^-:LiF lasers are efficient and reliable sources of tunable laser radiation in near IR spectral region (1.08–1.29 μm) [1-2]. Advantageous spectral position of absorption line allows to use commercially available ytterbium and neodymium solid-state and diode lasers as a pump source in order to get the F_2^-:LiF laser oscillation with an efficiency of up to 39% [1]. In [3] the F_2^-:LiF crystals was used as the effective laser amplifiers of picosecond pulses of the self-Raman Nd^{3+}:$KGd(WO_4)_2$ laser Stokes radiation with an output power of up to 10^{10} W and an energy of up to 30 mJ. In [4] the F_2^-:LiF crystals was used not only for passive Qswitch of the diode-pumped self-Raman Nd^{3+}:$SrMoO_4$ laser, but also as the laser amplifier of subnanosecond pulses of this self-Raman laser Stokes radiation. In [5] the spectral and lasing properties of F_2^- colour centers in new nanostructure LiF ceramics are studied and compared with those for single crystal samples at room temperature.

In this work, the laser oscillation spectra in the F_2^-:LiF crystal at various low temperatures and pumping levels are studied. The anomalous differences between the laser oscillation spectra and the luminescence spectra at 77 K are experimentally discovered. It is caused by influence of more that one phonon frequencies of the F_2^-:LiF crystal to the laser oscillation spectra formation. The mathematical model of multifrequency laser oscillation kinetics taking into account two phonons with frequencies of 250 and 270 cm^{-1} is proposed. The modeling results have an agreement with the experimental results and also provide insight into lasing and vibrational properties of the F_2^- colour centers in LiF crystals and ceramics.

References:

1. T.T. Basiev, P.G. Zverev, A.G. Papashvili, V.V. Fedorov, "Temporal and spectral characteristics of a tunable LiF: F_2^- colour-centre crystal laser" Quantum Electron., Vol. 27, pp. 574–578 (1997).
2. T.T. Basiev, S.V. Vassiliev, V.A. Konjushkin, V.P. Gapontsev, "Pulsed and cw laser oscillations in LiF: F_2^- color center crystal under laser diode pumping" Opt. Lett., Vol. 31, pp. 2154–2156 (2006).
3. T.T. Basiev, S.V. Garnov, V.I. Vovchenko, A.Ya. Karasik, S.M. Klimentov, V.A. Konyushkin, S.B. Kravtsov, A.A. Malyutin, A.G. Papashvili, P.A. Pivovarov, D.S. Chunaev, "Direct amplification of picosecond pulses in F_2^-:LiF crystals" Quantum Electron., Vol. 36, pp. 609–611 (2006).
4. T.T. Basiev, S.N. Smetanin, A.V. Fedin, A.S. Shurygin, "Intracavity SRS conversion in diode-pumped multifunctional Nd^{3+}:$SrMoO_4$ laser crystal" Quantum Electron., Vol. 40, pp. 704–709 (2010).
5. T.T. Basiev, M.E. Doroshenko, V.A. Konyushkin, V.V. Osiko, L.I. Ivanov, S.V. Simakov, "Lasing in diode-pumped fluoride nanostructure F_2^-:LiF colour centre ceramics" Quantum Electron., Vol. 37, pp. 989–990 (2007).

Paper LS-P-18

ENCHANCEMENT OF ACTIVE IONS CONCENTRATION IN Cr:Mg_2SiO_4 LASER CRYSTALS BY THE PROLONGED OXIDIZING ANNEALING

O.N. Zaytseva[1], K.A. Subbotin[1], D.A. Lis[1], A.A. Ivanov[2], E.V. Zharikov[1]

[1]A.M. Prokhorov General Physics Institute of the Russian Academy of Sciences, Vavilov str. 38, 119991 Moscow, Russia
[2]Photochemistry center of the Russian Academy of Sciences, Novatorov str. 7A, b. 1, 119421 Moscow, Russia

ozaytceva@mail.ru

Finding the ways to control the concentration of impurity chromium ions with a different valence in forsterite laser crystals is highly important for the wide usage of Cr: forsterite in tunable and femtosecond solid-state lasers emitting in the near infrared range (1.17–1.37 μm). Now it's restrained by the parasitic absorption of Cr^{2+} ions. Earlier, in Refs [1, 2] it was reported that oxidizing annealing can, in principle, reduce the concentration of divalent chromium ions and increase at the same time the content of active tetravalent chromium ions.

The results of our attempts to improve the characteristics of Cr:Mg_2SiO_4 laser crystals by the prolonged oxidizing annealing are presented in this talk. The evolution dynamics of chromium content in different oxidation states during the series of prolonged oxidizing annealings of forsterite single crystals grown in different growth conditions and having the initially different ratios of Cr^{2+}:Cr^{3+}:Cr^{4+} concentrations was studied.

Forsterite single crystals were grown by the Czochralski technique using iridium crucibles on seeds cut along the *a* crystallographic axis (*Pbnm* notation). The pulling and rotation rates were 3 mm/h and 12 rpm, respectively. Chromium concentrations in the melt were 0.13–0.14 wt %. As the growth atmosphere the extra-pure argon or a mixture of argon with oxygen (the oxygen partial pressure 2.2 kPa) were using. The last parameter was controlled in real time using the oxygen analyzer AKPM-01. Samples shaped as cubes ($5\times5\times5$ mm^3) were cut from single crystals and oriented using a DRON-4-13 X-ray diffractometer. The series of annealings of the samples in air was performed at 1573 K during 240 hours each treatment.

Room-temperature polarized absorption spectra were measured before treatment and after each subsequent annealing by a Shimadzu UV-VIS-NIR scanning spectrophotometer. The obtained absorption spectra were approximated by sums of elementary Gaussians corresponding to elementary transitions between spin-orbital components of the ground and excited states of chromium ions in different oxidation states (Cr^{4+}, Cr^{3+} and Cr^{2+}). The spectrum of the sample, in which the elementary band of the particular type is better resolved, had been used to determine the peak position ν_i^c and FWHM w_i for the corresponding Gaussian. Then, using the set of Gaussians with determined in such a way fixed ν_i^c and w_i values, we calculated the Gaussian amplitudes Ai and background levels y0 for each spectrum, which provided the best approximation of the experimental curve.

It was found, that the prolonged oxidizing annealing of Cr:Mg_2SiO_4 crystals leads to the fast decrease of the Cr^{2+} ion concentration and slow monotonic increase of Cr^{4+} ion concentration. The dynamics of both processes were studied and discussed.

References:

1. Y. Yamaguchi, K. Yamagishi, A. Sugimoto, Y. Nobe, OSA Proceedings on Advanced Solid-State Lasers, Vol. 10, pp. 52–56 (1991).
2. W. Chen, G. Boulon, Optical Materials, Vol. 24, pp. 163–168 (2003).

Paper LS-P-19

DEPOSITION OF INHALED DRUGS IN ARTIFICIAL LUNG MEASURED BY MAPPING LASER RAMAN SPECTROSCOPY

M. Veres, A. Nagy, A. Kerekes, D. Oszetszky, S. Tóth, L. Himics, M. Koós, A. Czitrovszky

Insititute for Solid State Physics and Optics, Wigner Research Centre for Physics, Hungarian Academy of Sciences, PO Box 49., H-1525 Budapest, Hungary

veres.miklos@wigner.mta.hu

Study of the characteristics and mechanisms of the deposition of the inhaled drugs in the lung and upper respiratory tracts are of great importance for the efficient delivery of the active agents to the required areas. The deposition is affected by a number of factors, including, but not limited to the size and velocity of the particles, geometry of the airways or the inspiration pattern of the patient. Some *in vivo* [1] and *in vitro* [2] studies were performed on this topic, but the methods used there were of poor resolution, complicated or had effect on the deposition process itself.

In this study the deposition of inhaled drug on the walls of an artificial lung was studied using laser Raman spectroscopy. The lung was prepared by 3D printing from computer tomographic data of a real human lung tract. The inhalation of the drug was performed on breath simulator equipment able to reproduce real human inspiration and respiration patterns. Small pieces of silicon wafer were attached to the inner surface of the different sections of the lung sample. After the inhalation experiments they were removed and measured using a micro-Raman spectrometer. The Raman measurements were performed on a Renishaw 1000 micro-Raman spectrometer attached to a Leica microscope, using the 488 nm line of an Ar ion laser for the excitation. The equipment allowed the characterization of the samples by both optical microscopy and mapping Raman spectroscopy.

Our results showed that Raman spectroscopy is an excellent tool for the characterization of the deposition of the inhaled drugs in different tracts of the respiratory system. It allowed determining and comparing the amounts of the active agent attached to the lung surface at the trachea, primary and secondary bronchi regions.

References:

1. S. Newman, A. Salmon, R. Nave, A. Drollmann, “High lung deposition of 99mTc-labeled ciclesonide administered via HFA-MDI to patients with asthma” Respiratory Medicine, Vol. 100, pp. 375–384 (2006).
2. A.F. Heenan, W.H. Finlay, B. Grgic, A. Pollard, P.K.P. Burnell, “An investigation of the relationship between the flow field and regional deposition in realistic extra-thoracic airways” Journal of Aerosol Science, Vol. 35, **pp.** 1013–1023 (2004).

SECTION PA

Photoacoustics

Paper PA-I-2

TEMPERATURE CONTROLLED RETINAL PHOTOCOAGULATION

R. Brinkmann[1,2], S. Koinzer[3], K. Schlott[1,2], A. Baade[1], J. Roider[3]

[1]*Medical Laser Center Lubeck, Lubeck, Germany*
[2]*Institute of Biomedical Optics, University of Lubeck, Lubeck, Germany*
[3]*Eye Clinic, University Hospital of Schleswig-Holstein, Campus Kiel, Germany*

brinkmann@bmo.uni-luebeck.de

Retinal photocoagulation is a long time established treatment for a variety of retinal diseases, most commonly applied for diabetic macular edema and diabetic retinopathy. The damage extent of the induced thermal coagulations depends on the temperature increase and the time of irradiation. So far, the induced temperature rise is unknown due to intraocular variations in light transmission as well as scattering and RPE/choroidal pigmentation, which can vary interand intraindividually by more than a factor of four. Thus in clinical practice, often stronger and deeper coagulations are applied than therapeutically required, which lead to extended retinal damage and strong pain perception.

In this project, an optoacoustic (OA) method is developed to determine the temperature rise during retinal photocoagulation. The principle of OA and OA temperature determination relies on the short pulsed laser irradiation and heating of an absorber, which subsequently leads to thermoelastic expansion and the emission of a bipolare pressure. The amplitude of the pressure wave $p(t)$ is proportional to the pulse energy E_0 and the material specific Gruneisen Parameter $\Gamma(T)$ according to $P(T) \sim \Gamma(T)E_0$. With proper calibration it can be used to measure the temperature rise during retinal thermal therapies in vivo in realtime [1].

A clinical study comprising 20 patients was conducted in order to determine the temperature rise during photocoagulation. Irradiation is performed with a modified photocoagulation laser (Carl Zeiss Meditec AG, Visulas 532s, $\lambda = 532$ nm). Pressure waves were detected with an acoustic ultrasonic transducer embedded in an ophthalmic contact lens anyway used for treatment.

The clinical data evaluation shows very similar temperature profiles and absolute temperatures for most of the lesions ranging from 60–80°C. The observed temperature slopes are within the range which is expected from heat diffusion theory [2]. However, Arrhenius parameter derived vary significantly from published values for the retina.

In conclusion, it has already been demonstrated on in vivo on rabbits that these data can be processed in real time and be used for an automatic treatment laser switch-off on preselected coagulation strengths, when the appropriate temperature is reached [3].

Acknowledgement: This collaborative project is supported by the German Ministry of Research and Technology (BMBF), Grant # 01EZ0732-35.

References:

1. J. Kandulla, H. Elsner, R. Birngruber, R. Brinkmann, "Noninvasive optoacoustic online retinal temperature determination during continuous-wave laser irradiation" J. Biomed. Opt., Vol. 11(4), 041111 (2006).
2. R. Brinkmann, S. Koinzer, K. Schlott, L. Ptaszynski, M. Bever, A. Baade, S. Luft, Y. Miura, J. Roider, R. Birngruber, "Real-time temperature determination during retinal photocoagulation on patients" J. Biomed. Opt., Vol. 17(6), 061219 (2012).
3. K. Schlott, S. Koinzer, L. Ptaszynski, M. Bever, A. Baade, J. Roider, R. Birngruber, R. Brinkmann, "Automatic temperature controlled retinal photocoagulation" J. Biomed. Opt., Vol. 17(6), 061223 (2012).

Paper PA-I-3

VOLUMETRIC OPTOACOUSTIC IMAGING IN REAL TIME FOR HIGH PERFORMANCE FUNCTIONAL AND MOLECULAR IMAGING

Xosé Luís Deán-Ben[1], Daniel Razansky[1,2]

[1]*Institute for Biological and Medical Imaging (IBMI), Helmholtz Center Munich, Ingolstädter Landstraße 1, 85764 Neuherberg, Germany*
[2]*Faculty of Medicine, Technical University of Munich, Ismaninger Straße 22, 81675 Munich, Germany*

dr@tum.de

Optoacoustic phenomenon is unique in a way it allows to generate complete volumetric tomographic datasets from the imaged object using a single interrogating laser pulse. This possibility does not exist in most other imaging modalities as it is usually necessary to perform sequential excitation of the object from multiple source locations in order to acquire tomographic data required for efficient volumetric image reconstructions. Yet, multiple technical limitations exist for efficient implementation of real-time optoacoustic imaging, such as lack of appropriate ultrasound detection and laser technologies and limitations on the digital sampling and processing capacities. Herein, we developed a handheld optoacoustic imaging system capable of acquiring volumetric optoacoustic data in real time. The system is based on the simultaneous acquisition of 256 optoacoustic signals by means of a transducer array with elements distributed on a spherical surface surrounding the region of interest. Thereby, volumetric reconstructions can be done at high frame rate, limited by the pulse repetition rate of the laser. We further developed accurate model-based algorithm for quantitative optoacoustic image reconstruction in three dimensions [1].

The presented optoacoustic tomography system presents important advantages over other systems that use scanning for attaining volumetric optoacoustic data. Due to scanning, the latter systems usually suffer from relatively long acquisition times, thus volumetric in-vivo images are generally affected by motion artifacts, which effectively reduce the spatial resolution and quantification abilities [2, 3]. Our approach, on the other hand, is capable of acquiring complete volumetric tomographic datasets from the imaged object with a single interrogating laser pulse. Along with the handheld design approach brings important advantages for both small animal imaging as well as clinical studies. First, dynamic processes, such as the biodistribution of molecular probes, can be monitored in the entire volume of interest. Second, out-of-plane and motion artifacts that could degrade the image quality when imaging living specimen can be avoided. Finally, real-time 3D performance can obviously save time required for experimental and clinical observations.

Acknowledgements: The research leading to these results has received funding from the European Union under grant agreement ERC-2010-StG-260991.

References:

1. X.L. Deán-Ben et al., "Accurate model-based inversion algorithm for three-dimensional optoacoustic tomography" IEEE Trans. Med. Imag., Vol. 31, pp. 1922–1928 (2012).
2. M.Á.A. Caballero et al., "Model-based optoacoustic imaging using focused detector scanning" Opt. Lett., Vol. 37, pp. 4080–4082 (2012).
3. D. Razansky et al., "Volumetric real-time multispectral optoacoustic tomography of biomarkers" Nature Prot., Vol. 6(8), pp. 1121–1129 (2011).

Paper PA-I-4

DEEP MEDICAL EPI-OPTOACOUSTIC IMAGING

Martin Frenz, Michael Jaeger, Sara Peeters, Stefan Preisser

Institute of Applied Physics, University of Bern, Sidlerstrasse 5, CH-3012 Bern

frenz@iap.unibe.ch

For versatile medical optoacoustic imaging an epi-illumination and detection technique is preferred to avoid strongly attenuating media such as gas in hollow organs or bones. Unfortunately, such an approach causes severe clutter from strong optoacoustic emissions close to the probe, which limits useful clinical imaging to depths of one centimeter of less when using 7.5 MHz transducer probes. Clutter signals may propagate directly to the acoustic probe (direct clutter), or reach the probe via acoustic scattering from echogenic structures (echo clutter). Several methods for clutter reduction or even clutter elimination had been developed and tested in phantom experiments and in-vivo applications. Deformation compensated averaging, which exploits clutter decorrelation during tissue strain, has achieved signal-to-clutter ratio improvements in clinical epi-optoacoustic imaging of about three, limited by the maximum achievable deformation and the minimum deformation step required for local clutter decorrelation [1–3]. To reach the noise limited depth however much larger gains are needed. A very promising new method uses vibration-induced localized displacements to tag optoacoustic signals at their place of origin, enabling signal identification and, in theory, full clutter cancellation if ideal conditions are met. Such localized transient vibration can be induced, among other potential methods, by means of an acoustic radiation force (ARF) generated by an ultrasonic focused beam. ARF generation using transmit beam forming is already implemented in radiation force ultrasound elastography, where ARF ultrasound transmission over a fraction of a millisecond generates a localised tissue displacement on the order of a few tens of micrometres.

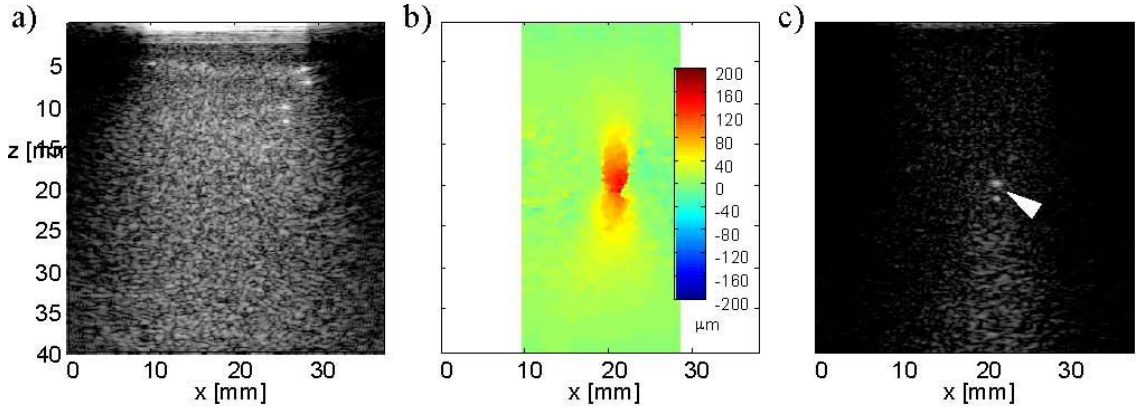

Figure. (a) Conventional optoacoustic image of gelatine phantom with cylindrical inclusions mimicking blood vessels. Owing to clutter, the cross-sections of only the most superficial two inclusions are visible as white double-arc structures. (b) Localised displacement after ARF push. (c) Resulting optoacoustic image, with the inclusion indicated by white arrowhead.

This clutter cancellation method may also offer benefits in conventional US and other imaging modalities where clutter limits image contrast.

Acknowledgements: This research was supported in parts by the Swiss National Science Foundation (No. 205320-103872) and the European Community's Seventh Framework Programme (FP7/2007-2013) under grant agreement No. 318067.

References:

1. M. Jaeger et al., "Reduction of background in optoacoustic image sequences obtained under tissue deformation" J. Biomed. Opt., Vol. 14, 054011-1-10 (2009).
2. M. Jaeger et al., "Improved contrast deep optoacoustic imaging using displacement-compensated averaging: breast tumour phantom studies" Phys. Med. Biol., Vol. 56, pp. 5889–5901 (2011).
3. M. Jaeger et al., "Deformation compensated averaging for clutter reduction in epiphotoacoustic imaging in vivo" J. Biomed. Opt., Vol. 17, 066007-1-8 (2012).

Paper PA-I-5

MEDICAL GRADE OPTOACOUSTIC SYSTEMS FOR NONINVASIVE DETECTION OF HEMATOMAS AND PATIENT MONITORING

Rinat O. Esenaliev

Laboratory for Optical Sensing and Monitoring, Center for Biomedical Engineering, Department of Neuroscience and Cell Biology, Department of Anesthesiology University of Texas Medical Branch, 301 University Blvd., Galveston, Texas 77555-1156, USA

riesenal@utmb.edu

Our group has pioneered biomedical optoacoustic imaging, sensing, and monitoring and developed this technology for a number of diagnostic applications. The optoacoustic technique utilizes time-resolved detection of thermoelastic ultrasound waves induced in tissues by short optical pulses under stress-confined irradiation conditions. This yields a noninvasive diagnostic modality with high optical contrast and ultrasound spatial resolution. One of the most important applications of this technique is noninvasive detection and characterization of intracranial hematomas and monitoring of blood parameters, in particular, oxygenation in specific blood vessels. We developed a number of laser optoacoustic systems that are based on solid-state lasers or laser diodes. In this work we report our results on development and pre-clinical and clinical tests of medical grade optoacoustic systems that are based on optical parametric oscillators (OPO)s tunable in the 700–1064 nm spectral range or on pulsed laser diodes. The systems generate nanosecond pulses to provide the condition of stress confinement. We have developed unique patient interfaces incorporating highly-sensitive, wide-band probes for detecting optoacoustic waves induced with these laser systems in hematomas and specific blood vessels such as the radial artery, superior sagittal sinus, and central and peripheral veins. Our results obtained in pre-clinical studies in small and large animals and in clinical studies in patients with traumatic brain injury, healthy volunteers, anemic patients, and neonatal patients indicate that the optoacoustic systems can provide rapid detection of hematomas and real-time, continuous monitoring of clinically important blood parameters. Further development of these systems will greatly facilitate prompt recognition and treatment of a variety of life-threatening illnesses in patients with traumatic brain injury, circulatory shock, surgical patients, critically ill patients, and neonates.

Acknowledgements: The authors acknowledge support of these studies by the NIH (Grants U54EB007954, R01EB00763, R01NS044345, R41HL103095, R43HD075551, and R41HD076568), John Sealy Memorial Endowment Fund for Biomedical Research, Moody Center for Traumatic Brain Injury Research, 2 DOD grants, UTMB Business Acceleration Program, and Texas Emerging Technology Fund. Drs. Esenaliev and Prough are co-owners of Noninvasix, Inc., a UTMB-based startup that has licensed the rights to optoacoustic monitoring, sensing, and imaging technology.

Paper PA-I-6

INTEGRATED PHOTOACOUSTIC/ULTRASONIC CONTRAST AGENTS USING THE NONLINEAR ACOUSTIC RESPONSE OF NANOEMULSIONS

Matthew O'Donnell[1], Chen-wei Wei[1], Kjersta Larson-Smith[2], Ivan Pelivanov[1,3], Camilo Perez[4], Jinjun Xia[1], Thomas Matula[4], Danilo Pozzo[2]

[1]*Bioengineering, University of Washington, 3720 15th AVE NE, Seattle, WA 98195, USA*
[2]*Chemical Engineering, Benson Hall, University of Washington, Seattle, WA 98195, USA*
[3]*International Laser Center, Moscow State University, Leninskie Gory 1/2, 119991 Moscow, Russia*
[4]*Applied Physics Lab, University of Washington, 1013 NE 40th Street, Seattle, WA 98105, USA*

odonnel@uw.edu

A dual-probing technique is proposed to increase sensitivity and specificity of both ultrasound (US) and photoacoustic (PA) molecular imaging in detecting abnormal cells or tissues targeted by a new type of composite contrast agent, which combines a 250 nm emulsion bead core with surface-assembled gold nanospheres (GNSs) [1]. GNSs absorb light efficiently in the near infrared due to a red shifted absorption spectrum from their high packing density. Under laser irradiation, they promote a phase transition of the emulsion bead into a transient bubble. This process produces stronger PA signals than from thermal expansion, thus enhancing PA responses. In addition, delivering an US probe pulse to the generated bubble creates harmonic signals, enabling nonlinear contrast-enhanced imaging of molecular targets.

The emulsion bead dispersion and a control linear GNS cluster dispersion with the same optical absorption were measured in a tube phantom. Figure 1 shows the acoustic signals received by a broadband (0.1–30 MHz) transducer at different probe conditions, including US pulse/echo signals, pulse laser (6.3 mJ/cm^2) induced PA signals, and dual-probing (US+PA) signals. The PA signal of the emulsion beads is three times larger than that of the linear sample, showing enhancement of PA sensitivity using this contrast agent. Also, the nonlinear residue signal of emulsion beads by subtracting single US and PA signals from the dual-probing signal is 10 times larger than that of linear GNS clusters, indicating the capability of this technique to sensitively and specifically detect targeted regions by locally activating the nonlinear contrast agent.

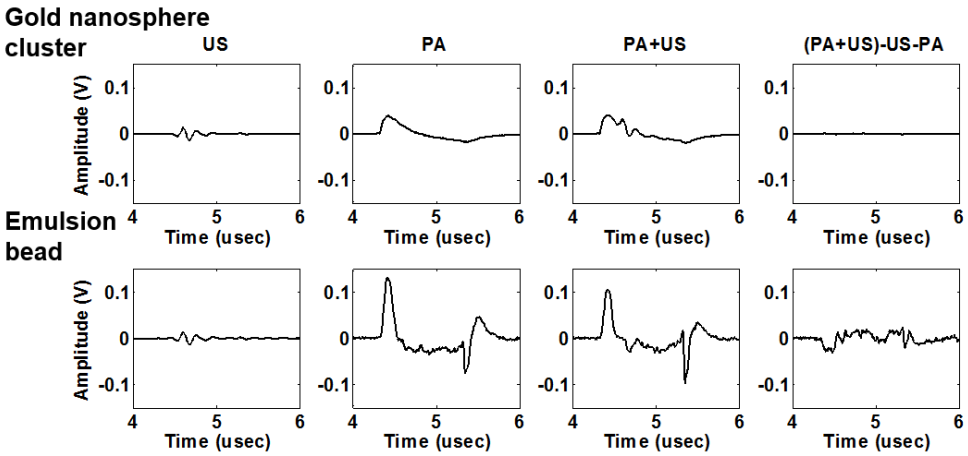

Figure 1. Signals of linear gold nanosphere cluster (top row) and nonlinear emulsion bead (bottom row). Differential signals between dual-probing (US+PA) and single US and PA signals show nearly complete suppression for the linear agent, but 10 time larger residue for the nonlinear emulsion beads.

References:

1. K. Larson-Smith, D.C. Pozzo, "Pickering emulsions stabilized by nanoparticle surfactants" Langmuir, Vol. 28(32). pp. 11725–11732 (2012).

Paper PA-I-7

ACOUSTIC SHEAR WAVE IMAGING IN THE EYE USING OPTICAL COHERENCE TOMOGRAPHY

Shaozhen Song[1,2], Zhihong Huang[2], Matthew O'Donnell[1], Ruikang K. Wang[1,3]

[1]*Bioengineering, University of Washington, 3720 15th AVE NE, Seattle, WA 98195, USA*
[2]*School of Engineering, Physics and Mathematics, University of Dundee, Dundee, DD1 4HN, UK*
[3]*Department of Ophthalmology, University of Washington, 325 9th ave., Seattle, Washington 98104, USA*

wangrk@uw.edu

Elastography is an ideal method to map local stiffness within soft tissue and provide useful information for clinical diagnosis. Optical methods are gaining increased interest for detecting mechanical response of tissue because of their ability to achieve high spatial resolution without tissue contact. A combined acoustical and optical method is proposed for tracking in time and space induced shear waves propagating within the cornea, leading to quantification of localized wave velocities with high resolution that cannot be achieved by traditional competing elastography modalities.

Shear waves were launched in mouse cornea *in vivo* at low kHz frequencies using a stacked piezoelectric actuator. A phase sensitive optical coherence tomography (PhS-OCT) system tracked the propagating waves in space and time. The PhS-OCT system was operated in M-B mode with an equivalent frame rate of 47 kHz, precisely synchronized with stimulation-induced 5 kHz tone bursts. Processing M-B scan data provided the time sequence of propagating wave displacement fields. Representative frames of wave propagation at 4 different time points during the experiment are shown Figure 1(a), where wave propagation in cornea from left to right is clearly visible. The procedure was carried out on age-varied C57 mouse corneas. Using a time-of-flight method, the localized group-wave velocity was calculated and mapped onto the structural OCT image. Figure 1(b) shows a comparison of the group velocity of mechanical waves for a young mouse (3 months) and an old mouse (15 months). Clearly, the old mouse has a higher wave velocity, i.e. higher stiffness, than the young one. These preliminary results demonstrate the potential of the proposed technique to sensitively detect and record tissue mechanical motion with high speed and high resolution, opening up opportunities for future studies of mechanical property measurements of corneal microstructures and potentially useful tools for clinical applications in ophthalmology.

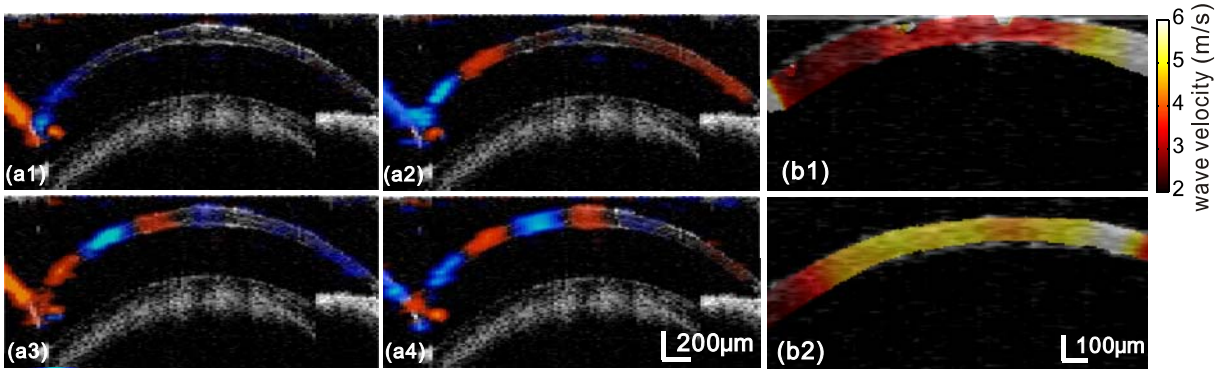

Figure 1. (a1–a4) Displacement field B-frame images at different time points: (a1) $t=2T_s$, (a2) $t=4T_s$, (a3) $t=6T_s$, (a4) $t=8T_s$ (T_s stands for sampling period), (b) group velocity map computed from dynamic wave fields: (b1) young mouse, (b2) old mouse.

Paper PA-I-8

HIGH SENSITIVE INTERFEROMETRIC FIBER OPTIC SENSORS FOR OPTOACOUSTIC IMAGING

H. Lamela[1], D. Gallego[1]

[1]*Optoelectronic and Laser Technology Group, Universidad Carlos III de Madrid, Madrid, Spain*

horacio@ing.uc3m.es

Recent advances in ultrasound and optoacoustic imaging techniques for clinical applications demands for miniaturized and wide bandwidth ultrasonic probes [1]. It has been presented in 2012 the images of internal organs in vivo using a 2.5-mm diameter optoacoustic and ultrasonic dual-mode endoscope [2]. In order to extend the use of these kind of dual mode endoscopes to complement the intravascular ultrasound (IVUS), adding to the morphological information the specificity of the optoacoustic imaging, it is necessary to miniaturize the probe to be fitted in less than 1mm to pass through thin vasculature. Moreover, for a practical IVUS/IVPA catheter is mandatory to have a wideband ultrasonic detector up to 50 MHz with enough sensitivity despite the necessary miniaturization. The optical detection of ultrasound using optical fiber sensor can provide the compactness, sensitivity and bandwidth required for this application.

Our group, previously, has demonstrated that ultrasonic sensitivity of an interferometric single mode polymer optical fiber sensor (SMPOF) is one order of magnitude higher than a silica counterpart [3]. However, these SMPOF are not easily commercially available and its performance in terms of loss and coupling light into is very poor what makes them impractical for real implementation. In contrast, microstructured polymer optical fiber (mPOF), exhibiting the same acoustic sensitivity, presents moderate low loss at visible wavelength regime and can be made endlessly single-mode.

In this contribution, we present a complete ultrasonic characterizations of intrinsic mPOF sensor based on PMMA and TOPAS. Most of the POFs are based on PMMA. However, TOPAS presents the fundamental advantage over PMMA of the humidity insensitive. This is important for ultrasonic measurements due to the sensor must be inside an inherently wet medium.

In order to make a more compact and reliable ultrasonic sensor, a Fabry-Perot interferometer embedded in PMMA mPOF made from two FBG is investigated. The results are compared with a straightforward fiber optic Mach–Zehnder interferometric sensor based on the same mPOFs.

References:

1. K. Jansen, A.F.W. van der Steen, H.M.M. van Beusekom, J.W. Oosterhuis, G. van Soest, “Intravascular photoacoustic imaging of human coronary atherosclerosis” Opt. Lett., Vol. 36, pp. 597–599 (2011).
2. J.M. Yang et al., “Simultaneous functional photoacoustic and ultrasonic endoscopy of internal organs in vivo” Nature Medicine, Vol. 18, p. 1297 (2012).
3. D. Gallego, H. Lamela, “High-sensitivity ultrasound interferometric single-mode polymer optical fiber sensors for biomedical applications” Opt. Lett., Vol. 34, pp. 1807–1809 (2009).

Paper PA-I-9

LASER EXCITATION AND DETECTION OF ULTRAFAST SHEAR ACOUSTIC WAVES IN LIQUIDS

T. Pezeril, V. Gusev, R. Busselez

IMMM, UMR CNRS 6283, Université du Maine, Le Mans, France

thomas.pezeril@univ-lemans.fr

Direct experimental access to ultrafast shear structural relaxation dynamics in liquids remains challenging. On slow time scales, dynamic mechanical analysis and sonic or related measurement methods can be used. Faster responses at MHz frequencies are accessible to ultrasonics and impulsive stimulated thermal and Brillouin scattering, and the low GHz range may be accessed through spontaneous Brillouin scattering. Recent work in x-ray Brillouin scattering has accessed THz longitudinal acoustic frequencies; however, this technique is not yet capable of measurements at shear acoustic frequencies in liquids. Deep-UV Brillouin scattering from longitudinal acoustic waves in this range has been demonstrated. However, it is poorly adapted to measurements of shear relaxation in non-visquous liquids where acoustic damping is strongest.

Picosecond ultrasonics, which applies femtosecond lasers for both generation and detection of coherent phonons, has provided tabletop access to most of the GHz frequency range for longitudinal acoustic waves. Adaptations of this method for GHz shear wave generation through sudden laser interaction with a peculiar sample with broken transverse isotropic symmetry have been developed in the recent years. However, studies of shear waves in liquids have remained elusive.

We will describe a novel approach of laser generation of frequency-tunable shear acoustic waves in the GHz frequency range. We will further demonstrate a sample and optical configuration that allows measurements on viscous and non-viscous liquids [1]. Frequency dependent results in the GHz frequency range and temperature dependent measurements for glycerol and water will be shown. Preliminary results on confined liquids with thicknesses down to a few monolayers will be presented. Finally, we will present the principle of the generation and detection of inhomogeneous shear acoustic waves by laser-induced gratings [2].

References:

1. T. Pezeril, C. Klieber, S. Andrieu, K.A. Nelson, “Optical generation of gigahertz-frequency shear acoustic waves in liquid glycerol”, Phys. Rev. Lett., Vol. 102, 107402 (2009).
2. M. Kouyate, T. Pezeril, D. Mounier, V. Gusev, “Generation of inhomogeneous plane shear acoustic modes by laser-induced thermoelastic gratings at the interface of transparent and opaque solids” J. Appl. Phys., Vol. 110, pp. 1235261–12352617 (2011).

Paper PA-O-1

APPLICATION OF THE THERMOACOUSTIC EFFECT FOR DETECTION OF THE THz PULSES

Valeriy Andreev[1], Vladimir Vdovin[2], Yuriy Kalynov[3]

[1]*Acoustics Dept., Faculty of Physics, Moscow State University, Moscow, Russia*
[2]*Institute of Radio Engineering and Electronics, Moscow, Russia*
[3]*Institute of Applied Physics, Nizhniy Novgorod, Russia*

andreev@acs366.phys.msu.ru

Results of measurements of electromagnetic pulses with 3 to 10 mcs duration at frequencies 0.55, 0.68, and 0.87 THz generated by a large orbit gyrotron are presented. Operation of the thermoacoustic probe is based on effect of acoustic signal generation when electromagnetic pulses are absorbed in the layered structure: radiotransparent substrate – absorber – immersion liquid. Thin metallic film of nanometer thickness sputtered onto the quartz substrate is used as an absorber. The transformation of electromagnetic radiation into acoustic pulse is performed in the film and in the immersion liquid contacting with the film. Acoustic pulse is detected by the broadband acoustic transducer and registered with a digital oscilloscope.

The profiles of THz pulses of 4.8 (curve 1) and 8 μs (curve 2) duration at frequency 550 THz detected by the thermoacoustic and control probes are shown in Fig. 1a. Calculated integrals of profiles 1 and 2 are presented in Fig. 1b. It is shown that for the pulse of microsecond duration the signal waveform detected by the thermoacoustic probe is completely matched to the derivative of a profile of terahertz pulse. When water and ethanol are used as immersion liquids the presence of additional film absorber is not compulsory because these liquids absorb effectively the electromagnetic radiation at the specified frequencies.

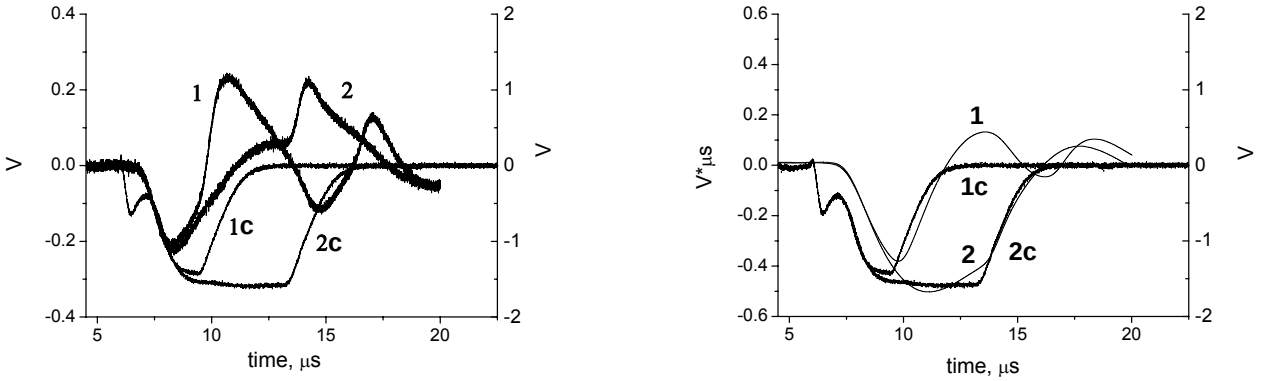

Fig. 1. Profiles of the pulses detected by the thermoacoustic probe (*a*) and their integrals (*b*). The signals of the control probe are marked with "c" letter. 4-mm layer of ethanol and 10-nm chromium film on a quartz substrate were employed in a construction of this thermoacoustic detector.

Acknowledgements: Work was supported by RFBR Grant 12-08-00921 and grant from the Government of the Russian Federation 11.G34.31.0066.

Paper PA-O-2

TWO-PHOTON ABSORPTION-INDUCED PHOTOACOUSTIC IMAGING

Gregor Langer[1], Klaus-Dieter Bouchal[2], Hubert Grun[2], Peter Burgholzer[1,2], Thomas Berer[1,2]

[1]*Christian Doppler Laboratory for Photoacoustic Imaging and Laser Ultrasonics, Altenberger Stra.e 69, 4040 Linz, Austria*
[2]*Research Center for Non-Destructive Testing GmbH (RECENDT), Altenberger Stra.e 69, 4040 Linz, Austria*

gregor.langer@recendt.at

In this paper we demonstrate two-photon absorption-induced photoacoustic imaging using pulses from a femtosecond laser. In contrast to earlier works [1] we extend the method to non-liquid samples and exclude that the photoacoustic signals are generated by second harmonic generation, white light generation, thermal radiation or plasma formation. For this we *in situ* measure the luminescence spectrum. To proof that the photoacoustic signal stems from two-photon absorption we measure the photoacoustic signal as a function of the excitation laser light intensity. We present theoretical predictions for the photoacoustic signal. Experimental signals of a Rhodamine B/water solution and of the Rhodamine B dyed microspheres exhibit a quadratic dependence on the incident laser light intensity, which match the theoretical predictions (Fig. 1b and 1d). In addition we show photoacoustic signals stemming from single-photon absorption (Fig. 1a) and from surface melting or plasma formation (Fig. 1c). Finally, we present two-photon induced photoacoustic imaging on dyed microspheres by scanning the laser beam utilizing galvanometer mirrors (Fig. 2).

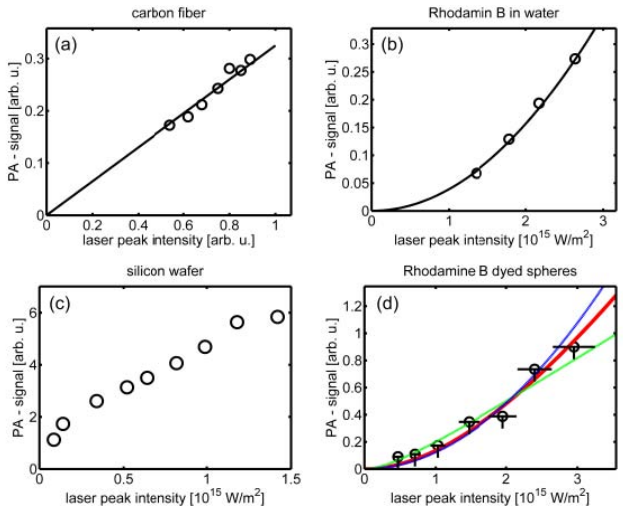

Fig. 1. Photoacoustic signal strength as function of the laser peak intensity for different materials.

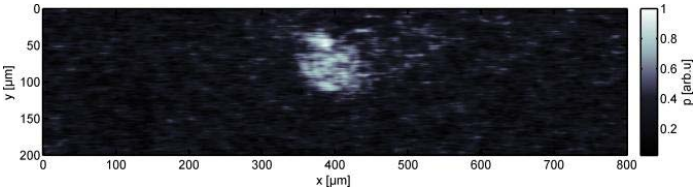

Fig. 2. Two-photon absorption-induced photoacoustic image of a polyethylene microsphere dyed with Rhodamine B.

Acknowledgements: This work has been supported by the Christian Doppler Research Association (Christian Doppler Laboratory for Photoacoustic Imaging and Laser Ultrasonics), the Federal Ministry of Economy, Family and Youth, the Austrian Science Fund (FWF), project number S10503-N20, the European Regional Development Fund (EFRE) in the framework of the EU-program Regio 13, and the federal state Upper Austria.

References:

1. Y. Yamaoka, M. Nambu, T. Takamatsu, “Fine depth resolution of two-photon absorption-induced photoacoustic microscopy using low-frequency bandpass filtering” Opt. Exp., Vol. 19, 13365 (2011).

Paper PA-P-1

ETHYLENE RELEASE FROM STRAWBERRIES BY PHOTOACOUSTIC SPECTROSCOPY ASSAY

S. Banita[1,2], C. Achim[1], M. Patachia[1], C. Matei[1], A.M. Bratu[1], M. Petrus[1], D.C. Dumitras[1,2]

[1]*National Institute for Laser, Plasma and Radiation Physics, 409 Atomistilor St., PO Box MG-36, 077125 Bucharest, Romania*
[2]*University Politehnica of Bucharest, Faculty of Applied Sciences, Romania*

stefan.banita@inflpr.ro

Fruits are important for humans in general, because they have been associated with lower risk of chronic diseases; people with health problems like cardiovascular diseases, cancer, hypertension and diabetes type two benefit of them due to their high content in dietary bioactive compounds. Metabolic disturbances (irradiation, toxicity, temperature, freezing, growth hormone etc.) in fruits are followed by significant and rapid changes in the rate of ethylene emission. Irradiation preserves the fruits by disrupting the biological processes that lead to the decay of fruits quality. Radiation interacts with water and other biological molecules in the fruit system and can lead to the decrease of the quality when lipid oxidation takes place, can cause several changes in the molecular structure of the organic matter [1].

We used a state-of-the-art trace gas Laser photoacoustic spectroscopy (LPAS) technique to quantify and to compare the ethylene gas released by organic strawberries fruits with ethylene gas from nonorganic strawberries fruits [2, 3].

We show the potential and capabilities of LPAS as a powerful method for trace gas detection with fruit quality assessment applications, focusing the attention on quantitative determination of ethylene contained in organic vs. nonorganic strawberries fruits.

Measurements were made to determine if the nonorganic fruits release more ethylene gas compared with organic ones. Ethylene was measured for 8 organic/nonorganic strawberries samples. We also assessed the effect of nitrogen flow for organic fruits quality using LPAS method.

Our findings proved that nonorganic fruits determine a greater increase of the ethylene concentration in the respiration of strawberries. Also, we demonstrated that organic strawberry fruit released ethylene in higher concentrations from opening flowers to mature red fruits.

References:

1. A.B. Oliviera, C.F.H. Moura, E. G-Filho, C.A. Marco, L. Urban, M.R.A. Miranda, PLOS ONE, Vol. 8, e56354 (2013).
2. D.C. Dumitras, S. Banita, A.M. Bratu, R. Cernat, D.C. Dutu, C. Matei, M. Patachia, M. Petrus, C. Popa, Infrared Physics & Technology Journal, Vol. 53, p. 308 (2010).
3. D.C. Dumitras, D.C. Dutu, C. Matei, A.M. Magureanu, M. Petrus, C. Popa, Journal of Optoelectronics and Advanced Materials, Vol. 9, p. 3655 (2007).

Paper PA-P-2

MULTICHANNEL PHOTOACOUSIC IMAGING USING A PLANAR FIBER-OPTIC DETECTOR ARRAY

Karoline Felbermayer, Johannes Bauer-Marschallinger, Hubert Grun, Peter Burgholzer, Thomas Berer

Research Center for Non-Destructive Testing GmbH (RECENDT),
Altenberger Stra.e 69, 4040Linz, Austria

karoline.felbermayer@recendt.at

In this paper we present multichannel photoacoustic imaging (PAI) using an integrating line-detector array. The individual integrating line detectors are realized by using optical fibers [1] and multichannel imaging is facilitated by a combination of parallelization and multiplexing. The optical fibers are part of fiber-optic Mach-Zehnder interferometers. Ultrasonic waves which impinge at the optical fibers change their index of refraction and the respective change in optical path length is demodulated by the interferometers.

Up to now we have demonstrated three-dimensional PAI with single channel detectors only, e.g. as presented in [1]. Multichannel imaging was mainly hindered by the high-cost per channel. Recently, we demonstrated parallelization of fiber-optic detectors by using in-house produced photodetectors and low-cost components from telecommunication industries [2]. In the present work we extend the system by introducing fiber-optic switches to multiplex the channels and demonstrate a planar eight channel array of integrating line detectors. The linear detector array consists of graded-index polymer optical fibers (GIPOFs), which exhibit a better sensitivity than glass optical fibers (GOFs) [3]. Light from a coherent laser source at 1550 nm is distributed into the GIPOFs and respective reference paths which include optical phase shifters. The light from those paths are superposed within fiber couplers; demodulation is done with self-made balanced photodetectors. The high frequency outputs of these detectors are fed to a multichannel sampling device. Self-made analog control circuits use the low frequency outputs of the photodetectors to stabilize the operating points of the interferometers. A 4:1 fiber-optic switch multiplexes four line detectors to one channel, thus, the amount of needed photodetectors, control circuits, phase shifters and sampling channels are reduced by a factor of four.

In addition, we compare the signal/noise ratio of the “standard” realization of the Mach-Zehnder interferometers [1, 2] with an improved detection scheme, including fiber-mirrors and circulators. Furthermore, we present measurements with the device and analyze the directivity of the sensors.

Acknowledgements: This work has been supported by the Austrian Science Fund (FWF), project number S10503-N20, project SenthermS (Sensorik fur innovative thermische Speichertechnologien) by the European Regional Development Fund (EFRE) in the framework of the EU-program Regio 13, and the federal state Upper Austria.

References:

1. Hubert Grun, Thomas Berer, Robert Nuster, Gunther Paltauf, Peter Burgholzer, “Three dimensional photoacoustic imaging using fiber-based line detectors” J. Biomed. Opt., Vol. 15(2), 021306 (2010).
2. J. Bauer-Marschallinger, K. Felbermayer, A. Hochreiner, H. Grun, G. Paltauf, P. Burgholzer, T. Berer, “Low-cost parallelization of optical fiber based detectors for photoacoustic imaging”, SPIEm Vol. 8581, 85812M (2013).
3. Thomas Berer, Istvan A. Veres, Hubert Grun, Johannes Bauer-Marschallinger, Karoline Felbermayer, Peter Burgholzer, “Characterization of broadband fiber optic line detectors for photoacoustic tomography” J. Biophotonics, Vol. 5(7), pp. 518–528 (2012).

Paper PA-P-3

LEAST SQUARES BASED ITERATIVE METHOD F OR MULTICOMPONENT GAS TRACES PHOTOACOUSTIC DETECTION

I.R. Ivascu[1,2], C.E. Matei[1], D.C. Dumitras[1,2]

[1]Department of Lasers, National Institute for Laser, Plasma, and Radiation Physics, 409 Atomistilor St., PO Box MG-36,077125 Bucharest, Romania
[2]University "Politehnica" of Bucharest, Physics Department, 313 Splaiul Independentei, Bucharest, 060042, Romania

ivascu_ioana@physics.pub.ro

The laser based photoacoustic method is among the most sensitive techniques in the world, being able to measure gas concentrations at sub-ppb levels (partial pressure of 10^{-10} atm) [1]. The unique properties of the laser based photoacoustic detection such as: high selectivity, large dynamic range, multicomponent capability has been exploited in designing of sensing devices for gas traces measurements. Though the photoacoustic systems have been intensively developed by a continuous upgrade which enlarged their utility areas (e.g. monitoring of the air pollution, industrial processes, medical diagnostics, etc.), there is still a challenge for optimization of the systems performance according to: the kind and number of detectable substances, the minimum detectable concentrations, the dynamic ranges, and the spatial and temporal resolution [2]. Based on the selectivity of the laser radiation absorbed by the specific gas molecules, the success of the photoacoustic technique is mainly related with the properties of the tunable laser source (accessible wavelengths, tuning characteristics) and of the detection scheme employed. Moreover, a multicomponent gas mixture detection rises additional problems due to a partial overlapping of the individual absorption spectra of several compounds, to a resonant energy transfer processes between vibrational energy levels of excited molecules or to a temporal delay in the production of the photoacustic signal leading to a phase shift of the photoacoustic signal, which make difficult to distinguish between the individual components without an *apriori* knowledge of the mixture composition [2, 3].

In this presentation we propose an algorithm based on the least-squares iterative method for the detection of multicomponent gas traces by photoacoustic technique. Based on this algorithm we calculated the individual gas concentrations from measured photoacoustic signal amplitudes and phases at selected CO_2 laser wavelengths used as source. For the first instance the algorithm was applied for the multicomponent analysis of a synthetical air sample with a known mixture composition. Further the algorithm test was extended to the air quality measurements, for the characterization of air samples collected from the Bucharest underground network, a heavy traffic street node and from a greenhouse. A comparative study of the results from performed measurements was also considered from the point of view of the exposure risk to both urban and rural pollution.

Acknowledgements: This work was supported by a grant of the Romanian Ministry of Education, CNCS – UEFISCDI, project number PN-II-RU-PD-2012-3-0207.

References:

1. D.C. Dumitras et al., "Ultrasensitive CO_2 laser photoacoustic system" Infrared Phys. Technol., Vol. 53(5), pp. 308–314 (2010).
2. P.L. Meyer, M.W. Sigrist, "Atmospheric pollution monitoring using CO_2 laser photoacoustic spectroscopy and other techniques" Rev. Sci. Instrum., Vol. 61, pp. 1779–1807 (1990).
3. M.A. Moeckli, C. Hilbes, M.W. Sigrist, "Photoacoustic multicomponent gas analysis using a Levenberg–Marquardt fitting algorithm" Appl. Phys. B, Vol. 67, pp. 449–458 (1998).

Paper PA-P-4

PHOTOACOUSTIC SEPARATION AND MANIPULATION OF MICROPARTICLES AND CELLS

V.Yu. Khomich, T.V. Malinskiy

Institute for Electrophysics and Electric Power of the Russian Acad. Sci., 18 Dvorzovaya nab., 191186 Sankt-Peterburg, Russia

tm2@newmail.ru

Microparticles, including cells, suspended in fluid can be separated and manipulated using acoustic fields that are generated with laser beam by means of photoacoustic (PA) effect. This technique can be used for: (a) holding particles in a given area, (b) trapping particles to the desired path, and (c) separating of dissimilar particles.

We consider the laser beam which passes near the particles through the liquid with small absorption. Due to PA effect the sound wave field is created. For specific laser beam geometry and duration the acoustic field have "potential well" [1, 2]. In this well small particles may be trapped.

For the case of circle-geometry laser beam acoustic field in linear theory for some range of nondimensional pulse duration $\tau_L = \tau c_0/r_0$ (τ – the laser pulse duration, r_0 – beam's radius, c_0 – sound speed in water) has potential well. Acoustic radiation force moves particle towards this well. The dependence of this force from nondimentional distance r/r_0, calculated for the polystyrene and pyrex glass microspheres in water for two different τ_L shown on Fig. 1. For $\tau_L = 7.5$ all particles move towards potential well near the beam's boundary (Fig. 1a). When the τ_L changed to 3.75 only glass particle moves towards the beam's boundary, while the polystyrene particle moves out of the beam axis (Fig. 1b). So, the particles can be separated and trapped by varying the laser pulse duration or beam diameter.

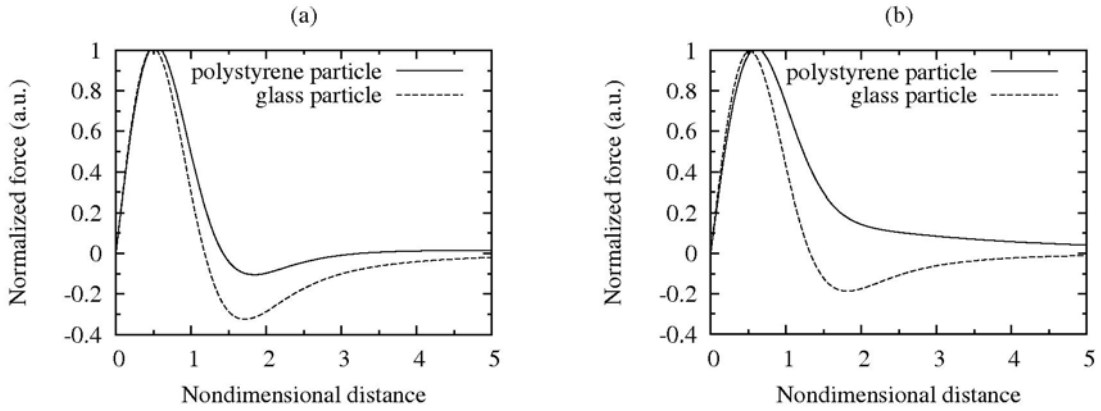

Fig. 1. Dependence of the acoustic radiation force from nondimensional distance for circular beam geometry for polystyrene and glass beards for $\tau_L = 7.5$ (a) and $\tau_L = 3.75$ (b) pulse duration.

References:

1. V.P. Zharov, T.V. Malinsky, R.C. Kurten, "Photoacoustic tweezers with a pulsed laser: theory and experiments" J. Phys. D: Appl. Phys., Vol. 38, pp. 2662–2674 (2005).
2. L.P. Gor'kov, "On the forces acting on a small particle in an acoustic field in an ideal fluid" Sov. Phys. Dokl., Vol. 6, pp. 773–775 (1962).

Paper PA-P-5

INVESTIGATION OF WET LASER CLEANING OF SURFACE FROM PAINT COATING BY MEANS ACOUSTICAL METHOD.

V.P. Veiko, A.A. Samokhvalov

St.Petersburg State University of Information Technologies, Mechanics & Optics, 49 Kronverksky pr., 197101, St.Petersburg, Russia

The mechanism of wet laser cleaning (WLC) is still not fully understood, in particular, laser removal of paint coatings by WLC virtually has not been investigated. Currently, for laser cleaning is economically feasible using of the multiple-pulse fiber lasers with pulse repetition rate of 20–100 kHz and a pulse energy of up to 1 mJ. Therefore, the aim of this work was investigating of the WLC, performed by means of fiber lasers, and the definition of an effective regime of laser cleaning of surfaces from paint coatings.

In our experiments the cleaning of surfaces of metering (anilox) roll, construction steel from paint coatings have been carried out by using laser machine “Mini-Marker 2”, it’s created on the based a pulsed 20 Watt-fiber laser (pulse energy 1 mJ, repetition rate 20–100 kHz, IPG-Photonics). The acoustic emission from laser irradiation surface was detected at an angle (45°) to the sample surface with a wide-band electret microphone (20–20000 Hz). The acoustic signal has been recorded using an oscilloscope (Tektronix TDS 3052C). The spectral analysis method, fast Fourier transform (FFT), was used to study the acoustic waves and to build the relationship between the acoustic waves and laser pulse energy.

As a result of experiments were obtained dependence between the fundamental frequency of the Fourier spectrum and the energy of the laser pulse. The amplitude of the fundamental frequency of the Fourier spectrum suffered a leap at the laser pulse energy of the order of 0.5–0.6 mJ, this indicated of the change of the mechanism of WLC. Obtained dependence was approximated by two straight lines. Also, the thickness of the liquid layer which was necessary for the most effective way to remove paint coatings was determined and appearsequal to 1 mm. At a thickness of the fluid layer 0.5 mm the optical interference were observed, which is significantly reduced the efficiency of laser removal of paint coatings.

It was concluded finally the optimal laser cleaning regime in the frames of WLC is a regime in a presence of developed bubbles collapse along with a shock waves in a liquid.

Acknowledgements: The work is supported by Russian State Contracts RSC № 14.B37.21.0144 and № 11.519.11.4017 Russian Federation President Grant for leading scientific school SS–619.2012.2.

References:

1. V.P. Veiko, E.A. Shakhno, “Physical Mechanisms of Laser Cleaning” (from book “Laser cleaning”). World Scientific Publ., pp. 311–340 (2002).

SECTION TH

Terahertz Technologies

Paper TH-I-1

ADVANCES IN STRONG THz FIELDS FROM BICOLOR FILAMENTS

A.D. Koulouklidis[1,2], A. Gorodetsky[1], M. Massaouti[1], S. Tzortzakis[1,2]

[1]*Institute of Electronic Structure and Laser (IESL), Foundation for Research and Technology - Hellas (FORTH), P.O. Box 1527, GR-71110 Heraklion, Greece*
[2]*Department of Materials Science and Technology, University of Crete, GR-71003, Heraklion, Greece*

stzortz@iesl.forth.gr

Gas-plasma strings from 2-color femtosecond laser filaments constitute one of the most convenient and promising sources of pulsed terahertz (THz) radiation. It is one of the approaches that allow one to achieve at the same time ultrabroadband THz spectra and very high amplitudes of THz electric fields. Such sources present major advantages for applications of sensing, spectroscopy, imaging, and nonlinear optics. In view of the numerous applications an understanding of the emission from the filament and the far field spatial distribution of the terahertz radiation, is crucial. One of the first works towards this direction [1], revealed a highly directional THz radiation while a more recent publication [2] proposes a donut-shape spatial pattern. The most recent results reported by Kim et.al. [3], propose an off-axis phase matched emission from the filament due to interference effects between the different point sources across the filament, resulting thus in a donut-shape profile. A simple theoretical model was also proposed in [3], which is though insufficient to explain all observations.

Here we present new experimental results and a more comprehensive model describing the THz spatial distribution in the far-field [4]. We find both on-axis and off-axis components, unifying previous scarce findings in the literature. As for the physical interpretation we demonstrate the failures of the model presented in [3] and suggest appropriate improvements. Our experimental and theoretical findings let us also suggest ways for controlled directional off-axis THz emission that can be useful in many applications.

Acknowledgements: This work was supported by the Aristeia project "FTERA" (Grant No. 2570), co-funded by the European Social Fund (ESF) and National Resources.

References:

1. Hua Zhong, Nick Karpowicz, X.-C. Zhang, "Terahertz emission profile from laser-induced air plasma" Appl. Phys. Lett. Vol. 88, 261103 (2006).
2. A.V. Borodin, M.N. Esaulkov, I.I. Kuritsyn, I.A. Kotelnikov, A.P. Shkurinov, "On the role of photoionization in generation of terahertz radiation in the plasma of optical breakdown" J. Opt. Soc. Am. B, Vol. 29, p. 1911 (2012).
3. Y.S. You, T.I. Oh, K.Y. Kim, "Off-axis phase-matched terahertz emission from two-color laser-induced plasma filaments" Phys. Rev. Lett., Vol. 109, 183902 (2012).
4. A.D. Koulouklidis, M. Massaouti, A. Gorodetsky, S. Tzortzakis, Under Review.

Paper TH-I-2

EFFICIENT THZ GENERATION BY FEMTOSECOND LASER PULSES AND APPLICATION OF THZ RADIATION FOR PLASMA DIAGNOSTICS

A. Stepanov

Institute of Applied Physics, Nizhny Novgorod, Russia

step@ufp.appl.sci-nnov.ru

Two schemes for efficient generation of THz radiation based on lithium niobate nonlinear crystal ($LiNbO_3$) were investigated experimentally. In the first one the Cherenkov radiation mechanism was implemented in sandwich geometry [1] consisting of a 35 μm $LiNbO_3$ layer, metal substrate and Si output prism. A record high optical-to-terahertz conversion efficiency of 0.25% was realized with femtosecond laser pulses propagated in such a planar Si-$LiNbO_3$-air-metal structure. Also it was demonstrated terahertz spectrum tuning by adjusting an air gap between the $LiNbO_3$ layer and the metal plate.

In another approach we investigated THz generation in $LiNbO_3$ by femtosecond laser pulses with a tilted intensity front at cryogenic temperatures at high (up to 10 mJ) pump energy for different laser pulse duration and crystal length. Maximum conversion efficiency of ~0.2% is obtained for 5 mm crystal length and 190 fs pulse duration. The mechanism responsible for the saturation of the efficiency of THz generation observed in the experiment will be discussed.

Terahertz generation by two-color femtosecond laser pulses in ambient air was recently proposed to produce broadband THz radiation which (tightly focused) allowed to reach electric field up to 1 MV/cm [2]. In this talk, to clarify the two-color mechanism, we report the results of the terahertz wave generation in air using inverted two-color excitation scheme. We used in addition to the strong laser field at fundamental frequency (at 800 nm) a weak subharmonic signal with frequency equal to one half of fundamental one (about 1600 nm). The wavelength of subharmonic field could be tuned. Polarization of THz radiation as a function of mutual polarization of fundamental and subharmonic frequencies was investigated altogether with dependence of THz radiation on energy in fundamental and subharmonic pulses. Resonant dependence of THz yield on frequency detuning was observed. Experimental findings agreed very well with the residual current density model.

We applied our expertise in THz generation to diagnose the crucial parameter of a plasma filament produced by intense femtosecond laser pulses in gases – the plasma concentration and its decay. Plasma density was found from the experimentally measured scattered THz signal [3]. The plasma decay was measured in different gases in a wide range of pressures (2–760 Torr). The influence of external DC electric field on plasma decay was also investigated.

References:

1. S. Bodrov et al. “Efficient terahertz generation by optical rectification in Si-$LiNbO_3$-air-metal sandwich structure with variable air gap” Appl. Phys. Lett., Vol. 100, 201114-1–4 (2012).
2. B. Clough, J. Dai, X.-C. Zhang, “Laser air photonics: beyond the terahertz gap” Mater. Today, Vol. 15, pp. 50–58 (2012).
3. S. Bodrov et al. “Effect of an electric field on air filament decay at the trail of an intense femtosecond laser pulse” Phys. Rev. E, Vol. 87, 053101-1–9 (2013).

Paper TH-I-3

APPLICATION OF TERAHERTZ-LASER-LAUNCHED EVANESCENT WAVES TO MATERIAL STUDY: SURFACE PLASMONS ON METAL-DIELECTRIC INTERFACE AND ATTENUATED TOTAL REFLECTION IN CIRCULAR DICHROISM SPECTROMETER

B.A. Knyazev[1,2], V.S. Cherkassky[1,2], Yu.Yu. Choporova[1,2], V.V. Gerasimov[1,2], I.A. Kotelnikov[1,2], A.K. Nikitin[2,3], D.G. Rodionov[1,2,4], G.N. Zhizhin[3], E.V. Grigorieva[5], L.A. Mostovich[5]

[1]*Budker Institute of Nuclear Physics SB RAS, Novosibirsk 630090, Russia*
[2]*Novosibirsk State University, Novosibirsk 630090, Russia*
[3]*Scientific and Technological Center for Unique Instrumentation of RAS, Moscow 117342, Russia*
[4]*Novosibirsk State Technical University, Novosibirsk 630091, Russia*
[5]*Institute of Molecular Biology and Biophysics, SB RAMS, Novosibirsk 630117, Russia*

ba_knyazev@phys.nsu.ru

Two techniques based on the measurement of the transmission and attenuation of evanescent waves have been developed at Novosibirsk terahertz free electron laser (NovoFEL), whose radiation wavelength can be gradually scanned in a wide spectral range, for sensing of metal and dielectric surface characteristics. In the first technique, the sensitivity of surface plasmon polaritons (SPPs) to the thickness and dielectric permittivity of thin layers covering a metal is employed in the study of metal-dielectric-air interfaces. A non-invasive study of SPP characteristics bases on characteristics of free wave arising when an SPP is diffracted at the surface edge. A theory tying characteristics of the diffracted wave with those of the initial SPP was developed and corroborated experimentally. The propagation lengths for SPPs travelling along Au-ZnS-air interfaces have been measured for plane and cylindrical surfaces with real-time detectors of three types. "Jumps" of SPPs through air gaps were studied both experimentally and theoretically. Possible application of the results obtained to the development of terahertz optical communication systems is discussed. In the second technique, attenuation of an evanescent wave produced by the laser radiation above the surface of a total internal reflection element is used for measurement of the absorption coefficient of a sample attached to the surface (attenuated total reflection (ATR) system). A broad-band terahertz circular-dichroism (TCD) spectrometer with an ATR element to study highly-absorbing substances has been developed. A Michelson interferometer with crossed photolithographic polarizers in the arms and one of the mirrors mounted on a translation stage generated the beam which elliptical polarization was modulating between left- and right-rotating polarization states. Polarimetric characteristics of a number of polysaccharide enantiomers in aqueous solution as well as of other optically active media were studied using the TCD spectrometer. The experiments have clearly shown high efficiency of both techniques for sensing of materials in the terahertz range.

Paper TH-I-4

GENERATION OF TERAHERTZ WAVES IN CRYSTALS WITH INHOMOGENEOUS DISTRIBUTION OF SECOND-ORDER NONLINEAR SUSCEPTIBILITY

G.Kh. Kitaeva

M.V. Lomonosov Moscow State University, Moscow 119991, Russia

The nonlinear-optical methods of terahertz wave (THz) generation are known to be among the best laser-based methods for effective THz generation, advantageous not only due to room-temperature operation, but also due to possibilities of instantaneous detection using inverse frequency-conversion process and the same laser source. The problem of matching the phases of optical and terahertz waves is avoided in some tasks by using the quasi-phase matched (QPM) crystal structures with a periodic inversion of the crystal axes. Due to spatial periodic variation of the sign of second-order optical susceptibility in such structures, by a proper selection of the variation period one can obtain narrowband generation with a high spectral power density at any necessary frequency within the THz range of the crystal transparency.

Recently we have studied characteristics of the QPM generation and detection of short THz pulses [1, 2] in periodically poled lithium niobate crystals (PPLN) with regular one-dimensional domain gratings of two different types, fabricated by applying the standard electrical poling technique, and obtained directly within the off-center Czochralski growth procedure. Due to the technical features of the post-growth method, the transverse sizes of the input and output windows of crystals of this type are limited to 0.5–1 mm. The windows of in-growth PPLN crystals are wider in 5–10 times, but domain grating periods are not spatially uniform. Our study demonstrates that the generation efficiencies of the post-growth samples and the most regular parts of the in-growth crystals are of the same order. Stochastic character of the in-growth samples did not affect appreciably the width of the generation spectrum, but decreased the peak power. However, the crystals changed their roles when we applied them in the electro-optical sampling scheme. The larger input aperture enabled us to realize the narrow-band QPM electro-optical detection in the in-growth PPLN crystals, while the detection efficiency of the post-growth samples was too low for this application.

We propose and demonstrate also the new schemes of QPM THz generation, such as optical rectification of nanosecond laser pulses [3], and generation of multi-line THz spectra in specially designed aperiodic QPM crystals. Theoretical models of the methods are developed with account of any arbitrary spatial distribution of the second-order optical susceptibility in the QPM structures. Engineering of non-linear optical elements opens a way to control both the spectrum of the THz generation and the spectral sensitivity of the QPM THz detection.

Acknowledgements: The author acknowledge support from the Russian Foundation for Basic Research (projects 12-02-12034 and 11-02-12102) and the Russian Ministry of Education and Science (grant 8393).

References:

1. G.Kh. Kitaeva, S.P. Kovalev, I.I. Naumova, R.A. Akhmedzhanov, I.E. Ilyakov, B.V. Shishkin, E.V. Suvorov, "Quasi-phase-matched probe-energy electro-optic sampling as a method of narrowband terahertz detection" Appl. Phys. Lett., Vol. 96, 071106 (2010).
2. G.Kh. Kitaeva, S.P.Kovalev, I.I. Naumova, A.N. Tuchak, P.V. Yakunin, Y.-C. Huang, E.D. Mishina, A.S. Sigov, "Terahertz wave generation in periodically poled lithium niobate crystals fabricated using two alternative techniques" Laser Phys. Lett., Vol. 10, 055404 (2013).
3. A.N. Tuchak, G.N. Gol'tsman, G.Kh. Kitaeva, A.N. Penin, S.V. Seliverstov, M.I. Finkel, A.V. Shepelev, P.V. Yakunin, "Generation of nanosecond terahertz pulses by the optical rectification method" JETP Lett., Vol. 96, pp. 94–97 (2012).

Paper TH-I-5

ELECTROOPTIC SENSING, FROM DC UP TO THZ FREQUENCIES

Gwenaël Gaborit[1,2], Lionel Duvillaret[2], Andrius Biciunas[3], Jean-Louis Coutaz[1]

[1]*IMEP-LAHC, UMR CNRS 5130, Université de Savoie, 73376 Le Bourget-du-Lac, France*
[2]*Kapteos, Savoie Technolac, BP347, 73377 Le Bourget-du-Lac cedex, France*
[3]*Semiconductor Physics Institute of Center for Physical Sciences and Technology, 01180 Vilnius, Lithuania*

gwenael.gaborit@univ-savoie.fr

Measurement of electric (E) field is of a major interest in versatile applications e.g. near field pattern, bioelectromagnetism, spectroscopy, … Among the available methods to perform an experimental assessment of the E-field vector, electro-optics constitutes a relevant non-invasive technique. This latter one is based on the E-field induced perturbation of an optical beam within a non-centrosymetric crystal. The first order non-linear optical effect (also called Pockels effect) actually can be expressed as a modification of the EO crystal eigen refractive indices with the E-field vector components. These latter ones can be probed both in magnitude and phase, thanks to a laser probe beam which sees its amplitude, its phase and its polarization state modulated [1]. The frequency bandwidth exceeds 10 THz and the spatial resolution can be diffraction limited and is actually as low as some 10 µm. The EO dynamics spreads from a minimum detectable field weaker than 1 V/m/√Hz to more than 1 MV/m. Furthermore, as the transducer is fully dielectric (only an EO crystal), the disturbance on the field to be measured remains very low comparatively to more commonly used sensors such as antennas. Remote measurement can be achieved thanks pigtailed EO devices.

Taking benefits of the previous mentioned intrinsic properties, recent development concerns not only in lab experiment aiming innovative and unprecedented results [2, 3] (e.g. real time evolution of the E-field vector) but also a lot of industrial applications (*e.g.* energy lines monitoring) requiring reliable and reproducible tools.

A concise tutorial of EO sensor principles will be given during the conference. Theoretical expectations as well as experimental developments and results will demonstrate the potentialities of such a technique. The presentation will also focus on the limiting factors of the EO bandwidth measurement concerning very low frequencies (down to DC) as well as for high cut-off frequency (up to a few tens THz).

References:

1. L. Duvillaret, S. Riallant, J.-L. Coutaz, "Electro-optic sensors for electric field measurements. I. Theoretical comparison among different modulation techniques" JOSA. B, Vol. 19, pp. 2692–2703 (2002).
2. G. Gaborit, J.-L. Coutaz, L. Duvillaret, "Vectorial electric field measurement using isotropic electro-optic crystals" Appl. Phys. Lett., Vol. 90, 241118 (2007).

Paper TH-I-6

TWODIMENSIONAL PLASMA EXCITATIONS FOR DETECTION OF THz RADIATION

W. Knap[1,2], N. Dyakonova[1], S. Rumyantsev[1,3], M.S. Vitiello[4], D. Coquillat[1], S. Blin[5], F. Teppe[1]

[1]*Laboratoire Charles Coulomb Université & TERALAB Montpellier 2 &CNRS, France*
[2]*Institue of High Pressure Physics UNIPRESS PAN, 02-845 Warsaw, Poland*
[3]*Rensselaer Polytechnic Institute, Troy, New York 12180, USA*
[4]*NEST, Istituto Nanoscienze - CNR and Scuola Normale Superiore, 56127 Pisa, Italy*
[5]*IES &TERALAB, Universite Montpellier 2 & CNRS, 34950 Montpellier, France*

Two-dimensional electron plasma in nanometre size field effect transistors can oscillate in Terahertz (THz) frequencies, far beyond transistors fundamental cut-of frequencies [1]. We present an overview of some important and recent results concerning the physics of nanometre scale field effect transistors showing that they can be used for the detection of terahertz radiation

The subjects were selected in a way to stress some new aspects/developments rather than purely technological/engineering improvements. The basic physics related problems like temperature dependence of the photoresponse [2], interferences of THz signals leading to helicity sensitive detection are presented [3].

Until now most of works on nanometer FETs detectors were considering only THz imaging applications. We show the first results on the application of nanometre FETs as detectors in wireless communication with signal modulated in GHz range [4]. Finally we present also results from THz detection by grapheme transistors [5]. A possible development of future THz detectors using grapheme structures is also addressed.

Examples of the imaging using using FET detectors with electronic sources and THz gas lasers will be also presented

References:

1. W. Knap, M.I. Dyakonov, 'Field effect transistors for terahertz applications' in D. Saeedkia, Handbook of terahertz technology for imaging, sensing and communications, Cambridge, Woodhead Publishing, 121-155(2013); W. Knap, S. Rumyantsev, M.S. Vitiello, D. Coquillat, S. Blin, M. Shur, F. Teppe, A. Tredicucci, T. Nagatsuma, "Nanometer size field effect transistors for terahertz detectors" Nanotechnology, Vol. 24 (2013).
2. O.A. Klimenko, W. Knap, B. Iniguez, D. Coquillat, Y.A. Mityagin, F. Teppe, N. Dyakonova, H. Videlier, D. But, F. Lime, J. Marczewski, K. Kucharski, "Temperature enhancement of terahertz responsivity of plasma field effect transistors" J. Appl. Phys., Vol. 112, 014506 (2012).
3. C. Drexler, N. Dyakonova, P. Olbrich, J. Karch, M. Schafberger, K. Karpierz, Yu. Mityagin, M.B. Lifshits, F. Teppe, O. Klimenko, Y.M. Meziani, W. Knap, S.D. Ganichev, "Helicity sensitive terahertz radiation detection by field effect transistors" J. Appl. Phys. Vol. 111, 124504 (2012).
4. S. Blin, F. Teppe, L. Tohme, S. Hisatake, P. Nouvel, D. Coquillat, A. Penarier, J. Torres, W. Knap, T. Nagatsuma, "Plasma-wave detectors for terahertz wireless communication" IEEE El. Dev. Lett., Vol. 33, p. 1354 (2012).
5. L. Vicarelli, M.S. Vitiello, D. Coquillat, A. Lombardo, A.C. Ferrari, W. Knap, M. Polini, V. Pellegrini, A. Tredicucci, "Graphene field-effect transistors as room-temperature terahertz detectors" Nature Materials, Vol. 11, p. 865 (2012).

Paper TH-I-7

THz GYROTRONS: DEVELOPMENT AND APPLICATIONS

M. Glyavin, A. Luchinin, V. Bratman, V. Zapevalov, G. Denisov

Institute of Applied Physics RAS, 46 Ul'yanov st., Nizhny Novgorod 603950, Russia

glyavin@appl.sci-nnov.ru

Terahertz frequency range (0.1–10 THz) has a number of specific features that make it very attractive for a wide range of basic and applied research in physics, chemistry, biology and medicine. Terahertz waves are promising for diagnosis and spectroscopy of various media, including the development of high resolution electron paramagnetic resonance (EPR) and nuclear magnetic resonance (NMR) spectroscopy. Powerful terahertz radiation can be used to create dense plasma and control its parameters (controlled thermonuclear fusion, "point" plasma X-ray sources, remote detection of ionizing radiation).

In the pioneering IAP works in 1970–1980's was shown the principle possibility of a high-power CW and pulsed gyrotrons operation at frequencies from 0.33 to 0.65 THz. Recent experiments using the original pulsed solenoid with a magnetic field up to 50 T yielded generation on the main cyclotron resonance with 5–0.5 kW power in single pulse duration of 50 microseconds at record frequencies 1–1.3 THz [1]. One of the promising applications of high power THz gyrotrons considered remote detection of ionizing radiation based on localized terahertz discharge at a time when the number of free electrons, slightly higher than the natural background. For this method at distances of several tens meters, 0.67 THz / 200 kW gyrotron has been developed [2]. Same gyrotron has been successfully used for THz discharges in gases in studies designed to create a point source of extreme ultraviolet light.

To obtain high-frequency radiation in the IAP along with traditional gyrotrons are also being developed so named large orbit gyrotron (LOG) with axis-encircling electron beam. Such beam result selection excitation of high harmonics with harmonic number equal to mode azimuthal index. In 80 kV voltage LOG excitation of second and third harmonics obtained single mode 10 microseconds pulses with frequencies 0.55–1.0 THz at power level 1.8–0.3 kW [3]. LOG with permanent magnet created by IAP in collaboration with FIR FU (Japan) implement the generation of 3–5 harmonics at frequencies up to 0.14 THz [4].

For technological, biological and medical research IAP jointly with FIR FU was developed CW gyrotron with a frequency of 0.3 THz and a power of 2.7 kW [5] based on helium-free 12-T cryomagnet.

To obtain high-resolution high-field NMR spectroscopy complex based on CW 100 W / 0.26 THz second harmonic gyrotron with internal mode converter of operating mode to narrow beam and high power and frequency stability has been realised. Experiments with this gyrotron allowed 80 times the sensitivity and resolution of the NMR spectrometer [6].

In recent years a number of new results have been obtained such as the penetration of gyrotrons in the frequency range above 1 THz, development and application of sub-THz gyrotrons for spectroscopy and plasma physics experiments.

References:

1. M. Glyavin, A. Luchinin, G. Golubiatnikov, Phys. Rev. Lett., Vol. 100(1), 015101 (2008).
2. M. Glyavin, A. Luchinin, G. Nusinovich, et al., Appl. Phys. Lett., Vol. 101, 153503 (2012).
3. V. Bratman, Yu. Kalynov, V. Manuilov, Phys. Rev. Lett., Vol. 102, 245101 (2009).
4. T. Idehara, I. Ogawa, S. Mitsudo, et al., IEEE Trans. on Plasma Sci., Vol. 32(3), pp. 903–909 (2004).
5. T. Saito, T. Nakano, et al., Int. J. of Infrared & MM Waves, Vol. 28(12), pp. 1063–1078 (2007).
6. V. Zapevalov et al., 35 Int. Conf. on Infrared, MM & THz Waves, Roma, Italy, We-E1.4 (2010).

Paper TH-I-8

ALL QUANTUM-DOT BASED COMPACT THz SOURCES

E.U. Rafailov, R. Leyman, N. Bazieva

Photonics & Nanoscience Group, School of Engineering, Physics and Mathematics, University of Dundee, Dundee, DD1 4HN, UK

The THz optoelectronics field is now maturing and semiconductor-based THz devices are becoming more widely implemented as analytical tools in spectroscopy and imaging. Research into ultrafast semiconductor materials for THz devices is predominantly devoted to improving the optical-to-THz efficiency of photoconductive materials that generate THz signals when driven by suitable ultrafast coherent optical sources.

Materials traditionally used for this include low temperature-grown gallium arsenide (LT-GaAs) and LT-InGaAs for longer wavelength operation, and are used because the growth process integrates lattice defects and carrier trapping sites throughout the bulk, which act to shorten carrier lifetimes but also compromises carrier mobility and PC gain. We demonstrate here photoconductive THz antenna devices comprising of GaAs/InAs quantum dot-based semiconductor structures, which utilise ultrafast carrier capturing offered by InAs QDs to allow THz operation. This allows optical pumping of the device with ultrafast pulsed (time-domain) or "dual-mode" continuous wave (CW, frequency-domain) laser(s) at wavelengths over the 800–1300 nm range, which is absorbed by *both/either* the high quality GaAs crystal and/or InAs QDs, with high carrier mobility and almost arbitrarily short carrier lifetimes (below 0.7 ps) which is strongly determined by the pre-chosen QD layer periodicity.

We discuss such THz devices which exhibit optical-to-THz conversion efficiency around 5 times greater than commercial LT-GaAs-based devices in time-domain setups, and exhibits efficient optical-to-THz operation in frequency-domain setups at both LT-GaAs and InAs absorption wavelength ranges, ≤850 nm and ≤1300 nm respectively.

Paper TH-I-9

TERAHERTZ AND INFRARED DETECTORS AND MIXERS BASED ON NbN SUPERCONDUCTING THIN FILM NANOSTRUCTURES

G.N. Goltsman

[1]*Moscow State Pedagogical University, 1 Malaya Pirogovskaya, 119991 Moscow, Russia*
[2]*CJSC ``Superconducting Nanotechnology'' (Scontel), 5/22 Rossolimo, 119991, Moscow, Russia*

goltsman@mspu-phys.ru

Hot-electron bolometers mixers have been established as detectors of choice for terahertz observational astronomy because they offer a noise temperature which is typically a few times the quantum limit, a relatively wide intermediate frequency bandwidth, and also because they require much less local oscillator power [1]. Typically HEBs are patterned as bridges from 3.5-nm NbN films deposited onto high-resistivity Si substrates. The length-to-width ratio of the bridge is usually 1:10 in order to ensure a better match between the sensitive element and the planar antenna. With respect to the method of coupling an HEB with electromagnetic radiation, one speaks about the waveguide design and quasioptical design. The advantage of the former is that corrugated horns reduce edge diffraction, improve beam pattern symmetry and reduce cross-polarization.

A promising type of the photon counting detector is SSPD. The SSPD is patterned from 4-nm-thick NbN film as 120-nm-wide and meander-shaped strip that covers a square area of 10×10 μm^2. At wavelength $\lambda \leq 1.3$ μm quantum efficiency (QE) of our best devices approaches 35% at 2 K with 35 ps timing jitter. The system has already found a number of practical applications for detection of radiation from the quantum dots with high temporal resolution, as well as in quantum cryptography and nanophotonics circuits [2].

Here we present also recent advances in the development of SSPDs. In an effort to promote SSPD to the middle infrared, we have developed SSPD made of 40-nm-wide strips connected in parallel. These detectors show a response to 10 μm photon. Another development was the SSPD on a silicon waveguides [2]. We have shown that such SSPD has a quantum efficiency up to 94% at telecom wavelengths, high speed of detection and ultrashort timing jitter of 18 ps.

In particular we used ZBLAN fibers, allowing operation at wavelengths beyond 1700 nm. The best achieved DE is up to 28% at a wavelength of 0.75 μm, 20% at 1.55 μm and 11% for 1.8 μm fiber ZBLAN at 10 dark counts per second at a temperature of 2 K.

Also we present our approaches to the development of fiber-coupled superconducting single photon detectors with enhanced photon absorption. For such devices we have measured detection efficiency in wavelength range from 500 to 2000 nm. The best fiber coupled devices exhibit detection efficiency of 44.5% at 1310 nm wavelength and 35.5% at 1550 nm at 10 dark counts per second [3].

References:

1. I.Tretyakov et al., Appl. Phys. Lett., Vol. 98, 033507 (2011).
2. W.H.P. Pernice, C. Schuck, O. Minaeva, M. Li, G.N. Goltsman, A.V. Sergienko, H.X. Tang, Nature Commun., Vol. 3(12) (2012).
3. A.A.Korneev et al., Applied Superconductivity, IEEE Transactions, Vol. 23, p. 3 (2013).

Paper TH-I-10

UNCOOLED RECTIFICATION AND BOLOMETER TYPE THz/SUB-THz DETECTORS

F. Sizov[1], M. Sakhno[1], A. Golenkov[1], V. Zabudsky[1], V. Petriakov[1], S. Dvoretskii[2]

[1]*Institute of Semiconductor Physics NASU, Kiev-03028, Nauki Av., 41, Ukraine*
[2]*Institute of Semiconductor Physics SB RAN, 630090 Novosibirsk, Russia*

sizov@isp.kiev.ua

Detectors are among the critical components of THz/sub-THz imaging systems. The questions related with performance of some type of THz uncooled detectors and the state of the art of arrays development in imaging systems are discussed.

To make THz/sub-THz ($\nu \sim 0.1$–10 THz) cost-effective it is desirable to use un-cooled detectors and arrays on their base. Estimations of ultimate noise equivalent power (*NEP*) of direct detection uncooled rectification and bolometer type detectors or arrays that define their applicability in active or passive imaging systems when comparing the estimated *NEP*s with experimental ones for given radiation frequency range are given.

The comparison of operational parameters for different types of thermal detectors (Golay cells, metallic bolometers, pyroelectric detectors) and rectification ones (Schottky barrier diodes (SBDs), field effect transistors (FETs) and some others) as un-cooled THz/sub-THz detectors is considered. Signal rectification by un-cooled THz/sub-THz detectors seems is an advantageous technique for fast direct detection of radiation, allowing combine such detectors into focal plane arrays for applications in real time active or passive imaging.

The analysis of silicon FETs as direct detection THz/sub-THz detectors using the allregion model (with account of both drift and diffusion current components) has shown that the FET detector performance is mainly limited by parasitic effects. Frequency dependence (in high frequency range) of detected signal is similar for direct detection FET and SBD and is $\sim\nu^{-2}$ or $\sim\nu^{-4}$ dependent on the antenna type and the measurement procedure. Taking into account the parasitics and detector-antenna matching one can describe FET detector parameters and estimate the ultimate performance limits of such detectors. Compared to SBD detectors the FET ones can be preferable in applications if possible better adjustment of advanced FET impedance to that of antenna is attained. To the date FET detectors have demonstrated NEP in the spectral range $\nu \sim 100$–300 GHz that is appropriate for active imaging $\sim(10^{-10}$–$10^{-11})$ W/Hz$^{1/2}$ and is about one order of magnitude worse or comparable to the best values of SBDs. To operate well in THz frequency range small area SBDs with lower barrier height, compared to GaAs one, are required.

The application of narrow-gap mercury-cadmium telluride for mm-wave/THz hotelectron bolometer is also considered and it is shown that it can be used in linear arrays for active mm-wave/THz vision systems. *NEP* of such detectors with antennas and silicon microlenses can achieve $NEP \sim (1$–$3)\cdot10^{-10}$ W/Hz$^{1/2}$ [1] in radiation frequency range of $\nu \sim 77$–200 GHz. Some small number (8 to 16 elements) arrays were designed and some pictures (see e.g. [2]) in the range of $\nu \sim 150$ GHz were obtained.

Acknowledgements: Authors are thankful to M. Smoliy, S. Bunchuk, and Z. Tsybrii for detectors manufacturing and V. Reva and J. Gumenjuk-Sychevska for useful discussions.

References:

1. F. Sizov, V. Petriakov, et al., “Millimeter wave hybrid uncooled hot-carrier and Schottky diodes direct detectors” Appl. Phys. Lett., Vol. 101, 082198 (2012).
2. F. Sizov, V. Zabudsky, et al., “Millimeter-wave narrow-gap uncooled hot-carrier detectors for active imaging” Opt. Eng., Vol. 52(3), 033203 (2013).

Paper TH-I-11

ULTRATHIN NbN SUPERCONDUCTING NANOWIRES SINGLE PHOTON DETECTOR: INFLUENCE OF PROTON IRRADIATION ON OPTICAL SENSETIVITY

M.A. Tarkhov, K.E. Prikhodko, E.A. Kuleshova, D.A. Komarov, A.G. Domantovsky, B.A.Gurovich

National Research Centre «Kurchatov Institute»

tarkhov.michael.ipad@gmail.com

We present a fabrication technique of ultra sensetivity NbN Superconducting Single Nanowire Photon Detectors (SSNPD) made by proton irradiation method based on selective displacement of atoms [1]. Showed, that proton irradiation process leads to change superconducting and optical properties of SSPD fabricated in standart technology [2]. At fixed dose about 10^{21} proton per second that correspond to displacement per ion (dpi) ~ 0.7 quantum efficiency to increases up to maximum possible value 30% at wavelenght 1.3 μm. But critical current I_c and critical temperature T_c to decreases in half times. XPS (x-ray photoelectron spectroscopy) analysis showed that Nb to N atom ratio to be 0.505/0.495 before irradiation and oxygen concentration to be 10%, but after proton irradiation oxigen concentration to be 25–30%. We are propose the phenomenological model of single photon detection fabricated by proton irradiation method.

References:

1. B.A. Gurovich, D.I. Dolgy, E.A.Kuleshova, et al., UFN, Vol. 171, p. 105 (2001).
2. G.N. Goltsman et al., “Ultrafast superconducting single-photon detector” Journal of Modern Optics, Vol. 4(10) (2008).

Paper TH-O-1

STUDY OF ELECTROMAGNETIC PROPERTIES OF MULTYLAYER GRAPHENE FRACTAL STRUCTURES BY REMOTE METHOD

N.A. Dugin, T.M. Zaboronkova, V.V. Chugurin, E.N. Myasnikov

Radiophysical Research Institute, 25B. Pecherskaya st., N. Novgorod 603950, Russia

t.zaboronkova@rambler.ru

Studies of electromagnetic characteristics of nanostructured composites based on graphene materials are the scientific and technological basis for a wide range of different radio devices and coating having the desired electromagnetic properties.

One of the main methods for the synthesis of graphene-based materials is the process of graphite intercalation with thermal expansion in induction chambers and the separation of multilayer graphene structures. However, this method to obtain the substance (expanded graphite) contains of the graphene film is not more than 0.1%, which is due on the one hand insufficient degree of intercalation of graphite and the other low rate of thermal degradation of the substance.

The authors of method of the microwave thermal destruction has been developed a facility consisting of an electrochemical graphite intercalation in high pressure reactor, unit microwave generator with the resonance chamber and an adjustable level of absorption of the microwave radiation in the environment of high-purity argon.

Experiments have shown a high degree of intercalation graphite and substantially more efficient absorption of microwave energy and the particulate material as a consequence of a high heating rate in the process of interaction with the high-frequency electromagnetic field.

The resulting material consists of multilayer graphene 10–20 nm thick structures, separated graphene films, complex filaments in length from 0.1 to 2 mm and an effective diameter of 0.001 to 0.03 mm, particle crystallites and amorphous carbon. Absorption surface of the substance reaches 700–900 m^2/g with a bulk density of 1.6 kg/m^3. After dynamic separation and processing the received substance by ultrasound chamber multilayer graphene structures were dispersing in the polymer matrix. The resulting material has high local conductivity and ability to produce two or three-dimensional cohesive structure (multifractal clusters) composed of a few atomic layers (including one) of the transverse dimensions of a few tens of micrometers, suitable for the study of their mechanical, optical and electronic properties.

The authors have been investigated polarization properties multilayer graphene structures depending on the concentration of the binder (polymer) in the centimeter wavelength range (3–10cm). With the help of a spectrum analyzer measured of the amplitude of a incident wave and the reflected wave from multilayer graphene composite.

We investigated the case of normal incidence of the electromagnetic wave to the composite film. Revealed the presence of anisotropy in the film which is rotated in a plane perpendicular to the direction of propagation of the wave. Polarization of the amplitude of the reflected wave under the rotation of the film was 20 to 30%, depending on the topological structure of the fractal clusters. The influence of the anisotropy of the medium on the reflective properties both of TE and TH polarized waves is theoretically analyzed. Based of this theoretical research the method of determination of electromagnetic parameters of multilayer graphene composite is developed and experimentally proved.

Acknowledgements: This work was supported by the Russian Foundation for Basic Research (Grant 13-02-97035_a).

Paper TH-O-2

FEMTOSECOND COHERENT CONTROL OF THz SPECTRA DRIVEN BY FREE- AND COUPLED ELECTRONS IN GAS PLASMA

M.N. Esaulkov, N.A. Panov, A.V. Borodin, O.G. Kosareva, A.P. Shkurinov

Lomonosov Moscow State University, Leninskie Gory, Moscow 119991, Russia

ashkurinov@physics.msu.ru

Abstract: Interference between the free electron photocurrent and the nonlinear polarizationof neutrals, can be used for the femtosecond coherent control of the THz spectra and polarization in a femtosecond filament.

OCIS codes: (190.0190) Nonlinear optics; (260.3090) Infrared, far; (300.6290) Spectroscopy, four-wave mixing.

Gas is one of the promising and convenient medium for generation of broadband pulsed terahertz radiation. The highest THz generation efficiency is reached in the case of high intensity dual-frequency femtosecond laser pulses. The most important contribution to generation of low-frequency field is provided by the photo-current of free charges, induced by photoionization, and the four-wave mixing process, which describes nonlinear response of bound electrons in a gas.

In this paper we show both theoretically and experimentally that the THz-range radiation produced by co-propagating in nitrogen and air 800 nm and 400 nm high-intensity femtosecond laser pulses consists of the contribution from both the free electron current and the nonlinear polarization of neutral molecules. The major contribution from free electrons is in the low-frequency part of the THz spectrum, while the higher-frequency part is dominated by the instantaneous and delayed Kerr nonlinear response of neutrals at the difference frequency. We discussed the polarization properties of the THz radiation versus the polarizations of the incoming light beams.

Paper TH-O-3

TRANSFORMATION OF RADIATION FROM THz QUANTUM CASCADE LASERS USING EXTERNAL OPTICAL ELEMENTS

E.E. Orlova

Institute for Physics of Microstructures RAS, N.Novgorod GSP-105, Russia

orlova@ipm.sci-nnov.ru

Specifics of the transformation of radiation from THz quantum lasers using external optical elements stems from their wire geometry: subwavelength cross section, and the length much larger than the wavelength. While beam shaping optics for the lasers with transverse dimensions much larger than the wavelength is well established [1], external transformation of the radiation from subwavelength sources is an emerging field. The importance of this field is determined by existing complications with effective coupling of radiation from wire lasers caused by high radiation divergence and non-uniform phase front [2]. It has been shown that the problem of effective coupling of radiation from wire lasers can be solved by altering the field distribution of the laser mode [3–5], however this approach requires elaborate cavity design which is not always robust and economic. In this talk the overview of results obtained in the field of external transformation of radiation from wire lasers is presented, including the development of specific methods of analysis of transformation of radiation field of wire lasers, approaches towards the construction of optical elements, and investigation of specific beam profiles, promising for applications, that can be created using wire lasers with external optical elements.

Acknowledgements: The work is supported by RAS, TERADEC joint NWO/RFBR project and NATO SfP 984068 grant.

References:

1. Laser beam shaping theory and techniques, Ed. F.H. Dickey, S. C. Holswade. New York: Marcel Dekker Inc., 2000.
2. J.L. Adam, I. Kasalynas, J.N. Hovenier, T.O. Klaassen, J.R. Gao, E.E. Orlova, B.S. Williams, S. Kumar, Q. Hu, J.L. Reno, “Beam pattern of TeraHertz quantum cascade lasers with sub-wavelength cavity dimensions” Appl. Phys. Lett., Vol. 88, 151105 (2006).
3. E.E. Orlova, J.N. Hovenier, T.O. Klaassen, I. Kasalynas, A. J.L. Adam, J.R. Gao, T.M. Klapwijk, B.S. Williams, S. Kumar, Q. Hu, J.L. Reno, “Antenna model for wire lasers” Phys. Rev. Lett., Vol. 96, 173904 (2006).
4. M.I. Amanti, M. Fischer, G. Scalari, M. Beck and J. Faist, “Low-divergence single-mode terahertz quantum cascade laser” Nature Photon., Vol. 3, p. 586 (2010).
5. T.-Y. Kao, Q. Hu, J.L. Reno, “Perfectly phase-matched third-order DFB THz quantum-cascade lasers” Opt. Lett., Vol. 37, p, 2070 (2012).

Paper TH-O-4

SPECTRAL LIMITATIONS OF THE AIR BASED COHERENT DETECTION (ABCD) TECHNIQUE OF THE THZ PULSE DETECTION

M.N. Esaulkov[1], N.A. Panov[1], A.V. Borodin[1], A.A. Frolov[2], O.G. Kosareva[1], A.P. Shkurinov[1]

[1]*Lomonosov Moscow State University, Leninskie Gory, Moscow 119991, Russia*
[2]*Joint Institute for High Temperature, Russian Academy of Sciences, Moscow 125412, Russia*

Esaulkov_mich@mail.ru

Abstract: The coherent plasma detection technique to detect pulsed terahertz (THz) signal based on the transient photocurrent mechanism is suggested.

OCIS codes: (190.0190) Nonlinear optics; (260.3090) Infrared, far; (300.6290) Spectroscopy, four-wave mixing.

1. Introduction

Nonlinear interactions during propagation of the two-color femtosecond laser radiation result in the effective generation of the THz radiation [1]. The spectral bandwidth of this radiation is inversely proportional to laser pulse duration [1, 2]. Zhang et al. [3] proposed an electric-field induced second harmonic generation (EFISH) process for terahertz detection. The use of external DC field allows to measure terahertz field amplitude at the given moment of time. Temporal waveform of the terahertz pulse can be obtained by scanning of delay stage in time-domain scheme. This method is known as air-biased coherent detection (ABCD) [4].

Initially, the second harmonic generation in the ABCD method was attributed to the anharmonic response of bound electrons [4]. Later, in the paper [5] it was shown that the free electrons can also contribute to generation of second harmonic radiation in this detection scheme.

In this paper we propose an ABCD method based on the transient photocurrent-induced mechanism of second harmonic generation. We investigate the bandwidth limitations of the detection technique both for bound and free electron mechanisms.

2. Theoretical background

The ABCD detection method requires interaction of three electric fields: $\mathbf{E} = \mathbf{E}_{\text{laser}} + \mathbf{E}_{\text{DC}} + \mathbf{E}_{\text{THz}}$, where $\mathbf{E}_{\text{laser}}$, $\mathbf{E}_{\text{THz}}$, and $\mathbf{E}_{\text{DC}}$ are the probe laser, THz, and DC fields, respectively, and $|\mathbf{E}_{\text{laser}}| >> |\mathbf{E}_{\text{THz}}|, |\mathbf{E}_{\text{DC}}|$. Here we take the $\mathbf{E}_{\text{laser}}$ field amplitude high enough for tunnel/multiphoton ionization of the gas. The radiative part of the photocurrent can be written as

$$\dot{\mathbf{J}} = \frac{e^2}{m} N_{\text{e}} \mathbf{E}, \tag{1}$$

where m, e are electron mass and charge respectively, N_{e} is free electron density.

The spectrum of $N_{\text{e}}(t)$ contains only even harmonics of the laser field frequency because the tunnel ionization rate reaches its maximum twice during each optical period. As a result, the radiative part of the photocurrent responsible for the second harmonic generation takes form

$$\dot{\mathbf{J}}_{\text{even}} = \frac{e^2}{m} N_{\text{e}} \left(\mathbf{E}_{\text{DC}} + \mathbf{E}_{\text{THz}}\right). \tag{2}$$

The spectral intensity of the second harmonic signal is written as:

$$S = \left|\hat{F}(\dot{\mathbf{J}})\right|^2 = f(\Omega)(\mathbf{E}_{\text{DC}}^2 + \mathbf{E}_{\text{THz}}^2 + 2\mathbf{E}_{\text{DC}}\,\mathbf{E}_{\text{THz}}), \tag{3}$$

where $f(\Omega)$ is a factor describing the spectral sensitivity of the ABCD method and Ω is terahertz wave frequency. The Eq. (3) is valid also for the bound electrons response if we use a corresponding factor $f(\Omega)$. The detection process requires heterodyne detection of a $S_{2\omega} = f(\Omega)\mathbf{E}_{\text{THz}}\mathbf{E}_{\text{DC}}$ component in the Eq. (3).

We consider numerically the reconstruction of the model THz signal $E_{\text{THz}} = E_{\text{THz}}^0 \cos\Omega t$ to determine the limitations of this technique. The quality of the reconstructed signal was estimated as $\xi(\Omega) = \Sigma(E_{\text{THz}}(\tau_i) - S_{2\omega}(\tau_i))^2$, where τ_i – time delay between laser probe and terahertz pulses. The dependence of the reconstruction quality on terahertz frequency Ω for 120 fs laser pulses is shown on the Fig. 1.

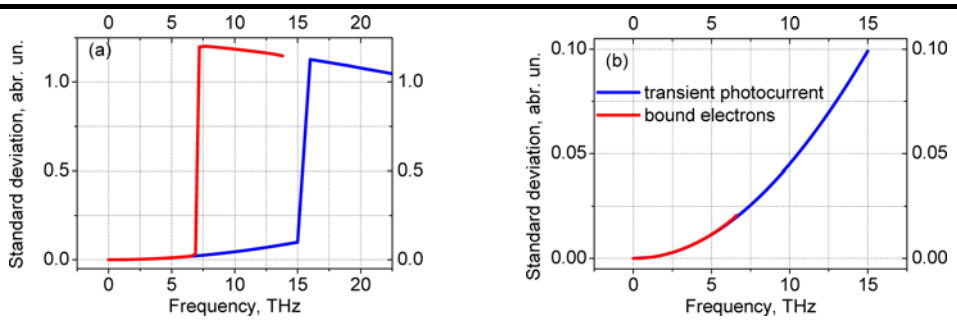

Figure 1. Dependence $\xi(\Omega)$ on terahertz frequency for bound electrons mechanism (red curve) and for transient photocurrent mechanism (blue curve).

One can see from Fig. 1 that the dependence $\xi(\Omega)$ monotonically increases at the low-frequency part of spectrum (see Fig. 1b) for both detection mechanisms in a similar way. At higher frequencies there is fast increase of $\xi(\Omega)$ due to incorrect reconstruction of the terahertz radiation phase (see Fig. 1a). The frequency of fast increase in case of transient photocurrent mechanism is higher than in case of bound electrons one due to lesser duration of the ionization front in comparison with the optical pulse duration.

3. Conclusions

We have introduced the transient photocurrent-induced mechanism for THz detection in the ABCD technique. We have shown that the critical frequency which limits the detection bandwidth at higher THz frequencies is caused by incorrect reconstruction of phase of terahertz radiation. This frequency is higher for the transient photocurrent mechanism due to lesser duration of the ionization front in comparison with the optical pulse duration.

References:

1. D.J. Cook, R.M. Hochstrasser, “Intense terahertz pulses by four-wave rectification in air” Opt. Lett., Vol. 25, pp. 1210–1212 (2000).
2. A.V. Borodin, N.A. Panov, O.G. Kosareva, V.A. Andreeva, M.N. Esaulkov, V.A. Makarov, A.P. Shkurinov, S.L. Chin, X.-C. Zhang, “Transformation of THz spectra emitted from dual-frequency femtosecond pulse interaction in gases” Accepted for publications to Optics Letters, 21.02.2013.
3. J. Dai, X. Xie, X.C. Zhang, “Detection of broadband terahertz waves with a laser-induced plasma in gases” Phys. Rev. Lett., Vol. 97, 103903-1-103903-4 (2006).
4. J.M. Dai, X.F. Lu, J. Liu, I.C. Ho, N. Karpowicz, X.-C. Zhang, “Remote THz wave sensing in ambient atmosphere” Terahertz Science and Technology (TST), Vol. 2, pp. 131–143 (2009).
5. A.A. Frolov, A.V. Borodin, M.N. Esaulkov, I.I. Kuritsyn, A.P. Shkurinov, “Theory of a laser-plasma method for detecting terahertz radiation” Journal of Experimental and Theoretical Physics, Vol. 114, pp. 893–905 (2012).

Paper TH-O-5

THz SPECTROSCOPY BASED ON QUANTUM CASCADE LASERS FOR MEDICINE AND BIOLOGICAL INVESTIGATIONS

V.L. Vaks

IPM RAS, Nizhny Novgorod, Russia

katja@ipmras.ru

Now the actual problems in the gas analysis field have been associated with development of novel methods of medical diagnostics. The analysis of composition of human exhaled air allows diagnosing some of pathology processes on the base of measuring concentrations of substance-markers, which are products of physiological and biochemical processes in human organism [1]. The investigations of biological compounds (DNA, proteins, sugars, etc) in solid and gaseous phases as well as liquids are important for medical and biological tasks. Dielectric properties of biomolecules in THz range are formed by low frequency vibrations, which specify collective motion of big atomic groups, and intermolecular hydrogen bonds, thus, providing information about molecular geometry and conformational flexibility and its chemical activity. During the variety of instrumental methods of analysis of exhaled air and biological compounds the spectroscopic methods including the spectroscopy of THz frequency range are more prospective. The THz technique can also be used for studying of biological tissues based on dielectric function analysis.

The essence of a nonstationary spectroscopy is as following: interaction of electromagnetic radiation with ensemble of absorbing molecules results in induction of macroscopic dipole. After a radiation impact is over, absorbed energy is reradiated coherently at the frequency of molecular transition. The operation of nonstationary spectrometers can be realized in a phase switching [2] or fast passage regime [3]. The advantages of the method involve frequency resolution about 10 kHz and high sensitivity. To provide a required resolution, spectroscopic characteristics of a radiation sources are to meet requirements for measurements at Doppler line resolution ($\sim 10^{-6}$) and frequency measurements with accuracy $10^{-8} \div 10^{-10}$. The cornerstone of the radiation source design based on quantum cascade laser (QCL) is a phase-lock loop (PLL) and modulation system. The first step in the elaboration of the PLL system involved studying of spectral, power and modulation characteristics of QCL. The PLL system for DFB QCL is designed using a room temperature superlattice (SL) harmonic mixer [4].

After the QCL based radiation source was shown to be operational a laboratory model of the spectrometer has been set up and tested. The exhaled breath analysis of oncopatients with cancer of lung which had radiotherapy and diabetes patient was carried out. The DNA spectra were measured preliminary.

Acknowledgements: This work is supported by the grant of the Government of RF № 11.G34.31.0066 (MedLab), TeraDec 047.018.005.

References:

1. E.V. Stepanov, “Methods of high-sensitivity gas analysis of biomarker molecules in studies of exhaled air”, Trans. A.M. Prokhorov Inst. Gener. Phys. Vol. 61, pp. 5–47, 2005 [in Russian].
2. V.L. Vaks, A.B. Brailovsky, V.V. Khodos, “Millimeter Range Spectrometer with Phase Switching – Novel Method for Reaching of the Top Sensitivity” Infrared & Millimeter Waves, Vol. 20, No. 5, pp. 883–896 (1999).
3. V.V. Khodos, D.A. Ryndyk, V.L. Vaks, “Fast passage microwave molecular spectroscopy with frequency sweeping” Eur. Phys. J. Appl. Phys., Vol. 25, pp. 203–208 (2004).
4. D.J. Hayton, A. Khudchencko, D.G. Pavelyev, J.N. Hovenier, A. Baryshev, J.R. Gao, T.Y. Kao, Q. Hu, J.L. Reno, V. Vaks, “Phase locking of a 3.4 THz third-order distributed feedback quantum cascade laser using a room-temperature superlattice harmonic mixer” [to be published].

Paper TH-P-1

TERAHERTZ TIME DOMAIN SPECTROSCOPY OF BLOOD COMPONENTS

O.P. Cherkasova[1], I.N. Smirnova[2], M.M. Nazarov[2], A.P. Shkurinov[3]

[1]*Institute of Laser Physics SB RAS, pr. Lavrentyeva, 13/3, Novosibirsk, 630090 Russia*
[2]*Institute on Laser and Information Technologies of RAS, 2 Pionerskaya St., Troitsk, 142092*
[3]*Lomonosov Moscow State University, Leninskie Gory, GSP-1, Moscow, 119991, Russia*

o.p.cherkasova@gmail.com

It is known that many diseases occur as a result of complex metabolic disorders. The disease diagnosis with a single marker could be uninformative that facilitates the transition of the disease to the chronic phase and leads to expensive and long-term treatment. The study of unique spectral "fingerprint" specific to the processes occurring in living organisms is an extremely important task. The methods of terahertz time-domain spectroscopy (THz-TDS) can be helpful for the study of specific markers of disease. This type of spectroscopy has a number of advantages such as the possibility to analyze a wide frequency band in a single measurement, to obtain time resolution and phase information and to measure the complex dielectric permittivity which completely characterizes the optical response of the matter [1].

Diabetes Mellitus is characterized by the high level of blood glucose, the changes of blood lipid profile and the elevation of corticosteroid hormones concentration. In preliminary studies we have shown that glucose and corticosteroids have characteristic absorption bands in the frequency range 0.7–3.0 THz [2, 3]. The aim of the present research is to perform the comparative analysis of the blood components in case of healthy and diabetic individuals by using of THz-TDS.

The absorption and refraction spectra of the whole blood, red blood cells and plasma have been measured. The used THz-TDS apparatus has been reported previously [2, 3]. For the case of solutions and thin films on quartz substrates we developed the total internal reflection (TIR) scheme using a silicon right angle Dowe prism. The practical advantage of TIR scheme consists in the larger signal amplitude (|R| is close to 1) for the strong absorbing media.

It was found that the greatest differences in the reflection amplitude spectra of blood components in case of healthy and diabetic individuals were located in the range 0.4–0.6 THz. A direct correlation between the amplitude of the absorption and blood glucose in rats with alloxan diabetes was established.

Acknowledgements: This work has been supported by RFBR (grant № 13-02-01364).

References:

1. M.M. Nazarov, A.P. Shkurinov, V.V. Tuchin, X.-C. Zhang, "Terahertz Tissue Spectroscopy and Imaging", Handbook of Photonics for Biomedical Science, Ch. 23, Editor: Valery V. Tuchin, Series in Medical Physics and Biomedical Engineering, CRC press, Taylor and Francis Group, pp. 519–617 (2010).
2. M.M. Nazarov, A.P. Shkurinov, E.A. Kuleshov, V.V. Tuchin, "Terahertz time-domain spectroscopy of biological tissues" Quantum Electronics, Vol. 38(7), pp. 647–654 (2008).
3. I.N. Smirnova, D.A. Sapozhnikov, A.V. Kargovsky, V.A. Volodin, O.P. Cherkasova, R. Bocquet, A.P. Shkurinov, "Lowest-lying vibrational signatures in corticosteroids studied by terahertz time-domain and Raman spectroscopies" Vibrational Spectroscopy, Vol. 62, pp. 238–247 (2012).

KEY FOR AUTHORS/CHAIRS